AMERICAN UNIVERSITY OF BEIRUT

PERSONAL COOLING STRATEGIES FOR ALLEVIATING THE THERMAL STRAIN OF PEOPLE WITH SPINAL CORD INJURY

by
FARAH KHALED MNEIMNEH

A dissertation
submitted in partial fulfillment of the requirements
for the degree of Doctor of Philosophy
to the Department of Mechanical Engineering
of Maroun Semaan Faculty of Engineering and Architecture
at the American University of Beirut

Beirut, Lebanon
September 2021

AMERICAN UNIVERSITY OF BEIRUT

PERSONAL COOLING STRATEGIES FOR ALLEVIATING THE THERMAL STRAIN OF PEOPLE WITH SPINAL CORD INJURY

by
FARAH KHALED MNEIMNEH

Approved by:

Dr. Nesreen Ghaddar, Professor
Mechanical Engineering Department
American University of Beirut

_____
Advisor

Dr. Fadl Moukalled, Professor
Mechanical Engineering Department
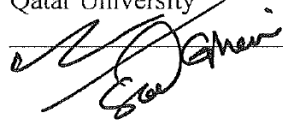American University of Beirut

_____
Chair of Committee

Dr. Kamel Ghali, Professor
Mechanical Engineering Department
American University of Beirut

_____
Member of Committee

Dr. Oussama Jadayel, (Ph.D., FRAeS)
Professor and Managing Director
AnNavCom Aeronatical Awareness and Outreach, DWC-LLC Dubai, UAE

_____
Member of Committee

Dr. Saud Abdul Aziz Abdu Ghani
Mechanical and Industrial Engineering Department
Qatar University

_____   Member of Committee

Date of dissertation defense: [September 10th, 2021]

AMERICAN UNIVERSITY OF BEIRUT

DISSERTATION RELEASE FORM

Student Name: Mneimneh   Farah   Khaled

I authorize the American University of Beirut, to: (a) reproduce hard or electronic copies of my dissertation; (b) include such copies in the archives and digital repositories of the University; and (c) make freely available such copies to third parties for research or educational purposes:

☒ As of the date of submission

☐ One year from the date of submission of my dissertation.

☐ Two years from the date of submission of my dissertation.

☐ Three years from the date of submission of my dissertation.

___Farah Mneimneh_____11-10-2021_____

Signature   Date

ACKNOWLEDGEMENTS

There are many who helped me along the way on this journey. I want to take a moment to thank them.

I wish to thank my advisors, Dr. Nesreen Ghaddar and Dr. Kamel Ghali. Without their guidance, I would not have made it as not only for their time and extreme patience, but for their intellectual contributions to my development as a researcher. They went above and beyond to help me reach my goal.

I want to thank my dissertation committee: Dr. Fadl Moukalled served as chair of committee; Dr. Oussama Jadayel and Dr. Saud Abdul Aziz Abdu Ghani served as wise committee members. I am most appreciative for agreeing to serve on the committee on short notice and knowing they would probably have less than two weeks to read my thesis.

To my lab-mates, thanks for the fun and support. My experience in the lab was greatly enhanced because of you. I greatly look forward to having all of you as colleagues in the years ahead.

Finally, but not least, I want to thank my family, especially my mother, who always encouraged me to pursue my PhD as they always believed that I could do it. Thanks for teaching me that it is important to try to leave the world just a little better than when you came into it, and how a career in research can be a worthy part of that pursuit. And, of course, thank you both for your constant support through the ups and downs of my academic career. It has been bumpy at times, but your confidence in me has enhanced my ability to get through it all and succeed in the end.

ABSTRACT
OF THE DISSERTATION OF

Farah Khaled Mneimneh   for   Doctor of Philosophy
                                                Major: Mechanical engineering

Title: Personal Cooling Strategies for Alleviating the Thermal Strain of People with Spinal Cord Injury

People with spinal cord injury (SCI) are prone to thermal strain (i.e. unsafe elevation in body core temperature) at hot conditions and/or high metabolic rates resulting in various levels of thermal discomfort based on injury level. This is due to the loss of motor/sensory functions at impaired body segments and disruption in both sweating and vasodilation responses. Therefore, for the health and well-being of people with SCI, it is of interest to investigate different personal cooling strategies. In literature, conventionally used phase change material (PCM) and evaporative cooling vests (ECVs) succeeded in reducing thermal strain for able-bodied people, but its application for people with SCI is still scarce and not conclusive in literature. Therefore, in this research, it is aimed to assess the effect of these two types of cooling vests on the physiological and psychological responses of people with SCI at different ambient conditions and metabolic rates. To achieve this goal, research methodology tracked two approaches; modelling and experimentation to assess the performance of proposed cooling vests for persons with SCI, and consequently, provide recommendations about the optimal design and use of these cooling strategies at different ambient conditions and physical activity levels.

To assess cooling vest performance, multi-segmented bioheat models for persons with SCI that can predict core and skin temperature values were developed and validated via previous studies in literature. Then, published fabric-PCM 1D-transient mathematical model was integrated into the bioheat model of person with SCI to predict the effect of PCM cooling vest on body core and skin temperatures as well as heat losses from sensate and insensate skin of the trunk. Validation of the developed combined model was done via previous studies in literature, and a parametric study about coverage area on the sensate/insensate skin of trunk and melting temperature of PCM cooling vest was done. Based on the findings of model predictions, human subject experiments were completed to test the proposed improvements in the design of PCM cooling vest for persons with SCI during exercise in heat.

Since PCM cooling vests caused additional weight burden and restricted movement of persons with SCI, the use of evaporative cooling vest (ECV) incorporated with ventilation fans (hybrid vest) is proposed to enhance heat losses at the limited sensate trunk skin area of person with PA. A 1-D transient mathematical model for the hybrid vest was developed

and integrated with the validated PA-bioheat model to predict body thermophysiological responses. The hybrid vest model was validated via experiments performed on a heated plate. A parametric study was then performed using the integrated models at range of ambient temperature and relative humidity for moderate and high activity levels. Evaluation of the hybrid ECV performance for persons with PA was based on the drop in local sensate skin, and sensible and latent heat losses, compared to No-Vest case. Furthermore, human subject experiments were done to evaluate the physiological and psychological responses of patients with SCI when using a commercially available of ECV.

TABLE OF CONTENTS

ILLUSTRATIONS

Figure

7

9

TABLES

13

ABBREVIATIONS

A	: area (m^2)
AB	: able bodied persons
AD	: arterial diameter
AIS	: ASIA impairment scale
ANS	: Autonomic Nervous System
ASIA	: American Spinal Injury Association
BMR	: basal metabolic rate
BMR$_{AB,core}$	: core basal metabolic rate of able-bodied persons
BMR$_{TP,Core}$	: core basal metabolic rate of people with tetraplegia
C_p	: specific heat (J/kg·K)
CO	: cardiac output
CTPM	: people with complete tetraplegia
e	: thickness (m)
ε_{ECV}	: enhancement factor
ECV	: evaporative cooling vest
EE	: energy expenditure
FES	: functional electrical simulation
FFM	: fat Free Mass
FM	: fat mass
h_{ads}	: heat of adsorption of water vapor (J/kg)
h_c	: convective heat transfer coefficient (W/m^2·K)
h_e	: evaporative heat transfer coefficient (kg/m^2·kPa·s)
h_r	: radiative heat transfer coefficient (W/m^2·K)
h_{fg}	: heat of vaporization of water vapor (J/kg)
h_{liq}	: enthalpy of liquid water (J/kg)
HP	: people with high thoracic SCI
HR	: heart Rate
H_{stored}	: rate of change in body heat storage
ISNCSCI	: International Standards for Neurological Classification of Spinal Cord Injury
K	: thermal conductivity (W/m·K)
K_{muscle}	: muscle conductance
$K_{fat-skin}$	: fat and skin layer conductance,
ITPM	: people with incomplete tetraplegia
LBM	: lean body mass
LBM$_{AB}$	: lean body mass of able-bodied persons
LBM$_{TP}$	: lean body mass of people with tetraplegia
LP	: people with low thoracic SCI
m	: mass (kg)
$\dot{m}_a$	: air mass flow rate (kg/s)
$\dot{m}_{evp}$	: rate of evaporation (kg/s)
$\dot{m}_{sw}$	: sweating rate (kg/s)
MR	: metabolic rate
M_{total}	: total metabolic rate of the human body

NV	: no vest
P	: vapor pressure (kPa)
P_{sat}	: saturated vapor pressure (kPa)
PA	: paraplegia
PCM	: phase change material
P1	: period before onset of sweating (mins)
P2	: period after onset of sweating (mins)
PE	: perceived exertion
Q_{lat}	: latent heat loss (W/m^2)
Q_{sens}	: sensible heat loss (W/m^2)
R	: regain
R_d	: dry thermal resistance (m^2·K/W)
R_e'	: shirt evaporative resistance (m^2·K/W)
R_e	: evaporative resistance (m^2·K/W)
R_{th}'	: shirt dry thermal resistance (m^2·K/W)
RH	: relative humidity
ρ	: density (kg/m^3)
RPM	: rotation per minute
SBP	: skin blood perfusion flow
SBP$_{AB}$	: skin blood perfusion for able-bodied persons
SBPR$_{LB}$	: skin blood perfusion ratio for lower body
SBPR$_{UB}$	: skin blood perfusion ratio for upper body
SBP$_{TP}$	: skin blood perfusion for people with tetraplegia
SCI	: spinal cord injury
SFT	: skin fat thickness
SNS	: sympathetic nervous system
SV	: stroke Volume
t	: time (s)
T	: temperature (℃)
TP	: tetraplegia
TPE	: people with tetraplegia participated in the experiment
$th_{fat+skin}$	: thickness of fat and skin layers
ΔT	: change of temperature
V1	: vest-type1 with phase change material of melting temperature 20 °C covering all trunk
V2	: vest-type2 with phase change material of melting temperature 20 °C covering all upper trunk
V20	: phase change material of melting temperature 20 °C covering all upper trunk
V14	: phase change material of melting temperature 14 °C covering all upper trunk
w	: humidity ratio (kg water/kg dry air)

SUBSCRIPTS

a	: microclimate air layer
acc	: accumulated
amb	: ambient
body	: body
cap	: captured
cr	: core
evp	: evaporation
i	: inner vest layer
insen	: insensate skin
o	: outer vest layer
sen	: sensate skin
sh	: shirt
sk	: skin
w	: water-absorbent layer
WB	: ambient wet bulb

CHAPTER 1

INTRODUCTION

In developed countries, reported incidence of spinal cord injury (SCI) ranged between 11.5 and 53.4 per million inhabitants per year (Sekhon and Fehlings, 2001). Globally, traffic accidents involving motor vehicles, bicycles or pedestrians account for the greatest number of SCIs, typically 50% of all injuries (Sekhon and Fehlings, 2001). Approximately 55% of the acute SCI occur in the cervical (C1-C7) region; whereas, approximately 15% occur in thoracic (T1-T12) region (Sekhon and Fehlings, 2001). Persons with cervical SCI, also named persons with tetraplegia (TP), present motor and sensory impairment in palms, arms, trunk, and legs; thus, considered most severe levels of SCI and requires continuous personal care as they are physically incapable to function independently. Persons with thoracic SCI, also named persons with paraplegia (PA), present impairment in region of the trunk and legs; accordingly, considered an active group compared to that of cervical SCI and can use wheelchair independently. Therefore, SCI became a major public health concern seeing that this injury is a debilitating and even life-threatening condition.

Not only SCI limits the physical mobility of the human body, but it also endures changes in the physiology, including cardiovascular responses, metabolic pathways, and thermoregulation. The severity of these changes is dependent on the injury level as defined by the International Standards for Neurological Classification of Spinal Cord Injury (ISNCSCI) (Kirshblum et al., 2011a). However, generally, SCI results in muscle atrophy, reduced energy expenditure (EE) as well as alterations in cardiovascular responses including cardiac output (CO), heart rate (HR) and skin blood perfusion (SBP)

because of changes in arterial blood vessel structure (Hostettler et al., 2012). More profoundly, persons with SCI experience poikilothermic behavior defined as unsafe elevation of body core temperature (T_{cr}) from its thermal neutral state (36.8±0.2 ℃). This induced thermal strain in persons with SCI results from the imbalance of body heat gains and losses as a consequence of the reduced afferent input to the thermoregulatory center and disruption in thermoregulatory responses at the impaired body segments (Attia and Engel, 1983; Petrofsky, 1992). The partial or complete loss of blood vasodilation and sweating at the insensate skin of the impaired body segments attenuates heat dissipation from the body which significantly reduces individual thermal comfort during outdoor activity exposure. Hence, the thermal strain and heat-illness risks that persons with SCI are prone to demand the use of cooling strategies that are adaptive to the body altered thermal physiology (Altus et al., 1985; Downey et al., 1992; Khan et al., 2007).

Among the proposed cooling strategies are phase change material (PCM) cooling vests and evaporative cooling vests (ECVs) (Golbabaei et al., 2020; Itani et al., 2018b). PCM cooling vests and ECVs have been the focus of many studies that target healthy able-bodied people (AB) for the sake of personal thermal management and thermal comfort in dry/humid and moderate/hot ambient conditions at different activity levels (seated at rest, walking, cycling…) (Bachnak et al., 2018; Ciuha et al., 2021; Eijsvogels et al., 2014; Golbabaei et al., 2020; Itani et al., 2018b; Procter). The effectiveness of such vests in alleviating the induced thermal strain on the human body is investigated based on maintaining the body core temperature (T_{cr}) around its thermal neutral state of 37 ℃. These cooling vests can enhance heat losses from the trunk which is the most vital segment for regulating body temperature due to its high metabolic heat generation and its relatively large skin surface area (Douzi et al., 2019; Dykes et al., 2002).

The use of PCM cooling vest was successful for outdoor workers, athletes, and firefighters considered heavy-duty activities in hot environments (Itani et al., 2017; Itani et al., 2018a). Nevertheless, the PCM vest was considered bulky in size, heavy in weight and had limited working duration although it was effective in dissipating heat in hot conditions for AB. To overcome the ergonomic problems and extra burden due to PCM weight, ECVs were suggested as an alternative for AB. Compared to PCM vests, ECVs were reported as more portable, affordable, lighter by∼80%, and convenient to use (Ciuha et al., 2021). In fact, up to now, two types of ECV were tested for AB via modelling and experimenting at various ambient conditions and activity levels.

The first ECV type (Type I) depends on sweat evaporation from the wetted inner fabric of the trunk (the shirt) using either meshed outer fabric layers or ventilation fans (Yi et al., 2017; Zhao et al., 2013). The second ECV type (Type II) is based on evaporation occurring at the outer surface of a saturated water-absorbent vest that can drop trunk-skin temperature by cooling the inner layer of the vest (Eijsvogels et al., 2014; Procter). Both types of ECV were tested for high activity levels in outdoor conditions for AB, and the results were positive showing significant reduction in T_{cr} values (Eijsvogels et al., 2014; Procter; Yi et al., 2017; Zhao et al., 2013). However, the performance of ECV Type I depended on sweat accumulation on the shirt, the renewal rate of the microclimate air, and ambient temperature and humidity that could limit sweat evaporation. Whereas, ECV Type II performance was reduced in humid conditions as it could be constrained by the ambient wet bulb temperature (Wang and Song, 2017); in addition to the restricted sweat evaporation due to its higher evaporative resistance compared to the case of not wearing a vest or using PCM cooling vests (Ciuha et al., 2020).

Few experimental studies in literature reported about the effect of cooling methods on the thermal response of persons with SCI during exercise (Armstrong et al., 1995; Bongers et al., 2016; Griggs et al., 2017; Trbovich et al., 2014). Griggs et al. tested the effectiveness of precooling of rugby players with TP using an ice cooling vest frozen at -20 °C, and that of precooling combined with water spraying between exercise times (Griggs et al., 2017). An intermittent sprint protocol was used, and the players exercised at ambient temperature (T_{amb}) 20 °C and relative humidity (*RH*) 33%. It was found that precooling did not affect HR, perceived exertion (Singh et al.) and thermal comfort. However, it decreased core and mean skin temperatures, but this decrease was not long-lasting during exercise. Trbovich et al. examined changes in T_{cr} values for persons with PA with and without cooling during a 60-min arm-crank exercise (Trbovich et al., 2014). Results showed insignificant variation in T_{cr} value when using PCM vest of melting temperature 15 °C. Yet, this study had limited outcomes as it did not include segmental trunk-skin temperatures (T_{sk}) nor estimated the heat losses at the trunk to evaluate the effectiveness of PCM cooling vest for persons with PA. Similar results were obtained by Armstrong et al. who tested the effect of ice cooling vest during exercise on persons with PA (Armstrong et al., 1995). Consequently, the insignificant effect of PCM cooling vests for persons with SCI, more profoundly for people with PA being more active group, cannot be conclusive as previous studies did not consider the effect of thermoregulatory impairment and limited trunk sensate skin; hence, this requires further investigation.

Other than PCM cooling vests, in literature to-date, ECV Type II was tested only for persons with PA at moderate and high activity levels (Bongers et al., 2017). As mentioned earlier, this type of ECV consists of an absorbent material soaked with water quilted by an impermeable layer near the wearer's body to prevent liquid flow to the inner

clothing of the trunk (Appolonia, 2002). The total activation weight of Type II ranges between 0.39 kg and 1.05 kg which remains lighter compared to PCM cooling vests (Appolonia, 2002; Ciuha et al., 2020). The cooling technology of Type II is based on cooling the outer surface via evaporation of water, which increases the temperature gradient between the skin surface and the inner surface of the vest (Havenith et al., 2013). In the study of Bongers et al., ten men with a thoracic lesion (T4-T5 or below) performed 45-min exercise at high activity level at ambient conditions (25.4 °C, 41 % *RH*) (Bongers et al., 2016). Their findings showed that ECV Type II decreased trunk skin temperature by ~3 °C compared to No-Vest test, and improved perception of thermal sensation. However, they did not report whether sweat accumulation at the shirt occurred and if it affected the ECV performance. Hence, the cooling capacity of Type II remains inconclusive for persons with SCI as it may not be sufficient and even drop when sweating occurs at the sensate skin due to the higher evaporative resistance of ECV Type II (Ciuha et al., 2021). As for ECV Type I, its effectiveness is questionable for this population due to the delayed and limited sweating response that reduces latent heat losses at the trunk. Therefore, the performance of either type of ECV used for persons with SCI cannot be deduced from the studies of AB, due to the partial or complete disruption in thermoregulatory responses at the impaired body segments below injury level as well as the limited sensate skin of the trunk after SCI.

Evidently, the research in this area is still picking, and the existing design of PCM cooling vests and ECVs needs to be rethought. Before being used by persons with SCI, the methods for enhancing the cooling effect should focus on the sensate skin. For PCM cooling vests, the placement on trunk-skin, coverage area and melting temperature of PCM should be investigated. Upon use of this type of cooling vest, it is important to

determine whether cooling the trunk-sensate skin is more effective than cooling the whole trunk sensate and insensate skin area. For ECV, a hybrid vest that combines ECV Type I and II where the water-absorbent material is integrated with ventilation fans needs to be studied. Cooling would then be enhanced at the inner shirt (ECV Type I) and at the inner surface of the water-absorbent material (ECV Type II) resulting in a two-fold cooling effect. The extent of the enhanced cooling when using the hybrid vest needs to be investigated to check whether it can compensate for the reduced sensate trunk-skin area in persons with SCI. Therefore, this research provides means of enhancing the existing cooling methods used by AB to overcome the lifestyle thermal challenges of persons with SCI for the sake of their health and well-being in disparate environments.

To achieve the objectives of the study, multi-segmented bioheat models for persons with TP and persons with PA need to be developed to be combined with cooling vest models. The predictions of PCM-PA and Hybrid ECV-PA models can be used to investigate the performance of PCM cooling vest and Hybrid ECV, while adopting the altered physiology of the body segments below injury level in the bioheat models. This approach would be cost and time-effective method. It can predict the thermophysiological responses (body core and skin temperatures) of a person with SCI in steady/transient environmental conditions and activity levels, with and without a cooling vest. Literature to date, the extensive empirical studies on AB thermoregulation resulted in the development of robust predictive AB- bioheat models. However, to the authors' knowledge, the scattered empirical studies for persons with TP or PA have not been utilized to develop bioheat models that can predict thermal response of a person with SCI. Additionally, upon the use of PCM cooling vest or hybrid ECV for persons with SCI, it is important to determine whether each cooling method can increase trunk heat losses at

different ambient conditions and activity levels. Then, human subject experiments can be conducted on the proposed enhancement of PCM cooling vests and commercially available ECV Type II to study the physiological and psychological responses of persons with PA, considered the group of interest in this research as these patients are more capable to engage in outdoor activities and exercises which may impose their body to thermal strain.

1.1. Objectives

This work aims to evaluate the performance of cooling vests for alleviating the thermal strain of persons with SCI. It is of great interest as i) it proposes optimizing approaches of PCM cooling vests adaptive to the thermal physiology of persons with SCI and ii) suggests new hybrid design for ECV that can promote cooling effect analogous to that of PCM cooling vests and evaluate its performance at range of dry/humid moderate/hot ambient conditions for certain activity level for persons with SCI. In fact, this research focuses in detail on:

a) The development of a bioheat model for persons with TP and a bioheat model for persons with PA from reasonably selected AB-model, while focusing on blood flow circulatory changes and perspiration that influence their thermal response in warm environments. The bioheat models will be derived from reasonably selected AB-bioheat model while taking into consideration observed physiological changes associated with SCI. The model predictions of segmental skin and core temperatures will be validated with published experimental data in literature under reported transient and steady thermal environments. The importance of TP- and

PA-bioheat models is to have a robust tool to predict thermal state of a person with SCI at different ambient conditions and activity levels.

b) Investigation of means of enhancement for the PCM cooling vests for persons with PA bearing in mind the limited trunk sensate skin. Published PCM cooling vest mathematical model will be integrated into PA-bioheat model to predict the thermal state of persons with PA while using a PCM cooling vest. Validation of the combined model will be done via previous studies in literature that tested PCM cooling vest of melting temperature 15°C and ice vests for persons with PA during exercise. A parametric study will be done to propose an optimized design of PCM cooling vest (placement of PCM packets, coverage area and melting temperature) via model thermophysiological predictions (body core and skin temperatures, trunk heat losses) for the cases: with PCM cooling vest compared to no vest.

c) Investigation of the effectiveness of the hybrid ECV for persons with PA. The hybrid ECV consisted of water-absorbent material incorporated with ventilation fans can be a good solution for maintaining the thermal homeostasis of the body without compromising the ergonomic preferences of the ECV design. A 1D-transient mathematical model for the hybrid ECV will be developed and validated via heated plate experiments, to be integrated into PA-bioheat model. A parametric study is conducted at ambient conditions and outdoor activity levels to identify the ambient conditions in which the hybrid vest performance is acceptable. Evaluation

is based on the drop in local sensate skin temperature, and corresponding sensible and latent heat losses, compared to No-Vest case.

d) Conduction of human subject experiments on persons with PA for the optimized design of the PCM cooling vest derived from model predictions. The testing will be done inside a climatic chamber of moderate conditions to perform an arm-crank exercise of fixed mechanical load, while monitoring and recording the physiological (heart rate, core and skin temperatures) and psychological responses (thermal sensation and comfort votes, skin wettedness and perceived exertion) of the recruited subjects.

e) Conduction of human subject experiments on persons with PA for the use of commercially available ECV Type II to be compared with the experimental findings of PCM cooling vests at same metabolic rate and ambient conditions. The testing will be done inside a climatic chamber of moderate conditions to perform an arm-crank exercise of fixed mechanical load, while monitoring and recording the physiological (heart rate, core and skin temperatures) and psychological responses (thermal sensation and comfort votes, skin wettedness and perceived exertion) of the recruited subjects.

1.2. Problem Statement

The purpose of this study is to assess the performance of cooling vests and recommend means of enhancing these cooling methods for persons with SCI to maintain T_{cr} values below threshold of thermal strain during exercise. These means require critical

understanding of the pathophysiology of SCI to accurately predict core and skin temperatures as well as sensible and latent heat losses at the sensate/insensate skin of the trunk. More profoundly, the magnitude of thermoregulation impairment for each of the cervical and thoracic SCI should be accounted for.

Persons with TP differ in their severity of impairments after SCI because each cervical level is related to a specific cervical motor which controls certain part of the body and its functionality as shown in Table 1. Also, based on ASIA impairment scale shown in Table 2, tetraplegia might be complete or incomplete based on whether the motor or sensory function is preserved below the neurological level related to the spinal cord vertebrae (Kirshblum et al., 2011b; Maynard et al., 1997). Because persons with injury level of C5-C7 are able to perform certain mobility functions, to sit in balance independently and to use manual wheelchair compared to higher cervical SCI levels with no need to a ventilator to breathe, it was proposed in this work to implement their pathophysiology into the selected bioheat model of AB. The changes in physical and physiological parameters pertinent to TP of C5-C7 with complete or incomplete injury were extracted from literature to attain a TP-bioheat model.

Table 1. Cervical nerves and corresponding body parts

Motor Level	Body Part	Functional Significance
C1 C2 C3	Head and Neck Head and Neck Diaphragm	• **unable** to perform mat mobility (set of rehabilitation exercises for people with SCI applied on the mattress such as rolling and prone on elbow), transitional movements, and sitting balance independently • **need power wheelchair** with adaptive set up for driving/tilting • require assistance to breathe
C4	Upper Body Muscles	• **unable** to perform mat mobility, transitional movements, and sitting balance independently • **need power wheelchair** with adaptive set up for driving/tilting • don't require a ventilator to breathe

C5	Wrist Extensors	• **able** to perform mat mobility, transitional movements, and sitting balance independently in case of strong muscles, and need assistance in case of weak muscles
C6	Wrist Extensors	• **need manual wheelchair** with custom modifications • don't require a ventilator to breathe
C7	Triceps	• able to perform mat mobility, transitional movements, and sitting balance independently • need manual wheelchair with custom modifications

Table 2. ASIA Impairment Scale (Melo et al.)

Impairment Type	Impairment Level	Description
A	Complete	No sensory or motor function is preserved in the sacral segments S4-5
B	Sensory Incomplete	Sensory but not motor function is preserved below the neurological level and includes the sacral segments S4-5 (light touch or pin prick at S4-5 or deep anal pressure) AND no motor function is preserved more than three levels below the motor level on either side of the body
C	Motor Incomplete	Motor function is preserved at the most caudal sacral segments for voluntary anal contraction OR the patient meets the criteria for sensory incomplete status (sensory function preserved at the most caudal sacral segments (S4-S5) by LT, PP or DAP), and has some sparing of motor function more than three levels below the ipsilateral motor level on either side of the body. (This includes key or non-key muscle functions to determine motor incomplete status.) For AIS C – less than half of key muscle functions below the single NLI have a muscle grade ≥ 3
D	Motor Incomplete	Motor incomplete status as defined above, with at least half (half or more) of key muscle functions below the single NLI having a muscle grade ≥ 3
E	Normal	If sensation and motor function as tested with the ISNCSCI are graded as normal in all segments, and the patient had prior deficits, then the AIS grade is E. Someone without an initial SCI does not receive an AIS grade

Likewise, persons with PA impose diversity in sensory and motor impairment within the twelve thoracic (T1-T12) vertebrae injuries, and the severity of injury might also be complete or incomplete (refer to Table 2) (Kirshblum et al., 2011b; Maynard et al., 1997). Any patient having injury between T1-T5 has an impairment at the upper chest, mid back, and abdominal muscles; whereas, patient having injury between T6-T12 has an impairment only at the abdominal and back muscles (Kirshblum et al., 2011a; Sekhon and Fehlings, 2001). Consequently, because thoracic injury of (T6-T12) would not

restrict the individual to use manual wheelchair and maintain independent body balance in seated position, **it was of interest in this work to focus on this range of injury as these individuals are likely to engage in high activity levels such as Paralympics**. The attributed sensory and motor functions of this injury range was taken into consideration to develop a bioheat model adaptive to thermal physiology of persons with PA. The development of PA-bioheat model proceeded the validation of TP-bioheat model to which the physiological modifications of persons with PA were applied.

Numerous bioheat models were reported in literature that predict the AB thermal responses under various thermal conditions and were validated with experiments on AB human subjects. The complexity of these models varied between simple such as Pennes' model (1948), Stolwijk's model (1966), Wulff's model (1974), Klinger's model (1985), and multi-segmented and detailed models such as Mitchell's model (1968), Huizenga's model (2001), Tanabe's model (2002), Salloum et al. model (2007), Al-Othmani's model (2008), Fiala's model (2011), Karaki's model (2013), and Fu's model (2016) (Al-Othmani et al., 2008; Fiala et al., 2001; Fu, 1995; Huizenga et al., 2001; Karaki et al., 2013; Klinger, 1985; Mitchell and Myers, 1968; Pennes, 1948; Salloum et al., 2007; Stolwijk and Hardy, 1966; Tanabe et al., 2002; Wulff, 1974). Since physiological adaptations following SCI include changes in muscular, cardiovascular, and respiratory systems, TP- and PA- bioheat models should be based on an AB model capable of integrating these systems. The selected model should be at a level of detail that can predict the thermophysiological responses in persons with SCI at different conditions and activity levels.

For this work, Salloum et al. model (2007) was selected as it is an appropriate model to modify to be adaptive to the thermal physiology of persons with SCI (Salloum

et al., 2007). Salloum et al. (2007) multi-node multi-segment bioheat model can easily be altered since it was based on exact anatomical data of the human body circulatory system, and real dimensions and anatomic positions of the arteries in the body (Avolio, 1980). Their model used the heart rate as input and calculated blood perfusion in the core tissue based on the pulsating arterial system model, which permits the incorporation of the variations of CO and HR in person with SCI on the heat transfer between the internal organs and skin layer. The bioheat model of Salloum et al. (2007) that was later modified by Karaki et al. (2013) to include the fingers is adapted in this work to develop TP- and PA- bioheat models (Karaki et al., 2013). As presented in Fig. 1(a), the body is divided into 15 segments: head, chest, pelvis, upper back, lower back, upper arms, forearms, hands, thighs, calves, and feet in addition to the 10 finger segments added by Karaki et al. (2013). As presented in Fig. 1(b), each segment is composed of a core node, skin node, artery node, and vein node where the core node represents the muscular part of the segment or the internal organs. Each of the upper and lower parts of the trunk has four skin nodes to account for any non-uniformity present in the environment. Salloum et al. (2007) modeled the two main systems: controlled (passive) and controlling (active) systems. In the controlled system, heat transfer between the body and surrounding was simulated by means of heat balance equations for each of the nodes. The active system was stimulated by warm/cold body signals that activate four thermoregulatory responses: vasodilation, vasoconstriction, shivering and sweating. The active system controls the passive system to adjust the tissue temperature when the human body is in a state of thermal discomfort. Salloum et al. (2007) and Karaki et al. (2013) modeled the blood circulation in the arteries and veins, and blood perfusion to the skin using the nonlinear formulation of the Avolio multi-branched model of the human arterial system (Avolio,

1980) presented in Fig. 1(c). The details of the model are not provided here as they are detailed in the respective references.
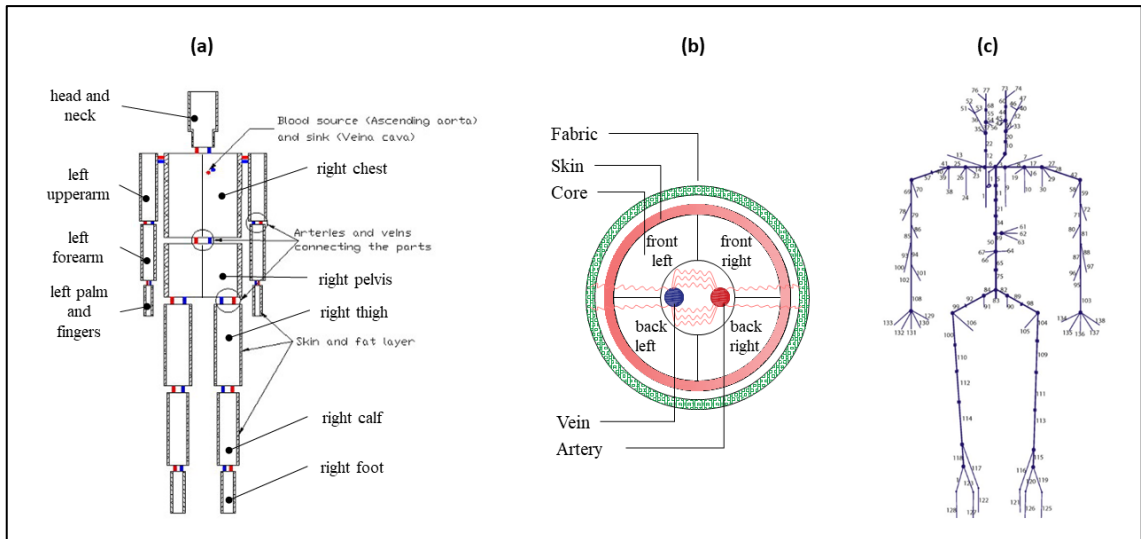
Figure 1. Schematic of (a) multi-segmental bioheat model (b) radial cross section of a body segment (c) human arterial tree used in Avolio model

Validation of TP- and PA- bioheat models was achieved via previous studies in literature that included human subject experiments for persons with SCI. The importance of having a valid robust bioheat is to be combined with cooling vests models to assess performance and recommend enhancement to the design of the vests. However, the integration of cooling vests models was only achieved using PA-bioheat model because persons with PA are more capable than persons with TP to be involved in outdoor activities and even extreme sports. In addition, persons with TP have impaired motor/sensory functions at the trunk which causes all its skin to be insensate. Whereas, persons with PA impose region of the trunk as sensate and region as insensate. This serves to answer the question about how magnitude of thermoregulation impairment affects the performance of cooling vest for a person with SCI especially that previous studies in

30

literature reported insignificant effect of cooling vests for persons with PA. Looking at the sensible and latent losses of the sensate and insensate skin of the trunk as shown in Fig. 2 will be useful to infer what region of the trunk should be targeted to ensure effective cooling of PCM cooling vests. Adding to the above, if a lightweight cooling vest is desired to be used, it is then important to assess hybrid ECV performance at range of ambient conditions in order to be recommended for persons with PA instead of heavier PCM cooling vest. Therefore, using modeling in this work brings a great insight as it can provides recommendations and suggestions to alleviate thermal strain in persons with SCI through critical understanding of their thermal physiology.
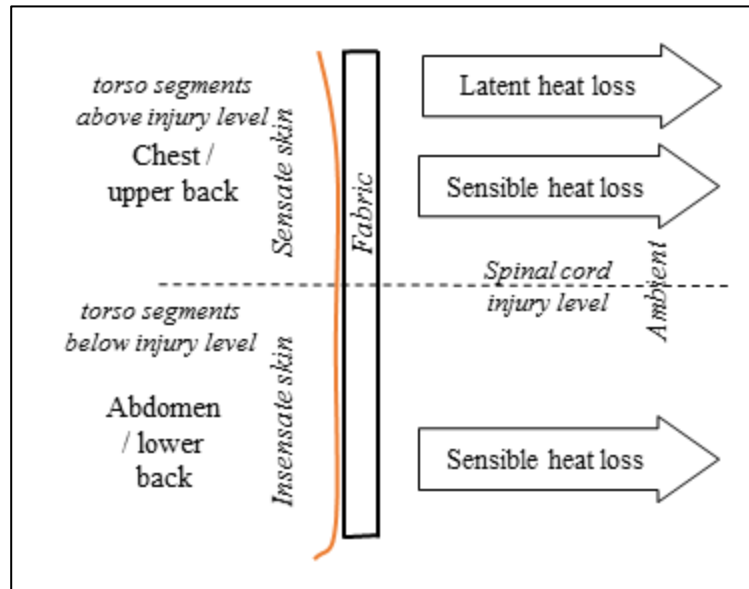
Figure 2. Schematic of sensate/insensate skin of trunk showing heat losses

Finally, by the findings of model predictions, human subject experiments were designed to test PCM cooling vests and ECVs for persons with PA. The aim of these experiments was to answer the question of how injury level affects performance of cooling vest for this vulnerable population. As previous studies in literature showed limitations in effectiveness of cooling vests, it was important to look at this problem by

the perspective of thermal physiology of persons with SCI (Armstrong et al., 1995; Trbovich et al., 2014; Bongers et al., 2016). That's why detailed categorization of participants of PA was considered in this work based on the portion of sensate and insensate skin of the trunk. This approach will be explained in detail in the coming section of "Human subject experiments".

CHAPTER 2

THEORETICAL RESEARCH METHODOLOGY

The development of bioheat model for person with SCI and integration of cooling methods were achieved through systematic approach as follows: i) extract data about physiological and thermoregulatory changes of the body in TP/PA compared to that of AB; ii) use extracted data to modify the published model of AB to be applicable for TP first, then altered to be adaptive to PA; and finally, iii) integrate published fabric-PCM model and newly developed hybrid ECV model to PA-bioheat model to assess the effectiveness of cooling on person with PA during exercise and heat exposure.

The alterations in the human body after cervical/thoracic SCI included: i) body composition as lean body mass (LBM) and skin fat thickness (SFT), ii) threshold temperatures of vasomotor, sudomotor and shivering, and, finally, iii) cardiovascular functions including arterial diameter (AD) and CO. These alterations were incorporated in the AB-bioheat model to predict overall and segmental skin and core temperatures for person with TP/PA at different climate conditions and activity levels. In addition, segmental heat losses have been predicted for sensate/insensate skin of the trunk.

Bioheat models and combined bioheat models with cooling vest models were validated via previous studies in literature or heated plate experiments and used to perform parametric study. For PCM cooling vest, the parametric study was done to address the significance of melting temperature and coverage area of trunk on performance of vest on person with PA. For hybrid ECV, the parametric study was done to address the ambient conditions at which ECV can be effective for a person with PA at moderate and high activity levels. According to the model predictions, human subject

experiments on persons with PA were performed. The following subsections describe the modelling features and experimenting details.

2.1. TP-bioheat model development

Changes in the physical and physiological parameters pertinent to TP of C5-C7 with complete or incomplete injury, derived from the experimental data on the physiology, anatomy, and thermal characteristics published in literature, are implemented in Salloum et al. model (2007) (Mneimneh et al., 2019c). Differences in anatomy, physiology, and thermoregulatory functions between persons with TP and AB can be organized by the following observed categories:

1) Energy expenditure: Basal metabolic rate (BMR) is lesser in persons with TP compared to AB due to drop in LBM after SCI (Chun et al., 2017; Spungen et al., 2003a; Yilmaz et al., 2007);

2) Body temperature regulation: In the absence of sudomotor, vasomotor and shivering responses, persons with TP are unable to maintain thermal neutral core and skin temperatures independent of the ambient conditions. Whereas, AB impose neutral thermal state even under extreme ambient conditions (Attia and Engel, 1983; Downey et al., 1992; Khan et al., 2007; Petrofsky, 1992);

3) Threshold value of core temperature of the vasomotor, sudomotor and shivering responses: After SCI, the thermal sensation of a large area of the body skin is lost. Thus, this loss limits the ability of the hypothalamus in the autonomic nervous system to interpret the external thermal changes in the surrounding and take on the necessary thermoregulatory responses.

34

Consequently, drifts in threshold values of vasomotor, sudomotor and shivering responses were observed as reported in literature due to the delay detection of heat imbalance in the body (Attia and Engel, 1983; Downey et al., 1992; Khan et al., 2007; Petrofsky, 1992);

4) Thermoregulatory responses: vasodilatation and sweating are disrupted in persons with TP. This causes an increase in body heat and rise of core temperature above its neutral state when exposed to hot ambient conditions with or without physical activity. Also, vasoconstriction and shivering are interrupted in persons with TP; thus, decrease in body heat and drop of core temperature occur when exposed to cold ambient conditions (Griggs et al., 2017; Petrofsky, 1992);

5) Circulatory system: CO and skin perfusion are diminished in persons with TP compared to AB due to modifications in arterial blood vessels' structure after SCI (de Groot et al., 2006; de Groot, 2005; Takahashi et al., 2004; Thijssen et al., 2012);

6) Skin blood perfusion: No blood fluctuations in the insensate skin are observed for the peripheral limbs because of disconnection of the adrenergic neurons from brain integration. This may mimic denervation and lead to abnormal vascular responses in the insensate skin (Hogancamp II, 2004).

Accordingly, the structural properties of the human body including those of LBM and Fat mass (FM), arterial blood vessels' structure, BMR, and skin perfusion flow of impaired segments will be modified; then, a shift in core temperature threshold ($T_{cr\_threshold}$) values of the thermoregulatory responses will be specified based on observations reported in literature. Finally, changes in control equations will be adapted

35

to reflect the vasomotor, sudomotor and shivering responses in persons with TP for active non-impaired segments.

2.1.1. *Energy Expenditure*

People with TP are susceptible to lean mass degeneration and fat gain after a minimum duration of one year after SCI. The alteration in body composition is justified by the physical inactivity of impaired limbs below level of injury and the severity of injury. However, if being committed to certain electrically simulated exercise such as arm-crank ergometer to assist in the performance of functional movements of the upper extremities, LBM would be improved and FM would be reduced as reported in literature (Hjeltnes et al., 1997; Singh et al., 2014).

For non-athletic persons with TP, the number of calories burned per day will be less compared to that AB when the person is seated at rest. To rephrase, sedentary energy expenditure defined as basal metabolic rate (BMR) is lesser in persons with TP than AB. In case of incomplete cervical spinal cord injury, the changes in LBM and FM are less than those of complete TP but insignificant since the preserved motor function of the upper arms and forearms in person with incomplete TP are useless with only slight difference in number of calories burnt per day between persons with complete and incomplete TP (Gorgey and Dudley, 2007; Spungen et al., 2003a). Adding to this, advancing in age and duration of injury has direct effect on body composition of person with TP accounting mainly for the arms and the trunk muscle and fat mass (Spungen et al., 2003a). Further decrement in LBM and FM are expected with aging and prolonged duration of injury if not being committed to certain physical activity.

The percentage of LBM reduction in each limb in the body of person with TP is multiplied by the initial values of the core BMR implemented in Salloum et al. model (2007). All impaired segments below level of injury have reduced metabolic rate compared to that of AB except for the head (Salloum et al., 2007; Spungen et al., 2003a). For the skin node, the current model uses the same skin metabolic rate of AB. Therefore, the sum of core metabolic rate and skin metabolic rate for each segment gives the total BMR for each segment (head, neck, arms…) in persons with TP as presented in **Table 3**. The segmental BMR_{AB} derived from Salloum et al. model is shown in the 2nd-4th columns; the segmental percentage of LBM reduction ($\frac{LBM_{TP}}{LBM_{AB}}$) extracted from Spungen et al. (2003) is shown in the 5th column, and finally the new segmental BMR_{TP} is shown in the last three columns of **Table 3**. Using Eq. (1), $BMR_{TP,core}$ is calculated by multiplying $BMR_{AB,core}$ by percentage of reduction in LBM in TP ($\frac{LBM_{TP}}{LBM_{AB}}$) while keeping BMR_{skin} same as that of AB. Then, the total segmental BMR for both AB and person with TP is obtained and the overall body BMR for both AB and person with TP is verified by reported data in literature (Chun et al., 2017; Yilmaz et al., 2007). The derived values of segmental *BMR* are adapted in the current model for cervical SCI (C5-C7) with all level of severity of impairment (A-D).

$$BMR_{TP,core} = BMR_{AB,core} \times \frac{LBM_{TP}}{LBM_{AB}} \tag{1}$$

The physical activity of the body obliges the individual to burn more calories than when seated at rest. For this reason, the defined core and skin basal metabolic rates are multiplied by metabolic index, a factor in "MET" to calculate the accurate rate of calories burnt by person with TP. This factor ranges between 1.2 ~ 6.6. However, it was reported in literature that the significance of metabolic index of person with TP is different than

of AB given that the daily activities and intensity of sports vary between the two groups (Collins et al., 2010). Therefore, the metabolic index implemented in current model is actually related to person with TP daily life activities.

Table 3. Segmental core, skin and total basal metabolic rate in Watt for AB and TP

Segment in the body	Able-bodied person (Salloum et al., 2007)			Lean Body Mass	Tetraplegia (C5-C7) & (A-D)		
	Core Metabolic Rate (W)	Skin Metabolic Rate (W)	Total BMR per segment = (core + skin) BMR (W)	Percentage of Reduction in TP compared to AB (Spungen et al., 2003)	Core Metabolic Rate (W)	Skin Metabolic Rate (W)	Total BMR per segment = (core + skin) BMR (W)
Head	18.43	0.22	18.65	0%	18.43	0.22	18.65
Chest	5.95	0.60	6.55	10%	5.36	0.60	5.96
Pelvis	46.86	0.60	47.46	10%	42.17	0.60	42.77
Left/Right upper arm	1.06	0.18	1.24	32%	0.72	0.18	0.90
Left/Right forearm	0.59	0.10	0.69	32%	0.40	0.10	0.50
Left/Right hand	0.10	0.09	0.19	32%	0.06	0.09	0.16
Left/Right thigh	1.70	0.34	2.04	39%	1.04	0.34	1.38
Left/Right calf	0.75	0.15	0.90	39%	0.46	0.15	0.61
Left/Right foot	0.14	0.12	0.26	39%	0.09	0.12	0.21
Total BMR (W)	**79.91**	**3.39**	**83.30**	-	**71.49**	**3.39**	**74.88**
Total BMR values reported in Literature							
Yilmaz, 2007	-	-	**71.54 ±19.30**	-	-	-	**55.0±15.0**
Chun et al., 2017	-	-	**80.65 ±10.0**	-	-	-	**62 ± 15.0**

Although fat gain in person with TP has no effect on the skin BMR, it does affect the thermal conductivity of the fat-skin layer, and eventually the conduction heat transfer between the skin and the core in person with TP. The increased fat thickness increases the thermal resistance of the skin-fat layer and reduces heat loss from the core (internal organs) to the skin (surrounding). Therefore, in hot ambient conditions, the human body stores the thermal energy causing an increase in the core temperature because heat release to the environment is reduced, while the skin temperature becomes closer to the ambient conditions. As reported in literature, the head and neck segments conserve their FM; whereas, for the trunk segment, FM is increased by 24%; for the arms and hands, FM is

incremented by 94%; and finally, for the legs and feet, FM is increased by 39% (Spungen et al., 2003a). Based on the below equations of total thermal conductivity, the fat thickness presented in **Table 4** is used to calculate the thermal conductivity of the fat-skin layer, whereas the muscle thermal conductivity is dependent on the area of the skin only:

$$\frac{1}{K} = \frac{1}{K_{muscle}} + \frac{1}{K_{fat-skin}} \tag{2a}$$

$$K_{muscle} = \frac{A_{skin}}{0.05} \tag{2b}$$

$$K_{fat-skin} = \frac{A_{skin}}{0.0048(th_{fat+skin}-2)+0.0044} \tag{2c}$$

where K is the skin to core conductance calculated from the two conductance of the skin-fat and the muscle, K_{muscle} is the muscle conductance, $K_{fat-skin}$ is the fat and skin layer conductance, A_{skin} is the area of skin layer, and $th_{fat+skin}$ is the thickness of fat and skin layers.

Table 4. SFT in AB and TP and percentage of reduction

Body element	AB	TP	Fat Mass
	Fat and skin thickness (mm)	Fat and skin thickness (mm)	Percentage of Fat Body Mass in TP compared to AB
Head + Neck	8.50	8.50	100%
Chest	19.12	23.61	124%
Pelvis	19.12	23.71	124%
Left/Right upper arm	4.51	8.75	194%
Left/Right forearm	4.51	8.75	194%
Left/Right hand	7.40	14.36	194%
Left/Right thigh	10.64	14.79	139%
Left/Right calf	10.64	14.79	139%
Left/Right foot	11.70	16.26	139%

2.1.2. Variability of body core temperature after SCI:

It was clearly reported in literature that people with SCI have stable core temperature similar to that of AB ($36.8 \pm 0.2°C$) in a limited range of ambient conditions (22-25 °C and 45-50% RH) and at sedentary physical activity (Attia and Engel, 1983; Downey et al., 1992). When exposed to ambient condition greater than 25 °C for a prolonged duration, core temperature rises above 36.8 °C and remains high in the absence of vasodilatation and sweating responses for the impaired segments below injury level. Similarly, when exposed to cold ambient conditions (less than 22 °C) for prolonged duration, core temperature drops below 36.8 °C and remains low in the absence of vasoconstriction and shivering responses for the impaired segments below injury level for a low clothing resistance criterion. Therefore, unlike AB, persons with TP lose the ability to regulate T_{cr} within a steady state value in hot and cold ambient conditions (Pledger, 1962). Instead, persons with TP body undergoes a range of thermal states obtained based on the heat balance of the body with its environment when the environmental ambient conditions vary. This dysfunction in temperature regulation can be explained by the absence of thermal sensation between the brain and surrounding conditions over large areas of the skin (Finnerup et al., 2003). Accordingly, limited vasomotor, sudomotor and shivering responses for the active segments above level of injury are observed in the head and neck in case of complete injury in addition to forearms and upper arms in case of incomplete injury. That's why persons with TP are more prone to the heat strain and thermal discomfort problems in hot and cold outdoor conditions (Lehmann et al., 1987).

It was also reported in literature that the threshold values of sweating and shivering were shifted for the active segments above level of injury due to the reduced

thermal sensation of skin area to the thermal changes in the surrounding (Downey et al., 1992; Petrofsky, 1992). Moreover, the vasomotor responses of these segments above injury level showed a drift in the threshold set point (Attia and Engel, 1983). Vasodilation starts to occur when T_{cr} rises above 36.8 °C (SD 0.575 °C), while vasoconstriction starts to happen when T_{cr} drops below 36.8 °C (SD 0.9 °C). This change in threshold set points can be explained by the irregular thermal physiological responses in persons with TP that changes the body heat balance and its ability to respond when the ambient condition varies. Thus, the body attains a new thermal steady state of core temperature.

Based on the observations in literature of the thermal steady state of core temperature and body heat balance of persons with TP in the absence of normal thermoregulatory functions, **Table 5** represents the altered threshold values of T_{cr} for controlling vasomotor, sudomotor and shivering responses in persons with TP. The basal thermal neutral state of persons with TP was set at 36.8 °C same as that of AB, but with standard deviation ±0.9°C as reported in literature (Attia and Engel, 1983). Moreover, the threshold set points of start of shivering and sweating showed different values than that of AB. These threshold values of T_{cr} in the current model are assigned for the active segments above injury level: head, neck and possibly forearms and upper arms; and they are implemented in the control equations of the current model as will be demonstrated in the next sections.

Table 5. List of thermoregulatory threshold parameters for persons with TP compared to AB

Thermoregulatory Action	Threshold Control Parameter	Person with TP	AB
Start of Sweating	T_{cr}	38.2 ± 0.6 °C (Petrofsky, 1992)	37.2 °C (Salloum et al., 2007)
Basal Thermal Condition	T_{cr}	36.8 ± 0.9 °C (Attia and Engel, 1983)	36.8 °C (Salloum et al., 2007)

Start of Shivering	T_{cr}	35.6 ± 0.6 °C (Downey et al., 1992)	35.8 °C (Salloum et al., 2007)
	T_{sk}	-	35.5 °C (Salloum et al., 2007)
Maximum Shivering	T_{cr}	35.0 °C (Khan et al., 2007)	33.0 °C (Salloum et al., 2007)

2.1.3. Changes in circulatory system after cervical spinal cord injury

2.1.3.1. The cardiac output and heart rate

Following SCI, the arterial blood vessels are subjected to changes in their structure, mainly for the impaired ones below level of injury. For this reason, all the arteries have modified dimensions based on the percentage of reduction in the structure except those of the head in case of complete tetraplegia or except those of the head, upper arms and forearms in case of incomplete tetraplegia. The AB values of blood vessels' radii are taken from Avolio arterial tree (Avolio, 1980) as implemented in Salloum et al. model (2007) for AB. As reported in literature on complete TP, all arteries located within the head segment conserve their width since they are above level of injury; whereas, those located in the neck and shoulder segments are lessen to 16% in diameter and for the remaining arteries located in the limbs (arms, legs, hands and feet) are decremented by 50% since located below level of injury (de Groot et al., 2006; de Groot, 2005; Thijssen et al., 2012). Subsequently, the segmental CO will be the same for the head; while reduced by 30% and 60% for the neck and shoulders, and for the limbs respectively. As for incomplete TP, the arteries located within the forearms and upper arms conserve their diameter and wall thickness same as the head; while the remaining arteries distributed in the body change in structure (de Groot et al., 2006; de Groot, 2005; Thijssen et al., 2012).

Consequently, CO for the forearms and upper arms will remain unchanged same as that of the head.

Concerning the vein dimensions, it is considered that the radius of the vein is almost twice the radius of the artery having the same index (Salloum et al., 2007). The effect of alteration in structure of arterial blood vessels is observed at the level of CO. Therefore, the total resulting CO is reduced in person with TP whether with complete or incomplete injury compared to that of AB when exposed to the same ambient conditions and level of physical activity (Takahashi et al., 2004).

In general, the overall CO value is dependent on the body core temperature. Hence the three values of CO, defined as basal (CO_{basal}), minimum (CO_{con}) and maximum (CO_{dil}), are calculated by applying the percentage of reduction in the arterial blood vessels' radii on the CO values reported by Salloum et al. (2007) of AB for each segment as shown in **Table 6**.

Table 6. Modification in basal, minimum, and maximum CO values obtained from Salloum et al. model

	Basal (cm³/hr.)		Maximum (cm³/hr.)		Minimum (cm³/hr.)	
Body Part	AB	TP	AB	TP	AB	TP
Head	55119	55119	63408	63408	53910	53910
Neck	1407	1083	3620	3296	1084	760
Trunk	198,164	141,890	247,650	191,376	190,947	134,673
Right or Left Upper Arm	3852	1619	11261	1619	2772	1619
Right or Left Thigh	6196	2607	17193	2607	4592	2607
Right or Left Forearm	2151	904	7196	904	1415	904
Right or Left Calf	2741	1159	10344	1159	1632	1159
Right or Left Hand	1378	1179	4718	1179	891	1179
Right or Left Foot	1339	1035	5683	1035	706	1035
Total CO (cm³/hr)	290,005	**215,100**	427,468	**275,086**	269,957	**206,349**
Total CO (cm³/hr.) for TP reported in Literature						

| De Groot (2006) | - | 222,600 ± 46,800 | - | - | - | - |
| Takahashi et al. (2004) | - | - | - | 306,000 ± 30000 | - | - |

Since the level of injury and its severity affect the degree of reduction of CO in person with TP, average values of CO_{basal}, CO_{con} and CO_{dil} are implemented in the current model as follows:

$$CO_{con} = \quad 206,351.0 \qquad cm^3/hr. \tag{3a}$$

$$CO_{dil} = \quad 299,250.0 \qquad cm^3/hr. \tag{3b}$$

$$CO_{basal} = 229,000.0 \qquad cm^3/hr. \tag{3c}$$

The overall CO in the human body at a certain average core temperature is calculated using **Eq. (4a)**. It is dependent on the values of CO_{basal}, CO_{con} and CO_{dil}. In the case of vasodilation, threshold value of mean core temperature ($T_{cr,thershold}$), presented in **Table 5** as the basal thermal condition, is the control temperature for calculating the maximum dilatation value of CO using **Eq. (4b)** (Attia and Engel, 1983; Petrofsky, 1992). In the case of vasoconstriction, and distinct from Salloum et al. model (2007), CO in person with TP is now controlled by T_{cr} only and calculated using **Eq. (4c).** Since T_{sk} in person with TP doesn't trigger any vasomotor, sudomotor or shivering responses, core temperature may rise or fall due to disruption in skin sensory feedback of the body limbs and trunk to the brain (hypothalamus). Therefore, in case of vasoconstriction, the threshold value of T_{cr}, presented in **Table 5** as the basal thermal condition, is assumed to override that of T_{sk}, whose threshold value in Salloum et al. model (2007) ranged between 10.7 °C and 33.7 °C. This is adapted for levels of cervical spinal cord injury (C5-C7) and at different impairment severity (A-D) because as shown in **Table 1** the connectivity

between the brain and body parts is interrupted, deactivating the sensory cells at the skin of upper body and lower body muscles.

$$CO = \frac{CO_{dil} \times CO_{con}}{CO_{basal}} \tag{4a}$$

$$CO_{dil} =$$

$$\begin{cases} CO_{basal} & for \ T_{cr} \leq T_{cr\_threshold} \ {}^{\circ}C \\ \frac{T_{cr}-T_{cr\_threshold}}{38.2-T_{cr\_threshold}}(CO_{max}-CO_{basal})+CO_{basal} & for \ T_{cr\_threshold}{}^{\circ}C \ < T_{cr} < 38.2 \ {}^{\circ}C \\ CO_{max} & for \ T_{cr} \geq 38.2 \ {}^{\circ}C \end{cases}$$

(4b)

$$CO_{con} =$$

$$\begin{cases} CO_{min} & for \ T_{cr} \leq 35.6 \ {}^{\circ}C \\ \frac{T_{cr}-35.6}{T_{cr\_threshold}-35.6}(CO_{basal}-CO_{min})+CO_{min} & for \ 35.6 \ {}^{\circ}C \ < T_{cr} < T_{cr\_threshold} \ {}^{\circ}C \\ CO_{basal} & for \ T_{cr} \geq T_{cr\_threshold} \ {}^{\circ}C \end{cases}$$

(4c)

Then, the obtained value of CO is used to calculate the artery radii of the head for the complete tetraplegia or for the forearms, upper arms and the head for the incomplete tetraplegia since the arteries in these segments undergo vasodilatation or vasoconstriction unlike the remaining branches whose radius remain constant throughout the whole heart beat cycle. The equation of arterial radius was used in Karaki's Bioheat model as follows for the head artery (Karaki et al., 2013):

$$R_a =$$

$$\sqrt{((R^2a,\max - R^2a,\min) * (CO - 206351)/(299250 - 206351) + R^2a,\min)} \tag{5}$$

Where: R_a is the radius of artery in mm, $R_{a,max}$ is the maximum arterial radius of vasodilatation in mm, and $R_{a,min}$ is the minimum arterial radius of vasoconstriction in mm.

Adding to the above, the CO is controlled by the sympathetic nervous system to compensate for the change in metabolic rate in the body when the individual is at different levels of activity (Collins et al., 2010). After SCI, the sympathetic signals are disrupted leading to a constant SV, while HR will vary based on CO demand in the body as per the metabolic rate variations (Teasell et al., 2000). Driven by the variation in heart rate, the maximum value obtained of CO is actually function of increase in HR; while SV remains stable in person with TP. The consequence of this dysfunction in regulating CO upon increase in oxygen demand is the higher rate of change in HR compared to that of AB at same level of activity and ambient condition. This necessitates the modification of the HR equation **(Eq. 6a)** used in Salloum et al. (2007) model to result in acceptable HR values for TP when simulating the case study (ASHRAE, 2001). TP corrected HR equation is given by **Eq. 6b** in beat/minute:

$$HR_{AB} = 3.4(0.0476M_{total} - 7) + 75 \qquad (6a)$$

$$HR_{TP} = 3.4(0.0476M_{total} - 7) + 90 \qquad (6b)$$

M_{total} is the total metabolic rate of the human body defined as summation of the basal metabolic rate and the shivering rate.

2.1.3.2.   Skin blood perfusion

In healthy AB, blood perfuse between the core node and the skin node at basal rate when the body temperature is within its thermal neutral state. When the core temperature rises above its thermal neutral level, skin blood perfusion increases in all body parts including head, trunk and limbs to release stored heat from the body and retain core temperature back to its thermal neutral level. Similarly, when the core temperature falls below its thermal neutral level, skin blood perfusion decreases to restrict heat release from the body and manage to keep core temperature within its thermal neutral state. This

changeability in skin blood perfusion is accomplished by the effect of dilatation and constriction in blood arterial radii in each segment in the body. However, the variability of blood arterial radii, due to vasodilatation effect under high core temperature or vasoconstriction effect under low core temperature, is not anymore observed in person with TP for the impaired body segments except above level of injury. Consequently, skin perfusion will not be affected by ambient conditions whether cold or hot; it will remain constant in persons with TP. Therefore, blood flow will not increase from the organs to the peripheral; thus, heat strain will be triggered and rise in core temperature will be observed in hot ambient conditions (Theisen and Vanlandewijck, 2002). In addition, when exposed to cold temperatures, the transfer of blood from the periphery to the central organs is prevented; thus, heat will be lost from the body and core temperature will be lower compared to that of AB under the same cold ambient conditions with or without physical activity. Therefore, blood skin perfusion maintains a constant rate at the skin node for the impaired segments below level of SCI.

To calculate the skin perfusion in each segment above level of injury, it is essential to find the value of basal ($\dot{m}_{skin,basal}$), minimum ($\dot{m}_{skin,min}$) and maximum ($\dot{m}_{skin,max}$) skin blood flow rates for this segment based on the mean core temperature of the body. The skin perfusion in each segment is given by:

$$\dot{m}_{skin} = \frac{\dot{m}_{skin,dil} \cdot \dot{m}_{skin,con}}{\dot{m}_{skin,-basal}} \tag{7a}$$

First at a given ambient condition, the mean core temperature of the body, calculated from the segmental core temperatures based on the thermal weighting of each segment, was compared to a threshold value that represented the thermal basal steady state of person with TP (**Table 5**). Then, the maximum vasodilatation of the skin

perfusion was calculated using **Eq. (7b)**, and the maximum vasoconstriction of skin

perfusion was calculated **using Eq. (7c)** as follows:

$\dot{m}_{skin,dil} =$

$$
\begin{cases}
\dot{m}_{skin-basal} & for \ T_{cr} \leq T_{cr\_threshold} °C \\
\frac{T_{cr}-T_{cr\_threshold}}{38.2-T_{cr\_threshold}} \left(\dot{m}_{skin,max} - \dot{m}_{skin-basal} \right) + \dot{m}_{skin-basal} & for \ T_{cr\_threshold} °C < T_{cr} < 38.2 °C \\
\dot{m}_{skin,max} & for \ T_{cr} \geq 38.2 °C
\end{cases}
$$

(7b)

$\dot{m}_{skin,con} =$

$$
\begin{cases}
\dot{m}_{skin,min} & for \ T_{cr} \leq 35.6 °C \\
\frac{T_{cr}-35.6}{T_{cr\_threshold}-35.6} \left(\dot{m}_{skin-basal} - \dot{m}_{skin,min} \right) + \dot{m}_{skin,min} & for \ 35.6 °C < T_{cr} < T_{cr\_threshold} °C \\
\dot{m}_{skin-basal} & for \ T_{cr} \geq T_{cr\_threshold} °C
\end{cases}
$$

(7c)

The difference between the skin perfusion correlations used in AB bioheat model

and those used in the current model (**Eq. 6(b-c)**) is the threshold value that control these

correlations. In Salloum et al. model, the vasodilation skin blood flow was dependent on

core temperature and vasoconstriction skin blood flow was dependent on skin

temperature; whereas, in the TP-bioheat model, the average body core temperature

overrides the skin temperature values to control the skin perfusion. Values of $\dot{m}_{skin,basal}$,

$\dot{m}_{skin,max}$ and $\dot{m}_{skin,min}$ were calculated starting from those used in Salloum et al.

model and multiplied by two skin blood perfusion ratios in TP compared to AB: one for

the upper body ($SBPR_{UB} = SBP_{TP}/SBP_{AB}$) and other for the lower body ($SBPR_{LB} = $

SBP_{TP}/SBP_{AB}), as reported in literature (Hogancamp II, 2004). The ratio for the upper

body is **0.355** for the arms and trunk, and the lower body ratio is **0.29** for the legs in case

of complete tetraplegia; otherwise the values of blood skin perfusion are multiplied by

0.355 for the trunk and palms only excluding the forearms and upper arms, and by 0.29

for the legs in case of incomplete tetraplegia (Hogancamp II, 2004). In both cases, the head segment preserves its values of skin perfusion. The basal, maximum and minimum values of the skin blood perfusion are summarized in **Table 7**. It is clear that in person with TP, all segments except those above level of injury and based severity of impairment have the same value of skin perfusion. This indicates no fluctuation in skin blood flow is assumed in person with TP model whether the average core temperature is high or low because in reality the vasodilatation and vasoconstriction responses are disrupted in the impaired limbs below level of injury as a result of sympathetic decentralization (Guttman, 1958). Other than that, due to the alterations in blood vessels structure after SCI and the changes in LBM, the skin perfusion values were noticed lesser in persons with TP compared to those of AB (Muraki et al., 1996). This surely will affect the heat transfer between the core and the skin nodes under different ambient conditions as mentioned earlier.

Table 7. Basal, minimum, and maximum segmental skin blood perfusion rate (cm³/hr.) for TP and AB (C: complete and I: incomplete)

Body Part	Basal			Minimum			Maximum		
	AB	TP		AB	TP		AB	TP	
		C	I		C	I		C	I
Finger	28	10	10	10	10	10	80	10	10
Palm	418	148	148	215	148	148	1727	148	148
Forearm	508	180	508	0	180	0	5553	180	5553
Upper arm	910	323	910	0	323	0	8319	323	8319
Foot	934	271	271	266	271	271	5278	271	271
Calf	651	189	189	0	189	189	8253	189	189
Thigh	1456	422	422	0	422	422	12453	422	422
Head	6050	6050	6050	1206	1206	1206	16552	16552	16552
Lower Chest	2273	659	659	0	659	659	21953	659	659
Lower Back	2273	659	659	0	659	659	21953	659	659
Upper Chest	3442	1222	1222	0	1222	1222	33246	1222	1222
Upper Back	3442	1222	1222	0	1222	1222	33246	1222	1222

2.1.4. *Control equations: vasomotor, sudomotor and shivering*

The vasomotor response is defined as the vasodilatation of blood vessels when body core temperature rises above its thermal neutral condition indicating a need to release heat stored in the body to the external surroundings at the level of skin. In addition, it is defined as the vasoconstriction of blood vessels when body core temperature drops below its thermal neutral condition indicating a need to restrict heat release from the body to the surrounding. Vasomotor response is controlled by the skin temperature as long as the sensory receptors at the skin layer are activated in AB. However, after SCI, the human body loses its thermal sensation as a result of decentralization of SNS (Ho and Freed, 1991). The skin temperature is affected by the environmental condition whether hot or cold; whereas, the core temperature is affected by the internal body heat generation due to metabolism and convective heat transfer of heat as result of blood circulation in the body. Therefore, heat exchange between the core and skin layers is minimized as a result of absence of vasomotor response. This physiology is implemented in TP-bioheat model by setting reduced constant value of arterial blood vessels radii and blood skin perfusion for impaired segments below level of injury as elaborated in earlier.

For the sudomotor response, it is mainly the production of sweat at the skin level when the skin temperature is above its threshold and also the core temperature is above its thermal neutral value. This is the case of AB. However, the cervical SCI leads to disruption in triggering the sweat glands at the level of insensate skin for impaired limbs below level of injury; thus, preventing the body from losing heat by vaporization of sweat. Referring to the level of the SCI, persons with incomplete TP can sweat at the forehead area with small rate of secretion compared to AB; whereas, people with complete

50

tetraplegia may show no sweating at all. To implement this phenomenon in the current model, the sweating weighting factor is actually limited to the head neglecting other segments and set to be equal to one. Therefore, when simulating a case study in hot ambient conditions, sweat rates obtained are related to the head segment only in persons with TP using the equations originally obtained from Salloum et al. model (2007) and are modified to be suitable for the current model as follows:

$$T_{sweat} =$$

$$\begin{cases} 42.084 - 0.15833 \times T_{cr} & for \ T_{cr} < 38.2°C \\ 38.2°C & for \ T_{cr} \geq 38.2°C \end{cases}$$

(8a)

$$m_{sweat} = \frac{0.265 \times (45.8 + 739.4 \times (T_{cr} - T_{sweat})}{3600} \qquad for \ T_{cr} > T_{sweat}$$

(8b)

The coefficient 0.265 is derived from literature, and it's used in the original sweating equation of Salloum's et al. model (2007) (Griggs et al., 2017; Petrofsky, 1992). Now, the obtained value of sweat mass flow rate is expected to be less in persons with TP compared to that of AB. Also, in the current model, in **Eq. (8a),** the threshold of core temperature overrides that of skin temperature, which was taken at 33.0 °C to calculate *T_sweat* in Salloum et al. model (2007). The reason for that is that the sudomotor response is actually triggered based on the body core temperature, rather than its skin temperature due to denervation after SCI.

Similar consideration will be implemented for the shivering response in person with TP. It is known that shivering is an involuntary response in human body when the core temperature falls below its thermal neutral value. In person with TP, shivering

response is limited only to the segments above level of injury, mainly the head. Therefore, all segments below level of injury will have a weighting factor of shivering equal to zero.

To calculate the shivering rate in TP, **Eq. 9(a-c)** are used to calculate the threshold of shivering temperature and the shivering rate at a certain body core temperature. Distinct from the correlations used in from Salloum et al. model (2007), the threshold value of the core temperature triggers the shivering response, and T_{cr} replaces T_{sk} in the equations as follows:

$$T_{shver} =$$

$$\begin{cases} -1.0222 \times 10^4 + 570.97 \times T_{cr} - 7.9455 \times T_{cr}^2 & for \ 35.6^{\circ} \ C \ < T_{cr} \ < T_{cr,threshold} \\ \qquad 35.0^{\circ} \ C & for \ \ T_{cr} \ \leq 35.6^{\circ} \ C \end{cases}$$

(9a)

$$M_{shiv,max} = \frac{-1.1861 \times 10^9 + 6.552 \times 10^7 \times T_{cr} - 9.0418 \times 10^5 \times T_{cr}^2)}{3600} \quad for \ T_{cr} \ < T_{cr,threshold}$$

(9b)

$$M_{shiv} = M_{shiv,max} \times (1 - \frac{T_{sk} - 20}{T_{shiver} - 20} \ ) \quad for \ (40 - T_{shiver}) \ < T_{sk} \ < T_{shiver}$$

(9c)

Using **Eq. (9a)**, the shivering temperature is calculated based on T_{cr}. The threshold value of T_{cr} at which shivering expected to occur in a person with TP is obtained from literature and supposed to be equal to 35.0 ℃ for $T_{cr} \geq 35.6$ ℃ (Downey et al., 1992). But when T_{cr} is between 35.6 ℃ and $T_{cr,threshold}$, the shivering threshold will decrease with the changes in T_{cr}. Then, the maximum shivering intensity of the body expected to occur for the segment above level of injury is calculated based on T_{cr} using **Eq. (9b)**. However, the actual shivering rate is calculated based on the skin temperature, shivering temperature and maximum rate of shivering as shown in **Eq. (9c)**. So, the

obtained value (in Watts) is the metabolic rate of the body when shivering occurs in case of cold ambient conditions.

2.2. PA-bioheat model development

The physical and physiological changes in the body after SCI at thoracic vertebrae were related to the anatomy, physiology, and thermoregulatory functions of persons with PA compared to that of AB. These changes were applied for the impaired body segments including **feet, calves, thighs, lower back and abdomen** because as mentioned previously this model applies for PA with thoracic injury above T5 (T6-T12) (Sekhon and Fehlings, 2001). The sensory active body segments including head, neck, upper back, chest, upper arms, forearms, palms, and fingers maintain similar characteristics and thermoregulatory functions as that of AB. These specifications about SCI and its severity were taken into consideration for the development of the bioheat model for persons with PA.

Impaired body segments lose muscular mass and gain fat leading to reduction in EE. Although there is increase in fat mass, the active segments above injury level have an increase in muscular mass mainly for the arms because of their extra usage for Mat mobility (*ability to change position independently in supine position*) and wheelchair movement (*ability to balance seating position*); thus, causing an increment in EE (Spungen et al., 2003a). Moreover, the impact of SCI on blood vessels structure is observed by the decrement in AD for impaired segments below injury level which increases with injury duration (de Groot, 2005). Whereas, AD increases for segments above injury level due to increased muscular use. Therefore, the model assumes that arterial blood flow is reduced for the segments below injury level and increased for those

above injury level. Adding to the above, the thermoregulatory responses which include vasomotor (vasodilation and vasoconstriction), sudomotor (sweating) and shivering are also affected after SCI in persons with PA; they are totally disrupted for segments especially for an injury located at or below T10; while they remain activated for segments above this injury level. This means that *SBP* and blood flow rates are constant for the lower body including feet, calves, thighs, abdomen and lower back; also, no perspiration or shivering are observed at these segments (Cooper et al., 1957). Following the approach reported in section of TP-bioheat model development, the detailed quantitative and qualitative changes for the body segments below injury level for person with PA were extracted from the reported experimental studies for persons with PA (Mneimneh et al., 2018). Whereas, for the body segments above injury level, AB physiology and thermoregulatory responses were applicable for them.

2.2.1. Energy Expenditure

Body segments below injury level are susceptible to muscle atrophy defined as the loss of LBM and transformation of muscle fibres to a less metabolically active type characterized as fat vacuoles (Biering-Sørensen et al., 2009). Consequently, their EE is decreased compared to that of AB even at very low activity level (at rest). Contrarily, upper body segments mainly arms undergo increase in LBM and EE due to continuous use of arms for Mat mobility and wheelchair movement (Spungen et al., 2003a). Moreover, since subcutaneous SFT is dependent on the caloric intake of the body, it is expected to increase in all body parts because of overall reduced physical activity after injury. Whereas, the head and neck maintain similar LBM and SFT to that of AB, and of course similar EE (Spungen et al., 2003a). The variation of SFT has direct effect on the heat transfer between the core and skin nodes, rather than skin BMR. Thus, the thermal

conductance of the fat-skin layer and the body part itself decreases as they are correlated in **Eq. 2(a-c).**

In **Table 8**, the segmental core and skin basal metabolic rates were calculated for person with PA based on values of BMR used in Salloum et al. model (2007) for AB. Reported data in literature about ratio of LBM in person with PA compared to that of AB ($\frac{LBM_{PA}}{LBM_{AB}}$) for each body segment was obtained and multiplied by its corresponding core BMR of AB ($BMR_{AB,core}$) for the same segment (Salloum et al., 2007; Spungen et al., 2003a). Then, the obtained value was the core BMR for person with PA at this segment ($BMR_{PA,core}$). It is noted that the skin BMR for person with PA was considered the same as for AB, and the total BMR was the sum of both skin and core BMR at this segment. In addition, new values of SFT were calculated as summarized in **Table 9,** where they were obtained by multiplying the ratio of SFT in person with PA by the SFT of AB ($\frac{SFT_{PA}}{SFT_{AB}}$) (Spungen et al., 2003a).

Table 8. Segmental core, skin and total basal metabolic rates in Watts for AB and PA

Body Part	AB (Salloum et al. 2007)			Ratio of LBM in PA compared to AB ($\frac{LBM_{PA}}{LBM_{AB}}$) (Spungen et al., 2003)	PA Thoracic Level (T1-T12)		
	BMR_{core} (W)	BMR_{skin} (W)	$BMR_{Total} = BMR_{core} + BMR_{skin}$ (W)		$BMR_{PA,core} = BMR_{AB,core} \times \frac{LBM_{PA}}{LBM_{AR}}$ (W)	$BMR_{PA,skin} = BMR_{AB,skin}$ (W)	$BMR_{Total} = BMR_{core} + BMR_{skin}$ (W)
				Body segments above injury level for PA			
Head	18.43	0.22	18.65	100%	18.43	0.22	18.65
Chest	5.95	0.60	6.55	98%	5.82	0.60	6.42
Left/Right upper arm	1.06	0.18	1.24	102%	1.08	0.18	1.26
Left/Right forearm	0.59	0.10	0.69	102%	0.6	0.10	0.70
Left/Right hand	0.095	0.09	0.19	102%	0.096	0.09	0.19
				Body segments below injury level for PA			
Pelvis	46.86	0.60	47.46	98%	45.82	0.60	46.42
Left/Right thigh	1.70	0.34	2.04	58%	0.98	0.34	1.32

Left/Right calf	0.75	0.15	0.90	58%	0.43	0.15	0.58
Left/Right foot	0.14	0.12	0.26	58%	0.08	0.12	0.20
BMR_{Total} **(W)**	79.91	3.39	**83.30**	-	76.6	3.39	**80.00**
Reported Data in Literature for BMR in PA compared to AB							
(Buchholz et al., 2003)		**81.2 ± 10.82**					**71.3 ± 11.04**
(Nightingale and Gorgey, 2018)		NA					**72.64 ± 7.85**

Mean ± SD; Abbreviations: LBM: lean body mass; BMR: basal metabolic rate; PA: paraplegic people; AB: able-bodied people; W: watts; NA: not available.

Table 9. SFT of AB and PA

Body element	AB (Salloum et al. 2007)	PA	Ratio of SFT in PA compared to AB (Spungen et al., 2003)
	SFT (mm)	SFT (mm)	$\dfrac{SFT_{PA}}{SFT_{AB}}$
	Body segments above injury level		
Head + Neck	8.5	8.50	100%
Chest	19.12	22.87	120%
Left/Right upper arm	4.51	8.94	198%
Left/Right forearm	4.51	8.94	198%
Left/Right hand	7.4	14.66	198%
	Body segments below injury level		
Pelvis	19.12	22.87	120%
Left/Right thigh	10.64	14.89	140%
Left/Right calf	10.64	14.89	140%
Left/Right foot	11.7	16.37	140%

2.2.2. *Variability of core temperature thresholds in PA*

It was reported in literature that person with PA may reach a stable core temperature like that of AB usually at 36.8±0.2 °C, but non-uniform distribution of skin temperature when exposed to neutral ambient conditions at a room temperature of range 22-25 °C and RH 45-50% (Attia and Engel, 1983). However, major deviations from the thermal steady state of the body is expected to occur in persons with PA as T_{cr} may drop

or rise at a rate higher than of AB when exposed to extreme environmental conditions and high activity levels (Attia and Engel, 1983; Wilsmore, 2007). This rapid change in T_{cr} is due to the of thermoregulatory disruption for segments below injury level, thus shifting the threshold values of both sudomotor and shivering responses at the sensate skin. However, at the basal thermal condition, the vasomotor onset temperature was still considered to be the same as that of AB for the segments above injury levels (Attia and Engel, 1983; Wilsmore, 2007). **Table 10** summarizes the list of thermoregulatory threshold parameters of persons with PA based on the reported data in literature (Salloum et al., 2007; Wilsmore, 2007).

Table 10. Threshold values of vasomotor, sudomotor and shivering responses for PA compared to AB

Thermoregulatory Action	Threshold Control Parameter	PA	AB
Sweat Onset	T_{cr}	37.1 ± 0.2 °C (Wilsmore, 2007)	37.2 °C (Salloum et al., 2007)
Basal Thermal Condition	T_{cr}	36.8 ± 0.9 °C (Attia et al., 1983)	36.8 °C (Salloum et al., 2007)
Shivering Onset	T_{cr}	35.12 ± 0.91°C (Wilsmore, 2007)	35.8 °C (Salloum et al., 2007)
	T_{sk}	-	35.5 °C (Salloum et al., 2007)
Maximum Shivering	T_{cr}	35.0± 0.5 °C (Wilsmore, 2007)	33.0 °C (Salloum et al., 2007)

Mean ± Standard deviation. Abbreviations: PA: paraplegic people; AB: able-bodied people; SFT: skin fat thickness

2.2.3. *Alterations in blood vessel diameter because of paraplegia*

The blood circulatory system undergoes alterations in structure and distribution because of PA. The blood vessels' structure is reformed at early stage of injury during which the arterial diameter is decremented for those below injury level, yet no change for the blood vessels above injury level (de Groot et al., 2006; de Groot, 2005). The rate of

change of blood vessel diameter was correlated to the injury level and its severity (Dawson et al., 1994; Mathias, 2006; Popa et al., 2010; West et al., 2012). Subsequently, the drop of arterial diameter is part of the body total adaptation to the paraplegic condition. Quantitatively, it was reported in literature that the arterial diameter was reduced by 30% for the blood vessels below injury level; thus, affecting the blood flow for the corresponding body parts (de Groot, 2005; Schmidt-Trucksäss et al., 2000; Wijnen et al., 1991). This reduction was implemented in the altered PA-bioheat model for blood vessels in the back, abdomen, thighs, calves, and feet. For the veins, its dimension is almost twice the radius of the artery having the same index (Salloum et al., 2007).

2.2.4. *The cardiac output and heart rate*

The consequence of the arterial structure remodeling after SCI is the resulting segmental arterial or regional blood flow rate changes in body parts below injury level. Nevertheless, the overall value of CO in person with PA showed insignificant difference from than that of AB (Hopman et al., 1993; Kessler et al., 1986; Takahashi et al., 2004). CO defined as the blood volume pumped per minute is a cardiovascular indicator for HR and SV (Dampney, 1994). In general, SV is lower in person with PA, but it follows the same pattern as SV in AB mainly during incremental exercise, i.e. an increase in SV until reaching 45-50% of peak of worked exercise and thereafter a stable SV. In order, to use CO correlations defined in **Eq. 10(a-c)** new values of basal, maximum and minimum CO values were obtained by applying reduction of arterial blood vessel structure on CO values of AB as presented in **Table 11** (Salloum et al., 2007). These values were validated by referring to reported data in literature (Jehl et al., 1991; Kessler et al., 1986).

$$CO = \frac{CO_{dil} \times CO_{con}}{CO_{basal}} \tag{10a}$$

$$CO_{dil} =$$

$$\begin{cases} CO_{basal} & for\ T_{cr} \leq T_{cr\_threshold}\ °C \\ \dfrac{T_{cr}-T_{cr\_threshold}}{38.2-T_{cr\_threshold}}(CO_{max}-CO_{basal})+CO_{basal} & for\ T_{cr\_threshold}°C\ < T_{cr} < 37.3\ °C \\ CO_{max} & for\ \ T_{cr} \geq 37.3\ °C \end{cases}$$

(10b)

$$CO_{con} =$$

$$\begin{cases} CO_{min} & for\ T_{cr} \leq 35.12\ °C \\ \dfrac{T_{cr}-35.6}{T_{cr\_threshold}-35.6}(CO_{basal}-CO_{min})+CO_{min} & for\ 35.12\ °C\ < T_{cr} < T_{cr\_threshold}\ °C \\ CO_{basal} & for\ \ T_{cr} \geq T_{cr\_threshold}\ °C \end{cases}$$

(10c)

Table 11. Cardiac output values at the basal, maximum, and minimum demands in person with PA compared to AB

Body part	Basal (cm³/hr.) AB	PA	Maximum (cm³/hr.) AB	PA	Minimum (cm³/hr.) AB	PA
Head	55119	55119	63408	63408	53910	53910
Neck	1407	1407	3620	3620	1084	1084
Trunk	198,164	198,164	247,650	247,650	190,947	190,947
Right or Left Upper Arm	3852	3852	11261	11261	2772	2772
Right or Left Forearm	2151	2151	7196	7196	1415	1415
Right or Left Hand	1378	1378	4718	4718	891	891
Right or Left Thigh	6196	*4779*	17193	*4779*	4592	*4779*
Right or Left Calf	2741	*2116*	10344	*2116*	1632	*2116*
Right or Left Foot	1339	*1219*	5683	*1219*	706	*1219*
Total CO (cm³/hr)	290,005	**285,682**	427,468	**377,258**	269,957	**272,327**
Total CO (cm³/hr) for PA reported in Literature						
(Kessler et al., 1986) (Mean ± standard deviation in cm³/hr.)	323,353 ± 83,832	353,293 ± 53,892	-	-	-	-
(Jehl et al., 1991) (Mean ± standard deviation in cm³/hr.)	-	-	461,078 ± 83,832	449,102 ± 53,892	-	-

Abbreviations: PA: paraplegic people; AB: able-bodied people; CO: cardiac output

2.2.5. Skin blood perfusion

It is one of the body thermoregulatory responses to the change in T_{cr} to maintain a stable thermal state. It is disrupted for the body segments below injury level including thighs, calves, feet, lower back and abdomen with a percentage of reduction of 12% in SPB compared to that of AB (Hogancamp II, 2004). When SBP becomes constant independent of body thermal state, it induces blood pooling in the lower body extremities and increase of T_{cr} of person with PA due to inability to redistribute blood to the active muscles in the body especially during exercise (Dawson et al., 1994; Mathias, 2006; Popa et al., 2010; West et al., 2012). Whereas, for the segments above injury level mainly the forearms, it is observed to have an increased SBP with a ratio of 3.296 compared to that of AB (Hogancamp II, 2004). The remaining active body segments (fingers, upper arms, palms, chest and upper back) maintain similar values to that of AB. Three values of SBP (basal, minimum, and maximum values) were modified for the thighs, calves, feet, abdomen, lower back and forearms. Then, the obtained values were used to calculate SBP of the body about its threshold T_{cr} in PA using **Eq. 11(a-c)**. This is applicable for all thoracic SCI levels (Cooper et al., 1957).

$$\dot{m}_{skin} = \frac{\dot{m}_{skin,dil} \cdot \dot{m}_{skin,con}}{\dot{m}_{skin,-basal}} \tag{11a}$$

$$\dot{m}_{skin,dil} =$$

$$\begin{cases} \dot{m}_{skin-basal} & for \ T_{cr} \leq T_{cr\_threshold}°C \\ \frac{T_{cr}-T_{cr\_threshold}}{38.2-T_{cr\_threshold}} \left(\dot{m}_{skin,max} - \dot{m}_{skin-basal} \right) + \dot{m}_{skin-basal} & for \ T_{cr\_threshold}°C < T_{cr} < 37.3°C \\ \dot{m}_{skin,max} & for \ T_{cr} \geq 37.3°C \end{cases}$$

(11b)

$$\dot{m}_{skin,con} =$$

$$\begin{cases} \dot{m}_{skin,min} & for\ T_{cr} \leq 35.12\ ^{\circ}C \\ \frac{T_{cr}-35.6}{T_{cr\_threshold}-35.6}\left(\dot{m}_{skin-basal} - \dot{m}_{skin,min}\right) + \dot{m}_{skin,min} & for\ 35.12\ ^{\circ}C\ < T_{cr} < T_{cr\_threshold}\ ^{\circ}C \\ \dot{m}_{skin-basal} & for\ T_{cr} \geq T_{cr\_threshold}\ ^{\circ}C \end{cases}$$

(11c)

2.2.6. *Hot and cold control equations (sudomotor and shivering):*

After thoracic SCI, persons with PA are prone to instability in T_{cr} in hot and cold climates (or even exercise) due to the absence of sudomotor (sweating) and shivering for segments below injury level. This is implemented in the altered PA-bioheat model by modifying the weighting factor of each SWEAT and COLD, representing the sudomotor and shivering responses respectively. Compared to AB, sweat rate is reduced by 10% from the whole body in PA, but it is increased by 1.5 and 1.2 for the head and palms respectively as reported in literature (Fitzgerald et al., 1990; Wilsmore, 2007). For the segments below injury level (T6-T12), neither sweat nor shivering was observed (Petrofsky, 1992; Wilsmore, 2007). Thus, in the altered bioheat model, the weighting factor of SWEAT and COLD was modified to zero for the impaired body segments including thighs, calves, feet, lower back (defined by right and left lower back in the model) and abdomen (defined by right and left lower front in the model). The remaining body segments above injury level had SWEAT, and COLD weighting factors as summarized in **Table 12**.

Table 12. SWEAT and COLD weighting factors for body segments above injury level of PA defined in the bioheat model

Body Segment	Head	Chest	Upper Back	Upper arm	Forearm	Palm	Finger
SWEAT	0.1215	0.275	0.275	0.0444	0.0326	0.093	0.00155

COLD	0.0775	0.515	0.515	0.0024	0.0014	0.0001	0.00002

2.3. Numerical methodology of TP/PA-bioheat model

Starting from the simulation program of the published AB-bioheat model, the TP/PA-bioheat model was developed using FORTRAN 90 that included the use of double precision real numbers and 8 significant bits complex numbers (complex(8)) as well as structures to describe the topology of the human body, the clothing data, and the output variables.

The input of the program consists of the initial thermal state of the human body, the metabolic rate, the ambient conditions, and clothing layers properties (number of layers, temperature, water vapor pressure). A fully explicit Euler-Forward integration scheme with a time step of 0.02 seconds over the desired simulation period is used to solve the energy balance equations of the human body nodes for any segment where the respiratory heat loss, blood flow rates, thermoregulatory responses and skin vapor pressure are calculated from previous time step. The regional blood flow rates in the arteries veins and tissue are obtained from the output of Avolio model which consists of the velocity ratios for any considered artery to the cardiac output. Therefore, the temperatures of the core, skin, artery, and vein nodes, and the artery blood flow rate are updated for each segment at each time step. Avolio model blood flow that gives the arterial blood velocity and thereafter the blood perfusion rates are computed after each complete cycle of the heart which approximately takes 0.8 sec for the neutral state of the body and which can vary depending on the metabolic rate.

Suitable initial conditions are determined starting from the neutral ambient conditions (24 °C, 50%) to simulate a relatively long exposure to obtain steady state values to be used as initial conditions for all other unsteady calculations of various node temperatures for all segments and the sensible and latent heat loss from the skin.

Certain steps are followed to solve the balance mass and energy equations:

1. The human body and clothing parameters are read from a database that are defined initially by the user before running the code.

2. The ambient and exercise conditions are assigned through the given time span in addition to the convection and radiation coefficients.

3. The initial temperatures are assigned for the human body nodes and clothing layers.

4. The initial mean skin temperature, the initial thermoregulatory controls and the initial blood flow rates are determined from initial conditions.

5. Loop over the time span.

    a. Compute the blood flow rates in the core, skin, arteries, and veins in the considered part.

    b. Compute the sweat and shivering rates.

    c. Compute the temperature and vapor pressure for all the layers existing on the part.

    d. Solve for the new temperatures of the considered parts for the new time step.

    e. If the computations are accomplished for all the body parts, go to step 6, otherwise go to the next part of the human body at step 5a.

6. Compute the total sweat rate, total shivering rate, mean skin temperature, cardiac output for the new time step.

7. Save the needed results of the new time step.

8. If the time is equal to the given time span, then the grogram run is finished. Otherwise, increase the time by a time step and return to step 5.

2.4. Integration of Fabric-PCM model into PA-bioheat model

The means of enhancement of the PCM cooling vest in alleviating the thermal strain of persons with PA is investigated. Persons with PA are the target group of interest in this research as they are more capable than persons with TP to be involved in outdoor activities and even extreme sports. Having thoracic (T1-T12) SCI, persons with PA possess a critical magnitude of thermoregulation impairment, and have at least 25% of the trunk skin as sensate (Kirshblum et al., 2011a).

In the current work, the published Fabric-PCM model of Itani et al. was chosen to be integrated into PA-bioheat model (Itani et al., 2016). The validation of the combined Fabric-PCM-PA model was achieved via previous studies in literature that investigated the cooling effect of PCM cooling vest for persons with PA (Armstrong et al., 1995; Trbovich et al., 2014). Armstrong et al. and Trbovich et al. tested ice cooling vest (melting point of 0 °C) and PCM cooling vest (melting point of 15°C), respectively for persons with PA performing certain activity level at specified T_{amb} and RH. Comparison of T_{cr} and T_{sk} was done between the reported experimental results and the combined model predictions. In addition, the sensible and latent heat losses at the sensate and insensate trunk-skin were obtained to assess the performance of PCM cooling vest for persons with

PA. The coming sections describe the Fabric-PCM model, its integration with PA-bioheat model, boundary conditions and numerical solution.

2.3.1. Fabric-PCM model:

The published Fabric-PCM model of Itani et al. was developed to simulate the mass and heat transfer through the different layers of the PCM cooling vest, while incorporating the transient period for moisture build-up in the inner fabric layer in contact with the trunk-skin. The model predicts the temperature and humidity ratio of the air layer forming the vest, as well as the PCM temperature during transients and its melted fraction during phase change.

As shown in **Fig. 3(a-c)**, the outer fabric layer of the vest was exposed to the ambient; while the inner fabric layer (assumed shirt) was assumed near the trunk skin layer. Between these two layers, there were two types of air layer: macroclimate and microclimate. The macroclimate occupied the free space between PCM packets and outer fabric layer, whereas the microclimate occupied the free space between PCM packs and the inner layer. PCM packets were located at the front and back of the vest covering the trunk sensate (chest and upper back) and insensate skin (abdomen and lower back).
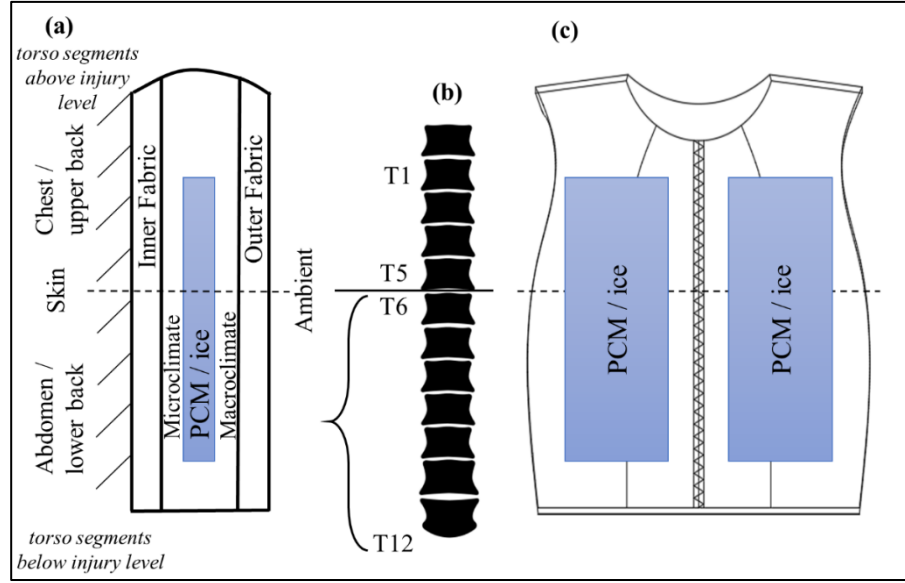
Figure 3. Schematic of a cooling vest with PCM or ice packets covering skin area at the impaired segments (abdomen and lower back), and active segment (upper back and chest): (a) side view of different layers of fabric-PCM or fabric-ice, (b) spinal cord injury level related to PA- (T6-T12) bioheat model, (c) front view of the vest with the packets

Because the PCM packet had the lowest temperature among the different layers, it absorbed heat by convection and radiation from the surrounding micro- and macro-climate air layers of the vest with possible effect of condensation. The microclimate air layer exchanged heat with the inner fabric and PCM. On the other hand, the macroclimate air layer exchanged heat with the PCM, inner fabric layer and outer fabric layer. The outer fabric layer exchanged heat with the surrounding environment. All the mass and heat transfer equations of the Fabric-PCM model are explained in detail in the study of Itani et al. and Hamdan et al. (Hamdan et al., 2016; Itani et al., 2016).

2.3.2. Boundary conditions

The integration of Fabric-PCM model into PA-bioheat model is done by ensuring the continuity of heat and mass fluxes between the skin of the trunk and the shirt at any time. At the sensate skin of the trunk (the chest and the upper back), liquid sweat would be captured by the shirt once the accumulated amount of sweat exceeds 31.5 g/m^2 (maximum mass of sweat accumulation for persons with PA) (Wilsmore, 2007), and the shirt vapor pressure would be equal to its saturated pressure (Jones, 1992; Umeno et al., 2001; Wan and Fan, 2008). In addition, a contact thermal resistance between the skin and inner fabric was considered due to the air gap between the two layers. With a thickness of 1.3 mm, air layer's thermal dry resistance was calculated using **Eq. 12** (Stephan and Laesecke, 1985):

Dry resistance: $R_{d\_airlayer} = \frac{th_a}{k}$ (m²·℃/W) (12)

where k = 24 mm W/ m²·C, and th_a=air layer thickness (assumed 1.3 mm in the model).

For the numerical simulations, it was aimed to validate the combined Fabric-PCM-PA model by simulations done for the cases study of Armstrong et al. and Trbovich et al. that investigated the performance of the ice cooling vest (melting point of 0 °C) and PCM cooling vest (melting point of 15°C); respectively, for persons with PA. The clothing, metabolic rate, ambient conditions, and the initial conditions of the thermal state (core and skin temperatures) of the body as well as that of the clothing temperature and regain were specified as per each case study. Then, the attained steady state trunk-skin and shirt temperatures were used as an initialization for the start of exercise in hot ambient conditions.

2.3.3. *Numerical Solution*

The mass and heat transfer balance equations of Fabric-PCM-PA bioheat model were solved numerically using the explicit Euler forward method, given the initial values of the body core and skin temperatures of the trunk, pressure of all different layers of clothing and air, and initial PCM temperature. Before running the PA-bioheat model, initial conditions for the remaining body segments including temperature and pressure of clothing layers were provided from saved database for person with PA at moderate sedentary conditions.

At a specified time reading (t + Δt where Δt = 0.02 sec taken in this model to capture complete cardiac cycle), the Fabric-PCM model was called first to calculate the core and skin temperatures of segments whose clothing layers included PCM or ice packet (chest, abdomen, lower back and upper back). Before looping into PA-bioheat model, PCM or ice computed temperature was compared to its melting temperature to identify whether to update its temperature if it's higher than its melting temperature else to keep it the same and calculate melted fraction of PCM or ice packet. Then, using bioheat model for PA, skin and core temperatures were calculated for the remaining body parts excluding the trunk.

After each complete iteration, the average values of core temperature and cardiac output were calculated and compared to threshold values of thermoregulatory responses in person with PA to identify whether vasomotor, sudomotor or shivering to be activated for body segments above injury level. These steps were looped over until the simulation time duration was finished. Consequently, the output parameters of the Fabric-PCM-PA model are the average and segmental body core and skin temperature as well as sensible and latent heat losses at the sensate and insensate skin of the trunk. The time step for the

numerical solutions of the PA-bioheat model and the combined Fabric-PCM-PA model are presented in **Fig. 4(a-b)**.
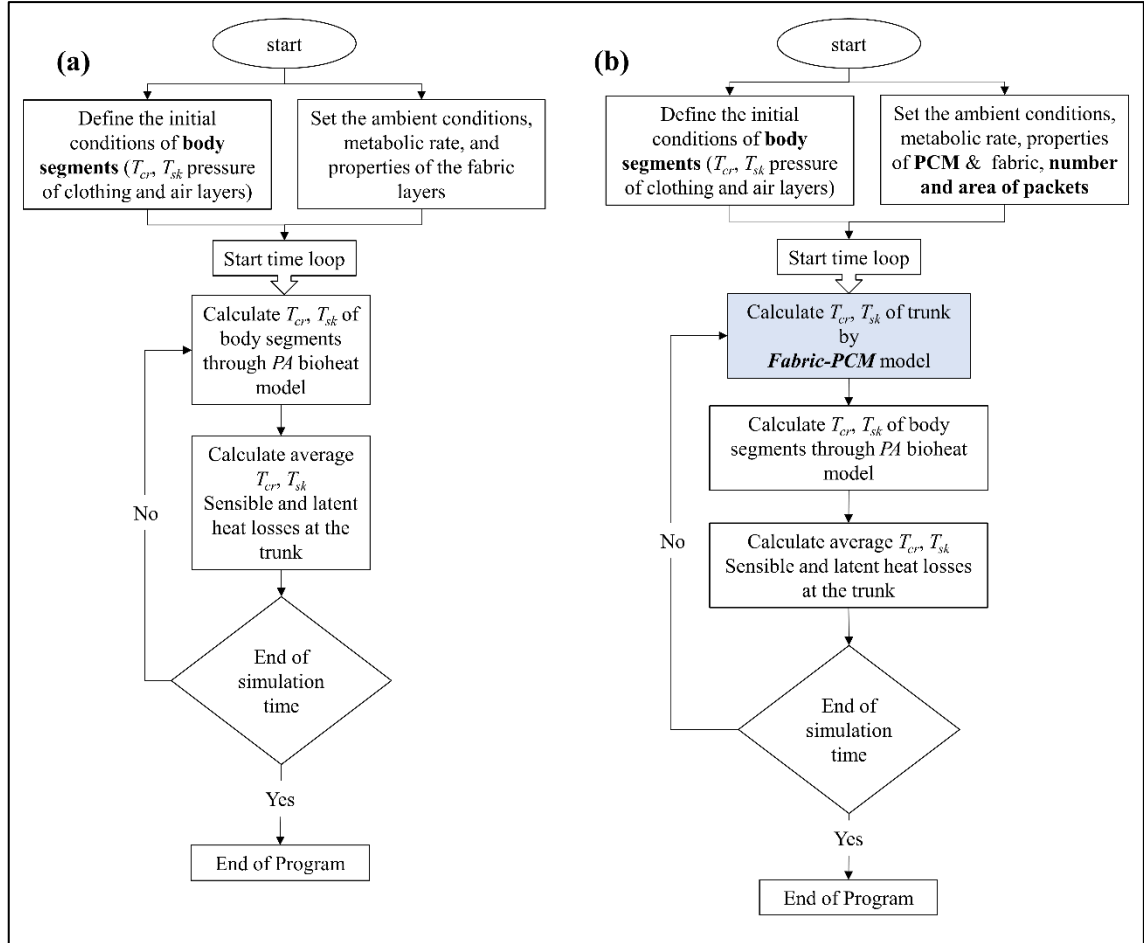
Figure 4. Flow chart of numerical methodology of the (a) PA-bioheat model and (b) integrated Fabric-PCM-PA bioheat model

2.5. Validation of Fabric-PCM-PA bioheat model

The Fabric-PCM-PA bioheat model was validated vi previous studies in literature of Armstrong et al. and Trbovich et al. (Armstrong et al., 1995; Trbovich et al., 2014). Each experimental study was focused on a specific material and melting temperature of the PCM cooling vest at moderate and high climate conditions and activity levels (specific metabolic rate). **Table 13** presents the protocol of the two experiments; Armstrong et al.

and Trbovich et al. The duration of the exercise in Trbovich et al. was twice that of Armstrong et al., but the indoor room conditions were higher in the latter. Both experiments aimed at studying the effectiveness of PCM cooling vest on reducing T_{core} for persons with PA; thus, each exercise was repeated twice, with and without the cooling vest. In both experiments, participants wore shorts and socks without shirts during *with-vest* case; while, the sleeveless vest covered the abdomen, back and chest, but the PCM packets or ice packs were mainly located at the abdomen and lower back area of the participant who was at seating position performing certain activity level.

Table 13. Experimental protocol of Armstrong et al. and Trbovich et al.

Experiment	Armstrong et al. (1994) Ice vest	Trbovich et al. (2014) PCM vest
Room temperature	32.9±0.1 °C	21.1-23.9 °C
Relative Humidity	75%	50%
Exercise Type	Pushing custom-built chair on a stationary roller	Intermittent sprint of wheelchair
Duration of exercise	30 mins	60 mins
Clothing	Shorts and socks without shirts	Shorts and socks without shirts
Cooling methodology	Ice vest	PCM vest
Melting Temperature	0 °C	15 °C
vest weight	3 kg	2.27 kg
coverage skin area	0.14 m²	0.061 m²
Number of packs	12 ice packs	4 PCM packs

Experiment	Armstrong et al. (1994) Ice vest	Trbovich et al. (2014) PCM vest
Vest used		
Vest Supplier	Steelevest; www.steelevest.com	Glacier Tek, Inc., West Melbourne, FL

2.6. Parametric study of Fabric-PCM-PA bioheat model

A parametric study using the integrated Fabric-PCM into PA-bioheat model was conducted to investigate the means of enhancement of PCM cooling vests via varying the PCM placement, coverage area and melting temperature to provide effective cooling for persons with PA during exercise.

Starting from the study of Trbovich et al. that tested PCM cooling vest at melting temperature of 15 °C (Trbovich et al., 2014), three design cases of cooling vest were simulated using the Fabric-PCM-PA model as presented in **Table 14**. In the first case, the melting temperature was set at 10 °C instead of 15 °C; this value was accepted for AB as shown to be effective in very hot ambient conditions without causing any skin breakdown (Gao et al., 2012). In the second case, the PCM coverage area at the sensate (chest and upper back) and insensate (abdomen and lower back) skin of the trunk was incremented up to 40% of total torso skin area. This is because it was reported that the critical body surface cooling area should not be below 40% to enhance heat losses from the body to the surrounding during exercise (Kume et al., 2009). Finally, in the third case, both melting temperature and PCM coverage area were modified to 10 °C and 40%,

respectively. At the end of each simulation, T_{cr} and T_{sk} values were plotted and compared. In addition, time-average sensible and latent heat losses were obtained at the sensate and insensate skin of the trunk segments.

Table 14. Protocol of Trbovich et al. experiment and three design cases of PCM cooling vest

Experiment	Trbovich et al.	case (1)	case (2)	case (3)
Room temperature	21.1-23.9 °C			
Relative Humidity	50%			
Exercise Type	Intermittent sprint of wheelchair			
Duration of exercise	60 minutes			
Cooling methodology	PCM vest			
Clothing criteria	Shorts and socks without shirts (0.3 clo)			
Melting Temperature (°C)	15	10	15	10
coverage skin area for lower back and abdomen (m²)	0.046	0.046	0.080	0.080
coverage skin area for upper back and chest (m²)	0.046	0.046	0.053	0.053

2.7. Hybrid ECV model development

The effectiveness of the hybrid ECV in alleviating the thermal strain of persons with PA is investigated. It consisted of the water-absorbent material incorporated with ventilation fans to enhance the heat losses at the trunk, bearing in mind the wettedness condition of the shirt covering the sensate skin. If sweat capture occurs at the shirt during a physical activity performed by person with PA, the use of ventilation fans enhances moisture removal and increases latent heat losses from the sensate skin. Since persons with PA show delayed and limited sweating response, the transient period before the shirt

becomes wetted should be considered in the design as it can be substantial compared to the duration of the outdoor physical activity that matches the lifestyle of persons with PA (Wilsmore, 2007). Therefore, the design of an effective hybrid ECV requires a clear understanding of the underlying heat and moisture transfer mechanisms between the wearer's body, the vest, and the environment. To account for the wettedness condition of the skin and the shirt, a transient mathematical model of the hybrid vest should be developed and integrated with a robust PA bioheat model for a person with PA (Mneimneh et al., 2019a, b).

As shown in **Fig. 5(a)**, ECV Type II is comprised of three fabric layers; i) inner layer made up of waterproof fabric (impermeable to vapor and liquid transport) to prevent fluid transport to the wearer's body, ii) middle layer made up of water-absorbent fabric, and iii) outer layer made up of breathable waterproof fabric that resists liquid water passing through, but allows water vapor to pass (Appolonia, 2002; Bongers et al., 2016). **Fig. 5(b)** shows the fans that are located at the lower front and back sides of the vest to blow the ambient air through the microclimate airgap (Klous et al., 2020). During the fan operation, the ambient air flows from the bottom to the top of the vest and leaves through the collar and channel at the upper part of the vest, as depicted in **Fig. 5(c)** (Yi et al., 2017; Zhao et al., 2013). Hence, ventilation in the microclimate is used to remove moisture when sweat capture occurs at clothing layer covering the trunk. In the case when fans are OFF, the microclimate acts as an enclosure with naturally driven air flow circulation and no ventilation.
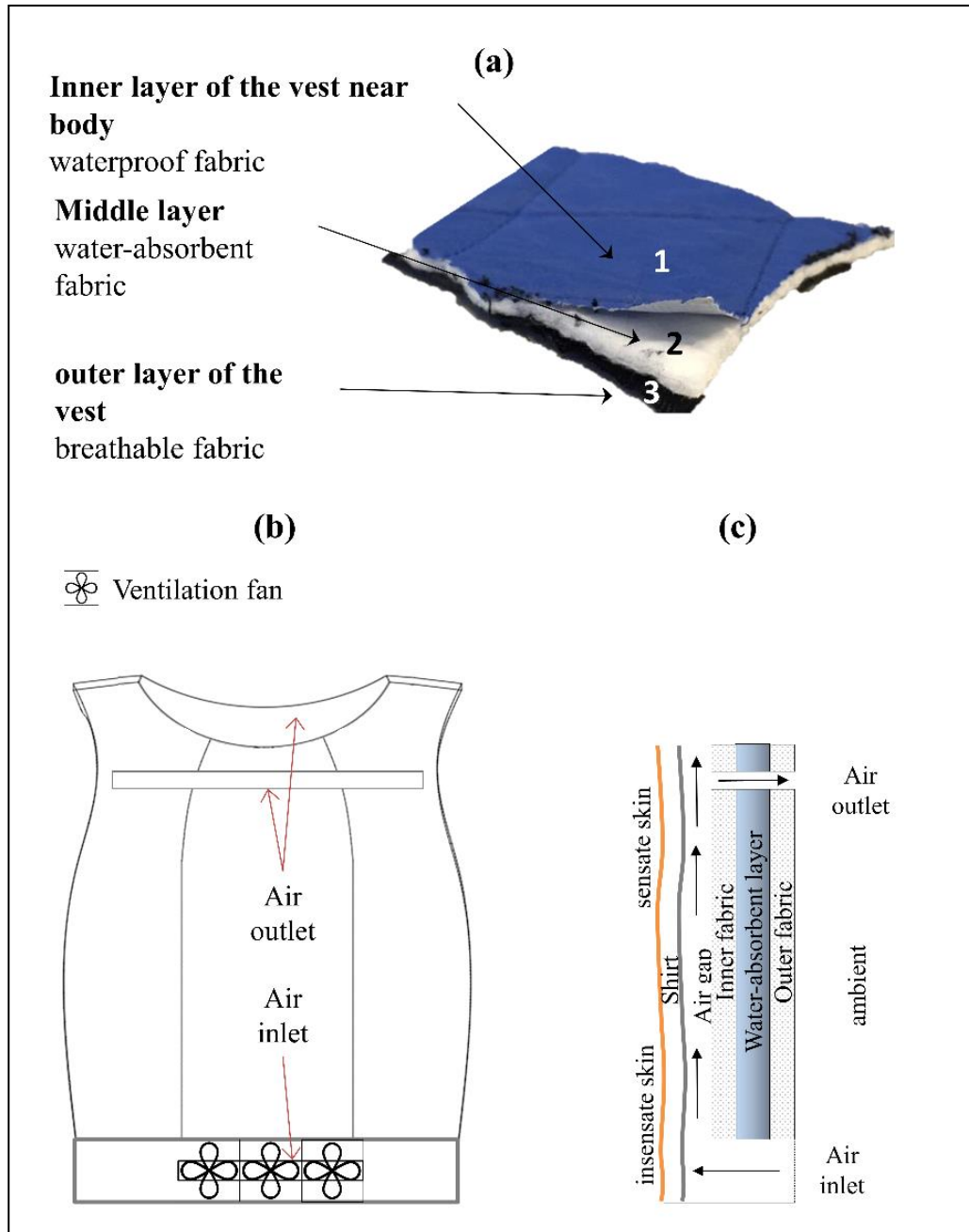
Figure 5. Picture of (a) material used in a commercially available ECV Type II (b) front view of hybrid ECV (c) section view of the vest layers with ventilation fans

2.6.1. System description

The system of the hybrid ECV consists of the vest layers, microclimate air, and shirt as shown in **Fig. 6**. The shirt layer is in contact with the skin of the trunk and is divided

into two non-interacting separate parts; one covering the sensate skin and the other covering the insensate skin. The microclimate air gap between the shirt and the inner surface of the hybrid ECV vest is divided into two nodes as well. Similarly, the inner layer of the vest, composed of liquid and vapor impermeable material is represented by two nodes. Whereas, the water-absorbent material, assumed initially saturated with water, consists of one node due to the high thermal conductivity of water. Finally, the outer layer of the vest is composed of breathable but liquid impermeable material, and also assumed of one node as it exposed to same boundary conditions along its height.

The hybrid ECV is subject to heat transfer by radiation and convection at the outer vest layer when used by an active person with PA for a given metabolic rate in outdoor conditions (see **Fig. 6**). Evaporation at the outer vest layer can happen by the virtue of water vapor pressure gradient across the water-absorbent layer to the ambient. Moreover, heat transfer can take place at the shirt by means of convection with the microclimate air and radiation with the inner vest layer. In case of sweat capture by the shirt at the sensate skin, cooling due to sweat evaporation can occur, which can also be enhanced using ventilation fans.
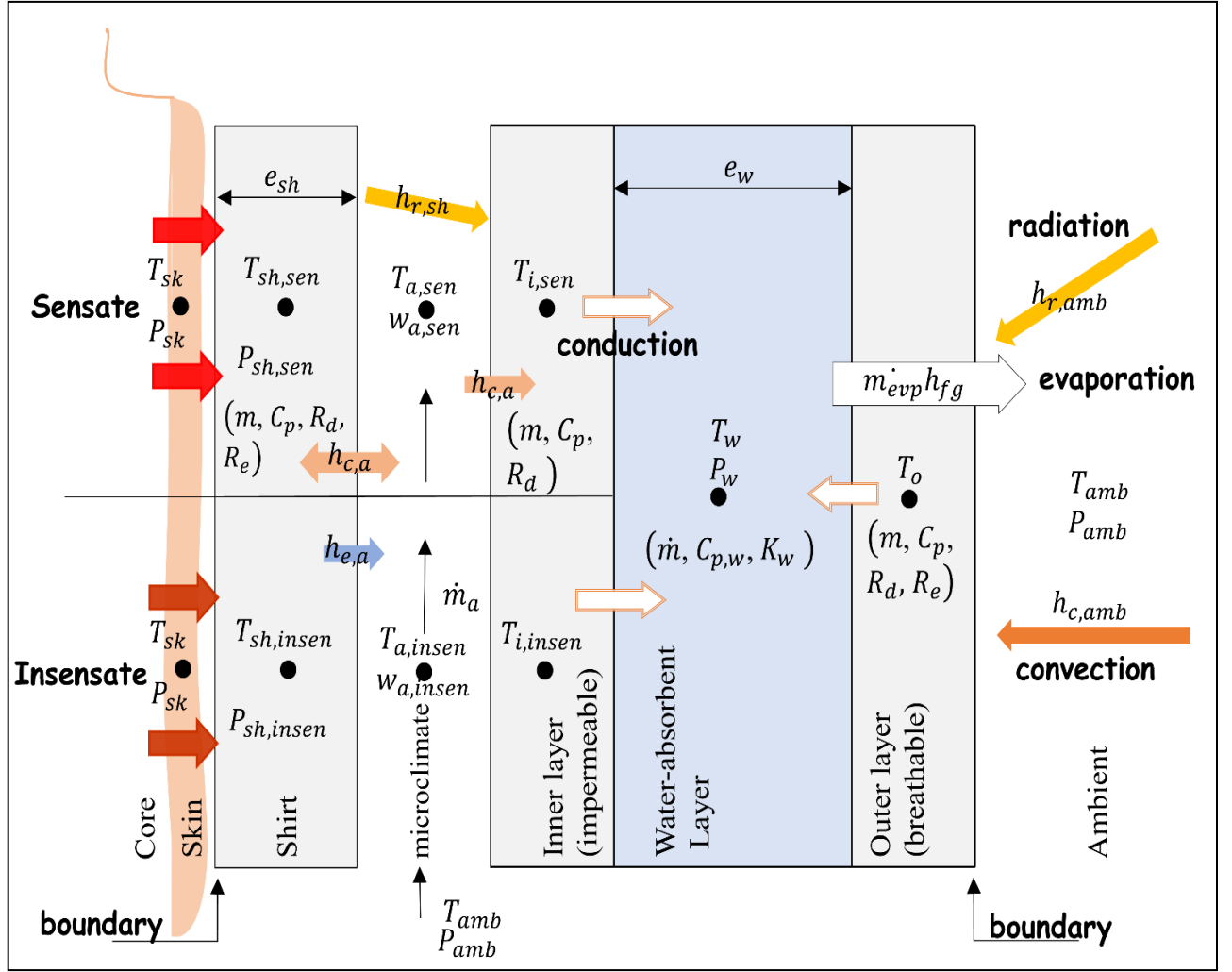
Figure 6. Schematic of the heat and mass transfer of the shirt, the microclimate, the inner layer, water-absorbent layer, and outer layer of the vest at the sensate and insensate skin of trunk

2.6.2. Mathematical model description

The hybrid ECV model consists of the three sub-models for each of: the layers of ECV Type II, the microclimate air layer, and the shirt (ECV Type I) covering the sensate and insensate skin of the trunk. It predicts the transient temperature profile of the vest layers, the microclimate air gap, and the shirt as well as the evaporation rate of the vest. The shirt model of ECV Type I is formulated to account for two phases of the shirt

wettedness including (1) the first phase where no sweat accumulation occurs in the shirt, i.e., *dry shirt phase*, and (2) the second phase where the sweat is captured in the shirt, i.e., *wet shirt phase*. The mass and heat transfer taking place in the shirt and in the microclimate air layer depend on the dry and/or wet state of the skin, taking into consideration the sensate and insensate parts of the trunk skin area. The shirt condition remains dry for the insensate skin, as no sweating occurs due to the thermoregulatory impairment for person with PA.

To simplify the formulation, the following assumptions are adopted: i) the fabric layers (the shirt and the vest layers) are assumed thin justifying the use of simplified unidirectional mass and heat transfer without lateral transport; ii) separate nodes for the shirt, microclimate air and inner vest layer are considered for the sensate and insensate skin regions; iii) no heat or mass transfer interaction is assumed between the sensate and insensate layer nodes; iv) since the sweat rate at the sensate skin is reduced for persons with PA, only the shirt adjacent to the sensate skin is assumed saturated when sweat capture occurs; whereas the shirt adjacent to the insensate skin is assumed to be below the saturation level even if some liquid may be wicked from the sensate skin; v) the change in the volume of air inside the vest upon fan operation has minimal effect on the microclimate air gap thickness; v) the inner and outer vest layers of the ECV material are modelled with constant dry thermal and evaporative resistances; and vi) volume changes of the fabrics due to the change of moisture content are neglected.

2.6.3. Hybrid ECV model

The hybrid ECV model considers three layers of vest: inner layer, water-absorbent layer, and outer layer. The inner layer of the ECV vest exchanges heat by convection and

radiation with the microclimate and the shirt; respectively (see **Fig. 6**). The water absorbent ECV layer modelled as one node exchanges heat and mass with the environment through the outer vest layer (similarly modelled as one node). The inner vest layer is consisted of two nodes to account for the sensate and insensate region of the trunk, which affects the wettedness condition of the shirt. The governing mass and energy balance equations are given as Eq. 13(a-c), where Eq. 13(a) applies to both nodes corresponding to the sensate and insensate skin.

- Inner vest layer:

$$\underbrace{m_i C_{p,i} \frac{dT_i}{dt}}_{\text{storage term}} = \underbrace{\frac{T_a - T_i}{\left(\frac{1}{2h_{c,a}} + \frac{R_{d,i}}{2}\right)} A_{sh}}_{\text{convection}} + \underbrace{h_{r,sh}(T_{sh} - T_i) A_{sh}}_{\text{radiation from shirt}} + \underbrace{\frac{T_w - T_i}{\frac{R_{d,i}}{2} + \frac{e_w}{2k_w}} A_{sh}}_{\text{conduction}} \tag{13a}$$

where m_i and $C_{p,i}$ are the mass and the specific heat of the inner vest layer. T_i, T_w, T_{sh}, and T_a are the temperatures of inner layer, water-absorbent layer, shirt, and microclimate air, respectively. $R_{d,i}$ is the dry thermal resistance of inner vest layer. The convection heat transfer coefficient ($h_{c,a}$) is calculated either via the correlation of forced convection over a plate in case of fan operation or via the correlation of natural convection inside an enclosure in case of no fan operation (Bergman et al., 2011). $h_{r,sh}$ is the radiative heat transfer with the shirt. e_w and k_w represent the thickness of water-absorbent layer and thermal conductivity of water, respectively. Finally, A_{sh} is the area of the shirt covering the sensate or insensate skin. It should be noted that all parameters are applied separately for the sensate and insensate skin regions.

- Water-absorbent layer:

$$C_{p,w} \underbrace{\frac{d(m_w T_w)}{dt}}_{\text{storage term}} = \underbrace{\frac{T_{i,sen} - T_w}{\left(\frac{R_{d,i}}{2} + \frac{e_w}{2k_w}\right)} A_{sh,sen}}_{\text{conduction}} + \underbrace{\frac{T_{i,insen} - T_w}{\left(\frac{R_{d,i}}{2} + \frac{e_w}{2k_w}\right)} A_{sh,insen}}_{\text{conduction}} +$$

$$\underbrace{\frac{T_o - T_w}{\left(\frac{R_{d,o}}{2} + \frac{e_w}{2k_w}\right)} (A_{sh,sen} + A_{sh,insen})}_{\text{conduction}} - \underbrace{\dot{m}_{evp} h_{fg}}_{\text{evaporation}}$$

(13b)

where m_w and $C_{p,w}$ are the mass and the specific heat of the water. $A_{sh,sen}$ and $A_{sh,sen}$ are the area of the shirt covering the sensate and insensate skin, respectively. T_o and $R_{d,o}$ are the outer surface temperature and dry thermal resistance of the outer vest layer. $\dot{m}_{evp}$ is the water evaporation rate from the vest calculated by Eq. (13c). h_{fg} is the heat of vaporization of water.

The mass balance equation governs the transient change in the amount of water in the vest due to evaporation $(\dot{m}_{evp})$ while taking into consideration the evaporative resistance of the outer vest layer $(R_{e,o})$ as follows:

$$\frac{dm_{evp}}{dt} = -\dot{m}_{evp} = -\frac{P_w - P_{amb}}{\left(R_{e,o} + \frac{1}{h_{e,amb}}\right) h_{fg}} (A_{sh,sen} + A_{sh,insen})$$

(13c)

where P_{amb} is the ambient vapor pressure, and P_w is the saturated vapor pressure obtained at T_w. $h_{e,amb}$ is the evaporative heat transfer coefficient at ambient conditions.

- Outer vest layer:

$$m_o C_{p,o} \underbrace{\frac{dT_o}{dt}}_{\text{storage term}} = \underbrace{\frac{T_w - T_o}{\left(\frac{R_{d,o}}{2} + \frac{e_w}{2k_w}\right)} (A_{sh,sen} + A_{sh,insen})}_{\text{conduction}} + \underbrace{\frac{T_{amb} - T_o}{\left(\frac{R_{d,o}}{2} + \frac{1}{(h_c + h_r)_{amb}}\right)} (A_{sh,sen} + A_{sh,insen})}_{\text{convection and radiation}}$$

(13d)

where m_o and $C_{p,o}$ are the mass and the specific heat of the outer vest layer. $h_{c,amb}$ and $h_{r,amb}$ are the convective and radiative heat transfer coefficients with the ambient, respectively.

2.6.4. Microclimate air layer

The mass balance of the microclimate air layer predicts the lumped air humidity ratio corresponding to either the sensate or the insensate skin, w_a, as shown in Eq. (14a). It considers moisture transfer by diffusion and convection with the shirt only. Furthermore, it accounts for the moisture transfer caused by air ventilation in case of fan operation, where the mass flow rate of the air, $\dot{m}_a$, is equal to the fan mass flow rate.

$$\underbrace{\rho_a e_a A_{sh} \frac{dw_a}{dt}}_{\text{storage term}} = \underbrace{\frac{P_{sh} - P_a}{R'_e h_{fg}} A_{sh}}_{\substack{\text{moisture transfer} \\ \text{by convection}}} - \underbrace{\dot{m}_a (w_a - w_{a,inlet})}_{\substack{\text{moisture transfer due to} \\ \text{air ventilation}}} \tag{14a}$$

where ρ_a and e_a are the density of air and the thickness of the microclimate air gap. P_{sh} and P_a are the vapor pressures corresponding to the shirt and air layer, respectively. R'_e is the evaporative resistance of the shirt, which depends whether the shirt is dry or wet. If the shirt is dry R'_e is equivalent to $\left[\frac{R_{e,sh}}{2} + \frac{1}{2h_{e,a}} \right]$ where $R_{e,sh}$ is the shirt evaporative resistance and $h_{e,a}$ is the evaporative heat transfer coefficient in the microclimate obtained by Lewis formula. Otherwise, R'_e for the wet shirt is equivalent to $\left[\frac{1}{2h_{e,a}} \right]$. $w_{a,inlet}$ denotes the humidity ratio of air entering the body segment, where it is equivalent to the ambient humidity ratio for the insensate skin, or the microclimate air humidity ratio leaving the insensate skin region and entering the sensate one, $w_{a,insen}$.

The energy balance for the air layer predicts the lumped air layer temperature (T_a) corresponding to either the sensate or the insensate skin shown in Eq. (14b). It considers the convective heat transfer between the microclimate air and the shirt as well as the inner layer of the vest corresponding to either the sensate or insensate skin, and the heat transfer due to air ventilation in case of fan operation mode.

$$\underbrace{\rho_a e_a A_{sh} C_a \frac{dT_a}{dt}}_{\text{storage term}} = \underbrace{\frac{T_{sh} - T_a}{R'_{th}} A_{sh}}_{\text{convection at shirt}} - \underbrace{\frac{T_a - T_i}{\left(\frac{R_{d,i}}{2} + \frac{1}{2h_{c,a}}\right)} A_{sh}}_{\substack{\text{convection at inner} \\ \text{layer of the vest}}} - $$

(14b)

$$\underbrace{\dot{m}_a C_a \left(T_a - T_{a,inlet}\right)}_{\substack{\text{heat transfer by} \\ \text{air ventilation}}}$$

where C_a represent specific heat of air. R'_{th} is the dry thermal resistance of the shirt, which depends whether the shirt is dry or wet. If the shirt is dry R'_{th} is equivalent to $\left[\frac{R_{d,sh}}{2} + \frac{1}{2h_{c,a}}\right]$ where $R_{d,sh}$ is the shirt dry thermal resistance. Otherwise, R'_{th} for the wet shirt is equivalent to $\left[\frac{e_{sh}}{2K_{eff}}\right]$ where e_{sh} and K_{eff} are the thickness and effective thermal conductivity of the shirt (Jones, 1992; Wan and Fan, 2008). $T_{a,inlet}$ denotes the temperature of air entering the body segment, where it is equivalent to the ambient temperature, T_{amb} for the insensate skin, or the microclimate temperature leaving the insensate skin region and entering the sensate one, $T_{a,insen}$.

In case of ECV Type II, the mass flow rate of the air, $\dot{m}_a$, in Eq. (14a) and Eq. (14b) is set to zero and the convection heat transfer coefficient ($h_{c,a}$) is calculated via the correlation of natural convection inside an enclosure (Bergman et al., 2011), as discussed earlier.

2.6.5. The shirt

The shirt model is adopted from previous studies focusing on PCM cooling vests for AB (Bachnak et al., 2018; Itani et al., 2017). Similarly, in this study, the mass and energy balance equations of the shirt covering the sensate and insensate skin of the trunk are developed for the hybrid ECV. These equations reflect the transient state of the shirt as it goes from a dry condition to a wet condition once sweat capture by the shirt starts.

2.6.5.1. Dry condition of the shirt at the sensate or insensate skin of the trunk

The mass balance equation of the shirt at the **sensate/insensate** skin of the trunk in the **dry state** is shown in Eq. (15a). In this condition, the skin vapor pressure (P_{sk}) and the shirt vapor pressure (P_{sh}) are below their saturation pressure.

$$\underbrace{\rho_{sh} e_{sh} \frac{dR_{sh}}{dt}}_{\text{storage term}} = \underbrace{\frac{P_{sk} - P_{sh}}{\left(\frac{R_{e,sh}}{2}\right) h_{fg}}}_{\substack{\text{moisture transfer} \\ \text{by diffusion}}} - \underbrace{\frac{P_{sh} - P_a}{\left(\frac{R_{e,sh}}{2} + \frac{1}{2 h_{e,a}}\right) h_{fg}}}_{\substack{\text{moisture transfer} \\ \text{by convection}}} \tag{15a}$$

where ρ_{sh} and R_{sh} represent the density and regain of the shirt. P_{sk} is obtained using the equation developed in the study of Jones (Jones, 1992).

Furthermore, the energy balance equation of the shirt at the **sensate/insensate** skin is written in Eq. (15b) (Bachnak et al., 2018):

$$\underbrace{\rho_{sh} e_{sh} C_{sh} \frac{dT_{sh}}{dt}}_{\text{storage term}} = \underbrace{\frac{T_{sk} - T_{sh}}{\frac{R_{d,sh}}{2}}}_{\text{conduction}} - \underbrace{\frac{T_{sh} - T_a}{\left(\frac{R_{d,sh}}{2} + \frac{1}{2 h_{c,a}}\right)}}_{\text{convection}} - \underbrace{h_{r,sh}(T_{sh} - T_i)}_{\text{radiation}} + \tag{15b}$$

$$\underbrace{\rho_{sh} e_{sh} (h_{ads} + h_{fg}) \frac{dR_{sh}}{dt}}_{\substack{\text{heat released by absorption} \\ \text{of water vapor or evaporation}}}$$

where C_{sh} is the specific heat of the shirt. T_{sk} is the local skin temperature for the sensate ($T_{sk,sen}$) or insensate ($T_{sk,insen}$) region of the trunk. The heat of adsorption of water vapor (h_{ads}) is correlated to the relative humidity of the shirt (RH) as reported in the study of Gibson (Gibson, 1996). In addition, RH is correlated to the shirt regain and can be predicted to find P_{sh} (Mortan and Hearle, 1975).

2.6.5.2. Wet condition of the shirt at the sensate skin of the trunk

The wet condition of the shirt is limited to the sensate skin since sweating can occur at a rate of $\dot{m}_{sw}$ once T_{cr} value exceeds that of the onset of sweating (37.1 ± 0.2

°C) (Wilsmore, 2007). The wet condition is established once sweat accumulated at the sensate skin, m_{acc}, reaches 31.5 g/m^2 for persons with PA, which is 10% less than that of AB (Fitzgerald et al., 1990; Wilsmore, 2007). When $m_{acc} \geq 31.5$ g/m^2, a finite amount of liquid is captured by the shirt (M_{cap}) depending on the transient mass change of accumulated sweat on the skin; thus, P_{sh} would be assumed equal to the saturated pressure at its temperature. The mass balance to predict the moisture mass of the shirt, M_{sh}, is shown in Eq. 15(c) (Bachnak et al., 2018):

$$\underbrace{\frac{dM_{sh}}{dt}}_{\text{storage term}} = M_{cap} - \underbrace{\frac{P_{sat}(T_{sh}) - P_a}{\frac{1}{2h_{e,a}}h_{fg}}}_{\text{moisture transfer by convection}} \tag{15c}$$

where M_{cap} is obtained using Eq. 15(d):

$$M_{cap} = \frac{dm_{acc}}{dt} = \dot{m}_{sw} - \frac{P_{sk} - P_{sh}}{R_{e,sh}h_{fg}} \tag{15d}$$

The energy balance equation of the **shirt facing sensate skin** of the trunk is given by (Bachnak et al., 2018):

$$\underbrace{\rho_{sh}e_{sh}C_{sh}\frac{dT_{sh}}{dt}}_{\text{storage term}} = \underbrace{\frac{T_{sk} - T_{sh}}{\frac{e_{sh}}{2K_{eff}}}}_{\substack{\text{conduction from} \\ \text{sensate skin to shirt}}} - \underbrace{\frac{T_{sh} - T_a}{\frac{e_{sh}}{2K_{eff}} + \frac{1}{2h_{c,a}}}}_{\text{convection}} - \underbrace{h_{r,sh}(T_{sh} - T_i)}_{\text{radiation}} +$$

$$\underbrace{h_{liq}M_{cap}}_{\substack{\text{enthalpy of captured} \\ \text{liquid water}}} - \underbrace{\frac{P_{sat}(T_{sh}) - P_a}{\frac{1}{2h_{e,a}}}}_{\text{evaporation}} \tag{15e}$$

where h_{liq} represents the enthalpy of liquid water.

2.8. Integration of Hybrid ECV model into PA-bioheat model

The transient PA-bioheat model adopted in this work is the multi-segmental bioheat model for persons with thoracic injury level below T6; T6 inclusive (T6-T12) of (Mneimneh et al., 2019a, b). The model can predict thermal response of a person with

SCI taking into consideration the disruption in thermoregulatory responses and limited sensate skin of the trunk. The model divides the human body into 31 segments: the head, chest, upper back, pelvis, lower back, upper arms, forearms, palms, fingers, thighs, calves, and feet. Each segment consists of 5 nodes: the core, skin, artery, vein, and superficial vein. Hence, it solves five energy balance equations for each node, taking into consideration the boundary conditions at the skin/clothing with the environment. The input parameters to the PA-bioheat model are defined at the beginning of the simulation which include the metabolic rate, clothing layers, and environmental conditions.

The PA-bioheat model was validated using previous studies in literature about persons with PA (Attia and Engel, 1983; Price and Campbell, 2003). In addition, it was used for modelling the effect of PCM cooling vest for this vulnerable population (Mneimneh et al., 2019a, b). The model predicted core and local sensate/insensate skin temperatures as well as sensible and latent heat losses at the trunk with good agreement with the findings of the published studies in literature.

2.7.1. Ambient conditions and initial body conditions

The integration of hybrid ECV model into PA-bioheat model is done by ensuring the continuity of heat and mass fluxes between the skin of the trunk and the shirt at any time. At the sensate skin of the trunk (the chest and the upper back), liquid sweat would be captured by the shirt once the accumulated amount of sweat exceeds 31.5 g/m^2, and the shirt vapor pressure would be equal to its saturated pressure (Jones, 1992; Umeno et al., 2001; Wan and Fan, 2008).

For the numerical simulations, it is aimed to simulate the real-life scenario of a person with PA who is at thermal neutrality and then gets exposed to outdoor ambient

conditions to perform certain activity while wearing the hybrid ECV knowing that the fan operation occurs from the beginning of the exposure till end of exercise. The initial conditions of the thermal state (core and skin temperatures) of the body as well as that of the clothing temperature and regain are specified for the case of a person seated at rest (1.4 met) in an environment of 23 °C, *RH* 50%. Then, the attained steady state trunk-skin and shirt temperatures were used as initialization for the start of exercise in outdoor ambient conditions. Furthermore, the initial temperature values of the vest layers were set equal to the indoor condition of 23 °C, and the estimated amount of water in the vest upon activation was set at 0.6 kg, similar to that reported in previous experimental studies (Ciuha et al., 2020; Eijsvogels et al., 2014; Procter, 2017). Three cases were investigated by the simulations: No-Vest (shirt without vest), Type II (shirt covered by ECV vest, but fan is off during the whole exposure period), and the hybrid vest (shirt covered by ECV vest while operating fan is on during the whole exposure period).

2.7.2. *Numerical solution*

The mass and heat transfer energy equations for the hybrid ECV model with PA-bioheat model are solved numerically using the explicit Euler forward method with a time step (Δt) of 0.02 sec over the desired simulation period. The selected time step was chosen small to account for the complete cardiac cycle of the heart which approximately takes 0.8 sec for the neutral state of the body and can vary depending on the metabolic rate (Salloum et al., 2007).

First, the simulation was conducted to reach the neutral steady thermal state of the body and clothing before using the hybrid ECV as explained in the previous section. Then, at specified time reading ($t + \Delta t$) where the neutral steady state of the core and

skin temperature was attained, the hybrid ECV model subroutine was then started. It calculated the temperature and vapor pressure of the shirt, microclimate and ECV layers covering each segment of the trunk (chest, upper back, abdomen, and lower back) at specified outdoor ambient condition and metabolic rate. The following parameters were then used in the hybrid ECV model: i) the temperature and vapor pressure for sensate/insensate trunk-skin; ii) the mass of sweat accumulated at the sensate skin, and iii) the fan flowrate. For the hybrid vest, the fans were ON during the whole exposure period of exercise; while for ECV Type II, the fans were OFF. Then, the new calculated values of shirt temperature and pressure were used as the input to the PA-bioheat model to update the trunk-skin temperature and vapor pressure to ensure continuity of heat and mass fluxes at any time. Moreover, the PA-bioheat model calculated the segmental skin and core temperature of the remaining body segments.

After each complete iteration, the average body values of core and skin temperatures as well as cardiac output were calculated and compared to threshold values of thermoregulatory responses in persons with PA to identify whether vasodilation and sweating need to be activated for body segments above injury level. These steps were repeated until the simulation time duration was finished. The flow chart for the numerical methodology of the hybrid ECV model integrated into the PA-model is presented in **Fig. 7**.
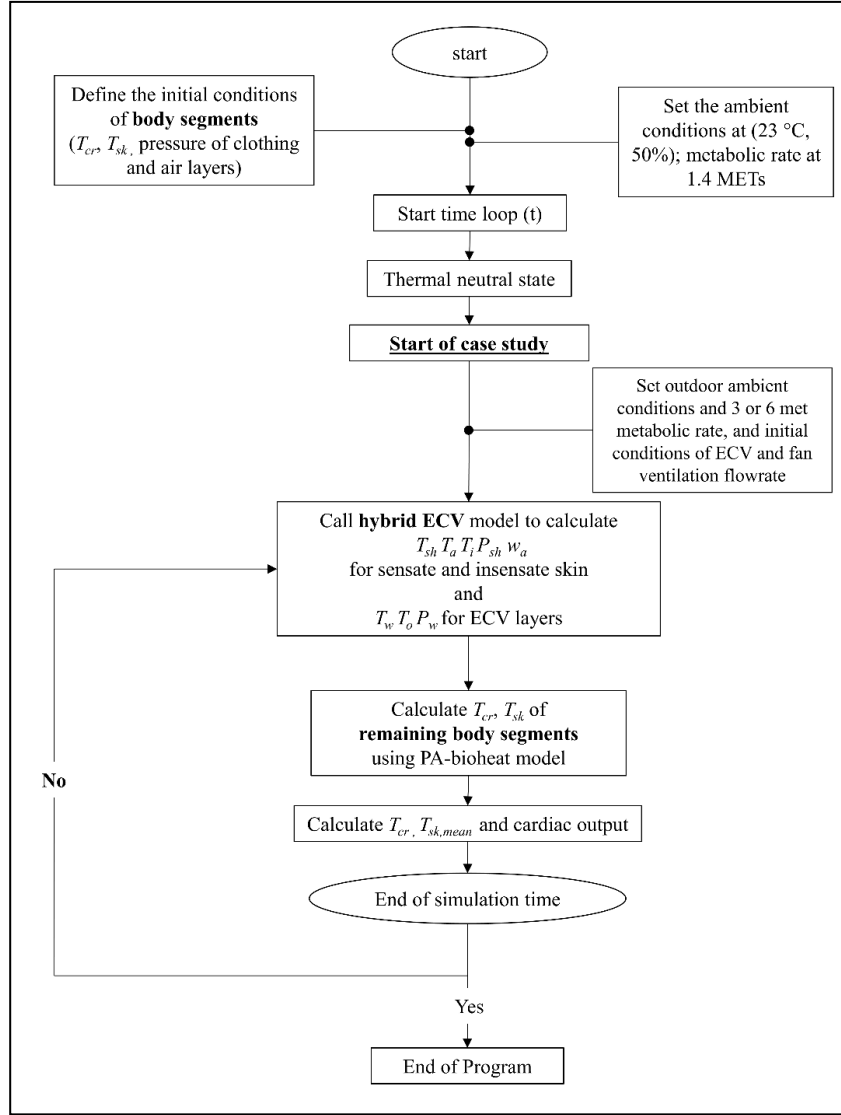
Figure 7. Flow chart of numerical methodology of hybrid ECV model integrated into

PA-bioheat model

2.9. Parameters for evaluating hybrid ECV performance

The combined hybrid ECV with PA-bioheat model is used to evaluate hybrid

ECV performance. Thermophysiology responses such local skin temperature variations

of the sensate and insensate skin nodes ($T_{sk,sen}$ & $T_{sk,insen}$) are predicted for the three

cases: No-Vest, Type II, and the hybrid vest, at a range of ambient conditions, and

moderate/high physical activity levels. In addition, the time-averaged sensible

87

(Q_{sens} W/m^2) and latent (Q_{lat} W/m^2) heat losses at the sensate/insensate skin of the trunk are predicted for two periods; before and after sweat capture by the shirt, in order to highlight the effect of sweat capture on heat loss.

Furthermore, for the hybrid ECV, the contributions of the fan and the ECV material on the heat losses at the sensate skin are presented. Finally, the enhancement factor (ε_{ECV}) in total hybrid ECV heat losses ($Q_{vest} = Q_{sens} + Q_{lat}$) from the sensate and insensate skin of the trunk compared to No-Vest ($Q_{No-Vest}$) case is defined in Eq. 16 as follows:

$$\varepsilon_{ECV} = \frac{Q_{vest}}{Q_{No-Vest}} \qquad (16)$$

2.10. Parametric study of Hybrid ECV-PA bioheat model

A parametric study using the integrated hybrid ECV and PA-bioheat model was conducted to investigate its effectiveness in providing cooling for persons with PA during exercise. In each case, a person with PA was initially at rest (1.4 met) at moderate indoor conditions (23 °C, 50 % *RH*) wearing a cotton T-shirt, trousers, underwear-pants, underwear-shirt, socks, and shoes with intrinsic dry thermal resistance of 0.5 clo (0.0775 m$^2\cdot$K/W). Then, the person engaged in a physical activity for a typical period of 60 min (Ginis et al., 2010; Urbański et al., 2021). For the hybrid vest case, the fan flowrate was set at 2.5 l/s to maintain low speed (< 1 m/sec) in the microclimate (air gap thickness = 1 cm). Initial temperature of the hybrid ECV layers was at the steady room temperature of 23 °C before being used by persons with PA. The simulated metabolic rates and outdoor ambient conditions are summarized as follows:

- Metabolic rate: 3 or 6 met (Collins et al., 2010)

- T_{amb}: 28, 32, or 36 °C

- *RH*: 30 or 60 %

The selected ambient conditions (temperature and relative humidity) cover the range of moderate/hot and dry/humid conditions at which persons with PA are prone to thermal strain upon heat exposure even at sedentary activity level (Attia and Engel, 1983).

CHAPTER 3

EXPERIMENTAL RESEARCH METHODOLOGY

3.1. Experimental methodology for validation of hybrid ECV model

The aim of the experiment is to validate the hybrid ECV model at the wet region of the shirt covering the sensate skin and the dry region of the shirt covering the insensate skin. The dry and wet shirt conditions reflect the thermal physiology at the trunk of a person with PA. The setup was conducted on a horizontal flat heated plate covered with a shirt in a climatic chamber. Commercially available material of ECV Type II and ventilation fans (Type I) were used. The transient temperature profile of the shirt, the microclimate air layer, the three layers of hybrid ECV and the transient change in the weight of the whole system (shirt and vest) were recorded.

3.1.1. Experimental Setup

Figure 8(a-b) presents the experimental setup showing (a) the shirt covering flat heated plate and ventilation fans and (b) ECV material mounted on a sensitive digital precision scale to monitor the weight loss from the system due to water evaporation. The heated plate is formed of a 30 cm × 40 cm rectangular plate covered with 4 metallic resistance heaters Omega-KH-412, used to generate a constant flux condition by monitoring the supplied voltage. Three similar ventilation battery-driven fans were mounted at the heated plate and operated at fixed flowrate of 3.5 L/s, which can be provided by commercially available fan cooling jackets (Itani et al., 2019; Xu and Gonzalez, 2011; Yi et al., 2017). A cotton shirt, placed in direct contact with the heated plate, was divided into two equal regions separated by an impermeable material to

90

account for two regions of the shirt: wet at the sensate and dry at the insensate skin. Additionally, commercially available ECV Type II material, Kewlshirt tank top (HyperKewl, TechNiche, Europe), was used in the experiment (see **Fig. 5(a)**. The properties of the shirt, inner and outer layers of ECV Type II material are presented in **Table 15**. Finally, Styrofoam insulation was used to insulate the sides and the back of the heated plate.

1. Wet shirt
2. Dry shirt
3. Ventilation fans
4. Pocket for iButton sensor
5. Thermocouple
6. ECV material support
7. ECV material
8. Sensitive digital precision scale
9. Styrofoam insulation
10. Datalogger
11. Impermeable liner
12. Flat heated plate
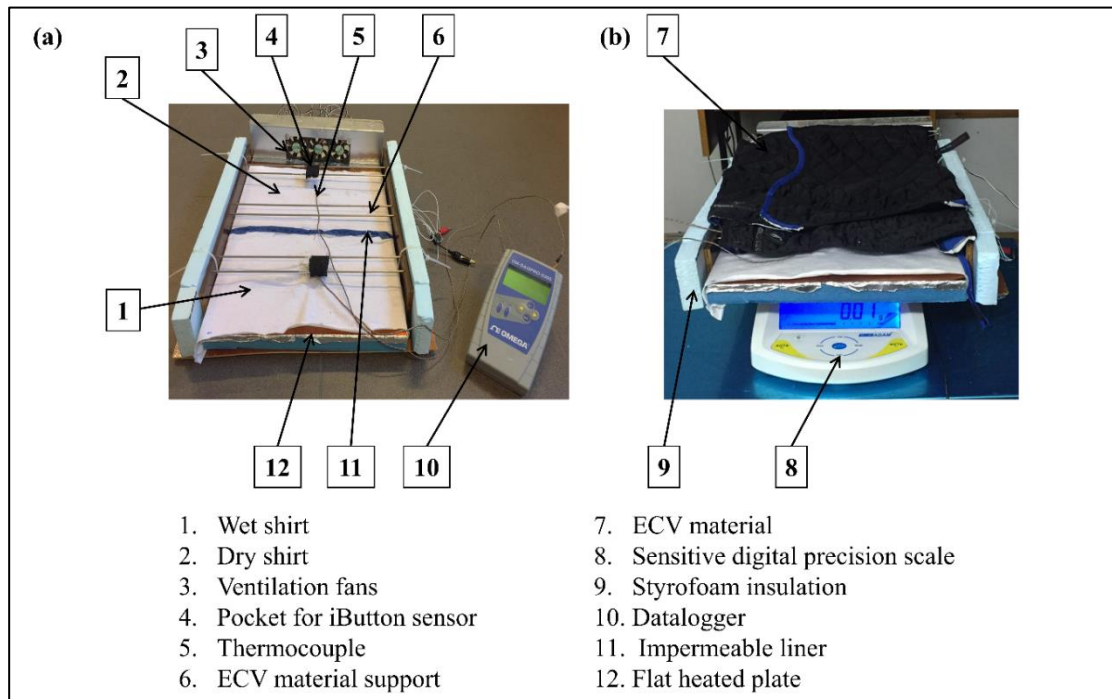
Figure 8. Experimental setup showing (a) shirt covering flat heated plate and ventilation fans and (b) ECV material mounted on a sensitive digital precision scale

Table 15. Properties of the shirt, inner and outer layers of ECV Type II material

Layer	Thickness (mm)	Dry thermal resistance in $m^2 \cdot K/W$ (clo)	Evaporative resistance ($m^2 \cdot kPa/W$)
Cotton shirt	4.0	0.006 (0.04)	0.0050

Inner vest layer: water-repellent 100% nylon	0.4	0.031 (0.20)	-
Outer vest layer: breathable 100% nylon	0.4	0.027 (0.17)	0.0005

The setup was tested at two ambient conditions inside the climatic chamber: 28 °C, 63% *RH* and 32 °C, 45% *RH*, depicting the common exposure conditions for persons with PA. Dry bulb temperature and *RH* sensor were used to measure the ambient conditions of the climatic chamber, as summarized in **Table 16** with the list of sensors used and their corresponding accuracy. OMEGA K-type thermocouples were placed at the dry and wet regions of the shirt, at the sensate and insensate regions of the inner layer of the vest, water-absorbent layer, and outer layer of the vest, as shown in **Fig. 8(a-b)**. Moreover, iButton sensors were placed inside small thin pockets between the shirt and the vest to measure the temperature and *RH* of the microclimate for the dry and wet regions of the shirt. Finally, hotwire anemometers were used to measure the air velocity at the exit channel.

Table 16. List of sensors with its corresponding accuracy used in this experiment

Equipment/Sensor	Measured Parameter	Accuracy
Digital precision scale PGW3502, Adam Equipment	Weight loss from shirt and ECV material	$\pm$ 0.01 g, with maximum reading of 3500 g
Sweating guarded hot plate (Model 306-200/400), Measurement Technology Northwest	Dry and evaporative resistances	error $< 0.1\%$

Dry-bulb temperature and RH sensor (OM-EL_WIN_USB, OMEGA, UK)	Ambient temperature and RH	± 0.5 °C at typical temperature range (35–80 °C) and 3% at typical RH range (20–80%)
K-type thermocouples, OMEGA	Sensate and insensate shirt temperature	± 1.1 °C accuracy, 0.1 °C resolution
iButton sensors (DS1923 Hygrochron Temperature/RH Data Logger, Maxim Integrated, CA, USA)	Microclimate air temperature and RH	± 0.5 °C accuracy, 0.0625°C resolution
Hotwire anemometer, SWEMA 03	Air speed and temperature leaving the vest air channel	±0.04 m/s and ± 0.1 °C

3.1.2. Experimental Protocol for ECV testing

The experiment was conducted for a period of 30 min as it was sufficient for temperature variations of the shirt, the microclimate, and the three layers of ECV to reach steady state. The climatic chamber was set at the desired ambient condition, the heaters were powered on at constant heat flux of 54.2 W/m^2, and the shirt was placed in contact with the heated plate without being wetted at first. Once ECV material was activated, one region of the shirt was wetted, and the weight was measured (0.42 kg/ m^2). ECV material was activated by being first immersed in water of initial steady state at room conditions (24 °C, *RH* 50%) outside climatic chamber; then, remove excess water by squeezing from top to the bottom without twisting the fabric to make sure that no more dripping of water from the vest occurred. The weight of ECV was measured before and after activation to obtain the initial amount of the water saturated (2.5 kg/m^2).

Thermocouples were located on each of the inner layer, outer layer, and the water-absorbent layer of ECV material, respectively. For the water-absorbent layer, small holes were made to fix the thermocouple inside this layer for accurate measurement of its temperature. For the inner and outer vest layers, adhesive thin tape (NITOTHROUGH, Nitoms) was used to fix thermocouples. Then, ECV material was placed in front of the shirt covering the heated plate using the support shown in **Fig. 8(a)** at a 15 mm gap and fixed by clamps. Finally, the fans located near the dry region of the shirt were operated.

During the 30-min duration of the experiment, all results of transient temperature profile and weight loss of the setup were recorded at a one-minute interval and were extracted for analysis and comparison with model predictions at two ambient conditions. To minimize the measurement errors, each test was repeated three times, and the measured temperatures were averaged to be compared with the simulations performed by the hybrid ECV model for validation (Wang and Song, 2017).

3.2. Human subject experiments with PCM cooling vests

Human subject experiments were conducted on persons with PA for the optimized design of the PCM cooling vest derived from the predictions of the Fabric-PCM-PA bioheat model. Testing was done inside a climatic chamber of moderate conditions (30°C, 50%) to perform an arm-crank exercise of fixed mechanical load (30 Watts), while monitoring and recording the physiological (heart rate, core and skin temperature) and psychological responses (thermal sensation and comfort votes, skin wettedness and perceived exertion) of the recruited subjects. As mentioned in previous sections, persons of PA were chosen to be the group of interest in this research since this group can be active and wheelchair dependent compared to the group of cervical SCI. The participants

were divided into three groups based on anatomy and physiology of thoracic injury (T1-T12).

Three types of PCM cooling vest were tested. With the first type, PCM packets of melting temperature 20 ℃ covered the trunk sensate and insensate skin area (chest, abdomen, upper back, middle back) and was tested in the three groups. With the second, the PCM packets of melting temperature 20 ℃ covered only the sensate skin of trunk (chest and middle back) based on injury level and was tested in the second group only. With the third type, PCM packets of melting temperature 14 ℃ covered the trunk sensate and insensate skin area (chest, abdomen, upper back, middle back) and was tested in the first two groups. All cases were compared to the case of no vest test. Accordingly, the hypothesis was that i) the effectiveness of PCM cooling vest can be significantly dependent on injury level; ii) cooling the sensate skin of the trunk rather than the whole trunk may be effective in attenuating the rise in T_{cr} for persons with PA.

3.3. Human subject experiments with ECV Type II

Human subject experiments were conducted on persons with PA for the use of commercially available ECV Type II (water-absorbent material) to be compared with the experimental findings of PCM cooling vests at same metabolic rate and ambient conditions. As mentioned earlier, testing was done inside a climatic chamber of moderate conditions (30°C, 50%) to perform an arm-crank exercise of fixed mechanical load (30 Watts), while monitoring and recording the physiological (heart rate, core and skin temperature) and psychological responses (thermal sensation and comfort votes, skin wettedness and perceived exertion) of the recruited subjects.

ECV covering the sensate and insensate region of trunk, it was tested for the second and third groups of participants with PA. All cases were compared to the case of no vest test. Accordingly, the hypothesis was that the performance of ECV Type II can be analogous to first type of PCM cooling vest at certain ambient condition and metabolic rate, but with the advantage of reducing perceived exertion due to less burden of vest weight and less restriction in body movement.

3.4. Categorization of human subjects

Persons with PA are in general distinctive by the paralysis of legs (thighs, calves, and feet) with the loss of physical sensation in the legs and trunk (Kirshblum et al., 2011a). However, the portion of impairment in the trunk is not the same among thoracic spinal cord injuries as shown in **Fig. 9(a-c)**. People with (T1-T2-T3) SCI have impairment in the whole trunk area except upper part of chest and shoulders and 75% of trunk skin area is insensate (see **Fig. (9a)**. People with (T4-T8) SCI have impairment from the level of the lower side of the chest (level of the nipples) and upper back until end of trunk and 50% of trunk skin area is insensate (see **Fig. (9b)**. Finally, people with (T9-T12) SCI have impairment in the portion of the middle back and the abdomen until end of trunk and only 25% of trunk skin area is insensate (see **Fig. (9c)** (Kirshblum et al., 2011a; Salloum et al., 2007). Not only is the degree of impairments in thermoregulatory responses different among thoracic SCI levels, but also metabolic rate obtained during exercise differed among them. Previous studies reported that the same external load of exercise performed by persons with PA produced different values of oxygen uptake, an indication of different metabolic rates (Veeger et al., 1991; WICKS et al., 1983). These studies showed that people with an injury level above T6 (T1-T5) had a significantly lower oxygen uptake

(by 22 ±6 %) compared to those of injuries below T6 (T6-T10) ($p<0.05$). Therefore, cardiorespiratory responses in persons with PA may vary based on injury level and affect amount of heat gained in the body during exercise.
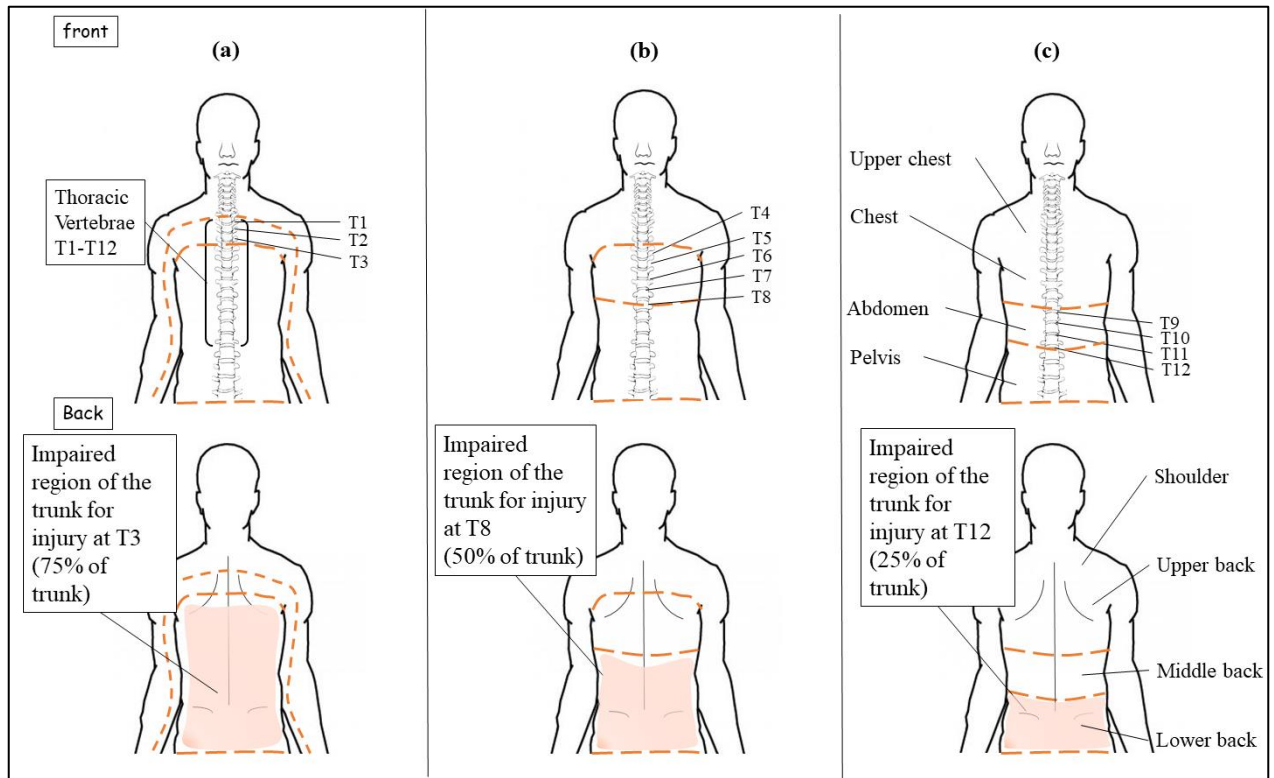
Figure 9. Schematic showing the frontal and back regions of impairment in the trunk
due to SCI at the thoracic vertebrae (a) T1-T3 (b) T4-T8 (c) T9-T12

During recruitment of persons with PA, the lesion level was obtained from participants' medical records and radiological findings. In addition, the severity of injury was determined based on a physical exam performed by the neurosurgeon in charge for recruitment, following the International Standards for Neurological Classification of Spinal Cord Injury (ISNCSCI) exam (Kirshblum et al., 2011a). According to the anatomy and physiology of thoracic spinal cord, the participants were divided into three groups: **Group I**: high-thoracic (T1-T3); **Group II**: mid-thoracic (T4-T8); and **Group III:** low-

thoracic (T9-T12) as shown in **Fig. 9(a-c)**. This categorization intended to compare thermoregulation during exercise with and without the vest on people with thoracic SCI based on their metabolic rate, portions of sensate skin area of the trunk, as well as, thermoregulatory disruptions (Kehn and Kroll, 2009; Melo et al., 2019).

3.5. Recruitment and medical examination of human subjects

Ethical approval to carry the study on persons with PA was obtained from the Institutional Review Board (IRB) at the American University of Beirut (AUB). Sixteen persons with SCI who are wheelchair dependent were selectively recruited for this study. The inclusion criteria were specified and approved by IRB as follows: i) complete/incomplete thoracic SCI (T1-T12); ii) the age in the range of 25-45 yrs.; iii) the average weight in the range of 75 ± 10 kg and the average height in the range of 170 ± 10 cm; iv) the duration of injury of minimum one year for medical stability; v) the participant of a wheelchair user; and vi) no implanted electro-medical device or gastrointestinal disease. As a result, the recruited participants were middle-aged (31 ± 6 yrs.) males and females with incomplete thoracic SCI (T3-T12) with an average weight (67 ± 11 kg) and an average height (171 ± 7 cm). The least injury duration was more than one year (9 ± 9 yrs.), and the cause was trauma of the spinal cord due to vehicle and constructions' work accidents.

All participants confirmed their commitment to a physiotherapy program provided by the recreation center and participated in exercise or performed outdoor chores at least two times per week. **Table 17** presents participants' physical properties including age, gender, weight, height as well as, injury level, its severity and its duration. No significant difference of these physical properties ($p>0.05$) was obtained between groups.

Since participants had the injuries older that one year, the medical status and physiological responses were assumed stable as the body would become adaptive to the complications of the injury (Krause and Crewe, 1991). In addition, because of lack of availability of eligible participants with complete thoracic SCI during recruitment, persons with incomplete thoracic SCI of ASIA B or C were accepted for participation. There is low likelihood of intact thermoregulation in these persons as previous studies reported that even when sensory innervation is partially preserved, complete loss of autonomic innervation can occur (e.g., ASIA B or C) (Mathias, 2004).

Table 17. Physical properties of participants

Subject	Age (yrs.)	Gender	Weight (kg)	Height (cm)	Level of Injury	Duration of Injury (yrs.)	ASIA Impairment Scale (Melo et al.)	Group
1	30	M	80	175	T3	2	B	I
2	33	M	71	178	T3	8	B	I
3	24	M	65	165	T3	2	B	I
Mean (SD)	29±5	-	72±8	173±7	-	4±3		
4	30	F	48	160	T8	12	B	II
5	42	F	62	162	T8	24	C	II
6	32	M	70	175	T8	11	B	II
7	25	M	77	180	T8	7	C	II
8	40	M	60	165	T6	33	C	II
9	22	M	55	170	T8	1	C	II
10	36	M	70	175	T7	6	B	II
11	25	M	70	172	T6	4	C	II
Mean (SD)	32±7	-	64±10	170±7	-	12±11		
12	30	F	60	165	T11	14	C	III
13	36	F	45	160	T12	10	B	III
14	31	M	80	175	T11	7	C	III
15	25	M	69	171	T12	6	B	III
16	35	M	82	183	T12	1.5	B	III
Mean (SD)	31±4	-	67±15	171±9	-	8±5		

B= sensory incomplete; C= motor incomplete (Melo et al.)

The clothing/uniform of the participants consisted of a 50% cotton- 50% polyester t-shirt, trousers, underwear-pants, underwear-shirts, socks, and shoes with an average dry thermal resistance of 0.5 ± 0.1 clo (0.0775 ± 0.01 m²·K/W). Each participant's first visit was a medical examination, a briefing about experimental protocol, listing the physiological and psychological parameters to be recorded, and signing a consent form.

3.6. Sample size

A minimum sample size per group was a requirement to detect the significant change in T_{cr} (ΔT_{cr}) and T_{sk} (ΔT_{sk}) to assess the effect of cooling vest on persons with PA. Thus, a priority power analysis calculated the minimum number of participants per group using GPower software of version 3.1.9.4. The sample size analysis was based on a power of test of 90% and a level of significance α of 5% (Griggs et al., 2017; Griggs et al., 2015; Price and Campbell, 2003). Sixteen participants with PA joined this experimental work. For **Group I**, a sample size of three participants (n=3) was assigned for a minimum significance of $\Delta T_{cr} = 0.6 \pm 0.2°C$ and $\Delta T_{sk} = 1 \pm 0.2°C$. For **Group II**, a sample size of eight participants (*n*=8) was defined for a minimum significance of $\Delta T_{cr} = 0.25 \pm 0.2°C$ and $\Delta T_{sk} = 1 \pm 0.2°C$. This number of participants was recruited to increase statistical power about effectiveness of the two configurations of the cooling vest for the mid-thoracic group. Finally, a sample size of five participants (*n*=5) was assigned for **Group III** for a minimum $\Delta T_{cr} = 0.3 \pm 0.2°C$ and $\Delta T_{sk} = 1 \pm 0.2°C$.

3.7. PCM cooling vest of melting temperature 20 ºC and 14 ºC

A polyester cooling vest that was commercially designed to hold up to 22 equally sized PCM packets was used in this study. The PCM packets used in the experiment were

made of a salt mixture of sodium sulfate and water known as Glauber's salt (Gao et al., 2012) with a melting point of 20℃. The thickness, area, mass, and heat of fusion of one PCM packet were 1.3 cm, 101.84 cm^2, 155 g, and 113.0 kJ/kg respectively (Swedish Emergency and Disaster Equipment AB, 2017; All Safe Industries, 2017). The melting period duration of the selected PCM packets could extend up to two hours under hot conditions (35℃) and moderate metabolic rates ($\cong 3\ METs$) as reported in previous studies in literature (Itani et al., 2017; Itani et al., 2016).

The current study focuses on two types of PCM vests of melting temperature 20 ℃ where each type covered a certain area of the trunk; however, it is worth noting that the covered trunk area might have different portions of sensate and insensate areas depending on the injury level. The first vest named, vest-type1 (V1), comprised of PCM packets, which covered the chest, upper back, middle back, and abdomen as seen in **Fig. 10(b)**. All three groups were tested with this type of vest. In the second type of vest, named vest-type2 (V2), PCM packets were placed on the chest and upper back to target sensate skin area only (**see Fig. 10c**), which resulted in lower vest weight. This type of vest was tested for **Group II** as this group had variation in the sensate/insensate portion of the trunk unlike **Groups I** and **III**.
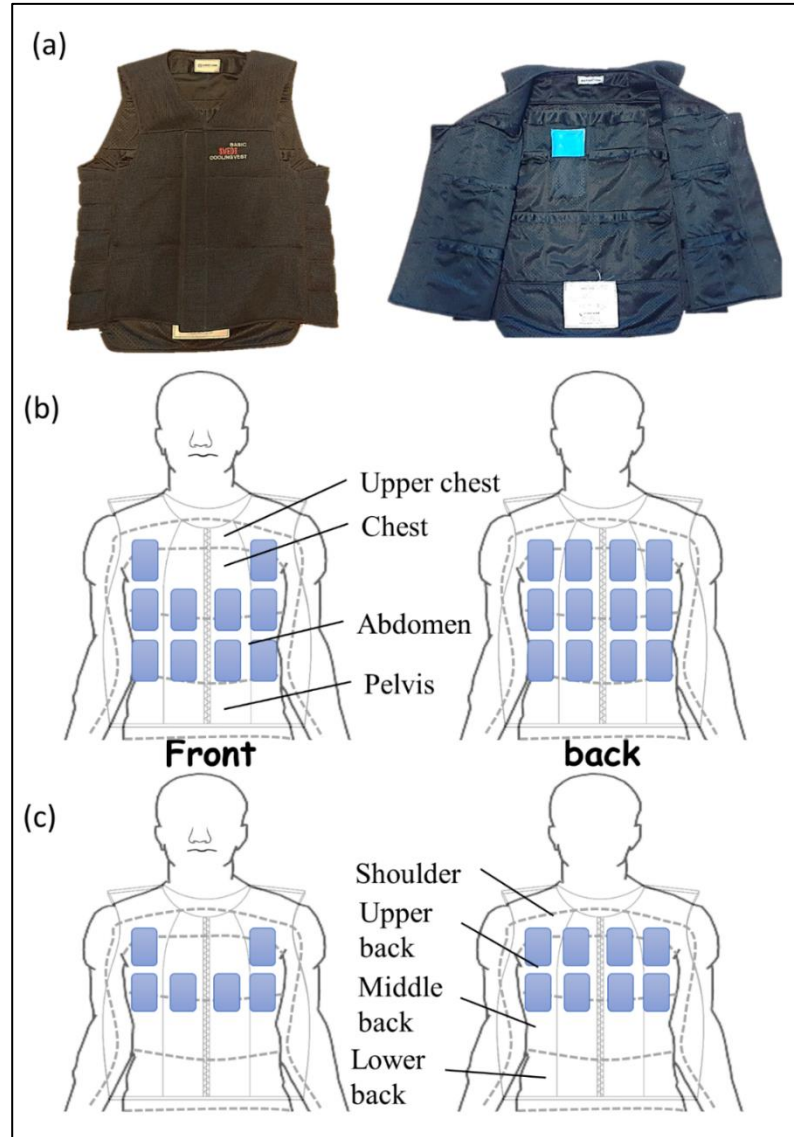
Figure 10. Picture of (a) PCM cooling vest and blue PCM packet inserted (b) configuration of type1 covering chest, upper back, middle back and abdomen, and (c) configuration of type2 covering chest and upper back

The comparison between two types of the vest is indicative whether cooling the sensate skin using V2 rather than whole trunk using V1 can be as effective in reducing T_{cr} for the mid-thoracic group. The mass of cooling vest and the PCM coverage area at the trunk were both 36% less in V2 than in V1. Based on the categorization of the

recruited participants, **Groups I** and **III** performed two experiments: no-vest (NV) and V1 tests; whereas, **Group II** performed three experiments: NV, V1, and V2 tests.

A commercially available PCM cooling vest of melting temperature 14 ℃ (V14) was selected for this study. It included 4 packets of non-toxic carbon-based liquid (Alkane Blend) of melting point (14°C) as seen in **Fig. 11**. The thickness, area, mass, and heat of fusion of one PCM packet were 1.1 cm, 550 cm2, 454 g, and 95.5 kJ/kg, respectively (Kewlshirt tank top, TechNiche Europe). The melting period duration of both selected PCM packets can extend up to two hours under hot conditions (35°C) and moderate metabolic rates ($\cong$3 METs), as reported in previous studies in the literature (Itani et al., 2017; Itani et al., 2016). Based on the categorization of the recruited participants, **Groups I** and **II** performed experiment using V14 to be compared with the findings of NV and PCM cooling vest of melting temperature 20 ℃ which covered the chest, upper back, middle back, and abdomen tests, named in this case V20. The comparison between two types of the vest is indicative whether lowering melting temperature can provide further effectiveness for persons with PA of higher thoracic SCI (T1-T8).

Figure 11. Picture of PCM cooling vest of melting temperature 14 ℃ (V14)

Table 18 summarizes the physical properties of the three types of the cooling vest of melting temperature 20 ℃/14 ℃ and the percentage difference between them.

Table 18. Physical properties three types of the cooling vest of melting temperature 20 ℃/14 ℃

Parameter	V1 (V20)	V2	% ($\frac{V2-V1}{V1}$)	V14
Total PCM mass (kg)	3.41	2.17	- 36%	2.7
Total PCM coverage (cm²)	2240.5	1425.8	- 36%	2200
% Coverage from total area (6666 cm²) of trunk	34%	21%	-	33%
Total PCM coverage at the front of trunk (cm²)	1018.4	611.1	- 40%	1100
Total PCM coverage at the back of trunk (cm²)	1222.1	814.7	- 33%	1100
% Coverage at the front of trunk (3333cm²)	31%	18%	-	33%
% Coverage at the back of trunk (3333cm²)	37%	24%	-	33%

3.8. ECV Type II

A polyester cooling vest commercially designed to achieve rapid absorption and stable water storage was used in this study. The Kewlshirt tank top (HyperKewl, TechNiche, Europe) is a lightweight cooling vest of 0.2 kg weight when dry; comprised of a quilted nylon outer layer with HyperKewlTM polymer; a water-repellent nylon liner and an elastic trim made of cotton and polyester as seen in **Fig. 12**. It was designed to thermoregulate the body during exercise based on evaporative technology without adding unnecessary weight. The vest was activated by simply submerging the item in water for 1-2 minutes allowing the fabric to absorb the water. Then, it was lightly squeezed to remove any excess water to be ready to wear. The garment was to remain activated up to three hours and can be re-hydrated by repeating these simple steps. This type of vest was tested on able-bodied persons in previous studies in literature (Eijsvogels et al., 2014; Procter). Based on the categorization of the recruited participants, **Groups II** and **III**

performed experiment using ECV to be compared with the findings of NV and PCM cooling vest of melting temperature 20 ºC which covered the chest, upper back, middle back, and abdomen tests, named in this case V20. The comparison between two types of the vest is indicative whether ECV can provide further effectiveness for persons with PA similar to PCM cooling vest.
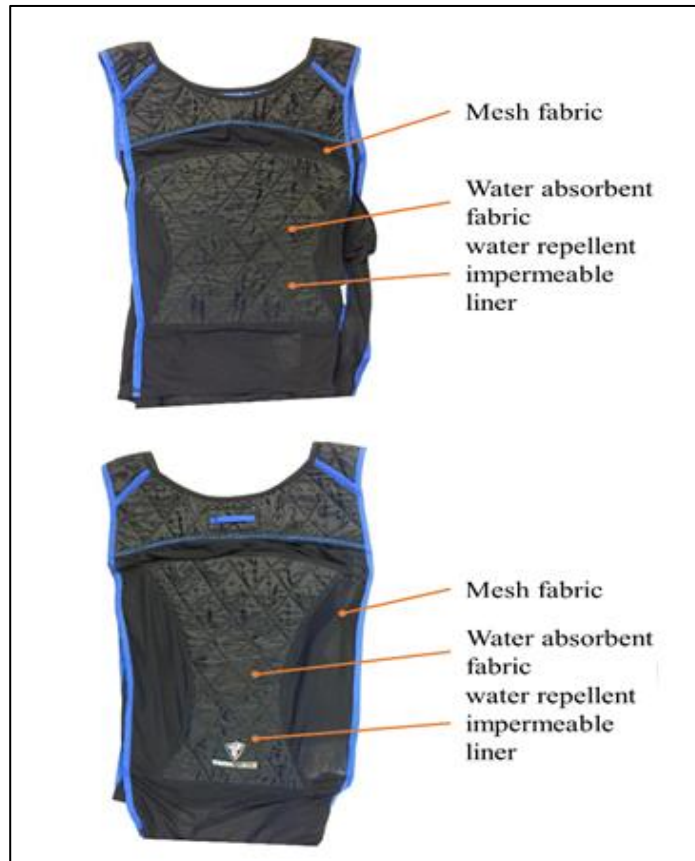
Figure 12. Picture of ECV Type II

3.9. Physiological and physical measurements

Dry bulb temperature and relative humidity sensor (OM-EL_WIN_USB, OMEGA, UK, 0.5°C and 0.5% resolution) measured every 1 min the ambient conditions of the climatic chamber. The accuracy of this sensor is reported to be $\pm 0.5°C$ at typical temperature range (35 to 80°C) and 3% at typical relative humidity range (20 to 80%).

Temperature iButton sensors (iButton DS19221, Maxim Integrated, CA, USA, 0.0625°C resolution) were taped on seven human body segments at 10 positions (chest, upper back, lower back, pelvis, forehead, forearm, palm, thigh, calf and foot) and recorded a measurement every 1 min throughout the one-hour period of preconditioning, exercise, and post exercise. The average accuracy of the iButton temperature sensors is 0.1°C when used at the environmental conditions of (30°C and 50%) with a maximum deviation of 0.4°C (van Marken Lichtenbelt et al., 2006). In order to ensure proper contact with the skin, a surgical tape was used to place the sensors on the different segments (van Marken Lichtenbelt et al., 2006). Mean skin temperature values were calculated using Hardy & Du Bois (1938) weighting formula of **Eq. 17**:

$$T_{sk,mean} = 0.35 \times T_{trunk} + 0.19 \times T_{thigh} + 0.14 \times T_{forearm} +$$
$$0.13 \times T_{calf} + 0.07 \times T_{forehead} + 0.05 \times T_{palm} + 0.07 \times T_{foot} \tag{17}$$

where the trunk skin temperature was calculated by averaging the skin temperatures of chest, upper back, lower back, and pelvis.

Heart rate was recorded every 5 min using a pulse oximeter (Model 2500A PalmSAT, NONIN, USA, ±3 bpm accuracy). The values of T_{cr} were measured in two ways: using an activated ingestible pill and using an infrared tympanic thermometer, IRTT. The ingestible pill (eCelsius, BodyCap, France) was configured using e-Celsius Performance Manager software and its monitor (eViewer Perf CE monitor, BodyCap, France) to read every 30 sec the gastrointestinal temperature, as an indicator of T_{cr}. The accuracy of the pill is ± 0.2°C. In addition, recording of the tympanic temperature was done every 5 min using IRRT (Braun ThermoScan 7 IRT6520, Braun, Kronberg, Germany, accuracy± 0.2°C).

Change in body temperature (ΔT_{body}) was calculated using the formula of **Eq. (18a)** (Burton, 1935; Griggs et al., 2015; Song et al., 2015):

$$\Delta T_{body} = 0.8 \times \Delta T_{cr} + 0.2 \times \Delta T_{sk,mean} \tag{18a}$$

In addition, the amount of heat stored (H_s) in the body during exercise when not wearing the cooling vest and during was defined as **Eq. (18b)** (Burton, 1935; Chou et al., 2008):

$$H_s = m_{body} \times C_p \times \frac{\Delta T_{body}}{t} \quad (W) \tag{18b}$$

where m_{body} is the mean body mass of sample (kg), C_p is the body specific heat (3490J/kg·°C), ΔT_{body} is the change in mean body temperature, and t (s) is the exercise duration.

The thermal sensation of head, neck, shoulders, and trunk on a scale of 0 to 5; wetness sensation on skin and clothing on a scale of 1 to 6; overall thermal comfort sensation on a scale of 0 to 5; and the rating of perceived exertion on a scale of 0 to 6 were evaluated from the actual votes of the subjects at the beginning of exercise and every 10 minutes throughout the test (Gagge et al., 1967; Griggs et al., 2015; Toner et al., 1986). **Table 19** summarizes the different reference scales of the subjective voting by the participants. These subjective questionnaires were explained to the participants on their first visit before any scheduled experiment.

Table 19. Reference scales for subjective ratings

Thermal Comfort Scale (Gagge et al. 1967)	0 neutral	1 comfortable	2 slightly uncomfortable	3 uncomfortable	4 very uncomfortable	5 extremely uncomfortable

Wetness of Skin and Clothing Scale (Grigg 2015)	1 *more dry than normal*	2 *normal dryness*	3 *slightly wet*	4 *wet*	5 *body wet*	6 *body wet, clothing sticks to the skin*
Head, neck and shoulders Thermal Sensation Scale (Toner et al. 1986) Trunk Thermal Sensation Scale (Toner et al. 1986)	0 *neutral*	1 *slightly warm*	2 *warm*	3 *hot*	4 *very hot*	5 *extremely hot*
Perceived Exertion Scale (Borg 1982)	0 *extremely light*	1 *very light*	2 *fairly light*	3 *somewhat hard*	4 *hard*	5 *very hard*

3.10. Experimental design

All experiments conducted were at the same time in the afternoon inside a climatic chamber. The chamber was equipped by a centralized air-conditioning ducted system and contained the arm-crank ergometer (Angio rehab with automatic stand, Lode, Netherlands). All participants performed the arm-crank exercise at constant load of 30 W to limit the variability in metabolic rate generation between subjects of the same group (Trbovich et al., 2016). Furthermore, previous studies in literature reported similar experiments for persons with SCI at constant load of exercise (Ishii et al., 1995; Petrofsky, 1992; Yamasaki et al., 2001). However, performing the same load of exercise, persons

with PA are expected to generate different metabolic rates based on injury level because SCI affects maximal oxygen uptake as lung capacity is lower in high thoracic levels (Brown et al., 2006; Veeger et al., 1991; WICKS et al., 1983). **Fig. 13(a-b)** shows two of the recruited participants: (a) one female not wearing the vest and (b) one male wearing the vest doing the arm-crank exercise inside the climatic chamber.
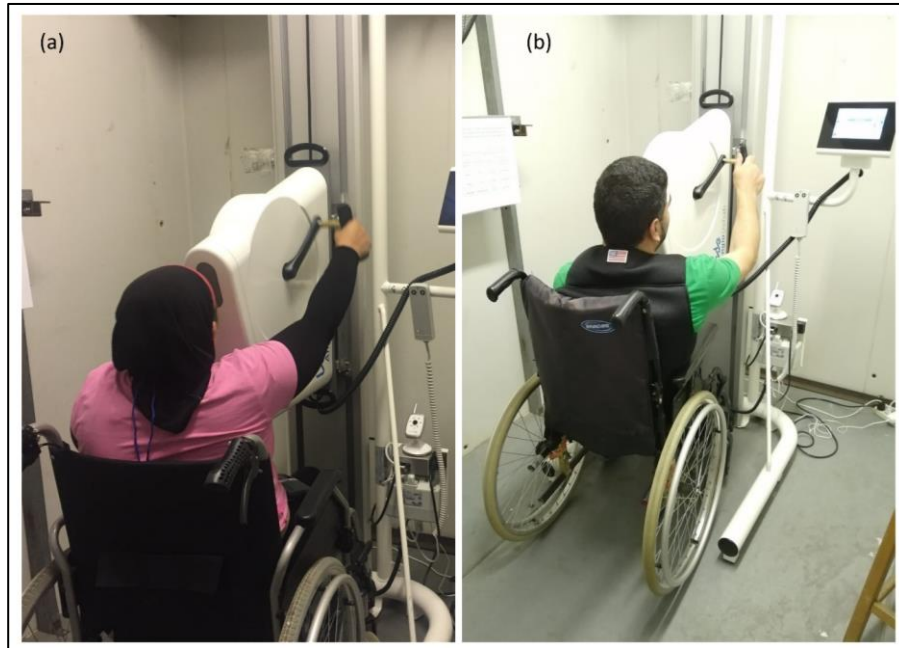
Figure 13. Pictures showing (a) one female participant doing exercise without vest and (b) one male participant doing exercise with vest

The climatic chamber conditions were set at warm humid conditions of 30°C room temperature set point and 50% relative humidity. These conditions were monitored and measured using temperature and a relative humidity sensor. The reported measurements for all experiments showed a small deviation from set conditions ($30.6 \pm 0.1°C$ and $50 \pm 5\%$). **Fig. 14** summarizes the detailed steps of the protocol on the day of the experiment. During the one-hour experiment, core and skin temperatures were recorded every minute using the ingestible pill and skin sensors respectively, but for monitoring purposes, tympanic temperature and heart rate values were checked every five

minutes under the surveillance of a nurse. Precautions were implemented for stopping the

experiment if any of the two conditions occurred to avoid any risk for the participants: i)

the core temperature reaches 38.5 °C and/or ii) if the participant wishes to stop any time

during the experiment (Griggs et al., 2015).

Location:
Heat Transfer & Energy Research Laboratory, Irani Oxy Building

Prior to the experimental session
- ingest an activated telemetric pill at a minimum of 2-3 hours

Arrival on-site
- Briefing on experiment
- Empty bladder and avoid fluid/food intake
- Preparation of participant (skin sensors allocation, synchronization of pill with monitor, attachment of pulse oximeter sensor to the ear
- Rest for 30 minutes in the research laboratory (24°C , 50%)

Time= 0 mins → **Enter the climatic chamber**
$(30.6 \pm 0.1°C, 50 \pm 5\%)$
- Participant rests for 15 minutes
- Beginning of tympanic (core) temperature and heart rate recording

Time= 15 mins → **Start of arm-crank exercise**
- Participant exercises on a arm-crank ergometer at a power load of 30 W (at about 2.8 Mets) for a period of 30 minutes

	Group I	Group II	Group II
NV	x	x	x
V1	x	x	x
V2		x	
V14	x	x	
V20	x	x	
ECV		x	x
V20		x	x

- Votes are reordered every 10 minutes about thermal comfort, thermal sensation, skin wettedness and perceived exertion

Time= 45 mins → **End of exercise**
- Recovery period of 15 minutes

Time= 60 mins → **Exit the climatic chamber**

Figure 14. Schematic of a brief description of the experimental procedure

3.11. Data Analysis Methodology

Comparison of the effectiveness of the cooling vest was considered within each group separately due to the variability of metabolic rate among thoracic SCI levels at the same load of arm-crank exercise (30W). The physiological responses (T_{cr}, T_{sk}, HR), as well as, subjective voting (thermal comfort, sensation, skin wettedness and perceived exertion) of the participants were analyzed using the Statistical Package for Social Sciences (SSPS version 25).

For NV and V1 tests, for groups **I** and **III**, paired-sample tests (parametric and non-parametric tests), were found suitable since this study aimed to compare the measured parameters before and after using the cooling vest (paired sample: NV vs. V1) at an interval of five minutes for the whole one-hour experiment. If the data was normally distributed, paired sample t-Test was used; otherwise, the data was evaluated using the Wilcoxon signed-rank test. The sample size of **Group (I)** (n=3) was found not to affect the data analysis of this group due to the fact of limited heterogeneity in the sensate skin portion of the trunk of the high-thoracic SCI group (Griggs et al., 2015; Hazra and Gogtay, 2016; Price and Campbell, 2003). For NV, V1 and V2 tests, for **Group II**, two-way ANOVA with repeated measures (test x time) was chosen since the changes in the physiology were investigated under three conditions. Previous studies in literature applied this test (Armstrong et al., 1995; Price and Campbell, 2003; Trbovich et al., 2014). For NV, V20 and V14 tests, the physiological and psychological responses for groups **I** and **II** were compared also using two-way ANOVA with repeated measures (test x time). Significance was accepted at the $p < 0.05$ level. Similarly, For NV, V20 and ECV tests, the physiological and psychological responses for groups **II** and **III** were compared also using two-way ANOVA with repeated measures (test x time). Where significance was

obtained, Scheffé *post hoc* analysis was undertaken. All data were reported as mean (±SD).

CHAPTER 4

THEORETICAL RESULTS

4.1. Validation of TP-bioheat model

The TP-Bioheat model validation was done by comparing its predictions of core and skin temperature with a number of physiological studies on human subjects with TP published by other researchers (Attia and Engel, 1983; Gass et al., 2002; Griggs et al., 2017; Guttmann et al., 1958; Trbovich et al., 2016). These independent studies included reporting experimental data on the thermal response in different steady-state and transient thermal environments with different level of physical activities appropriate for the SCI. However, some of the experimental limitations were difficulty and challenge in recruiting human subjects for experiments with all level of injuries. For each published experimental study about persons with TP, a description is provided of the conditions reported in the experiment followed by the comparison with model predictions of reported measured physiological and thermal parameters.

4.1.1. Comparison with steady-state ambient conditions and different activity levels

4.1.1.1. Comparison with Attia et al. (1983) data on seated at rest in steady-state conditions

Attia et al. (1983) performed an experimental study for the behavioral and autonomous thermoregulation in a group of nine patients with SCI compared against a control group of six AB under various room climate conditions (Attia and Engel, 1983). Among these subjects, one was with cervical spinal cord injury. All subjects were dressed

in light summer costumes of an estimated 0.4 Clothing-value. The subjects were exposed to a constant room temperature for 45 minutes on different days at the same time of the day in the climatic chamber. Each subject was exposed to a total of six ambient temperatures, namely, 15, 20, 25, 30, 35 and 40 °C; the air speed (0.2-0.3 m/s) and *RH* (45%) were kept constant. Every exposure was preceded by a 15-min fore-chamber exposure of the ambient temperature 22.25 ± 0.95 ºC and *RH* 50 %. The subjects were sitting comfortably on a wheelchair. Segmental skin temperatures were measured to calculate the mean skin temperature based on the weighting factor of each selected segment using **Eq. 19** proposed by Nadel (1977) which considers both area and sensitivity weighting:

$$T_{skin} = 0.21T_{face} + 0.17T_{abdomen} + 0.10T_{back} + 0.15T_{thigh} +$$

$$0.06T_{lowerarm} + 0.11T_{chest} + 0.08T_{calf} + 0.12T_{upperarm} \tag{19}$$

Validation was done by comparing the altered model predicted values of core temperature and mean skin temperature at different room temperatures to the experimental data of both AB and people with SCI. Salloum et al. model (2007) was also used to predict the thermal state of core temperature and the transient change in skin temperature for AB.

T_{cr} at different ambient conditions were compared between the simulated results and that of Attia et al. (1983). In **Fig. 15(a)**, the thermal state of person with TP obtained at the end of each simulation done using the altered model presents the steady-state reached by the mean core temperature at each room temperature (T_{room}) ranging between 15 – 40 ºC and *RH* 45% within a 45-min duration of exposure. The plotted results of the altered model and the experimental data showed that person with TP experienced higher T_{cr} than that of AB and persons with PA when $T_{room} > 25$ ºC (supposed to be range of hot

ambient condition). Contrarily, when $T_{room} < 25\ ^{o}C$ (supposed to be range of cold ambient condition), TP showed lower T_{cr} than that of AB and persons with PA. The predicted results included those of people with complete (CTPM) and incomplete tetraplegia (ITPM): ITPM showed closer values to that of experimental results of AB and persons with PA when $T_{room} < 25\ ^{o}C$, but both models CTPM and ITPM showed similar higher results when $T_{room} > 25\ ^{o}C$.

$T_{sk,mean}$ at two room temperatures were compared between the simulated results and that of Attia et al. (1983). **Fig. 15(b)** presents the transient change in $T_{sk,mean}$ when the participants, seated at rest, were subjected to hot ambient conditions at T_{room} 35 °C and RH 45%. The predicted $T_{sk,mean}$ followed similar pattern of change for both complete and incomplete tetraplegia, where it increased with time but at a higher rate of change than that of the experimental data until it reached the same value of the experimental data at the end of 60-minute simulation.

Fig. 15(c) presents the transient change in $T_{sk,mean}$ when the participants, seated at rest, were subjected to cold ambient conditions at T_{room} 20 °C and RH 45%. The predicted $T_{sk,mean}$ in this case follows the same pattern of change but at lower values in both ITPM and CTPM when compared to the experimental data. This could be justified by the fact that the current model implemented the vasomotor and sudomotor behaviors of person with TP whose level of injury varied between B (incomplete, sensory function but not motor function preserved below the neurological level and include the S4-S5 sacral segments) and C (incomplete, motor function preserved below the neurological level, and more than half of key muscles below the neurological level have a muscle grade less than 3) as compared to ASIA impairment scale; whereas, in the current literature data of Attia et al. (1983), majority of participants were with paraplegia; this means, that some of the

vasomotor and sudomotor responses are still activated in the arms and hands, unlike people with TP. This contributes to the great difference in body heat balance between the two groups; mainly in cold ambient conditions.
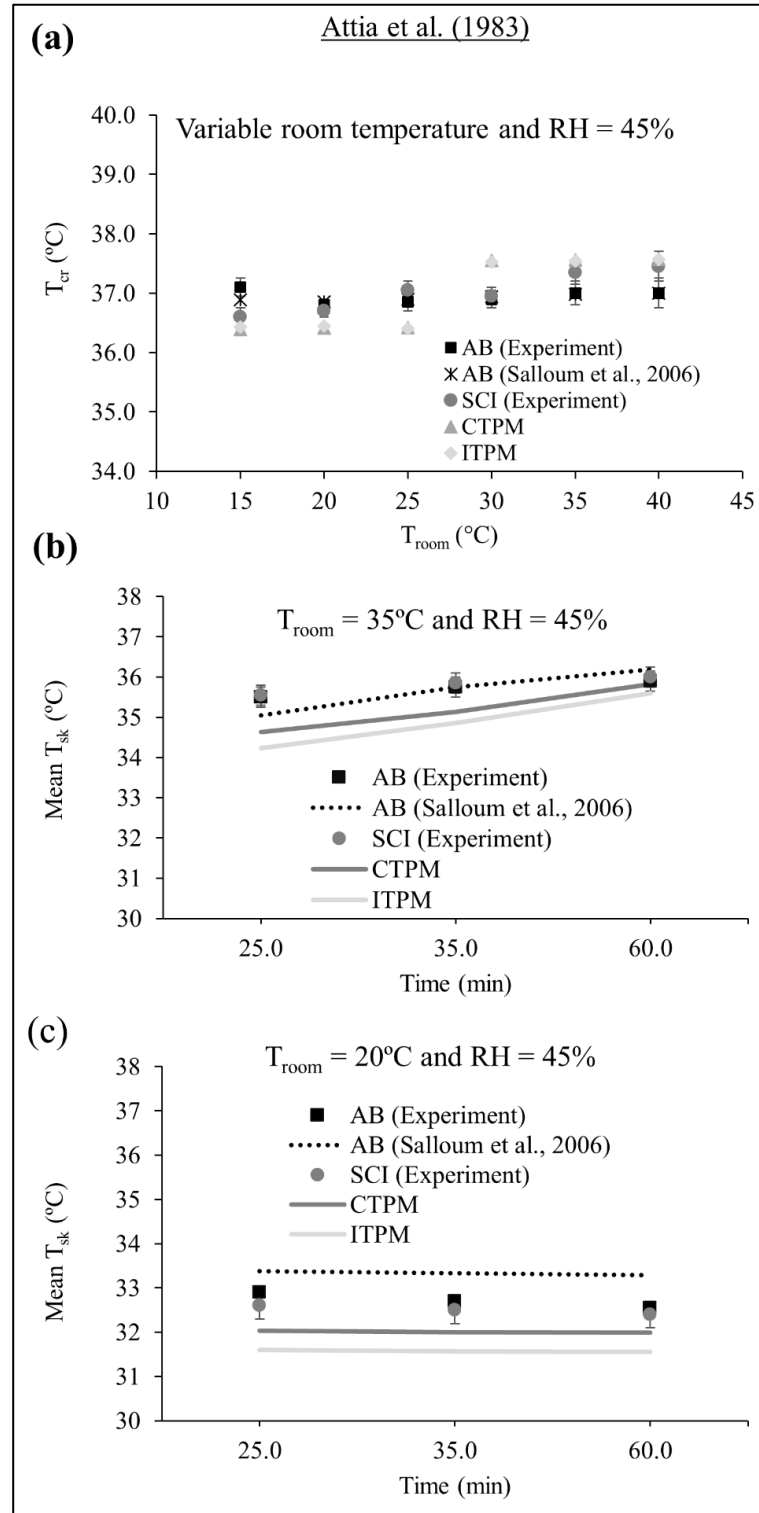
Figure 15. Comparison between the experimental data and the current model results of (a) T_{cr} at different T_{room} and same RH 45% (b) $T_{sk,mean}$ in hot condition (35°C) (c) $T_{sk,mean}$ in cold condition (20°C)

The current model displayed a steady state T_{cr} at the end of each simulation. The predicted T_{cr} presented the thermal steady state of person with TP at a certain ambient condition with a maximum error ±0.5°C including the maximum deviation of the experiment. Distinct from AB whose thermal neutrality ranges around 36.8 °C, the poikilothermic behaviour in person with TP is actually a new steady-state reached by the body whenever the environmental condition is changed as a result of new heat balance attained by the body with the surrounding (Attia and Engel, 1983).

The skin temperature, plotted for two ambient conditions 20 and 35°C, showed a difference of range (0.11°C - 0.70°C) for room temperature 35°C which is within the standard error of the experiment, whereas it showed a difference of range (0.07 °C – 1.0°C) for room temperature 20°C. The difference in T_{sk} between the experimental and the current model data presented in **Fig. 15(b-c)** can be justified by the discrepancy in SCI level among the participants. The studied group was a mix of different level of injury including cervical and thoracic level of injury, and the plotted data was the mean value among the subjects. This can explain the error in the accuracy of the obtained results. Therefore, it is expected to have a deviation of 1 °C in T_{cr} and T_{sk} between the results simulated and the ones from the experimental studies in literature due to the difference in the thermoregulatory responses between persons with TP and persons with PA. Actually, in persons with PA, not all vasomotor, sudomotor and shivering responses are interrupted

except for impaired segments; whereas, in case of person with TP, all segmental physiological responses are interrupted after cervical SCI (Guttman, 1958).

<u>4.1.1.2. Comparison with Trbovich et al (2016) data on arm-crank exercise in steady-state hot-exposure</u>

Trbovich et al (2016) performed an experimental study about the possibility of heat acclimation in persons with SCI. The groups were divided in to two: tetraplegic and paraplegic, consisted each of five subjects with different level of injury. Only the experiment with TP was simulated, where the participants were classified as complete and incomplete TP with C5-C7 level of injury.

First, the subjects were seating at rest in a preconditioning chamber at room temperature 22.4±1.1 ºC and < 40% *RH* for 15-min. Then, they entered an environmental chamber set at 35 ºC and 40% *RH* to begin 30-min arm crank ergometer exercise. Finally, the participants rested for 15-min post-exercise. This protocol has been applied for seven days. Segmental skin temperatures and aural temperature were measured. The experimental results showed increase in T_{cr} during the 30-min exercise and post exercise with insignificant change during the seven days of applying protocol. The resting aural temperature at t = 0 min was 35.9 ± 0.4 ºC during the seven days showing no heat acclimation in persons with TP. In addition, $T_{sk,mean}$ was calculated using Ramanathan (1964) **Eq. 20**:

$$T_{sk,mean} = 0.3T_{chest} + 0.3T_{arm} + 0.2T_{thigh} + 0.2T_{calf} \tag{20}$$

For the resting aural temperature (t = 0 min), the current model showed at time=0 sec T_{cr} = 36.20 ºC which is within resting aural temperature range obtained experimentally (35.9 ± 0.4 ºC). **Fig. 16(a)** shows the change in T_{cr} during a 30-min arm-

crank exercise in the hot conditions. The rate of increase in the predicted values of T_{cr} is similar to the ones extracted from the experimental data of (Trbovich et al., 2016). **Fig. 16(b)** presents the change in $T_{sk,mean}$ under the same ambient condition and metabolic rate. The rate of increase in the predicted values of $T_{sk,mean}$ is similar to the ones extracted from the experimental data of Trbovich et al. Compared against the experimental data, the current model displayed the same trend of change in T_{cr} with a maximum deviation 0.53 ℃, and $T_{sk,mean}$ with a maximum deviation 0.26 ℃.
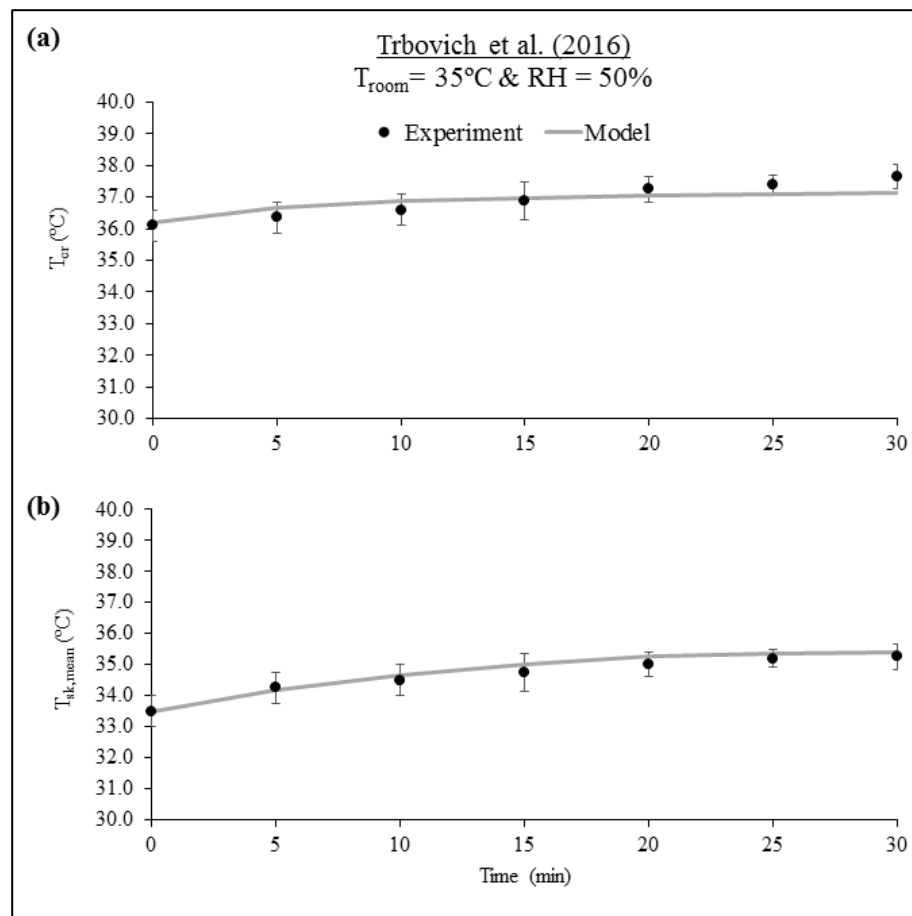
Figure 16. Comparison (a) Core and (b) mean skin temperatures, of people with TP at room temperature 35℃ and 50% *RH* for 30 minutes of arm-crank exercise compared between Experimental results and the simulated ones

4.1.1.3.Comparison with Gass et al. (2002) data on moving wheel chair exercise in steady-state neutral and humid exposure

Gass et al. (2002) performed an experimental study about the performance of athletic people with SCI during exercise in a hot environment (Gass et al., 2002). Four subjects with cervical SCI who were physically trained participated in this experiment. The experiment was a 40-min treadmill exercise which the participants were requested to roll their wheel chair on. It was performed in room temperature 23 ⁰C and *RH* 61.3%. Rectal temperature was measured. In **Fig. 17**, the predicted values in the current model are in compliance with experimental results where T_{cr} increases during the treadmill exercise due to the heat gain in the body and lack of sweating and vasodilatation to release heat. The maximum deviation between the two results obtained was 0.2 °C.
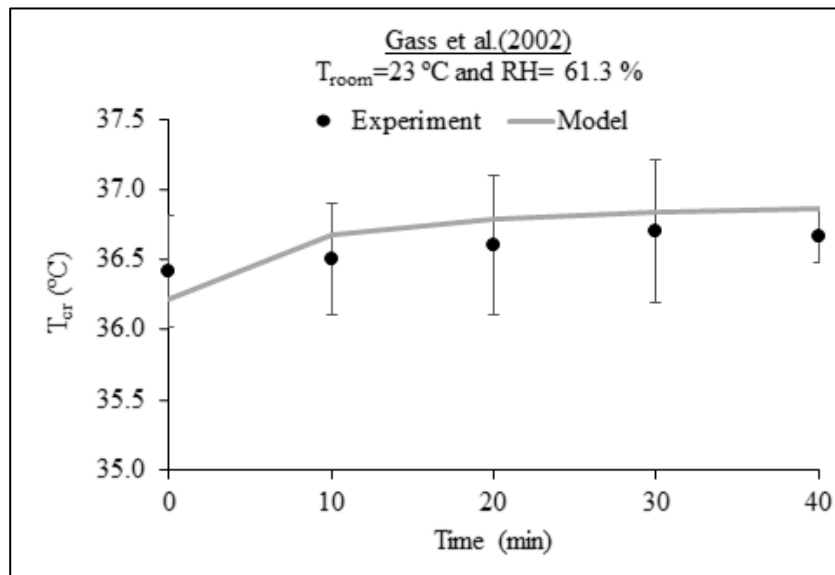
Figure 17. Plot of Tcr values of person with TP at room temperature 23⁰C and *RH* 61.3% obtained by the model and compared to experimental results

4.1.1.4.Comparison with Griggs et al. (2017) data on intermittent Sprint Exercise at steady thermal condition

Griggs et al. (2017) aimed to determine the extent of the thermoregulatory impairment for the athletes with an SCI during an intermittent sprint wheelchair exercise and post recovery in conditions representative of an indoor playing environment (Griggs et al., 2017). Eight wheelchair rugby players with TP participated in 60-min intermittent exercise in a room temperature 20.6 ± 0.1 °C and RH 39.6 ± 0.8 %, wearing thee light weight track suit trousers and short/long sleeved fitted top. The protocol of the exercise was an alternating scenario between three pushes forwards and backwards followed by maximum effort of sprint, and between active recoveries of low intensity. At the end, a passive recovery was taken for 15 minutes by all participants. As mentioned earlier in the transient at rest case study, T_{cr} was measured by swallowing pills (gastrointestinal temperature), and $T_{sk,mean}$ was calculated using Ramanathan (1964) stated in **Eq. 20**.

The current model adapted all the necessary exercise conditions including: temperature, RH, convection and radiation heat transfer coefficients, clothing resistance, and metabolic rate. The change in core temperature (ΔT_{cr}) and in mean skin temperature ($\Delta T_{sk,mean}$) has similar pattern compared to that of experimental results. **Fig. 18(a)** presents ΔT_{cr} with respect to intermittent exercise (exercise (E) and recovery (R) intervals), and the predicted values in the current model is in agreement with that of the experimental data; it followed similar trend of increase during the exercise. **Fig. 18(b)** presents $\Delta T_{sk,mean}$ with respect to intermittent exercise (exercise (E) and recovery (R) intervals), and predicted values are in agreement with that of the experimental data at the early stages of the intermittent exercise, but continued with higher trend than that of the experimental data. The mean error between the predicted value and the reported data in experiment was ± 0.5°C. Both skin and core temperature rise with time during performing the intermittent exercise by persons with TP. This variability in the core and skin temperatures of people

with complete or incomplete TP prove the thermoregulatory dysfunction and absence of vasomotor and sudomotor controls after SCI when the individual is doing certain physical activity.
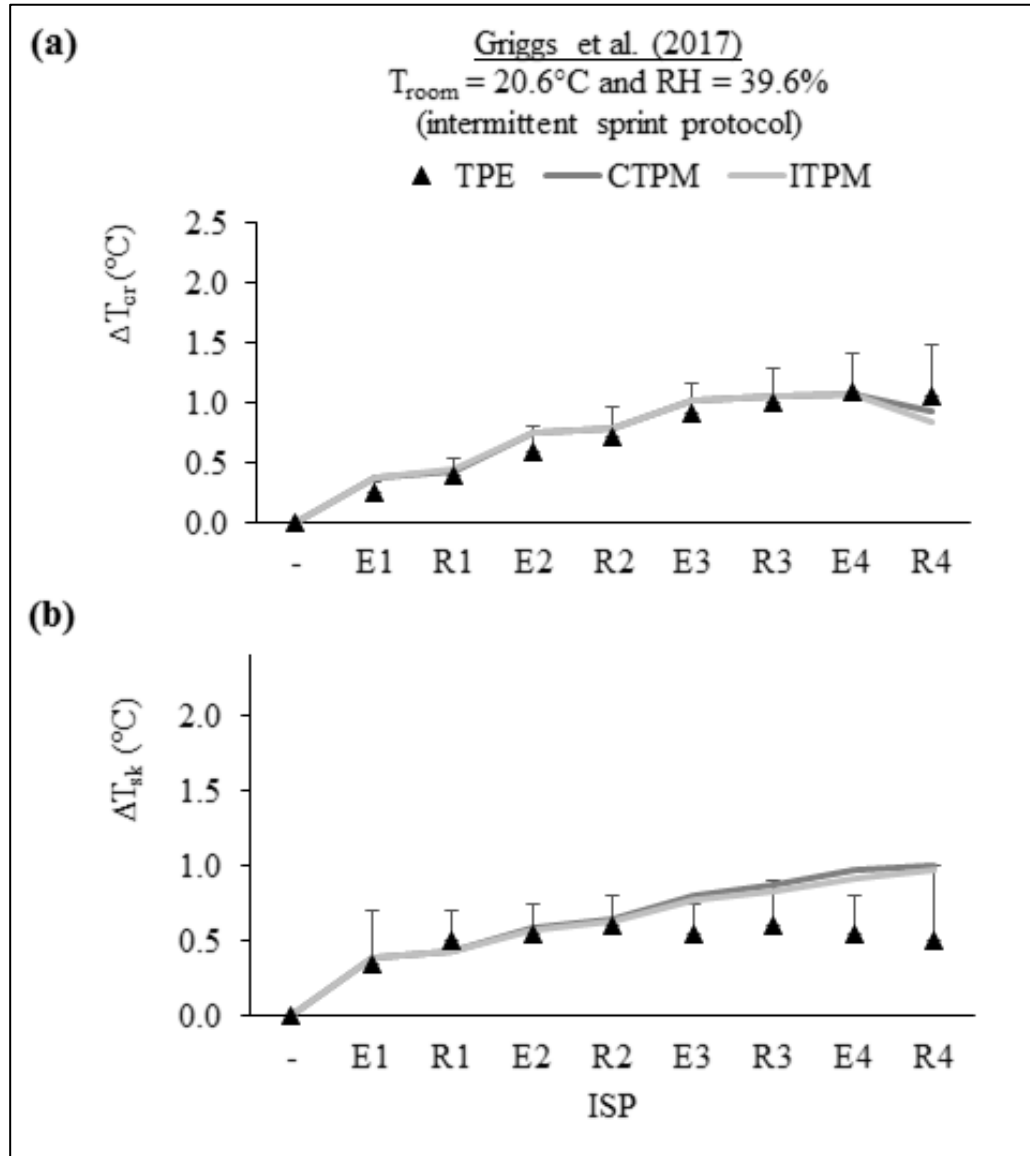
Figure 18. Comparison of simulated (CTPM: complete and ITPM: incomplete) and experimental values of (a) ΔT_{cr} and (b) $\Delta T_{sk,mean}$. E: exercise and R: recovery

4.1.2. Comparison with transient ambient conditions and different activity levels

4.1.2.1. Comparison with Guttmann et al. (1958) data on supine position in
transient environment exposure

Guttmann et al. (1958) performed an experimental study to understand the thermoregulation processes in spinal man. A group of human male patients with different level of SCI was exposed supine and naked first to an environmental temperature 27 ℃ and *RH* 40 % - 50 % for one hour. Then, the subject was transferred from the preconditioning zone to either cooler chamber (18 ~ 20 ℃) or hotter one (35 ~ 37 ℃) for the same *RH* for an hour and half or maximum two hours to assure the steady state is reached. The core temperature was measured rectally, and the skin temperature was measured at the segments (trunk, foot, finger, and forehead) using the following weighting segmental skin temperature (**Eq. 21**):

$$T_{skin} = 0.7T_{trunk} + 0.1T_{foot} + 0.1T_{finger} + 0.1T_{forehead} \tag{21}$$

The reported experimental measurements were compared to another research done by Hardy & du Bois (1941) on AB to bring out the alteration in the thermoregulatory responses due to the cord lesions. Therefore, the simulated results are validated by the results of two experiments mentioned above: one with person with TP and one with AB.

The patient with TP showed a high core and skin temperatures in the hot environmental condition (35 ~ 37 °C), and a low core and skin temperatures in the cold environmental condition (18 ~ 20 °C), indicating a poikilothermic behavior. Compared to the experimental results of Guttmann et al. (1958) as presented in **Table 20**, a maximum difference of 0.06 °C was observed between the average core temperature of the four participants and the simulated value in the current model for an environmental temperature 18~20 ℃. Also, a maximum variance of 0.75 °C was observed in the mean skin temperature predicted and the one extracted from the experimental data for the same

ambient conditions. In case of hot ambient condition (35~37 ℃), the body core temperature differed by 0.84 °C, while, the mean skin temperature differed by 0.9 °C. When compared to AB core and skin temperatures obtained by Hardy & du Bois (1941) and the one simulated by Salloum et al. model (2007), person with TP presented variability in both temperatures under hot and cold conditions whereas AB showed a steady state core temperature and great change in the skin temperature due to change in ambient conditions.

Table 20. Summary of Steady-state core temperature based on cold and hot environmental conditions

Room Temperature 18-20ºC and 50% RH at Supine Position			
Case Study (1)	**Subject**	**Core Temperature (ºC)**	**Mean Skin Temperature (ºC)**
Hardy & du Bois (1941)	AB	37	27.2
Salloum et al. model (2007)	AB	36.86	33.29
Guttmann et al. (1958)	C5 - C7	36.3 ± 0.2	30.85 ± 0.65
TP-Model	TP	36.17	31.6
Room Temperature 35-37ºC and 50% RH at Supine Position			
Case Study (2)	**Subject**	**Core Temperature (ºC)**	**Mean Skin Temperature (ºC)**
Hardy & du Bois (1941)	AB	37	35.2
Salloum et al. model (2007)	AB	36.86	36.36
Guttmann et al. (1958)	C5 - C7	38.07 ± 0.07	37.3 ± 0.1
TP-Model	TP	37.23	36.4

For the case study (1), **Fig. 19(a)** presents the chest skin temperature variation when the patient was initially preconditioned in $T_{room} = 27°C$ and then exposed to $T_{room} = 18\sim20$ °C. The predicted values in the current model followed similar rate of change compared against that of Guttmann et al. (1958) experimental data. It decreased when room temperature decreased at same *RH*. Similarly, **Fig. 19(b)** presents the same segmental skin temperature (chest) but for case study (2), where the subject was exposed to $T_{room} = 35\sim37$ °C after being preconditioned in $T_{room} = 27°C$. In addition, the predicted values in the current model followed similar rate of change compared against that of experimental data. It increased when room temperature increased at same *RH*.
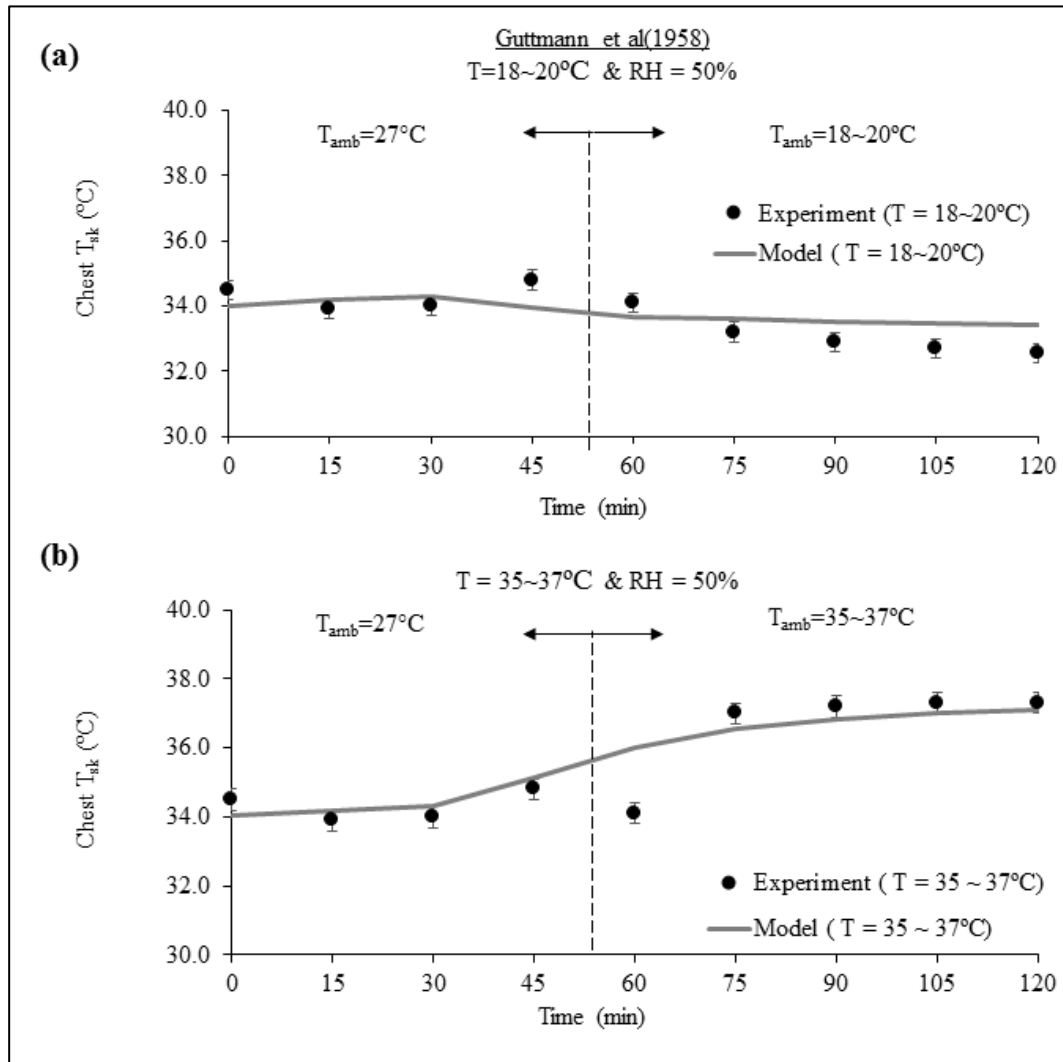
Figure 19. Skin Temperature of Chest at room temperature 27 ℃ for 1 hr. and at room

temperature (a)18 ℃~20 ℃ and (b)35 ℃~37 ℃ for extra 2 hr. compared between

Experimental results and the simulated ones

The current model displayed good outcomes compared to the literature data of Guttmann et al. (1958) for the case of supine position in transient environment exposure. In hot ambient condition, the maximum deviation of chest skin temperature simulated value from the experimental literature data is 0.44°C. In cold environmental condition, the simulated skin temperature is higher than that of the experiment with a maximum deviation 0.88°C.

4.1.2.2. Comparison with Griggs et al. (2017) data on seated at rest in transient thermal condition

Griggs et al. (2017) performed an experimental study to compare the evaporative heat loss and heat balance between AB and individuals with SCI with different lesion level. A group of 23 male participants, consisting of eight AB, eight persons with PA and seven persons with TP, were involved in a transient thermal condition experiment while being seated at rest (no activity using wheelchair). The room temperature was set at 37.2 ± 0.2 °C for the whole experiment, while the RH was incremented by 5% each seven minutes starting from an initial value of 20 %. All subjects were dressed in light summer costumes of an estimated 0.69 Clothing-value. Measurements of skin temperature were taken at the forehead, the right forearm, upper arm, chest, abdomen, upper back, thigh, calf, hand, and foot. Accordingly, the mean skin temperature was calculated using the mean skin formula of Ramanathan (1964) stated in **Eq. 20**. The core temperature was

determined by the gastrointestinal temperature, which was measured using telemetric pills swallowed by the participants.

Figure 20(a-b) shows ΔT_{cr} and $\Delta T_{sk,mean}$ respectively, within a transient ambient condition (increase in RH at a constant room temperature) for the people with TP obtained from the current model and compared to the experimental results. In **Fig. 20(a)**, the transient trend of ΔT_{cr} resulting from the model showed difference than that of experimental results with an error ± 0.45 °C including standard deviation of the experiment. In **Fig. 20(b)**, for the skin temperature, the results of $\Delta T_{sk,mean}$ in the model were higher with error ± 0.35 °C including standard deviation of the experiment. The increase in $\Delta T_{sk,mean}$ in the current model could be explained by the effect of not enough increment in the core temperature of either CTPM or ITPM as seen in **Fig. 20(a)** which limited the sweat rate in the model and reduced the effect of vaporization on cooling the skin temperature.
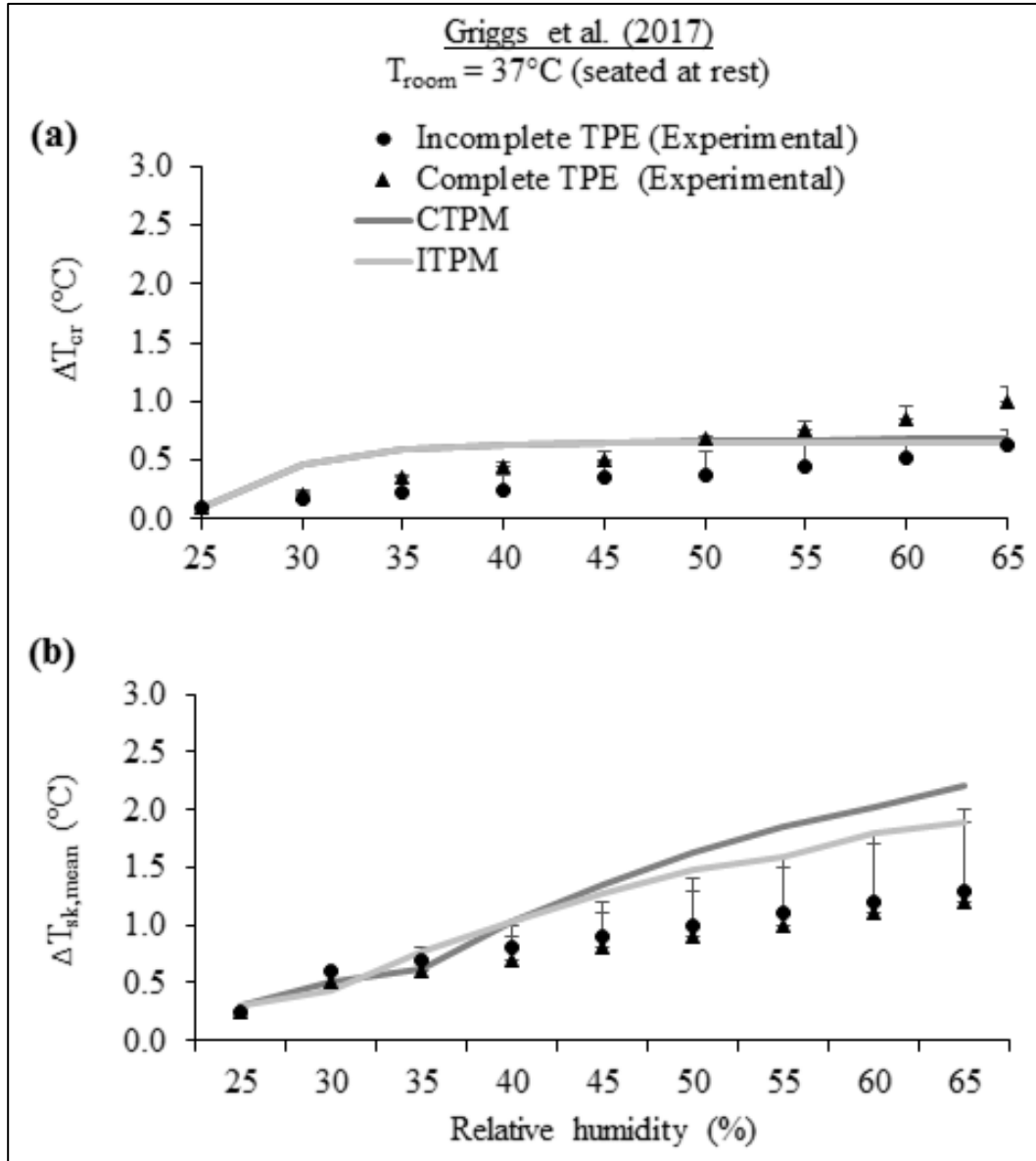
Figure 20. Plot of (a) ΔT_{cr} and (b) $\Delta T_{sk,mean}$ of person with TP at room temperature 37ºC

and incrementing RH by 5% obtained by the model (TPM) and compared to

experimental results by Griggs et al. (TPE)

However, the initial values of the core and mean skin temperatures at room temperature of 37 °C and *RH* 25 % showed great compliance between the simulated results and the ones measured in the experiment. Also, at the final increment in *RH* (65%), simulated core temperature was slightly below that of the experiment but within the

standard deviation. **Fig. 21(a)** presents the predicted values of core temperatures by the altered bioheat model and that Salloum et al. model (2007), at two ambient conditions: $RH = 25\%$ and $RH = 65\%$ compared to the experimental results of persons with TP and AB in Griggs et al. (2017). The modelled values showed similar results for the case of low RH at 25%, and higher difference for the case of high RH at 65%. However, negligible difference was observed in the predicted core temperature between complete and incomplete TP. **Fig. 21(b)** presents the predicted values of T_{cr} and $T_{sk,mean}$ by the altered bioheat model and that Salloum et al. model (2007), at two ambient conditions: $RH = 25\%$ and $RH = 65\%$ compared to the experimental results of persons with TP and AB in Griggs et al. (2017). Both models showed good agreement in T_{cr} values at both conditions. For $T_{sk,mean}$ values, it was noted that predicted values were higher than that of the experimental data at RH 25 %, however, similar values to that of experimental data at RH 65%. Moreover, slight difference was observed in the predicted mean skin temperature between complete and incomplete TP at RH 25%, while no difference is observed at RH 65%.
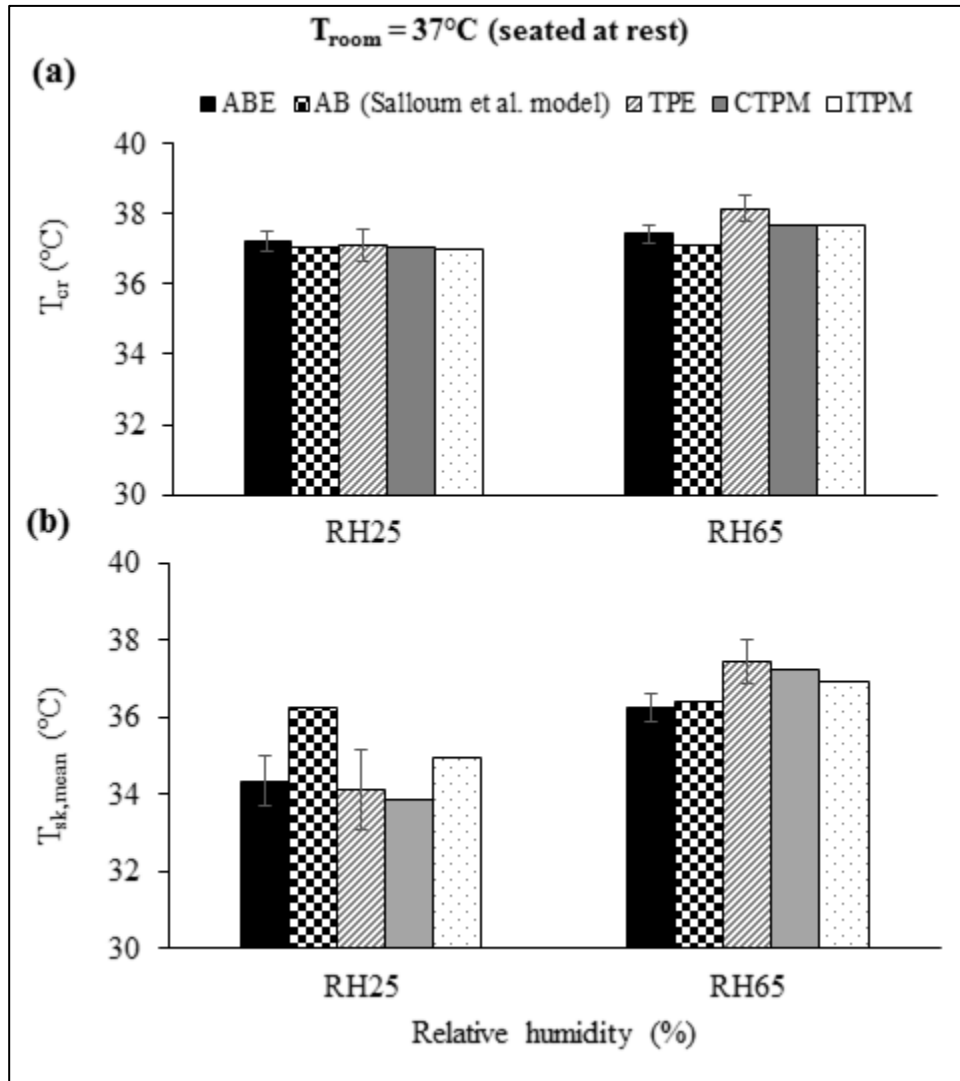
Figure 21. Bar graph presentation of (a) T_{cr} and (b) $T_{sk,mean}$ of AB (E: experimental), and

person with TP participated in the experiment (TPE) and that of TP-model (CTPM:

complete and ITPM: incomplete)

Figure 22 shows the predicted segmental skin temperature of the thigh for

complete and incomplete tetraplegia compared to experimentally reported values of

Griggs et al. (2017). The increase in thigh skin temperature was coupled with the increase

in the *RH*. The current model showed similar trend in thigh skin temperature compared

to that of the experiment, and no difference between the two cases of injury. Therefore,

it is possible to predict the segmental skin temperature of the lower body for person with

TP using the current model.
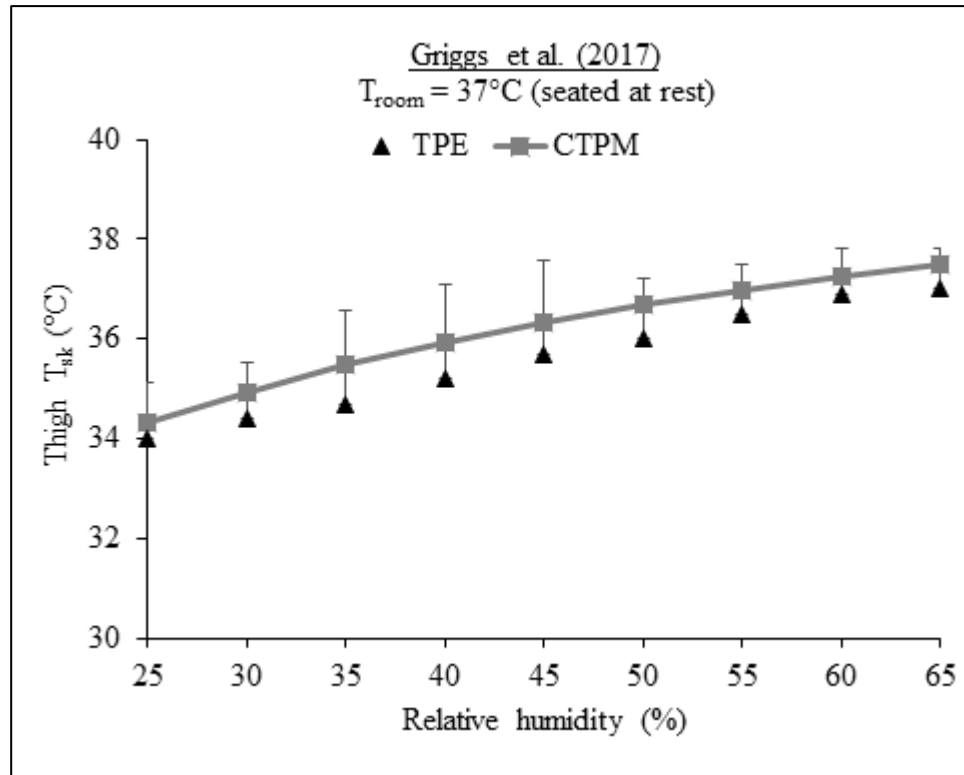
Figure 22. Comparison of simulated (CTPM: complete and ITPM: incomplete) and

experimental (TPE) values of thigh skin temperature plotted at incrementing RH at

constant room temperature for people with TP

4.1.3. Conclusion

To sum up, TP-bioheat model was developed to predict the thermoregulatory

responses in people with TP with complete and incomplete injury. The model examined

their thermal state under steady and transient ambient conditions, and at different activity

levels. Starting from Salloum et al. model (2007) that was developed for AB, main

parameters, such as arterial blood structure, LBM, FM, CO and skin perfusion rate, were

modified to reflect the thermal physiological and cardiovascular behaviors of people with TP.

The current model predictions of core and mean skin temperatures were validated with published experimental data of: i) Attia et al. (1983) on steady-state thermal conditions with participants seated at rest, ii) Trbovich et al. (2016) on arm-crank exercise in steady-state hot-exposure, iii) Gass et al. (2002) on moving wheel chair exercise in steady-state neutral and humid exposure, iv) Guttmann et al. (1958) on supine position in transient environment exposure, and finally v) Griggs et al. (2017) on seated at rest in transient thermal condition and on intermittent Sprint Exercise at steady thermal condition. The maximum error of core and mean skin temperature was 0.86 °C and 0.9 °C respectively, when comparing the predicted values in the current model to the ones in the literature.

However, the current model has some limitations that need to be taken in to consideration when implementing the model. These limitations include: (1) the group of tetraplegic patients participated in the study had different cervical spinal cord injury and different impairment severity. This diversity resulted in high standard deviation in transient conditions; (2) the physical status of the body in the altered model was considered for untrained people with spinal cord injury; otherwise, new observations needed to be extracted from literature to simulate the case of athletic or trained persons with TP because it will affect LBM, FM and energy expenditure in the body as well as possible increase in shivering and sweat rates; and finally (3) the altered model considered that the human body was deprived of any type of medication that may affect the blood circulatory system in the body which may be unavoidable in real life experimental study with human subjects for people with SCI (McKinley et al., 1999).

In conclusion, the interest in understanding the thermal physiology of people with TP helped to develop this bioheat model as a useful tool to predict the core and mean skin temperatures of the body. For this, it is possible to suggest cooling strategies for people with SCI to use, and implement these strategies, using the current model, to assess their effectiveness on the thermal state of people with SCI. In addition, the current model can be extended and modified for predicting the thermoregulatory responses in people with PA, who have more flexibility in their daily life activities and much intensive level of sportive activities.

4.2. Validation of PA-bioheat model

To validate the robustness of PA-bioheat model, three published experimental studies were selected. **Table 18** presents the detailed criteria of the selected experimental studies of each of Attia and Engel (1983), and Price and Campbell (1997, 2003). It was noted that the difference in injury level was taken into consideration and presented in the form of standard deviation for the measured variables (core and skin temperatures). In addition, the clothing thermal characteristics were specified based on reported data in each work. Additional thermal fabric resistance was incorporated in the model for the back and thighs that are in contact with wheelchair support material of the seated participant. Each of the three protocols was implemented in the altered PA-bioheat model, and values of T_{cr} and segmental T_{sk} were plotted for each climate/experiment. Moreover, the Salloum et al. model (2007) was used to predict the steady state of T_{cr} and segmental T_{sk} for AB for the first two studies only. Results showed that the model predicts T_{cr} and segmental T_{sk} within a limited accuracy in core and local skin temperature values compared to the experimental studies: 0.46 ℃ and 1.48 ℃ compared to Attia and Engel

(1983), experiment, 0.22 ℃ and 3 ℃ compared to Price and Campell (1997), and 0.75 ℃ and 1.83 ℃ compared to Price and Campell (2003). However, the model limitation can be justified by the fact that persons with PA present diversity in their level of injury, its severity and duration, disruption in thermoregulation and physical fitness.

Table 21. Criteria of experimental studies of Attia and Engel (1983) and Price and Campbell (1997, 2003)

Experiment	Reference	sample size (Injury level)	Activity level and duration	Climatic conditions	Measured variable	Clothing
Seated at rest in steady state thermal condition	Attia and Engel (1983)	$n_{PA} = 9$ (L1-T5) $n_{AB} = 6$	Seated at rest 45 minutes	15, 20, 25, 30, 35, 40 ℃ Relative humidity 45%	Rectal temperature (T_{cr}) T_{sk} of upper arm, lower arm, upper leg, and lower leg	light summer clothing ($\simeq 0.4$ clo)
Arm-crank exercise in moderate environmental conditions	Price and Campbell (1997)	$n_{PA} = 10$ (T3/4-L4) $n_{AB} = 9$	arm-crank exercise at intensity of 80% peak heart	21.5 (1.7) ℃ Relative humidity 47.0 (7.8) %.	Aural temperature T_{cr} forehead, chest, and thigh T_{sk}	light weight tracksuit trousers and training shoes
Arm-crank exercise in hot environmental conditions	Price and Campbell (2003)	$n_{LP} = 10$ (T7 and below) $n_{HP} = 10$ (T1-T6)	arm-crank exercise at intensity of 60% oxygen uptake	31.5±1.7 ℃ Relative humidity 42.9±8.0 %.	Aural temperature T_{cr} back and thigh T_{sk}	light weight tracksuit trousers and training shoes with no clothing covering the upper body

Abbreviations: PA: paraplegic people; AB: able-bodied people; LP: people with low thoracic SCI; HP: people with high thoracic SCI

4.2.1. Comparison with seated at rest in steady state thermal condition

Figure 23 shows the predicted and observed values of T_{cr} of Attia and Engel (1983) experiment for both groups of persons with PA and AB. Predicted values by PA-bioheat model show an average deviation of 0.28 ± 0.17 ℃ from experimental results, while the predicted values by AB model show an average deviation of 0.06 ± 0.05 ℃. At

low indoor temperatures (< 20 °C) and high indoor temperatures (> 35 °C), the PA-bioheat model appears to under predict T_{cr} values by 0.46 ℃, while at moderate room temperatures (20 - 35 °C), the model seems to show less deviation from the experimental results (0.08 ℃). Therefore, the PA-bioheat model can predict T_{cr} values within a maximum error of 0.46 ℃ at high and low ambient conditions.
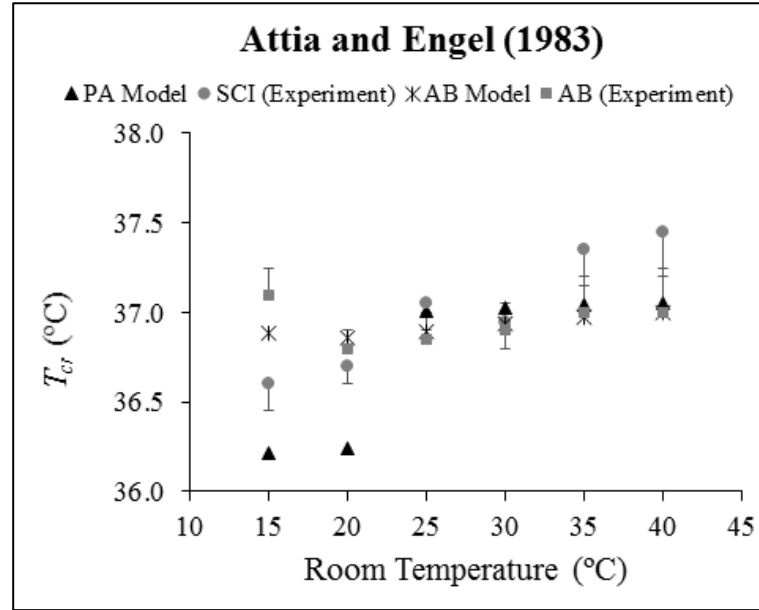
Figure 23. Scatter plot of predicted values and experimentally measured mean (±standard deviation) values of T_{cr} for both groups PA and AB seated at rest at different room temperatures and 45% *RH*

Figure 24(a-d) presents the transient change in segmental skin temperatures for upper arm, lower arm, upper leg and lower leg respectively, at room temperature 35 ^{o}C and *RH* 45% when seated at rest of Attia and Engel (1983) experiment (Attia and Engel, 1983). The predicted values of T_{sk} for upper arm and lower arm and upper leg and lower leg followed similar trends as observed experimentally. **Fig. 24(a)** shows the increase in upper arm skin temperature of person with PA predicted by the model with deviation

mean of 1.31 ± 0.14 °C from the experimental values. **Fig. 24(b)** shows the increase in

lower arm skin temperature of person with PA predicted by the model with deviation

mean of 0.22 ± 0.17 °C. Because vasodilation is still active for the lower arm (forearms)

in person with PA, its skin temperature showed transient change similar to that of

experimental results of AB. Yet, the higher absolute values of T_{sk} of the lower arm is due

to the increased SBP after SCI injury. **Fig. 24(c)** shows the increase in upper leg skin

temperature of person with PA predicted by the model with deviation mean of 0.97 ±0.45

°C. It remained lower than that of AB due to absence of vasodilation for upper leg which

is a body segment below injury level. Finally, **Fig. 24(d)** shows the increase in lower leg

skin temperature of person with PA predicted by the model with deviation mean of 0.63

± 0.43 °C. It showed lower values than that of AB due to lack of vasodilation in that body

segment as seen in upper leg skin temperature of **Fig. 19(c)**.
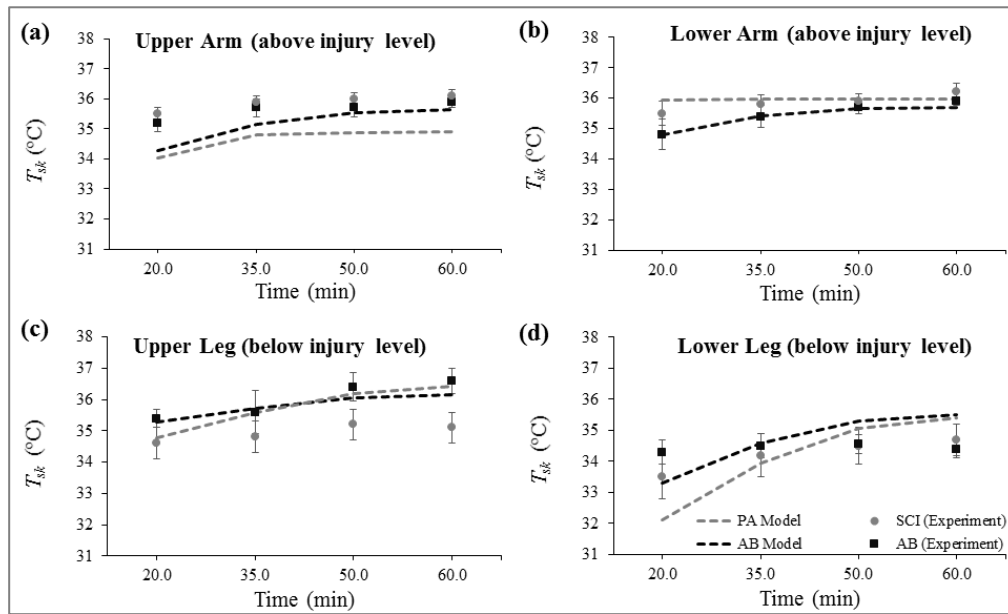
Figure 24. Line plot of predicted and observed values of T_{sk} of (a) upper arm (b) lower

arm (c) upper leg and (d) lower leg, for both groups PA and AB seated at rest at

different room temperatures and *RH* 45%

Figure 25 presents the transient change in the simulated results and observed measurements of T_{cr} of persons with PA and AB in the study of Price and Campbell (1997) (Price and Campbell). T_{cr} values showed a slight increase prior to the exercise during preconditioning phase of the experiment when participants were at rest. Then, an increase in T_{cr} values was obtained until a steady state was reached till the end of exercise (time = 90 mins) when heat gain and heat dissipation of the body were balanced. Finally, a drop in T_{cr} values was observed in the passive recovery post exercise (time > 90 mins). The predicted values for persons with PA showed similar trend to that of the observed experimental results but with an average deviation of 0.11 (0.056) °C from them. Whereas, predicted values by AB model were higher than that of experimental values with an average deviation of 0.426 (0.075) °C. Although the predicted values by PA- and AB- bioheat models showed difference not seen in the experimental results, predicted T_{cr} values were still within the standard deviation of those of the experiment. Moreover, the obtained difference for PA- model prediction is justified by the difference in injury level between participants and their physical characteristics whether trained and trained. In general, PA- bioheat model seems to over predict T_{cr} values but with an acceptable accuracy at moderate ambient conditions (21.5±1.7 °C, 47.0 ± 7.8 %) as seen in the case study of Attia and Engel (1983) at moderate indoor conditions (20-35 °C and 45 %).
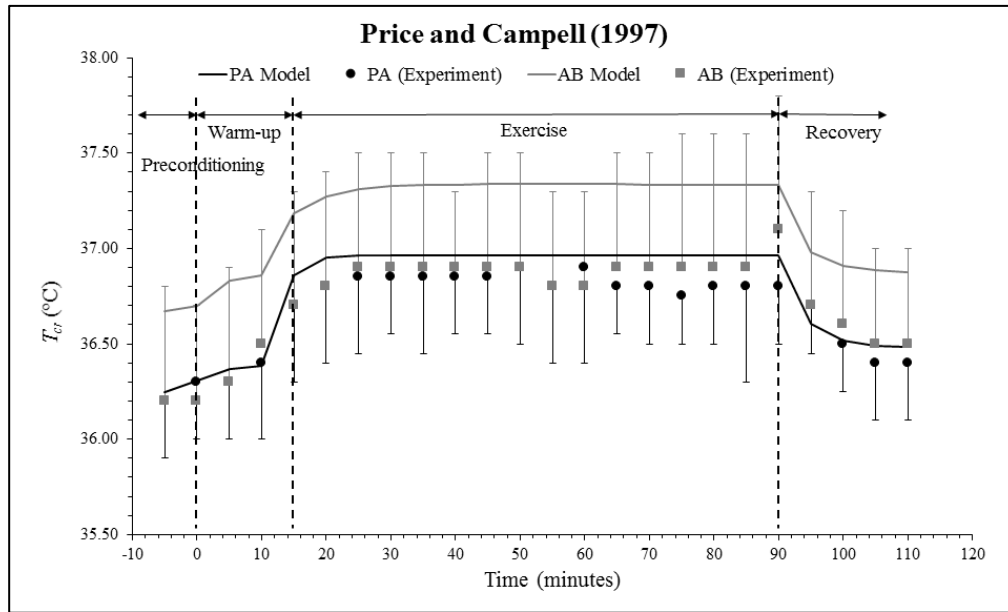
Figure 25. Line plot of predicted and observed values of T_{cr} for both groups PA and AB during rest, exercise and post recovery at room temperature 21.5 (1.7) °C and relative humidity 47.0 (7.8) %

In **Fig. 26(a-c)**, the transient change in the segmental skin temperatures for forehead, chest and thigh were plotted for both AB and persons with PA and compared to the experimental ones. **Fig. 26(a)** showed an increase in the predicted values of forehead skin temperature during exercise at a deviation mean 0.855 (0.278) °C for persons with PA and at a deviation mean 0.749 (0.15) °C for AB, both compared to that of experimental results. **Fig. 26(b)** showed an increase in the predicted values of chest skin temperature during exercise at a deviation mean 1.5 (0.413) °C for persons with PA compared to that of experimental results. **Fig. 26(c)** displayed an increase in the predicted values of thigh skin temperature during exercise at a deviation mean 1.96 (0.55) °C for persons with PA and at a deviation mean 1.48 (0.46) °C for AB, both compared to that of experimental results. It was observed that T_{sk} values of the active body parts in persons with PA (head and chest) were similar that of AB because sweating and vasodilation were

active for the sensate skin in persons with PA. Whereas, T_{sk} values of the impaired body parts in persons with PA (thigh) was lower than that of AB due to reduced SBP responsible for heat dissipation from the core to the skin and surrounding (Muraki et al., 1996). Therefore, any increase in T_{sk} values for body segment below injury level would be the result of: i) progressive heat storage in the core that is transferred by conduction to the skin, ii) the effect of convection and radiation heat transfer at the skin with the environment and finally, iii) lack of perspiration for these segments.
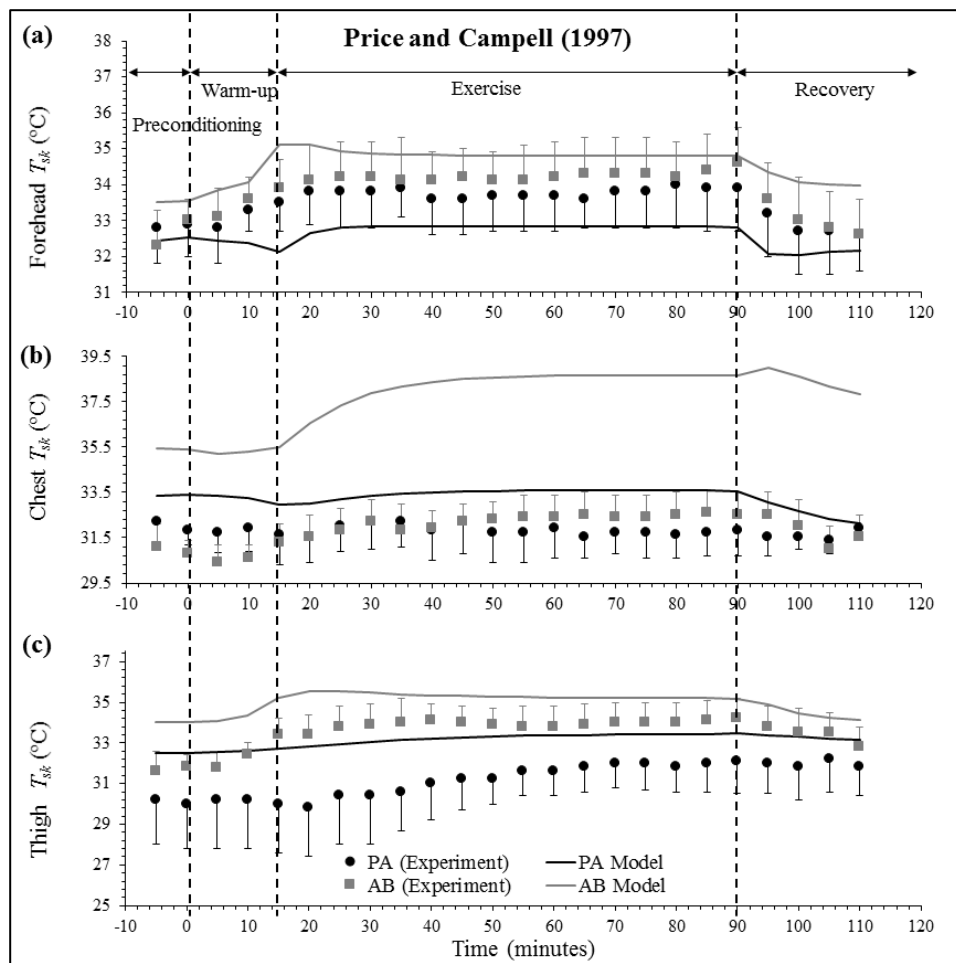
Figure 26. Line plot of predicted and observed values of T_{sk} of (a) forehead (b) chest and (c) thigh for both groups PA and AB during exercise at room condition 21.5 (1.7) °C and 47.0 (7.8) %

4.2.3. Comparison with arm-crank exercise in hot environmental conditions

Figure 27 shows the simulated results of T_{cr} of persons with PA for the study of Price and Campbell (2003) where a slight increase was observed during warm-up phase of the exercise (time < 20 mins) (Price and Campbell, 2003). Then, T_{cr} started to rise till the end of exercise (time = 60 mins). Finally, a drop in T_{cr} values was observed in the post recovery (time > 60 mins). The predicted values for persons with PA showed similar trend to that of the observed experimental results for people with high thoracic SCI (HP) with a mean of difference of 0.24 (0.15) °C, and for people with low thoracic SCI (LP) with a mean of difference of 0.57 (0.22) °C. The gradual increase in T_{cr} values for persons with PA during exercise indicated that heat gain in the body was higher than heat dissipation due to the disrupted thermoregulatory responses for impaired segments (absence of vasodilation and sweating).
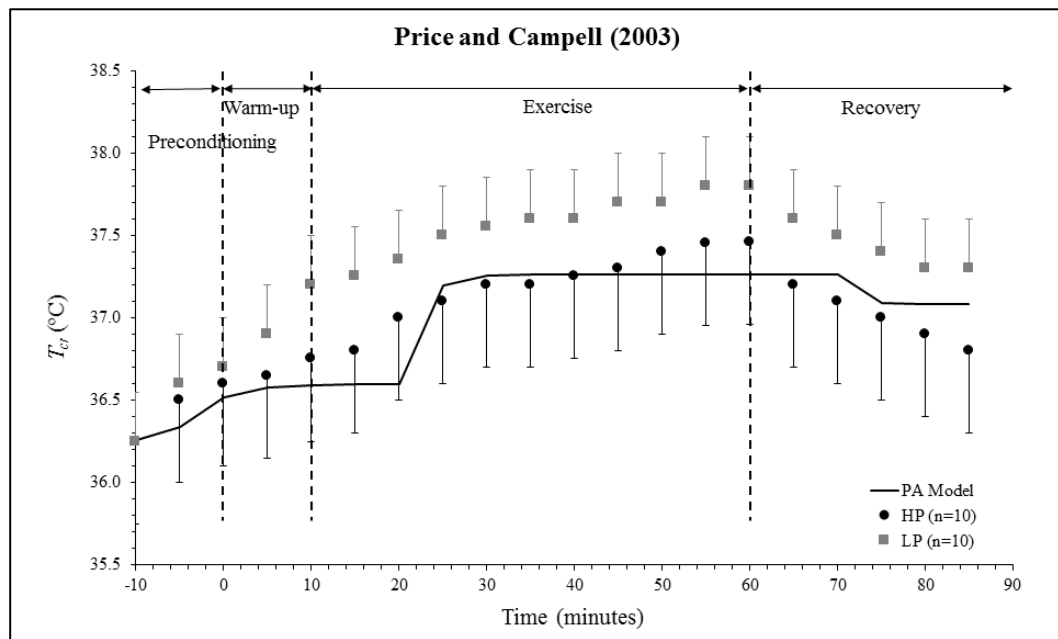
Figure 27. Line plot of predicted values of T_{cr} for persons with PA compared to that of experimental values of people with high thoracic SCI (HP) and people with low thoracic SCI (LP) during exercise at T_{room} 31.5 ± 1.7 °C and RH 42.9 ± 8.0 %

Figure 28(a) shows an increase in the predicted values of back skin temperature during exercise at a deviation mean 0.98 (0.69) °C compared to HP and at a deviation mean 1.02 (0.57) °C compared to LP. **Fig. 28(b)** showed an increase in the predicted values of thigh skin temperature during exercise at a deviation mean 2.96 (0.23) °C compared to HP and at a deviation mean 2.49 (0.31) °C compared to LP. At time ≥ 20 mins, back skin temperature predicted by PA-bioheat model showed 1.3 ℃ rise within 20 minutes and remained steady till the end of the exercise. This transient change in T_{sk} reflected the increase of MR of persons with PA defined in the model with respect to the protocol of the exercise reported in the study. In the experiment, the subjects were initially preconditioned at lab room temperature at rest within 10 minutes prior to exercise. Then, they performed certain warm-up for 10 minutes until they started exercising at gradual increase in the exercise intensity to a specific power till the end. Consequently, as MR increased, heat generation in persons with PA increased and was transferred to the skin. Thus, back's skin temperature of person with PA increased. For both predicted and experimental results, the absence of the vasodilation and sweating at the insensate skin of the back and thigh, T_{sk} increased during exercise in a rate and trend different from that of sensate skin.
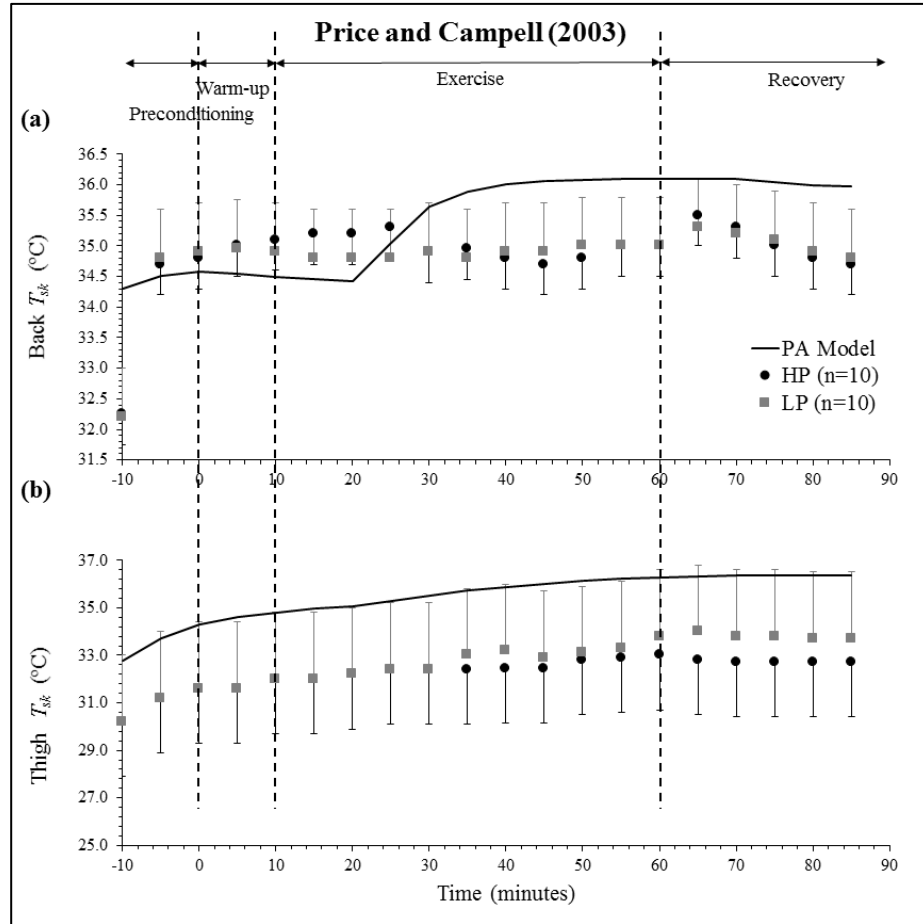
Figure 28. Line plot of predicted values of T_{sk} of (a) back and (b) thigh for persons with PA compared to that of people with high thoracic SCI (HP) and people with low thoracic SCI (LP) during exercise at T_{room} 31.5 ± 1.7 °C and RH 42.9 ± 8.0 %

4.2.4. Predicted sensible and latent heat losses at the sensate and insensate skin of the trunk for the case study of Attia and Engel (1983)

The continual increase in T_{cr} values and segmental T_{sk} values for the impaired body parts of persons with PA during exercise indicated their inability to regulate their body temperature. Although they maintained vasomotor response and sweating for body segments above injury level, they were still susceptible to thermal strain at high ambient conditions because of the disruption in thermoregulatory responses for the impaired body

142

segments below injury level. To understand the changes in thermal response of persons with PA compared to that of AB, segmental sensible and latent heat losses were calculated using the PA-bioheat model and AB bioheat model for the case study of Attia and Engel (1983).

Figure 29 shows the predicted heat losses of the chest and upper back and the abdomen and lower back parts of the trunk at different ambient temperatures for both AB and persons with PA. Starting with trunk segments below injury level, at $T_{room} < 25°C$, the latent heat loss of abdomen and lower back was similar between persons with PA and AB, but the sensible heat loss was higher for persons with PA than AB due to the lack of vasoconstriction at the impaired trunk segments (see **Fig. 29a**). Thus, heat dissipation at the insensate skin increased and eventually T_{cr} value for PA was lower than that of AB (see **Fig .23**). While at $T_{room} > 35°C$, the latent heat dissipation in AB increased rapidly because of perspiration at the abdomen and lower back, but no increase was noticed for that of person with PA due to absence of sweating. Sensible heat gain at $T_{room} = 40°C$ showed an increase in body heat resulting in higher value of T_{cr} for persons with PA compared to that of AB (see **Fig .23**). The heat gain experienced was due to higher environmental temperature.

For the trunk segments above injury level, **Fig. 29(b)** shows that at $T_{room} < 25°C$, chest and upper back witnessed higher sensible heat losses than latent ones for both persons with PA and AB, but the losses were similar between the two groups due to conservation of vasoconstriction and SBP rates for the active parts of trunk above injury level as explained in previous section. $T_{room} > 25°C$, the latent heat losses of persons with PA were much higher than that of AB due to higher rates of sweating at the sensate skin of chest as T_{cr} value reached onset of sweating (see **Table 12**). Furthermore, at hot

ambient condition (30°C and above), the latent heat losses were less than the case of moderate ambient condition (below 30°C) because skin vapor pressure approached ambient vapor pressure of saturation at the trunk segments above injury level. Regardless, because the sensible and latent losses in hot conditions were significant only at the sensate skin of trunk for persons with PA, T_{cr} value was observed to be higher compared to that of AB (see **Fig .23**).
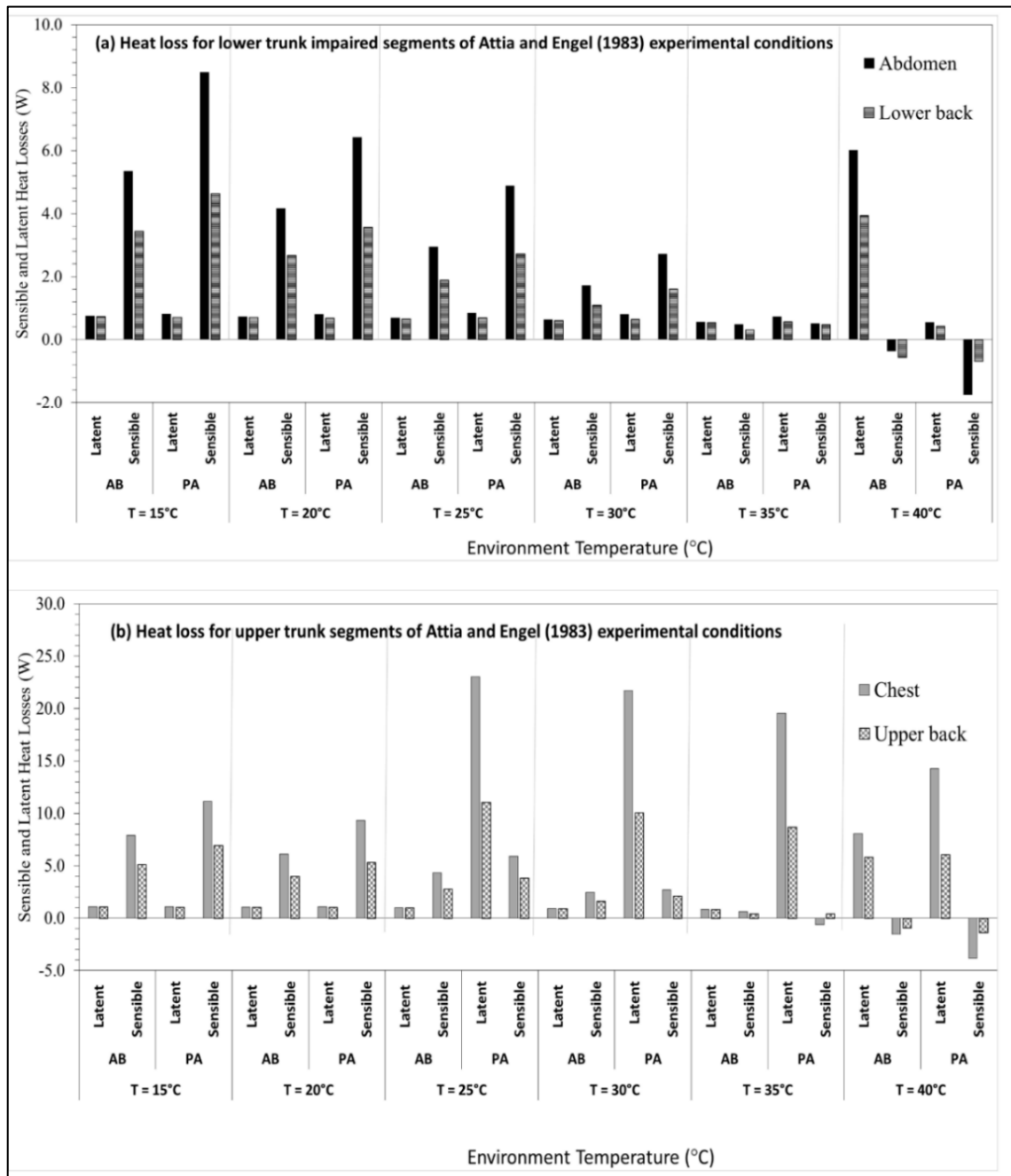
Figure 29. Bar graph of sensible and latent heat losses in AB and persons with PA at different room temperatures (15,20,25,30,35,40°C) at the (a) inactive parts of trunk (abdomen and lower back) and (b) active parts of trunk (chest and upper back)

4.2.5. Conclusion

In summary, PA-bioheat model predicted accurately PA thermal response compared to the experimental results of Attia and Engel (1983) and Price and Campbell (1997, 2003). Furthermore, the calculated latent and sensible heat losses at the active body segments were higher than those of inactive as presented by PA-model for the case study of Attia and Engel (1983). Therefore, for the purpose of enhancing the effectiveness of cooling in persons with PA at hot climatic condition and intense activity, cooling should target the skin site of trunk where sensible heat losses may be incremented to reduce T_{cr} values and avoid thermal strain.

4.2. Validation of Fabric-PCM PA-bioheat model

4.3.1. Comparison with the study of Armstrong et al. (1995)

Figure 30(a-b) shows the predicted values of T_{cr} for no-vest and with-vest simulations compared to that of the experiment of Armstrong et al. (1995) study where the participants were wearing ice cooling vests. An average deviation from the experimental results was obtained at 0.12 ± 0.03 °C for the no-vest case, and at 0.17 ± 0.15 °C for the with-vest case. Although the experimental values of T_{cr} were increasing in both cases, the maximum value reached with-vest was slightly less than that obtained in no-vest (no vest: $T_{cr} = 38.3\pm0.1$°C, with vest: $T_{cr} = 38.0\pm0.1$°C). However, the predicted values of T_{cr} by the Fabric-PCM-PA model showed negligible difference

between the two cases indicating that using ice cooling vest didn't affect T_{cr} value of person with PA during exercise. This outcome was obtained in the experimental study of Armstrong et al. (1995).
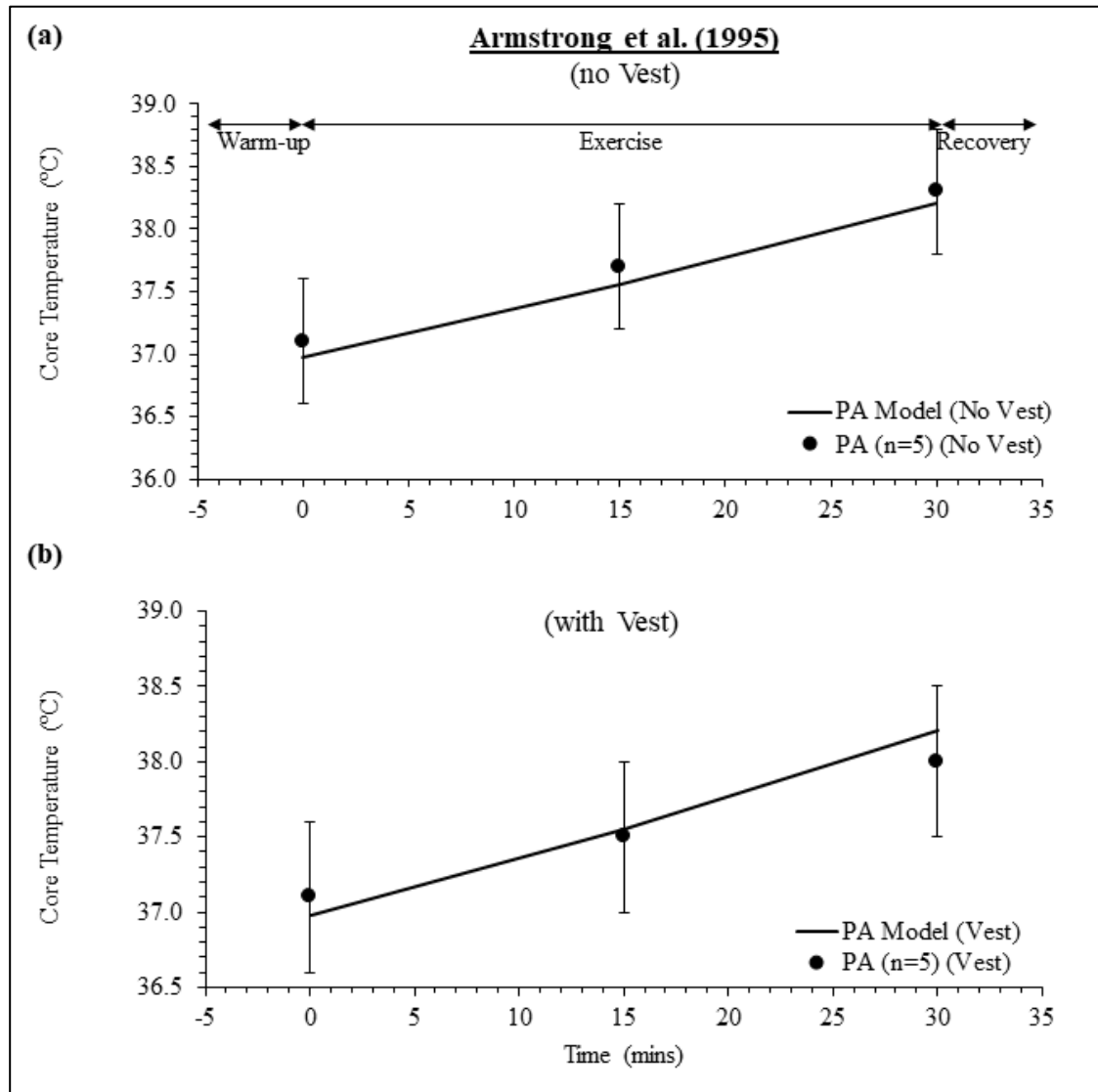
Figure 30. Line plot of predicted values of T_{cr} for persons with PA with and without PCM cooling vests compared to that of experimental values during exercise at T_{room} 32.9±0.1°C and RH 75%

To understand the effect of ice vest on thermal response of person with PA during exercise, the latent and sensible heat losses of the trunk were calculated using **Eq. 22(a, b)**:

$$Q_{latent} = A_{skin} \times \frac{P_{skin} - P_{if}}{R_{e\_air\ layer} + R_{inner\ fabric}} \ (W) \tag{22a}$$

$$Q_{sensible} = A_{skin} \times \frac{T_{skin} - T_{if}}{R_{d\_air\ layer} + R_{inner\ fabric}} \ (W) \tag{22b}$$

where A_{skin} is skin area in m², P_{skin} is skin pressure in kPa, P_{if} is the inner fabric pressure, T_{skin} is skin temperature (°C), T_{if} is inner fabric temperature (°C), $R_{d\_airlayer} = \frac{th_a}{k}$ (m². °C/W), $R_{e\_airlayer} = a(1 - e^{-th_a/b})$ (m²·kPa/W), k=24 mm.W/m²·C, th_a=air layer thickness (assumed 1.3mm), a = 0.034 m²·kPa/W and b=15 mm (Stephan and Laesecke, 1985).

Table 22 summarizes the calculated heat losses of impaired trunk segments (abdomen and lower back) and active trunk segments (chest and upper back) of persons with PA for both cases of *no-vest* and *with-vest* at the steady state attained at the end of the exercise (Armstrong et al., 1995). In the *no-vest* case, sensible heat losses obtained were higher at the front side of trunk that had less resistance with the ambient. Also, latent heat losses were minimal for abdomen and lower back as they are below injury level compared to the chest and upper back. After wearing the ice vest during exercise, sensible heat losses increased at the four skin sites of the trunk; while, the latent heat losses decreased. The difference in effect of ice vest at different skin sites of the trunk is justified by the different fabric resistances between the trunk and the ambient condition that was set at 32.9 ± 0.1 °C. However, it can be concluded that wearing ice vest during exercise

can contribute in increasing total skin sensible heat losses at the trunk for persons with PA. This increment may be insignificant for reducing T_{cr} because when considering the coverage skin area by the ice vest, lower back and abdomen (trunk area) were mostly covered by the ice packets compared to the chest and upper back (Armstrong et al., 1995). In the absence of vasodilatation at the lower trunk area, less heat will be transferred from the skin layer to the inner core layer because skin blood perfusion is disrupted at the trunk skin site (trunk is an impaired body segment below injury level). Heat transfer between the core and skin layers was enhanced by conduction only in the vest case. Therefore, locating ice packets mainly at the lower trunk affected the performance of this cooling method on reducing T_{cr} of persons with PA during exercise.

Table 22. Steady state of latent and sensible heat losses of trunk in PA for *no-vest* and *with-vest* cases of study in Armstrong et al. (1995) experiment

Trunk segment	*no-vest heat loss*		*with-vest heat loss*	
	Latent (W)	Sensible (W)	Latent (W)	Sensible (W)
Abdomen	0.52	2.10	0.33	6.56
Lower back	0.44	1.19	0.36	6.81
Chest	14.65	2.51	0.24	8.40
Upper back	6.21	1.33	0.45	8.49

4.3.2. *Comparison with the study of Trbovich et al. (2014)*

Figure 31(a-b) shows the predicted values of T_{cr} for person with PA in cases of *no-vest* and *with-vest* compared to that of the experiment of Trbovich et al. (2014) where LP and HP participants were wearing PCM vest (Trbovich et al., 2014). For the *no-vest* case, an average deviation of 0.42 ±0.33 °C were obtained in comparison to HP, and an

average deviation of 0.42 ± 0.7 °C in comparison to LP. For the *with-vest* case, a mean difference of 0.36 ±0.42 °C were obtained in comparison to HP, and a mean difference of 0.5 ± 0.56 °C in comparison to LP. Independent of injury level (T1-T12), T_{cr} was increasing in both cases of exercising, but the rate of increase of T_{cr} was attenuated during early stage of exercise when using vest as presented experimentally and by simulations.
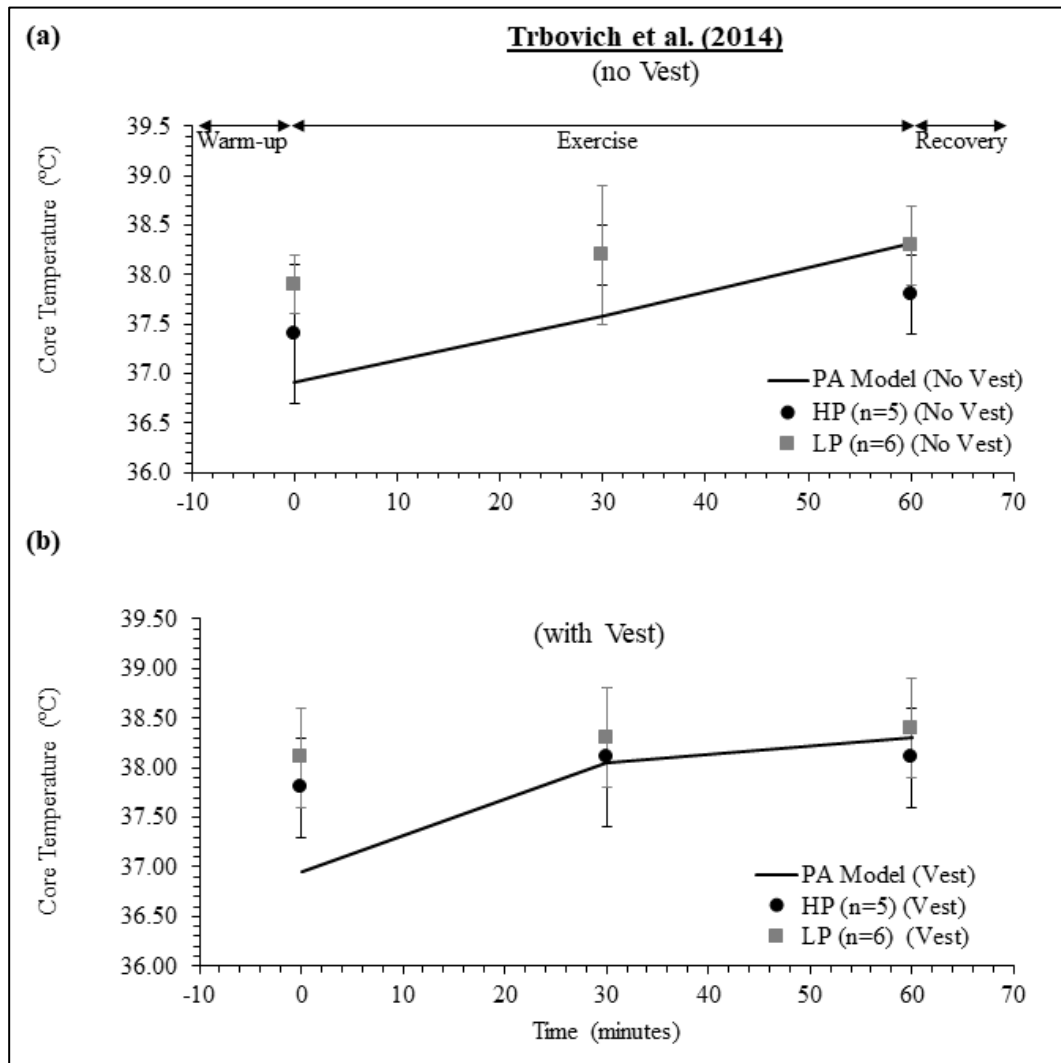
Figure 31. Line plot of predicted values of T_{cr} for persons with PA with and without PCM cooling vests compared to that of experimental values during exercise at T_{room} (21.1-23.9°C) and *RH* 50%

As summarized in **Table 23**, sensible heat losses of back side of trunk were lower than that of front side of trunk due to extra insulation by chair; whereas, latent heat losses were higher for upper part of trunk compared to lower one due to reduced effect of sweating for trunk segments below injury level (abdomen and lower back). Comparing *no-vest* and *with-vest*, sensible heat losses at the four trunk segments (abdomen, lower back, chest and upper back) showed an increase for the case of the *with-vest* case; while latent heat losses decreased. Therefore, wearing a PCM-vest during exercise can help increase total skin sensible heat loses for person with PA. However, the obtained results of PCM vest performance were not satisfactory because there was no change in T_{cr} values after wearing the vest during exercise. The coverage skin area of the PCM packets wasn't enough to target upper body skin sites, mainly the upper back. Instead, the packets were located at the abdomen and lower back which are insensate and below injury level. Therefore, the cooling capacity of PCM vest was insufficient to remove stored heat from the core through skin to the surrounding because vasodilation disruption at these body segments decremented convective heat transfer through blood circulation (Cooper et al., 1957).

Table 23. Steady state of latent and sensible heat losses of trunk in PA for *no-vest* and *with-vest* cases of study in Trbovich et al. (2014) experiment

Trunk segment	no-vest heat loss		with-vest heat loss	
	Latent (W)	Sensible (W)	Latent (W)	Sensible (W)
Abdomen	1.05	4.40	0.08	6.22
Lower back	0.81	2.67	0.15	5.72
Chest	21.71	5.75	0.14	9.66

Upper back	13.62	3.10	0.26	8.61

To assess further the effect of each of ice and PCM cooling vests on thermal response in person with PA, the change in body heat storage was calculated at the end of each exercise in both studies: Armstrong et al. (1995) and Trbovich et al. (2014). Using **Eq. 18(a-b)** and based on the initial and final average values of T_{cr} and T_{sk} obtained by Fabric-PCM-PA bioheat model, the rate of change in body heat storage was obtained as shown in **Table 24**.

Table 24. Stored heat values calculated for *no-vest* and *with-vest* cases in the studies of Armstrong et al. (1995) and Trbovich et al. (2014)

PA Case	Rate of Body Heat Storage (Sekhon and Fehlings)	
	Ice vest (Armstrong et al., 1995)	PCM vest (Trbovich et al., 2014)
no-vest	165 W	124 W
with-vest	161 W	109 W

The heat stored in the body was reduced by 2.4% during a 30-min pushing wheelchair exercise in hot and humid room conditions in the study of Armstrong et al. (1995). Also, it was decremented by 12% during a 60-min intermittent-sprint exercise in moderate room condition in the study of Trbovich et al. (2014). However, this attenuation was insufficient for both studies which could be justified by the limited skin coverage area cooled by the packets which was below the critical body surface cooling area (~40%) (Kume et al., 2009).

4.3.3. Conclusion

To sum up, although wearing a cooling vest can help increase sensible heat losses at the trunk skin site in person with PA, the effect of cooling was minimal on T_{cr} values and stored heat in the body of PA during exercise. Based on obtained observations of **Tables 23 and 24**, locating the ice or PCM packets at trunk can increase sensible heat losses, but decrease latent losses. The location of ice or PCM packs can enhance overall performance of the vest for the sake of regulating thermal response in person with PA. However, other than pack location, the melting temperature should be taken into consideration when designing the cooling vest. Usage of ice may induce local cutaneous vasoconstriction that may prevent heat dissipation through convective cooling and predispose insensate skin to breakdown (House et al., 2013). Therefore, using PCM agents of melting points greater than 0°C is recommended to avoid individual's skin damage and occurrence of local vasoconstriction that restricts blood flow to the skin and turns it paler (Trbovich et al., 2014). Similar approaches were tested on athletic AB to find the optimum melting temperatures of PCM to attain acceptable comfort and sensation levels for the individual without causing any skin breakdown (Itani et al., 2017). A minimum of 10 °C melting point was shown to be effective in very hot ambient conditions for AB (Gao et al., 2012; Ouahrani et al., 2017). Therefore, further investigation on the selection of optimal melting temperature should be done for enhancing cooling effectiveness during exercise for PA.

When thinking about the health safety issues for persons with PA especially during exercise, it was worthwhile to develop a robust tool defined as a PA-bioheat model to predict their thermal response. Extending TP-bioheat model, necessary modifications were done based on the changes in the thermal physiology of the body after thoracic SCI. Then, the obtained model was combined with two cooling methods (ice and PCM vests)

that were studied experimentally and published. Validation of PA-bioheat model with and without each of the two cooling techniques was achieved showing good agreement between the predicted values T_{cr} and the observed ones. Predicted results of core and skin temperatures as well as sensible and latent heat losses in PA may serve as a database for addressing the effectiveness of cooling on PA. Hence, means of enhancement of the cooling vest for person with PA can be investigated by assessing the needed skin coverage area, PCM melting point and location of packets.

4.4. Results of parametric study of Fabric-PCM-PA bioheat model

The validated Fabric-PCM-PA bioheat model was used in the parametric study presented in section 2.5, to determine the means of enhancing the performance of PCM cooling vest in reducing the thermal strain on persons with PA. The effectiveness was evaluated based on the analysis of the drop in T_{cr} as well as the improvement in the heat losses at the sensate and insensate skin of the trunk compared to the no-vest case and published experimental results of Trbovich et al. (2014).

Figure 32 presents the final T_{cr} values obtained at the end of exercise in the experimental study of Trbovich et al. (2014) and those simulated of the three proposed cases for PCM cooling vest design as well as the no-vest case for AB. For AB, T_{cr} value reached 37.76 °C which less than the experimental results of persons with high-thoracic (T3-T5) SCI and persons with low-thoracic (T7-T9) SCI (37.76 °C, 38.3 °C; respectively). This validates the potential of induced thermal strain for persons with PA during exercise compared to AB. Although data obtained from the experiment of Trbovich et al. (2014) showed insignificant change in T_{cr} values when using PCM vest, the predicted findings for the three proposed cases showed an average drop of 0.13±0.06

⁰C compared to no-vest case (model and experiment). This shows that using a low melting point and covering at least 40% of the trunk can reduce heat gain in person with PA at moderate metabolic rate and ambient conditions, but the duration of exercise should not be prolonged. This is because thermal strain is still possible to build up in their body as T_{cr} value may exceeded 37.5 °C (threshold of thermal strain in the human body) even when using PCM cooling vest. This restricted efficacy of using cooling vest is justified by the absence of vasodilation for trunk segments below injury level that limited heat transfer between the skin and the core layers to conduction heat transfer (Cooper et al., 1957; Wilsmore, 2007). That's why disruption in thermoregulatory responses after SCI affects T_{cr} regulation in persons with PA and limits the effectiveness of cooling vest when used in these conditions.
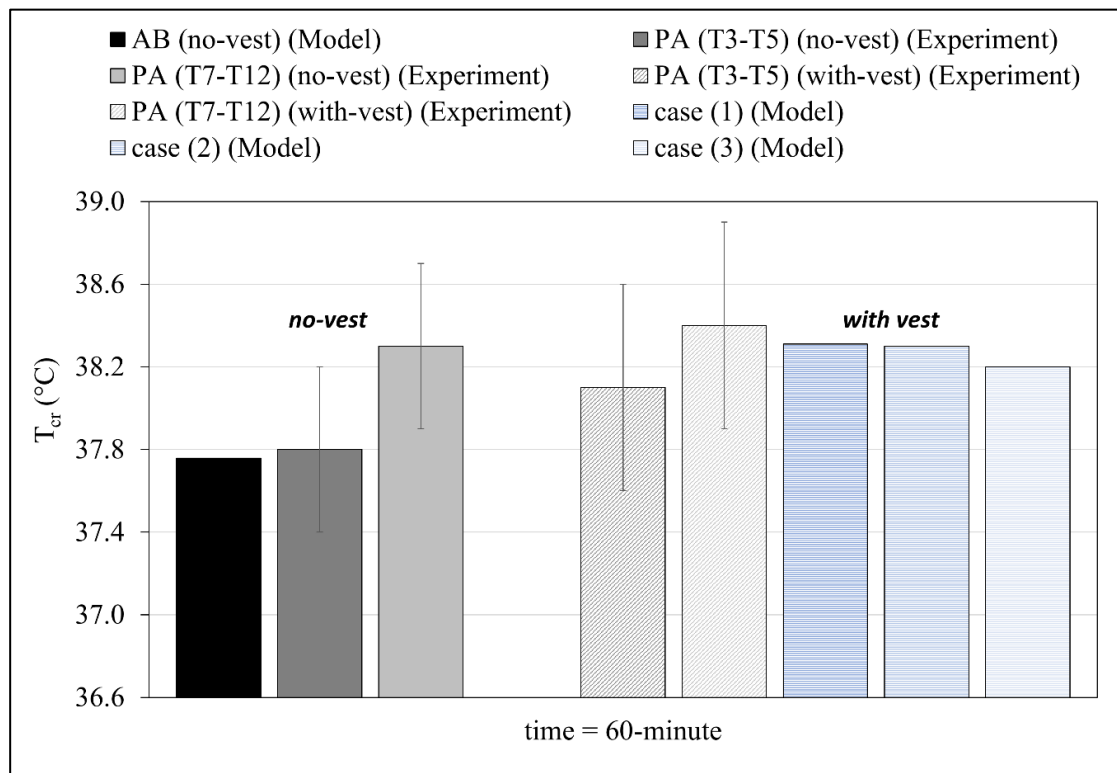
Figure 32. Comparison of T_{cr} values between experimental results and three cases study

Further to the above, **Fig. 33(a-b)** shows the difference in the heat losses between trunk segments above (chest and upper back) and below (abdomen and lower back) SCI with and without cooling vest. In **Fig. 33(a)**, in the no-vest case, the latent heat losses were negligible from the abdomen and lower back as they were below injury level which lack perspiration at the insensate skin of the trunk. Whereas, the latent heat losses were higher at the chest and upper back which were above injury level where sweating was still active. In the case of with-vest, latent losses of the chest and upper back were reduced compared to that of no-vest due to exposure to low temperature of the PCM packet that depressed sweating effect at the sensate skin.

In **Fig. 33(b)**, in the case of no-vest, although sensible heat losses occurred at both sensate and insensate skin of the trunk, these loses were not enough to reduce T_{cr} value. With PCM cooling vest, the heat losses at the abdomen, lower back, chest and upper back were magnified by (17%, 86%, 30%, 130%) in case (1); by (83%, 193%, 139%, 327%) in case (2); and by (110%, 240%, 170%, 390%) in case (3). This enhancement in heat losses at the trunk revealed the effect of lowering melting temperature of PCM used in the cooling vest and coverage area of the skin of the trunk. The most significant heat losses were in case (3) at which T_{cr} value was reduced by 0.2 °C. Furthermore, heat losses at the sensate skin of the trunk were significantly greater compared to the of the insensate skin of the trunk.
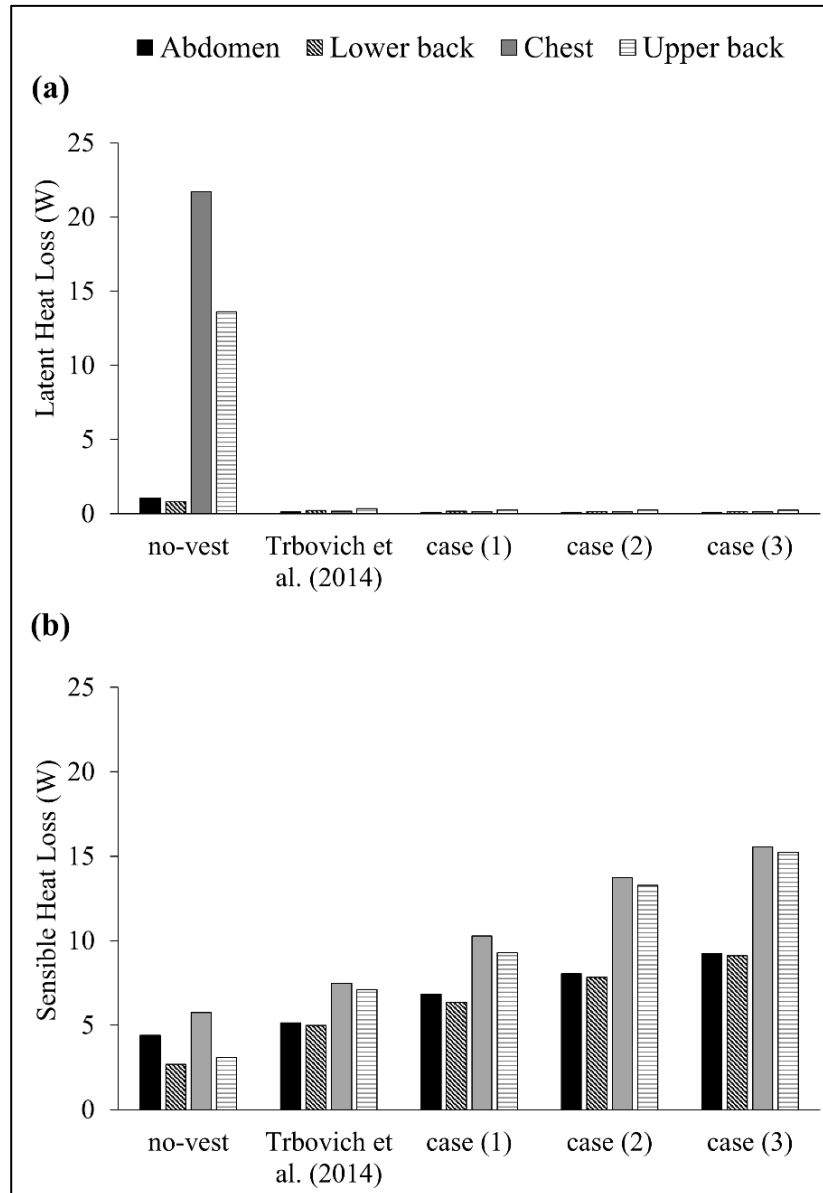
Figure 33. Comparison of (a) latent heat losses and (b) sensible heat losses heat losses at the four segments of the trunk

Consequently, in the means of enhancing the performance of the PCM cooling vest for persons with PA, it is proposed to locate PCM packets near the sensate skin at a coverage area of 40% of the trunk with low melting temperature.

4.5. Results of parametric study of Hybrid ECV-PA bioheat model

The Hybrid ECV model was validated via the heated plate experiment in a climatic chamber, explained in section 3.1. The model validation results are presented in the next section of the experimental findings of this research work.

The validated mathematical model used in the parametric study presented in section 2.9, to determine the effectiveness of the hybrid vest and ECV Type II in reducing the thermal strain on persons with PA at moderate and high activity levels. The effectiveness was evaluated based on the analysis of thermophysiological parameters of the skin and core temperatures as well as heat losses. Moreover, the contribution of the ventilation fans and ECV material in the hybrid vest to the drop in skin temperatures from the No-Vest case was evaluated to determine the conditions at which the use of the hybrid vest would be recommended.

4.5.1. Thermophysiological parameters at moderate physical activity level (3 met)

Figure 34(a-f) shows the temperature variations of the sensate ($T_{sk,sen}$) and insensate ($T_{sk,insen}$) skin at activity level of 3 met for No-Vest, Type II, and hybrid vest, at 30% *RH* and T_{amb} 28, 32 and 36 °C. **Table 25** summarizes the corresponding time-averaged latent (Q_{lat}) and sensible (Q_{sens}) heat losses at the trunk skin (sensate and insensate).

In **Fig. 34(a)**, it was observed that at 28 °C, $T_{sk,sen}$ increased slowly from a thermal neutral state of 35.6 °C to reach a final state of 36.39, 36.64 and 36.36 °C for No-Vest, Type II, and hybrid vest, respectively at the moderate metabolic heat generation. In **Fig. 34(b)**, $T_{sk,insen}$ had an initial value of 30.8 ℃ which was much lower than $T_{sk,sen}$ due to: 1) muscle atrophy defined as the loss of lean body mass and transformation of

muscle fibres to a less metabolically active type (Biering-Sørensen et al., 2009); 2) increase in the skin fat thickness which reduces the thermal conductance of the fat-skin layer and the core (Spungen et al., 2003b); and 3) reduced skin blood perfusion (Hogancamp II, 2004). In the first few minutes, $T_{sk,insen}$ showed a minor decline due to admittance of cooler air (28 °C), followed by a gradual increase due to increasing blood temperature. During the whole period, $T_{sk,insen}$ was lower than that of sensate skin since relatively little change in blood flow to the insensate skin of the trunk occurred as a result of the impaired vasodilation response as reported in previous studies (Price and Campbell, 1997b, 2003). However, the increase in $T_{sk,insen}$ was greater than that of $T_{sk,sen}$ since $T_{sk,insen}$ did not reach steady state conditions. Moreover, the body core temperature did not drop to the threshold value of 35.12 °C for persons with PA when using the hybrid vest, especially in the first few minutes at T_{amb} 28 °C. Hence vasoconstriction did not happen during that period (Mneimneh et al., 2019b; Wilsmore, 2007).

At the low *RH* and moderate ambient condition (28 °C and 30% *RH*), the hybrid vest achieved cooler sensate skin temperature but comparable to No-Vest as the drop in $T_{sk,sen}$ and $T_{sk,insen}$ did not exceed 0.2 °C and 0.4 °C, respectively over the whole exercise period (see **Fig. 34(a-b)**). The improved performance of the hybrid vest over No-vest was mainly due to the use of ventilation fans that: i) enhanced moisture evaporation thus increased time-averaged latent heat losses from the skin (Q_{lat} increased from 51 to 56 W/m^2) and ii) admitted ambient air cooled by the ECV material that enhanced time-averaged sensible heat losses (Q_{sens} increased from 111 to 143 W/m^2), as presented in **Table 25**. It can be noticed that the sensible heat losses were higher than the latent heat losses due to the absence of sweating at 3 met and the cooling effect of the ECV material with fan operation. On the other hand, Type II caused a maximum increase from No-Vest

by 0.3 °C and 0.7 °C in $T_{sk,sen}$ and $T_{sk,insen}$, respectively (see **Fig. 34(a-b)**). The absence of ventilation effect in the microclimate for Type II caused an increase in the microclimate moisture content thus decreased latent heat losses from the skin (Q_{lat} decreased from 51 to 38 W/m^2) and resulted in temperature increase of the skin (Q_{sens} decreased from 111 to 56 W/m^2). This was due to the additional evaporative resistance of ECV Type II that reduced heat losses at the trunk compared to No-Vest, as was experimentally reported by Ciuha et al. (Ciuha et al., 2020). Moreover, there was no direct contact between the shirt and ECV inner layer, due to the microclimate air gap that acted as an enclosure with natural convection due to the temperature difference between the two surfaces.
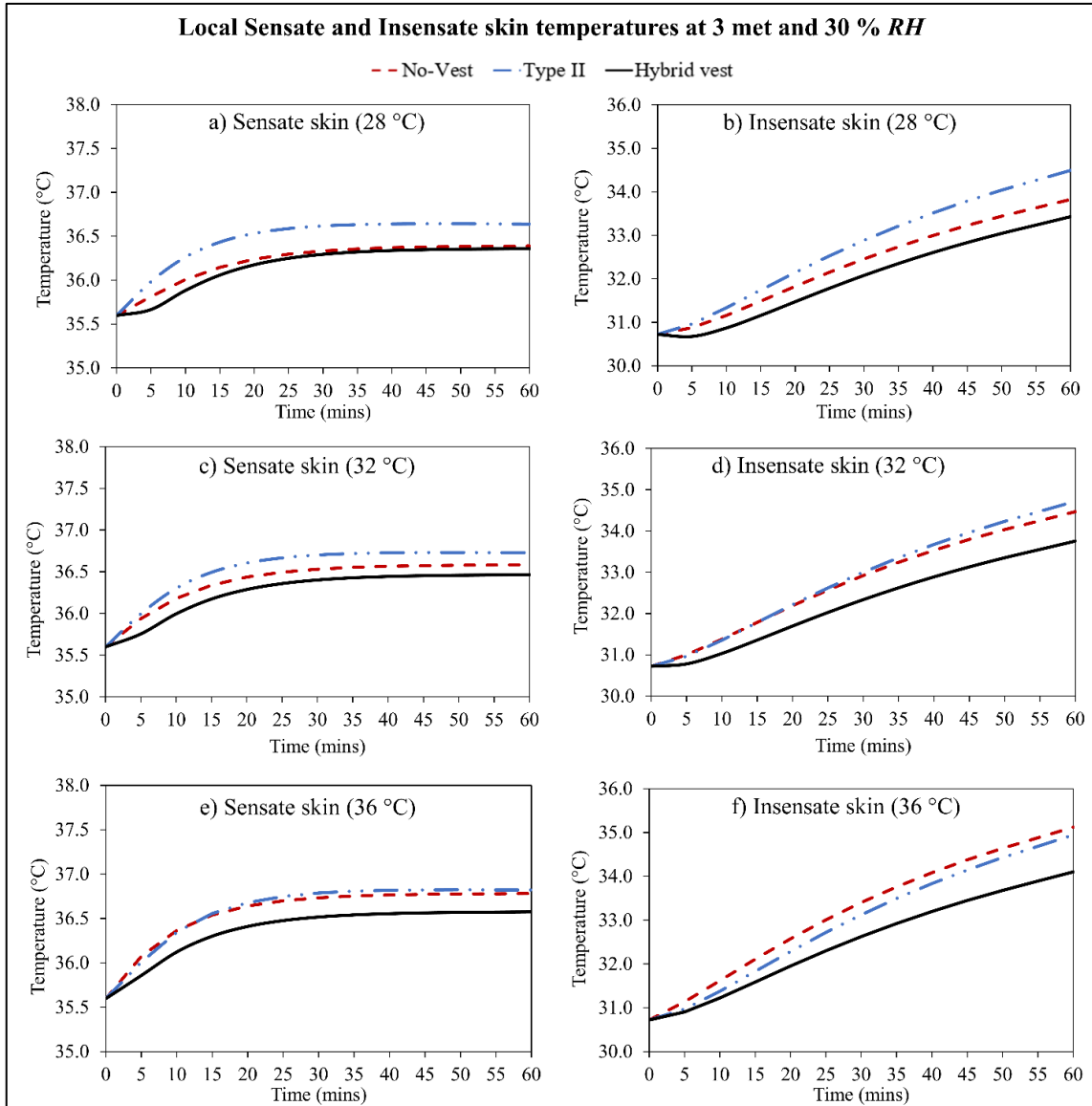
Figure 34. Plot of skin temperature variations at 3 met and 30 % *RH* of the a) sensate

and b) insensate at 28 °C, c) sensate and d) insensate at 32 °C, e) sensate and f)

insensate at 36°C for No-Vest, Type II, and hybrid vest

Table 25. Time-averaged Q_{lat} (latent heat loss), Q_{sens} (sensible heat loss) and Q_{tot} (total latent and sensible heat loss) of trunk skin, at 3 met and different ambient conditions

At 30% *RH*									
T_{amb}	**28**			**32**			**36**		
Case	Q_{lat} (W/m²)	Q_{sens} (W/m²)	Q_{tot} (W/m²)	Q_{lat} (W/m²)	Q_{sens} (W/m²)	Q_{tot} (W/m²)	Q_{lat} (W/m²)	Q_{sens} (W/m²)	Q_{tot} (W/m²)
No-Vest	51	111	162	49	56	105	46	1	47
Type II	38	56	94	38	37	75	38	18	56
Hybrid vest	56	143	199	54	117	171	51	90	141
At 60% *RH*									
T_{amb} (°C)	**28**			**32**			**36**		
Case	Q_{lat} (W/m²)	Q_{sens} (W/m²)	Q_{tot} (W/m²)	Q_{lat} (W/m²)	Q_{sens} (W/m²)	Q_{tot} (W/m²)	Q_{lat} (W/m²)	Q_{sens} (W/m²)	Q_{tot} (W/m²)
No-Vest	41	88	129	36	27	63	30	-37 (heat gain)	-7
Type II	38	37	75	38	14	52	38	-9 (heat gain)	29
Hybrid vest	46	102	148	40	66	106	34	26	60

At the same *RH* (30%), but higher T_{amb} of 32 and 36 °C, reduced heat loss was observed in the No-Vest case due to hotter environment as T_{amb} increased (see **Fig. 34**), which was reflected by the significant drop in Q_{sens} from 111 W/m² at 28 °C to 1 W/m² at 36 °C (see **Table 25**). Nevertheless, the hybrid vest cooling effect on both sensate and insensate skin became more significant over the No-Vest case due to evaporation from the cooling vest, as shown in **Fig. 34**. Regarding ECV Type II, its cooling effect on the

insensate skin was better than that of No-Vest case at T_{amb} of 36 °C (see **Fig. 34(f)**), as No-Vest case changed towards heat gain (see **Table 25**).

Based on the observed drops in sensate and insensate skin temperatures as well as trunk heat losses, the hybrid vest showed the best performance over No-Vest and ECV Type II for moderate activity level at low *RH*, indicating the advantage of ventilation in the microclimate even if no sweating occurred at the sensate skin.

The effect of increasing *RH* from 30% to 60 % on the sensate and insensate skin temperatures for all cases at the same metabolic rate of 3 met is shown in **Fig. 35**, and the corresponding time-averaged heat losses are summarized in **Table 25**. The fast rate of increase in sensate skin temperatures in the first 10-15 min due to metabolic heat generation is still observed (see **Fig. 35(a**, **c** and **e)**), but the hybrid vest performance became similar to the No-Vest due to admitting humid air in the microclimate and thus reducing evaporation from the shirt. Due to the heat gain from the environment and the restricted evaporation in the No-Vest, reflected by the drop in Q_{lat} and Q_{sens} (see **Table 25** at 60 % *RH)*, the advantage of using the hybrid vest became more obvious by the end of the exercise period at the sensate and insensate skin, as shown in **Fig. 35**. On the other hand, the advantage of using ECV Type II over the hybrid vest was more distinct at the beginning of exposure time during exercise, as T_{amb} increased from 28 to 36 °C, as shown in **Fig. 35** for both sensate and insensate skin. Compared to the hybrid vest, ECV Type II did not admit hot and humid air in the microclimate from the start of exercise. Instead, its microclimate humidity started building up due to moisture accumulation and lack of ventilation. Moreover, the rate of increase of the skin temperatures for ECV Type II were similar at all T_{amb}, unlike the No-Vest case that showed higher rates of increase as T_{amb} increased in the first few minutes. Thus, the difference between ECV Type II and No-

Vest case became more obvious as T_{amb} increased. However, with time and due to lack of ventilation in the microclimate of ECV Type II, the shirt moisture content increased, and the microclimate temperature and relative humidity exceeded that of the ambient conditions. Hence, the performance of ECV Type II became worse compared to No-Vest at $T_{sk,insen}$ from 30 min °C at $T_{amb} = 32$ °C and from 45 min at $T_{amb} = 36$ °C, and at $T_{sk,sen}$ from 20 min °C at $T_{amb} = 32$ °C and from 35 min at $T_{amb} = 36$ °C.

Local Sensate and Insensate skin temperatures at 3 met at 60 % *RH*
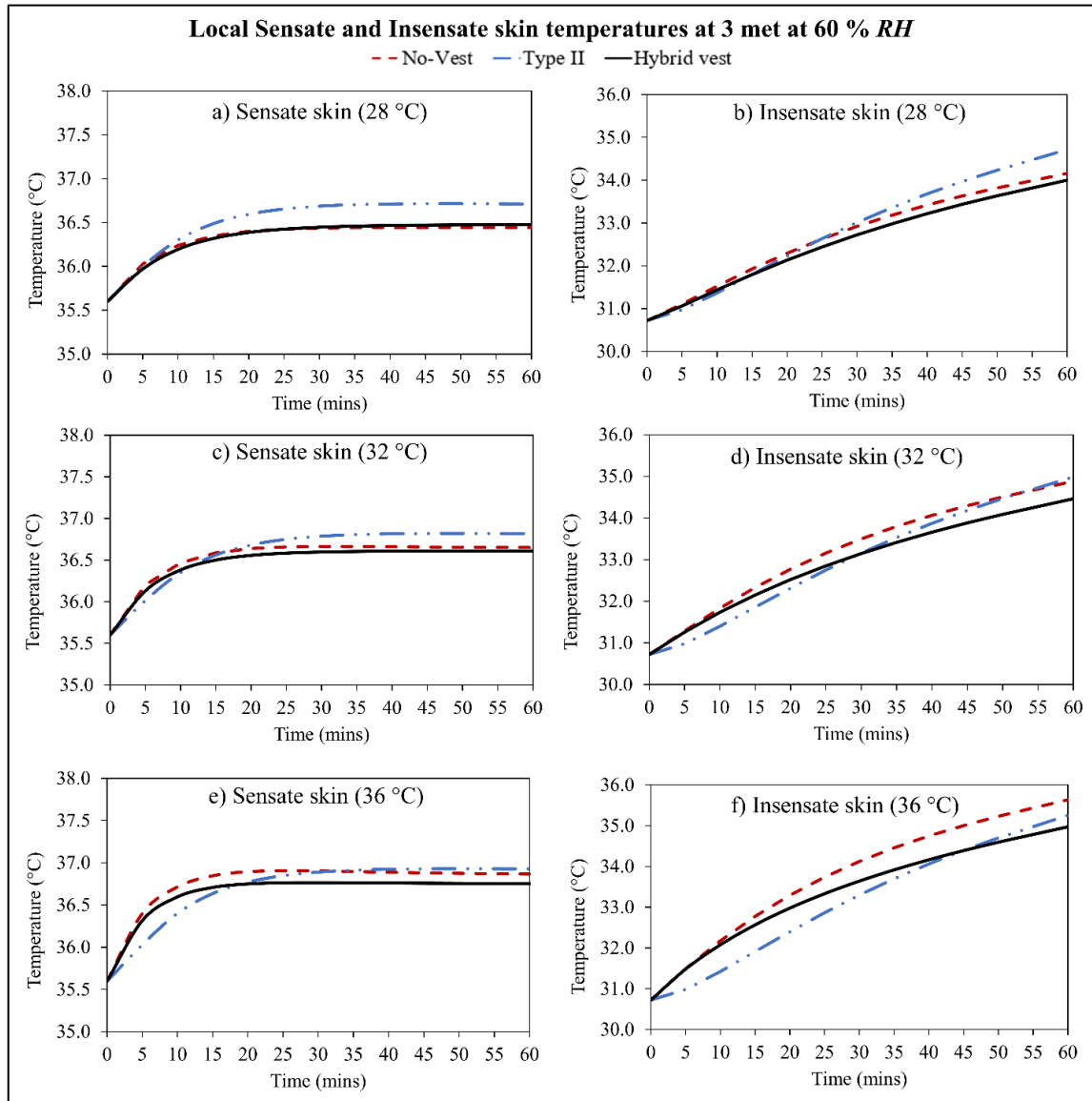
Figure 35. Plot of skin temperature variations at 3 met and 60 % *RH* of the a) sensate

and b) insensate at 28 °C, c) sensate and d) insensate at 32 °C, e) sensate and f)

insensate at 36°C for No-Vest, Type II, and hybrid vest

At moderate activity level of 3 met, for all ambient conditions, the temperature variations of the shirt and microclimate at the sensate skin and that of water-absorbent layer showed similar trend analogous to that of $T_{sk,sen}$ for the hybrid vest case. Due to the absence of sweat on the sensate skin in all the conditions for No-Vest, ECV Type II and hybrid vest, shirt temperature at the sensate node, $T_{sh,sen}$, and microclimate temperature at the sensate node, $T_{a,sen}$, remained significantly greater than that of water-absorbent layer, T_w, and did not approach the ambient wet bulb temperature, T_{WB}. Additionally, the increase in T_w caused an increase in $\dot{m}_{evap}$ in the first 5 - 10 mins of exercise, followed by steady state conditions of the temperature and evaporation rate of the hybrid vest, indicating that evaporation occurred at the outer layer of the vest. Subsequently, m_w decreased with time but remained substantial as only ~ 30 % of the hybrid vest weight was lost at the end of exercise. The hybrid vest may then be used for a significantly longer duration than 1 hr., during physical activity of persons with PA (Ciuha et al., 2020). Finally, at the moderate activity level of 3 met, T_{cr} showed an increasing trend over the exercise period for the three cases; however, this increase was not significant enough to reach the onset of sweating (37.3 °C) of a persons with PA nor the threshold of thermal strain at 37.5 °C (Miller and Ziskin, 1989; Wilsmore, 2007).

4.5.2. Thermophysiological parameters at high physical activity level (6 met)

Figure 36(a-f) show the temperature variations of the sensate ($T_{sk,sen}$) and insensate ($T_{sk,insen}$) skin at 6 met for No-Vest, Type II, and hybrid vest, at 30% *RH* and T_{amb} 28, 32 and 36 °C. **Table 26** summarizes the corresponding time-averaged latent (Q_{lat}) and sensible (Q_{sens}) heat losses at the trunk skin (sensate and insensate) in the period before onset of sweating (**P1**) and the period after sweating started (**P2**).

In **Fig. 36(a)**, for 28 °Cfor 28 °C, $T_{sk,sen}$ increased from a thermal neutral state at 35.6 °C due to build-up of the metabolic heat generation and the active vasodilation effect. After 8 mins of exercise, (**P1= 8 mins**), sweating started at the sensate skin (as marked on **Fig. 36(a)**), and $T_{sk,sen}$ continued increasing after **P1** for about 2 min due accumulated sweat on the skin before being wicked to the shirt where it can be evaporated to the microclimate in the case of hybrid vest or to the ambient in case of No-Vest. This delay in evaporation from the shirt caused the increase in $T_{sk,sen}$ for very small period of time (~ 2 min). This finding agrees with the experimental results of Fontana et al. and Atasağun et al. that investigated the cooling effect of sweating and evaporation on the trunk skin using a sweating torso setup and human subject testing (Atasağun et al., 2018; Fontana et al., 2017). Fontana et al. found that the delay in the cooling effect of sweat evaporation was about 3.1 ± 0.9 min (Fontana et al., 2017). The presence of wicked moisture in the shirt increased its pressure enhancing evaporation and thus lowering $T_{sk,sen}$. With evaporation occurring, $T_{sk,sen}$ decreased. This decrease in $T_{sk,sen}$ affected the shirt temperature, and the amount of evaporated moisture from the shirt and therefore lowering $T_{sk,sen}$ drop. The change in skin temperature drop during sweat evaporation was also observed experimentally in the study of Fontana et al. (2017) and Atasağun et al. (2018). This rate of temperature drop was more significant in the case of

hybrid vest and No-vest over ECV Type II, due to the cooler temperatures of the shirt and effect of evaporation.

A similar trend of $T_{sk,sen}$ occurred between the No-Vest, Type II, and hybrid vest cases. However, the hybrid vest showed the slowest rate of increase in the first 5 mins of exercise, attained lowest peak, followed by the highest drop in $T_{sk,sen}$ compared to No-Vest and ECV Type II. The better performance of the hybrid vest over No-Vest and Type II was due to sweat evaporation at the shirt which enhances Q_{lat}, as presented in **Table 26** by comparing the values at **P1** and **P2** for all the cases at 28 °C and 30 % *RH*. For example, the hybrid vest Q_{lat} increased from 66 W/m^2 at **P1** to 480 W/m^2 at **P2**. In addition, the start of sweat capture by the shirt decreased the driving potential for sweat evaporation from the skin for the three cases, but it occurred at an earlier time for the No-Vest and Type II due to lower capability for sweat evaporation. This also justified the highest $T_{sk,sen}$ attained by ECV Type II, with a higher evaporative resistance than the No-Vest case, restricted sweat evaporation and lack of ventilation (Ciuha et al., 2020).

Regarding $T_{sk,insen}$ shown in **Fig. 36(b)**, it showed a drop from the initial state before 5th min of exercise due to admitting relatively cool air at 28 °C and lack of vasodilation although the metabolic heat was being generated. After that, $T_{sk,insen}$ showed an increasing trend toward the end of exercise, while the hybrid vest showed the lowest values and ECV Type II the highest ones due to the added resistance. The lowest skin temperatures attained by the hybrid vest were reflected by the highest values of the time-averaged heat losses (*Q$_{lat}$* and *Q$_{sens}$*) at **P1** and **P2**, as summarized in **Table 26**. Hence, $T_{sk,insen}$ did not follow the same trend as the sensate skin. Instead, it showed drop in temperature within the first five minutes, as observed more profoundly in the case of **hybrid vest** (Garstang and Miller-Smith, 2007), due to blood flowing at its basal minimal

flow rate in the absence of vasodilation. Moreover, the drop in $T_{sk,insen}$ in the first five minutes decreased as T_{amb} increased as was observed in the case study of 3 met at 30% *RH* (**Fig. 35**).
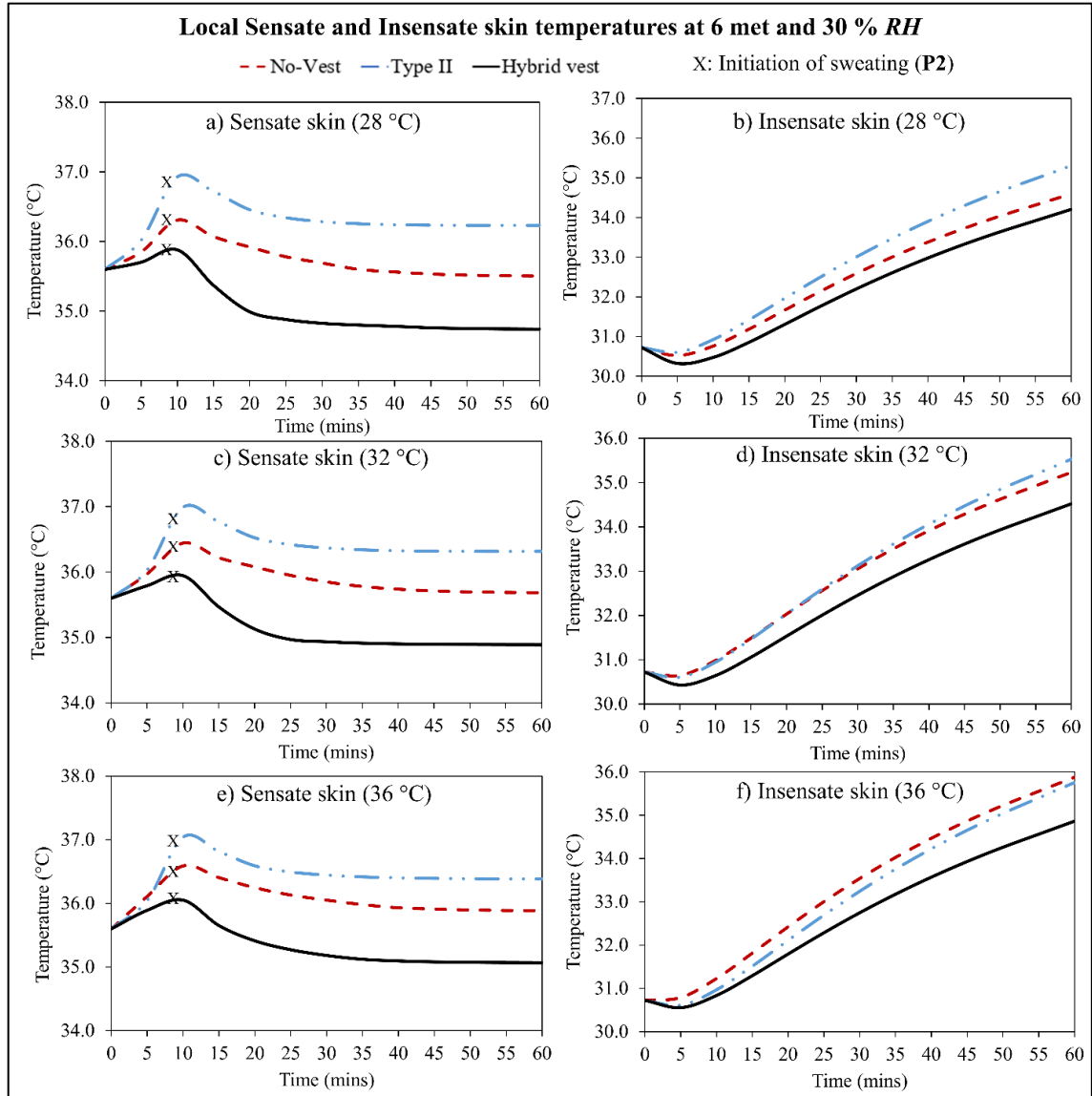

Figure 36. Plot of skin temperature variations at 6 met and 30 % *RH* of the a) sensate and b) insensate at 28 °C, c) sensate and d) insensate at 32 °C, e) sensate and f) insensate at 36°C for No-Vest, Type II, and hybrid vest

Table 26. Time-averaged Q_{lat} (latent heat loss), Q_{sens} (sensible heat loss) and Q_{tot} (total latent and sensible heat loss) in the period before sweating (**P1**) and in the period after sweating (**P2**) of trunk skin, at 6 met and different ambient conditions

	At 30% *RH*																	
T_{amb}	28 (°C)						32 (°C)						36 (°C)					
Case	Q_{lat} (W/m²)		Q_{sens} (W/m²)		Q_{tot} (W/m²)		Q_{lat} (W/m²)		Q_{sens} (W/m²)		Q_{tot} (W/m²)		Q_{lat} (W/m²)		Q_{sens} (W/m²)		Q_{tot} (W/m²)	
	P1[a]	P2[b]	P1[a]	P2[b]	P1[a]	P2[b]	P1[a]	P2[b]	P1[a]	P2[b]	P1[a]	P2[b]	P1[c]	P2[d]	P1[c]	P2[d]	P1[c]	P2[d]
No-Vest	45	327	139	187	184	514	43	315	105	99	148	414	42	280	51	35	93	315
Type II	50	193	57	29	107	222	50	183	54	-13 heat gain	104	170	50	173	53	-58 heat gain	103	115
Hybrid vest	66	480	238	360	304	840	65	466	210	309	275	775	64	433	190	306	254	739
	At 60% *RH*																	
T_{amb}	28 (°C)						32 (°C)						36 (°C)					
Case	Q_{lat} (W/m²)		Q_{sens} (W/m²)		Q_{tot} (W/m²)		Q_{lat} (W/m²)		Q_{sens} (W/m²)		Q_{tot} (W/m²)		Q_{lat} (W/m²)		Q_{sens} (W/m²)		Q_{tot} (W/m²)	
	P1[a]	P2[b]	P1[a]	P2[b]	P1[a]	P2[b]	P1[a]	P2[b]	P1[a]	P2[b]	P1[a]	P2[b]	P1[c]	P2[d]	P1[c]	P2[d]	P1[c]	P2[d]
No-Vest	43	283	80	122	123	405	41	230	39	45	80	275	38	184	-40 heat gain	-20 heat gain	-2	164
Type II	48	183	48	-10 heat gain	96	173	48	173	46	-65 heat gain	94	108	48	164	45	-116 heat gain	93	48
Hybrid vest	63	402	150	293	213	695	60	355	100	221	160	576	57	293	41	135	98	428

[a] **P1**= 8 mins for T_{amb} = 28 and 32 °C at 30% and 60% *RH*;
[b] **P2**= 52 mins for T_{amb} = 28 and 32 °C at 30% and 60% *RH*;
[c] **P1**= 7 mins for T_{amb} = 36 at 30% and 60% *RH*;
[d] **P2**= 53 mins for T_{amb} = 36 at 30% and 60% *RH*

At the same *RH* (30%), but higher T_{amb} of 32 and 36 °C, the hybrid vest had the best cooling effect on both the sensate and insensate skin over the No-Vest and Type II cases, as shown in **Fig. 36** with the highest attained Q_{lat} and Q_{sens} summarized in **Table 26**. However, this cooling effect dropped as T_{amb} increased due to the admittance of relatively hotter air in the microclimate. Similarly, the No-Vest and Type II had higher

skin temperatures by the end of exercise as T_{amb} increased, mainly due to the significant decrease in Q_{sens} as shown in **Table 26**. For example, the No-Vest case showed a drop in Q_{sens} from 139 W/m² (**P1**) and 187 W/m² (**P2**) at 28 °C, to 51 W/m² (**P1**) and 35 W/m² (**P2**) at 36 °C. It should be noted that ECV Type II showed a better performance than the No-Vest at the high T_{amb} of 36 °C on the insensate skin, as shown in **Fig. 36(f)**. This was due to exposing the shirt to cooler microclimate without admitting hot and humid ambient air.

The effect of increasing *RH* from 30 to 60 % on the sensate and insensate skin temperatures for all cases at the same metabolic rate of 6 met is shown in **Fig. 37**, and the corresponding heat losses before period **P1** and after **P2** in **Table 26**. The fast rate of increase in sensate skin temperatures in the first 5 mins due to metabolic heat generation is still shown (see **Fig. 37(a**, **c** and **e**)), but the hybrid vest performance became similar to the No-Vest due to admitting humid air in the microclimate, as was found at 3 met. The advantage of using the hybrid vest over the No-Vest became more noticeable in the presence of significant sweat evaporation by ventilation at the sensate skin. This is reflected by the increase in Q_{lat} and Q_{sens}, (see **Table 26** at 60 % *RH*) at the sensate and insensate skin, as shown in **Fig. 37**. On the other hand, the advantage of using ECV Type II over the hybrid vest became more pronounced as T_{amb} increased from 28 to 36 °C, as shown in **Fig. 37** for both sensate (before sweating) and insensate skin, similar to the results obtained at 3 met. Due to no admittance of hot and humid air in the microclimate and the absence of fan operation, ECV Type II showed lower temperature rise in the first 15, 30 and 45 minutes than the hybrid vest, as shown in **Fig. 37(b**, **d**, and **f)**, respectively. However, the total heat losses (Q_{lat} and Q_{sens}) from the sensate and insensate skin for the hybrid vest, remained higher than those of the No-Vest and ECV Type II for all ambient

conditions at 6 met, as shown in **Table 26**. This was due to the combined effect of sweat evaporation from the sensate skin using ventilation fans and water evaporation at the outer vest layer. Moreover, as was observed at 3 met, in the first few minutes, the rate of increase of the skin temperatures for ECV Type II were similar at all T_{amb}, unlike the No-Vest case that showed higher rates of increase as T_{amb} increased.
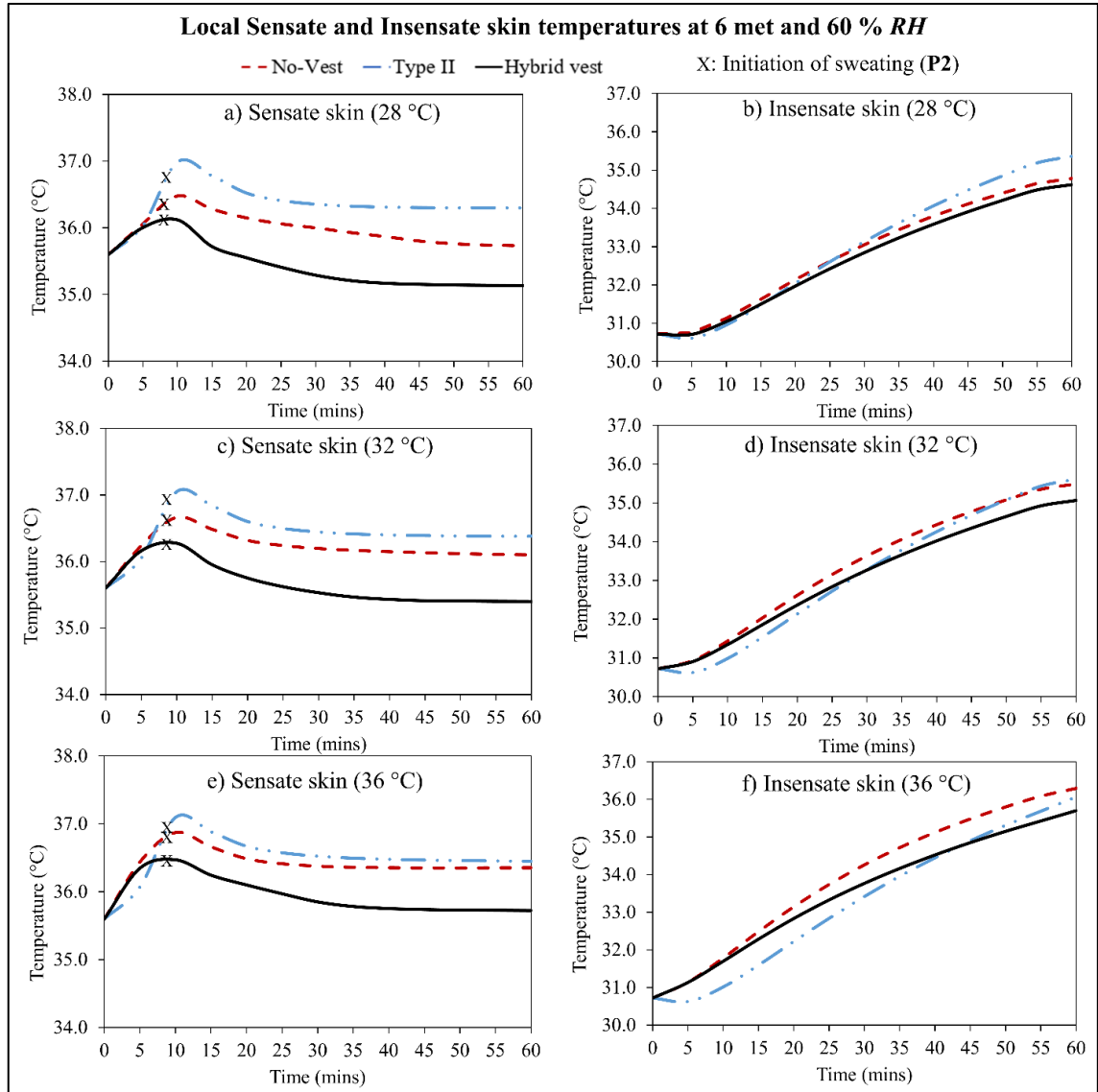

Figure 37. Plot of skin temperature variations at 6 met and 60 % *RH* of the a) sensate and b) insensate at 28 °C, c) sensate and d) insensate at 32 °C, e) sensate and f) insensate at 36°C for No-Vest, Type II, and hybrid vest

At the high activity level of 6 met, for all ambient conditions, the temperature variations of the shirt and microclimate at the sensate skin and that of water-absorbent layer showed similar trend analogous to that of $T_{sk,sen}$ for all cases. Due to sweat formation on the sensate skin, $T_{sh,sen}$, $T_{a,sen}$, and T_w dropped significantly by the hybrid vest due to ventilation effect in the microclimate. Hence, the hybrid vest had lower $\dot{m}_{evap}$ compared to that of Type II due to lower T_w which reduced the drop in m_w of the hybrid vest during exercise.

Finally, at activity level of 6 met, T_{cr} increased from the thermal neutral state of the body at 36.71 °C to 37.88 °C, 37.89 °C, 37.85 °C at the end of exercise for the cases of No-Vest, Type II and hybrid vest, respectively, for the ambient conditions of 28 - 36 °C and 30 - 60 % RH. The rapid increase in T_{cr} at high activity level was an indication of the impaired thermoregulatory response in persons with PA, as the predicted results agreed with the findings of previous studies in literature (Bongers et al., 2016; Petrofsky, 1992; Price and Campbell, 2003). Moreover, the body of a person with PA was under thermal strain as T_{cr} exceeded 37.5 °C (Miller and Ziskin, 1989).

4.5.3. *Effectiveness of the hybrid vest at moderate and high physical activity level*

Table 27 presents the time-averaged heat losses in the hybrid vest before (**P1**) and after (**P2**) sweating at the sensate skin, at 3 and 6 met and different ambient conditions. The heat losses of the hybrid vest calculated at the shirt can be divided into two parts: the first showing the contribution of the ventilation fans due to the convective heat and mass transfer from the shirt, and the second showing the contribution of the water evaporation

at the outer ECV material, which was reflected by radiation cooling between the shirt and the inner ECV layer.

At 3 met, heat losses due to ventilation and ECV material were more significant at low T_{amb} and RH with the highest values of 123 W/m^2 and 49 W/m^2, respectively, attained at 28 °C and 30 % where no sweating occurred, as shown in **Table 27**. These values dropped as T_{amb} increased from 28 to 36 °C at the same RH of 30 % due to the reduced sensible cooling effect by admitting hotter air in the microclimate. Similarly, as RH increased from 30 to 60 % at the same T_{amb}, the heat losses dropped due to limited evaporation at the shirt and the outer ECV layer.

At 6 met, similar drops in heat losses were attained as T_{amb} or RH increased as in the 3 met cases. However, all the 6 met cases had sweating and thus, the operation of the ventilation fans before sweating starts (**P1**) is not recommended due to the heat gain that occurs, which is reflected by the ventilation heat gains at T_{amb} of 32 and 36 °C and 60 % RH, as shown in **Table 27**. On the other hand, the use of ECV material at **P1** was still reasonable as indicated by the positive heat losses at the same ambient conditions. After sweating started (**P2**), most of the heat losses were contributed to the presence of ventilations fans that resulted with significant improvement in the heat losses as shown in **Table 27** at all ambient conditions.

Table 27. Time-averaged heat losses in the hybrid vest at the sensate skin at 3 and 6 met and different ambient conditions

T_{amb}	RH	3 met		6 met			
		Heat loss due to ventilation (W/m^2)	Heat loss due to ECV material (W/m^2)	Heat loss due to ventilation (W/m^2)		Heat loss due to ECV material (W/m^2)	
				P1	P2	P1	P2
28 ºC	30 %	123	49	156	591	48	47
	60 %	89	40	55	468	45	38
32 ºC	30 %	89	40	123	552	41	37

	60 %	63	28	(5) heat gain	396	37	26
36 ºC	**30 %**	87	29	97	510	36	27
	60 %	32	16	(73) heat gain	309	28	14

Table 28 summarizes the enhancement factor (ε_{ECV}) in the time-average total heat losses at both sensate and insensate skin and the time-average drop in $T_{sk,sen}$ of the hybrid vest over that of No-Vest at moderate and high activity levels, and all ambient conditions. Based on the findings of the thermophysiological responses obtained in the parametric study, the ambient conditions at which the hybrid vest succeeded in causing a significant drop in $T_{sk,sen}$, are marked in bold in **Table 28**.

At moderate physical activity (3 met), ε_{ECV} of the hybrid vest ranged between 1.15 and 3.61 for high T_{amb} ($\geq$ 28 °C). Nevertheless, at moderate activity level in high T_{amb} ($\geq$ 32 °C) and RH ($\geq$ 60 %), it is recommended not to operate the fans at the beginning of exercise, since during that period, ECV material without ventilation can be enough to provide the desired cooling effect.

At high physical activity (6 met), ε_{ECV} ranged between 1.64 and 3.25 for high T_{amb} ($\geq$ 28 °C), although similarly, it is not recommended to use the fans at $T_{amb} \geq 32$ °C and $RH \geq 60$ %. The hybrid vest showed a significant drop in $T_{sk,sen}$ from No-Vest above 0.6 °C at 6 met only for (i) low RH of 30 % at all T_{amb}; (Tanabe et al.) at high RH of 60 % but at $T_{amb} < 36$ °C (see **Table 28)**.

This implies that the use of the hybrid vest at moderate activity (3 met) with no sweating present and at high activity level (6 met) but with hot and humid ambient conditions is not recommended. Additionally, it was noted that both the ε_{ECV} and the drop in $T_{sk,sen}$ increased as T_{amb} and RH increased in most of the cases, since the No-Vest case had sensible heat gain rather than heat loss, while the hybrid vest was still able to provide

sensible cooling due to the presence of the water-absorbent layer of the ECV material. Moreover, sweat evaporation was enhanced due to ventilation in the microclimate of the hybrid vest, whereas the No-Vest case had limited evaporation with the environment.

The cases with a substantial cooling effect could enhance thermal comfort and sensation levels for persons with PA, as it was reported in published experimental studies in which the local sensate skin temperature dropped by ~ 1 °C compared to No-Vest case (Mneimneh et al., 2020a; Mneimneh et al., 2020b). Hence, this shows the advantage of ventilation in the microclimate to decrease the regain of the shirt, admit cool air, and sustain low moisture content in the microclimate that enhance heat losses of the hybrid vest over the No-Vest and Type II. At low met and in the absence of sweat or at high met with delayed sweating, the hybrid vest for persons with PA would perform better than Type I (without water-absorbent layer). The main advantages of blowing air in the hybrid vest are: i) preventing overheat of the microclimate beyond the ambient air temperature, and ii) preventing the build-up of moisture inside the microclimate, thus enhancing evaporation from the shirt.

Table 28. ε_{ECV} (Enhancement factor) in time-average total heat losses at sensate and insensate skin and time-average drop in $T_{sk,sen}$ of the hybrid vest over that of No-Vest

		At 3 met			At 6 met		
RH (%)	T_{amb} (°C)	28	32	36	28	32	36
30	ε_{ECV}	1.23	1.63	3.00	**1.64**	**1.87**	**2.43**
	Drop in $T_{sk,sen}$ (°C)	0.06	0.14	0.22	**0.80**	**0.83**	**0.84**
60	ε_{ECV}	1.15	1.69	3.61	**1.72**	**2.07**	3.25
	Drop in $T_{sk,sen}$ (°C)	0.00	0.06	0.07	**0.65**	**0.63**	0.54

4.5.4. Conclusion

Based on the findings of the parametric study of the Hybrid ECV-PA bioheat model, the hybrid vest succeeded in enhancing both sensible and latent heat losses for persons with PA compared to No-Vest and ECV Type II. However, the significance of this enhancement was dependent on the activity levels and ambient conditions. At moderate activity level, the hybrid vest improved heat losses at the trunk by a factor between 1.15 and 3.61, but it did not show a significant drop in local skin temperatures (< 0.6 °C) of the trunk for persons with PA compared to No-Vest. At high activity level, the hybrid vest improved heat losses at the trunk by a factor between 1.64 and 3.25, and its performance was effective in reducing skin temperatures at low *RH* for all simulated T_{amb} conditions, and at high *RH* but with T_{amb} lower than 32 °C, with a maximum of 0.84 °C drop in local sensate skin temperature of the trunk. This drop might be sufficient to improve the thermal comfort and sensation level for persons with PA. The above hybrid vest limitations imply that the use of the hybrid vest is recommended at $T_{amb} \leq 32$ °C and *RH* < 60% at both metabolic rates. Whereas, at $T_{amb} \geq 32$ °C and *RH* ≥ 60 %, before sweat and moisture accumulation start, the use of ECV Type II is recommended over the hybrid vest.

CHAPTER 5

EXPERIMENTAL RESULTS

5.1. Validation of Hybrid ECV model

The applied heat flux on the heated plate, and the ambient condition (temperature and *RH*) in the space were the input boundary conditions of the hybrid ECV model. The ventilation air flow rate was measured and used as input value. The initial temperature of the shirt and three layers of the vest; inner layer, water-absorbent layer, and outer layer; as well as the initial weight upon activation of the ECV and wet shirt were used as the initial conditions of the model.

Figure 38(a-c) shows the predicted and experimental temperature variations of the (a) shirt, (b) microclimate, and (c) inner vest layer at sensate (wet region) and insensate (dry region) nodes at both ambient conditions (28 ℃, 63% *RH* and 32 ℃, 45% *RH*).

In **Fig. 38(a)**, at both ambient conditions, the insensate node temperature of the dry shirt, $T_{sh,insen}$, showed a fast increase by $\sim$2 ℃ in the first two minutes of the 30-min period and continued increasing but at a relatively slow rate due to the heat flux gain. Whereas, the sensate node temperature of the wet shirt, $T_{sh,sen}$, dropped by $\sim$3 ℃ also in the first two minutes, and remained stable till the end of the experiment due to the effect of water evaporation from the wet shirt.

In **Fig. 38(b)**, the microclimate temperature at the sensate node, $T_{a,sen}$, followed similar trend as that of $T_{sh,sen}$ indicating that the air layer was cooled by the effect of evaporation at the wet shirt at both ambient conditions. At 28 ℃, 63% *RH*, the microclimate temperature of the insensate node, $T_{a,insen}$, had a slight increase above T_{amb} in the first few minutes due to the heat exchange with the hotter dry shirt as shown in **Fig.**

38(a). After that, $T_{a,insen}$ stabilized around T_{amb} of 28 °C. Whereas, at 32 °C, 45% RH, $T_{a,insen}$ dropped from the initial condition by $\sim$1 ℃ and remained below that of $T_{sh,insen}$ till the end of experiment; indicating the admitted air was cooled near the inner vest layer.

Finally, in **Fig. 38(c)**, the inner vest layer temperatures at the insensate node, $T_{i,insen}$, and sensate node, $T_{i,sen}$, increased by $\sim$1.5 ℃ and $\sim$0.5 ℃ from the initial state at 28 °C, 63% RH, and by $\sim$2 ℃ and $\sim$1 ℃ from the initial state at 32 °C, 45% RH, respectively. In summary, the insensate and sensate nodes of the hybrid ECV have different thermal response represented by the temperature variations of the shirt, microclimate, and inner vest layer due to the underlying different physics at wet and dry surfaces.
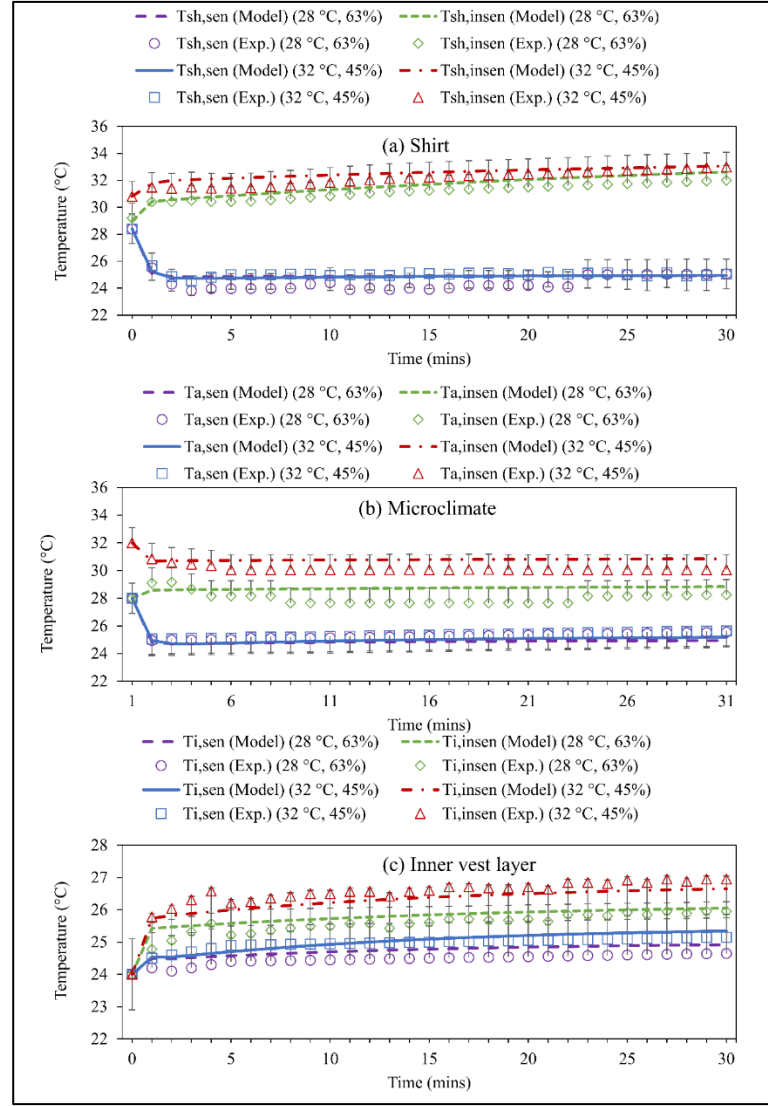
Figure 38. Plot of the predicted and experimental temperature variations of the (a) shirt, (b) microclimate, and (c) inner vest layer at sensate (wet region) and insensate (dry region) nodes

Figure 39 shows the predicted and experimental temperature variations of water-absorbent and outer layers of the hybrid vest model at both ambient conditions. The increase in water-absorbent layer temperature, T_w, was at a slow rate and did not exceed $\sim$0.5 ℃ from its initial state due to water evaporation process during the experiment. Hence, T_w remained below that of $T_{i,insen}$ and $T_{i,sen}$ while approaching the wet-bulb temperature of the ambient condition (22.56 ℃ at 28 ℃, 63% *RH* and 22.60 ℃ at 32 ℃,

45% *RH*). Whereas, the outer vest layer temperature, T_o increased from its initial state in the first two minutes by ~1.0 °C at 28 °C, 63% *RH* and by ~1.5 °C at 32 °C, 45% *RH* due to the heat exchange with the ambient. Then at both ambient conditions, T_o remained above T_w and attained steady state condition.

Finally, measurements of weight variations of the system (wet shirt and ECV material) showed a maximum drop of ~7% from the initial mass of the system by the end of the experiment, verifying the occurrence of water evaporation from the wet shirt and water-absorbent layer of the vest, leading to heat losses and a drop in $T_{sh,sen}$.
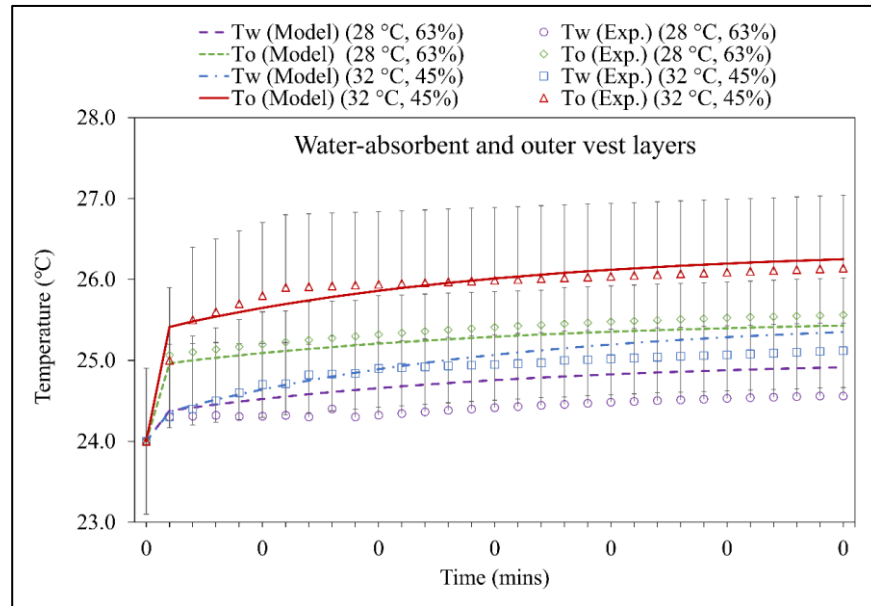
Figure 39. Plot of the predicted and experimental temperature variations of water-absorbent and outer layer of the hybrid vest

The model predictions of the temperature variations of the sensate (wet region) and insensate (dry region) nodes of the shirt, microclimate, and inner vest layer showed good agreement with the experimental ones. A better agreement was observed at the sensate (wet region) than the insensate (dry region), with a maximum error of 1 °C (0.5 °C) at 28 °C (at 32 °C) at the sensate and 1.1 °C (0.8 °C) at 28 °C (at 32 °C) at the insensate. The

maximum error in the prediction of water-absorbent and outer vest layers was 0.4 ℃ at 28 ℃ and 32 ℃, indicating a good agreement with the experimental results. Finally, at both ambient conditions, there was a maximum error of 2 g in the drop of the wet shirt and ECV material mass. The validated hybrid ECV model could be used to conduct the parametric study explained in section 2.9.

5.2. Human subject experiments: Effect of PCM location and coverage skin area on the performance of PCM cooling vest (V1, V2 and NV tests)

All experiments were completed by the three groups with no change in the number of participants by the end of the test inside the climatic chamber. A description of physiological and subjective findings, as well as, its corresponding discussion were established for each group in this section.

5.2.1. Group I: High-thoracic SCI T1-T3

At the baseline of the experiment, Group I showed insignificant difference in the values of HR, T_{cr} and $T_{sk,mean}$ between NV and V1 tests (94.0±6.6, 93.7±6.5 bpm; 37.07±0.46, 37.10±0.52 ℃; 31.25±0.23, 30.54±0.69 ℃). **Fig. 40(a-c)** presents the values of HR, ΔT_{cr} and $\Delta T_{sk,mean}$ during the complete one-hr. of the experiment. In **Fig. 40(a)**, HR values showed insignificant difference in V1 compared to NV ($p > 0.05$). In **Fig. 40(b)**, there was no significant difference in ΔT_{cr} between NV and V1 during preconditioning, exercise, and recovery period ($p > 0.05$). In **Fig. 40(c)**, $\Delta T_{sk,mean}$ was lower in V1 compared to NV during the complete one-hr. experiment (average difference $=0.82 \pm 0.1℃$).
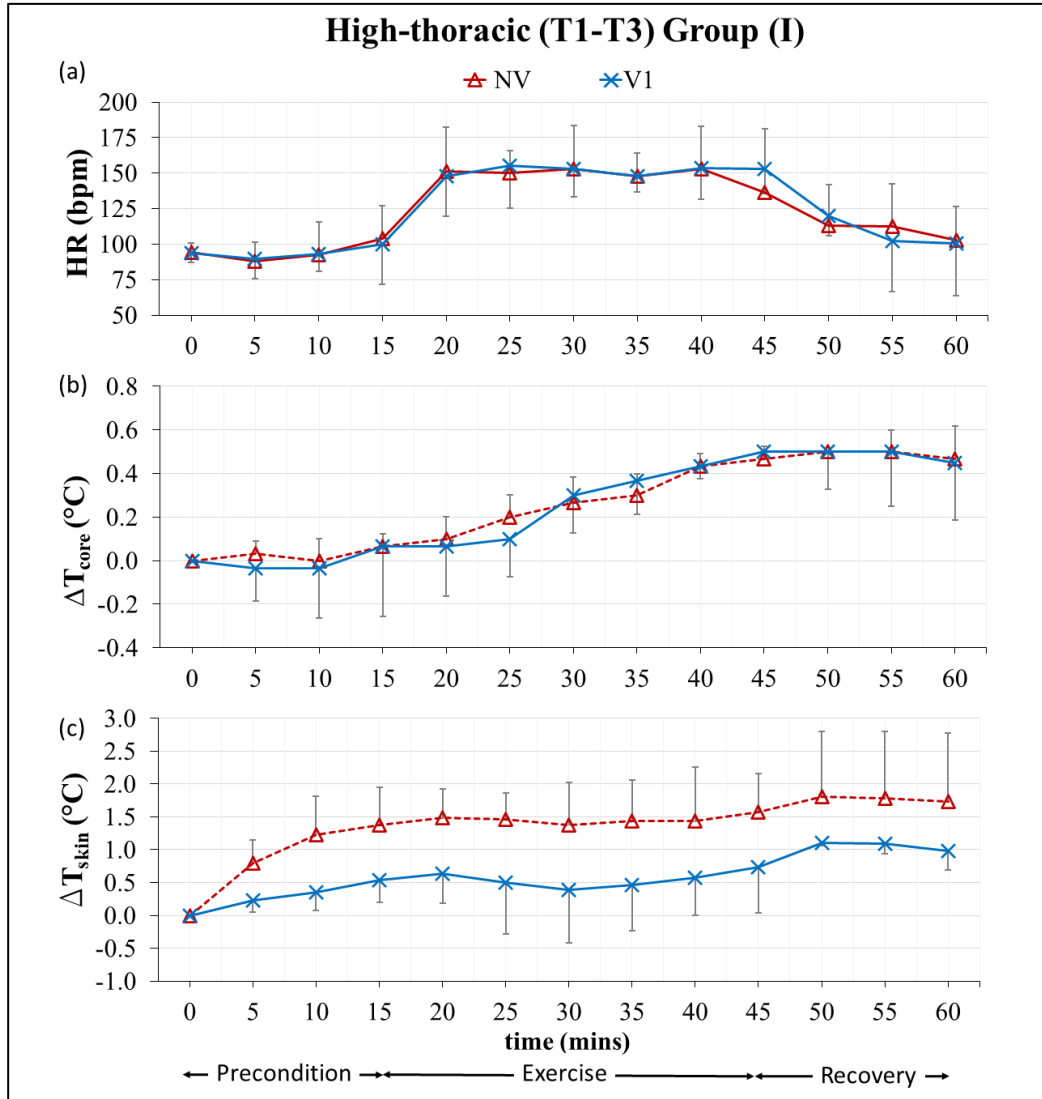
Figure 40. Plot of (a) heart rate values (b) change in core temperature (ΔT_{cr}), and (c)

change in skin temperature (ΔT_{sk}) (mean ± SD) for Group (I)

No significant difference of T_{sk} values of trunk segments was found at the baseline of the experiment for NV and V1 tests (chest: 32.48±0.27, 32.44±1.53; upper back: 33.13±0.48, 33.44±0.58; pelvis: 33.62±1.54, 32.94±1.61; lower back: 34.76±0.77, 34.94±1.48; p > 0.05). **Fig. 41(a-d)** shows the change in segmental skin temperature (ΔT_{sk}) for the trunk segments (a) chest, (b) upper back, (c) pelvis, and (d) lower back. In all segments of the trunk, ΔT_{sk} was less in V1 compared to the NV test (mean difference

of ΔT_{sk} $1.1 \pm 0.5°C, 1.0 \pm 0.2°C, 1.0 \pm 0.5 °C$ for chest, pelvis, and lower back; respectively; p<0.05) except for the upper back that showed no difference. The trend of increase of T_{sk} at the sensate skin of the trunk (for this group, the upper part of the chest and upper back) was analogous to that of T_{cr} due to active vasodilation that transferred metabolic heat generated at the core of the segment. whereas, this trend was absent at the insensate skin as seen more profoundly at the lower back, due to the absence of vasodilation effect.
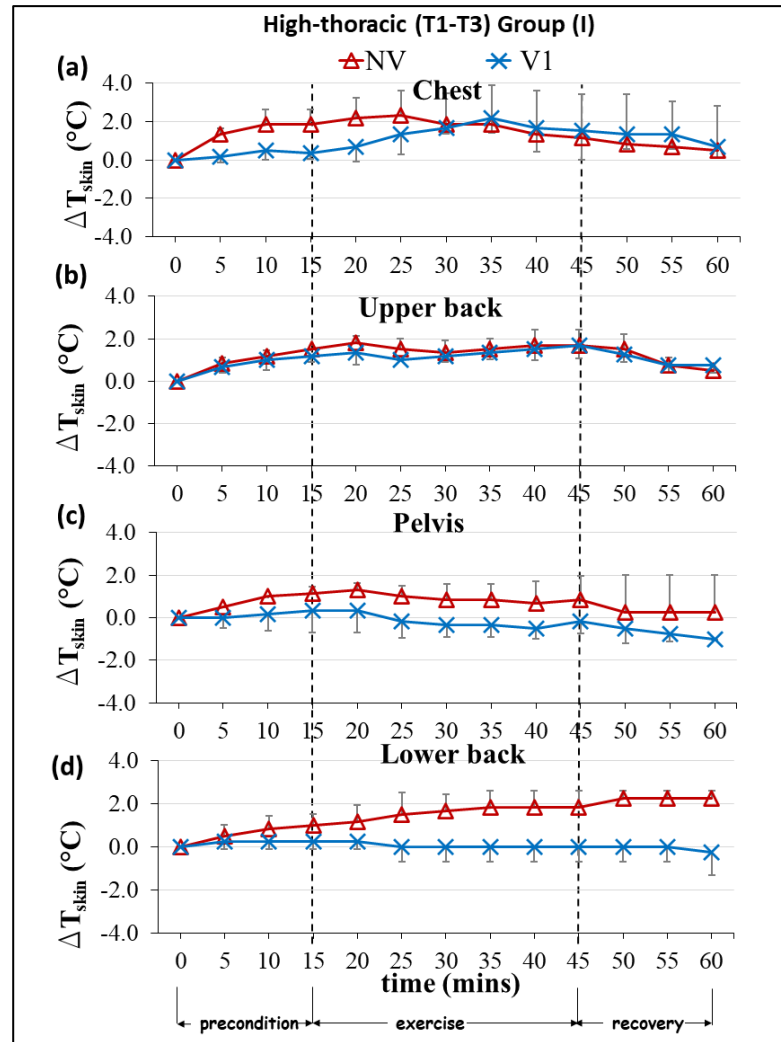

Figure 41. Plot of change in skin temperature (ΔT_{sk}) (a) chest (b) upper back (c) pelvis (d) lower back for Group (I)

Figure 42(a-e) demonstrates the results of subjective voting of the participants on (a) skin wettedness, (b) perceived exertion, (c) thermal comfort, and (d) thermal sensation at the head, shoulders, and neck, and (e) thermal sensation at the trunk during exercise. It is clear from **Fig. 42(a)** that wearing the vest has no effect on skin wettedness. **Fig. 42(b)** does not show an improvement in the perceived exertion of subjects (mean difference: 1 ± 0.5) which indicates that wearing the vest did not reduce exhaustion during exercise. Furthermore, **Fig. 42(c)** shows improvement in thermal comfort from "slightly uncomfortable" to "comfortable" during the first 15 mins of the exercise in V1 test compared to NV, but changes to "uncomfortable" until the end of the exercise. Thus, the improved comfort is insignificant during exercise (p>0.05). **Fig. 42(d)** shows an insignificant decrease in thermal sensation at head, shoulders, and neck except at time=15 min (mean difference: 0.9 ± 1; $p > 0.05$). Whereas, **Fig. 42(e)**, thermal sensation at the trunk was neutral when wearing V1 and not warm as in NV case during exercise (mean difference: 1.6 ± 0.3; $p < 0.05$).
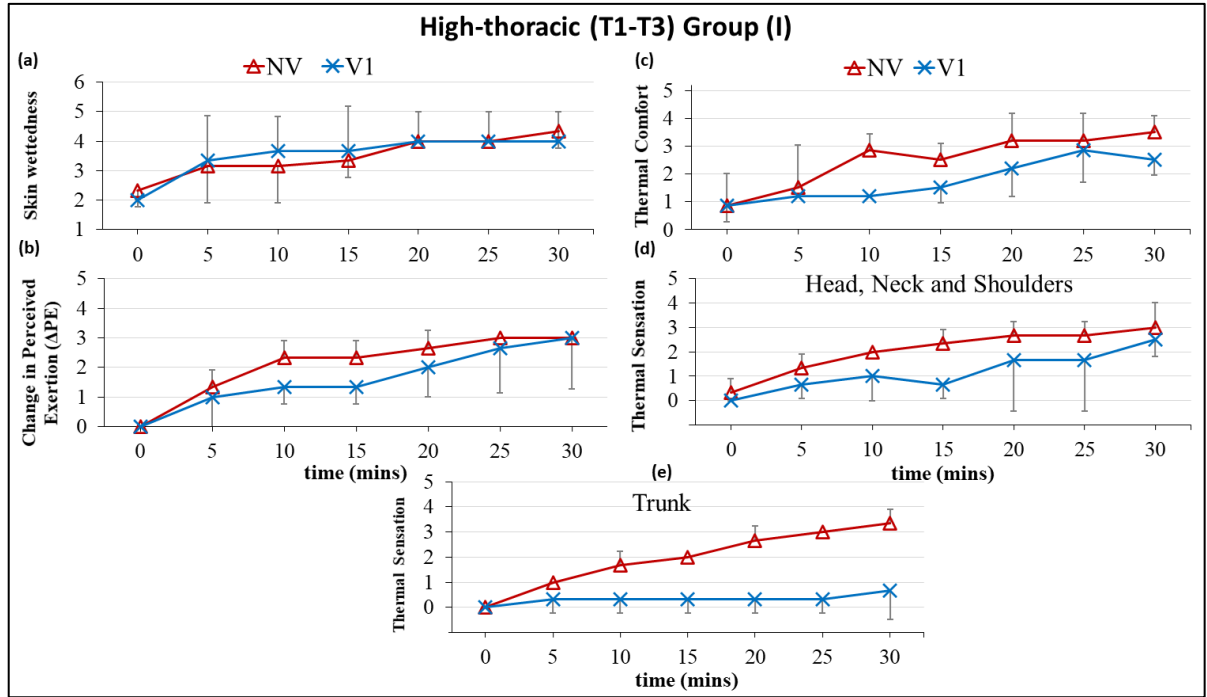
Figure 42. Plot of (a) skin wettedness (b) ΔPE (change in perceived exertion) (c) thermal comfort (d) thermal sensation at head, neck, and shoulders (e) thermal sensation at trunk, for Group (I)

The physiological findings of Group I indicated that although $T_{sk,mean}$ values were reduced while using V1, the cooling vest had no effect on reducing T_{cr} values. More precisely, when the sensate skin of the trunk (chest and upper back) cooled, its temperature increased similarly to the NV condition at the end of the experiment. Hence, preserved vasodilation response at the sensate skin of the trunk in Group I allows cooler blood to circulate from the periphery to the core when using V1. Whereas, insensate skin temperature dropped significantly when covered with V1 compared to NV because of absence of vasodilation response in this area. However, the limited sensate skin area at the trunk (not exceeding 25% from its area) was not sufficient to reduce T_{cr} values for Group I. Furthermore, cooling the insensate skin of trunk had no effect in enhancing body

184

heat dissipation at the periphery. Subjective voting of thermal comfort during exercise showed insignificant improvement in psychological perception analogous to the insignificant effect on T_{cr} values. Thus, persons with high-thoracic injury should seek out other cooling methods that reduce the rise in T_{cr} values and improve thermal comfort and sensation during exercise in heat (Trbovich, 2019).

5.2.2. *Group II: Mid-thoracic SCI T4-T8*

Initially (time=0 mins), Group II had insignificant difference in the values of HR, T_{cr} and $T_{sk,mean}$ between NV, V1 and V2 tests (85±12, 86.8±10, 85.8±15 bpm; 36.95±0.23, 37.08±0.33, 36.96±0.32 ℃; 32.2±1.05, 32.47±0.68, 32.65±1.1 ℃). **Fig. 43(a-c)** presents values of HR, ΔT_{cr} and $\Delta T_{sk,mean}$ during a complete one-hour exercise. In **Fig. 43(a)**, HR values do not show significant difference in V1 and V2 compared to NV($p > 0.05$). **Fig. 43(b)** shows ΔT_{cr} for the three tests. From the initial time of preconditioning (t=0 min) until the end of the exercise (time=45 min), the average ΔT_{cr} values showed negligible difference between the three tests ($p > 0.05$). However, the deviation started to appear during V1 ($0.26 \pm 0.04℃; p = 0.024$) and V2 ($0.20℃ \pm 0.03℃; p = 0.034$) at the end of exercise (time=45 mins) until the end of the recovery period (time=60 mins) both compared to NV. **Fig. 43(c)** at the end of exercise shows that $\Delta T_{sk,mean}$ values were lower in V1 compared to NV and V2 (mean difference =$0.45 \pm 0.15℃; p = 1.03E - 11$); whereas, no significant difference was found between V2 and NV ($p > 0.05$).
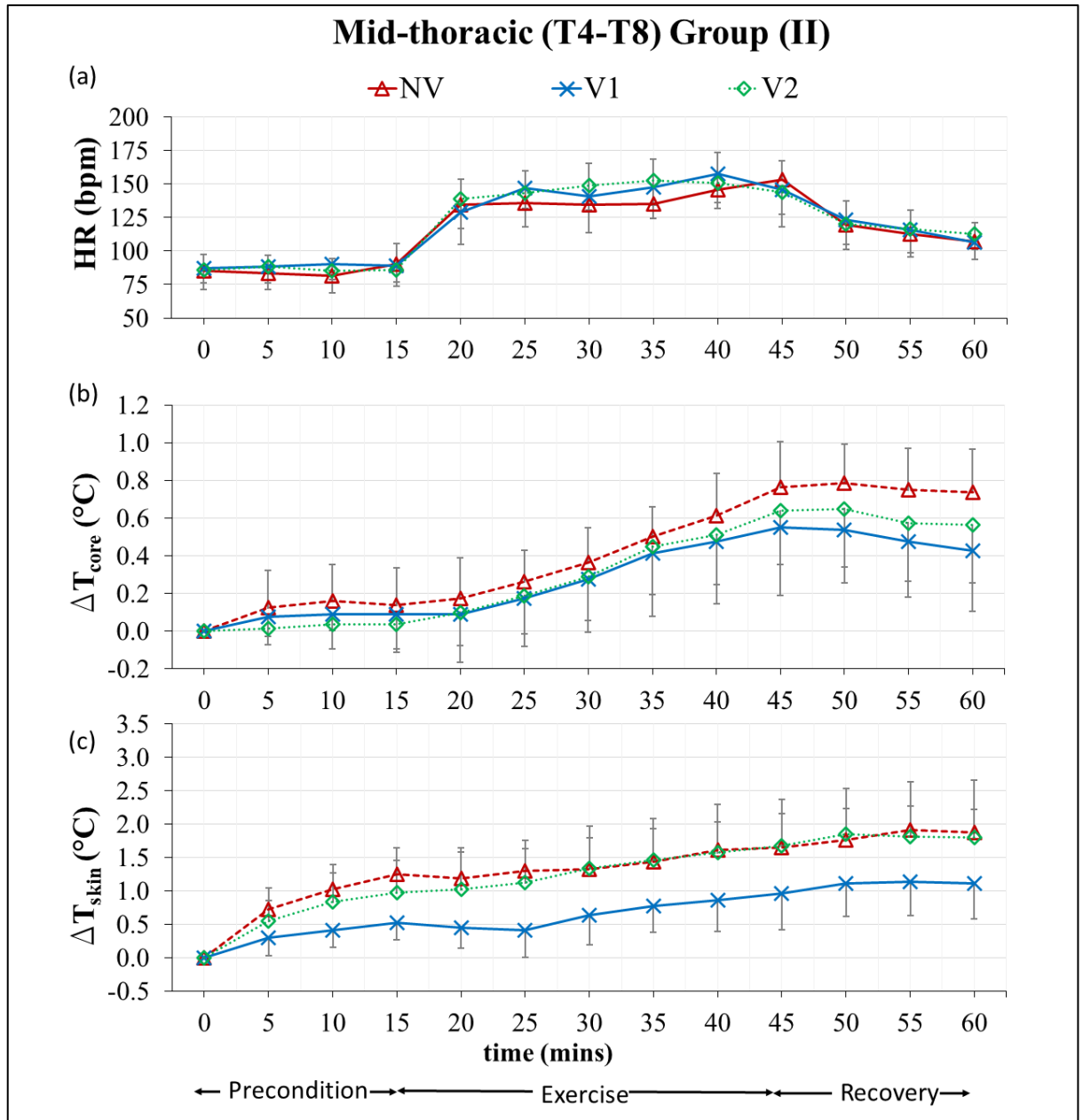
Figure 43. Plot of (a) heart rate values (b) change in core temperature (ΔT_{cr}) and (c) change in skin temperature (ΔT_{sk}) (mean $\pm$ SD) for Group II

No significant difference of T_{sk} values of trunk segments was found at the baseline of the experiment for NV, V1, and V2 tests (chest: 33.49±0.8, 33.43±1.0, 33.43±1.0; upper back: 33.16±0.8, 33.79±1.4, 33.75±1.3; pelvis: 32.72±1.5, 32.52±1.3, 32.92±1.7; lower back: 33.85±1.6, 32.40±2.1, 34.22±1.1; $p > 0.05$). **Fig. 44(a-d)** shows

the values of ΔT_{sk} for the trunk segments (a) chest, (b) upper back, (c) pelvis, and (d) lower back. In **Fig. 44(a)**, chest shows lower change during preconditioning and first 15-min of exercise (time=30 mins) at mean difference 0.7℃ and 0.85℃ for V1 and V2 compared to NV, respectively. This difference was minimized after this period to become statistically insignificant ($p > 0.05$) during recovery. **Fig. 44(b)** shows that the upper back did not have significant change between three tests ($p > 0.05$). Whereas, as seen in **Fig. 44(c-d)**, the pelvis and lower back showed significant decrease during V1 compared to NV and V2 ($p = 0.001$).
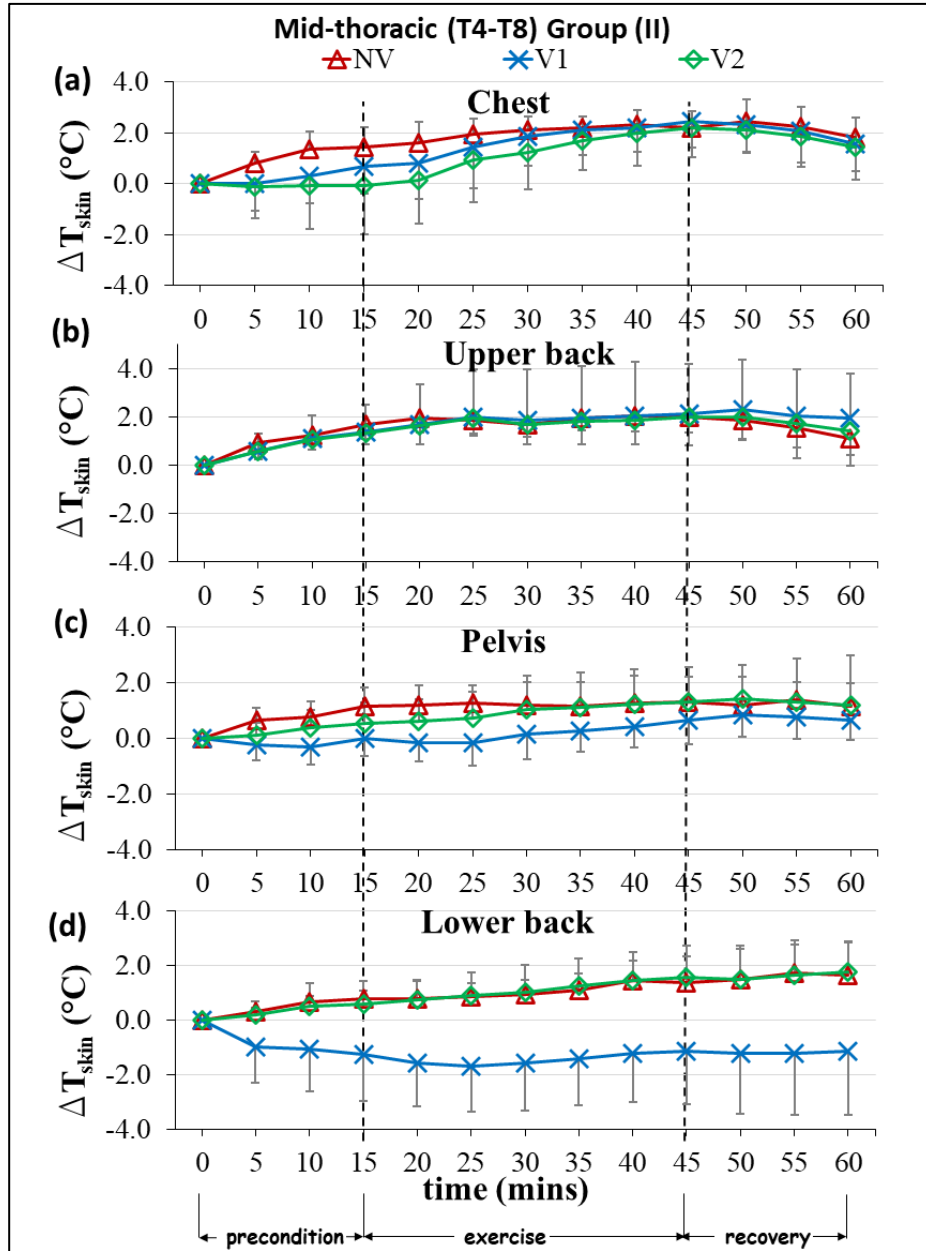
Figure 44. Plot of change in skin temperature (ΔT_{sk}) (a) chest (b) upper back (c) pelvis

(d) lower back for Group II

Figure 45(a-e) shows the results of subjective voting of the participants on (a) skin wettedness, (b) perceived exertion, (c) thermal comfort (d) thermal sensation at the head, shoulders and neck, and (e) thermal sensation at trunk during exercise. Skin wettedness was reduced by mean difference 1.25 ± 0.6 ($p = 0.002$) when wearing the

vest for both configurations (see **Fig. 45a**). Change in perceived exertion (p=0.01) was improved in V2 compared to V1 and NV tests (see **Fig. 45b**). Finally, thermal comfort (p=0.03), thermal sensation at head, neck, shoulders (p=0.03), as well as, trunk (p=0.001) were improved in both V1 and V2 compared to NV tests (see **Fig. 45(c-e)**).
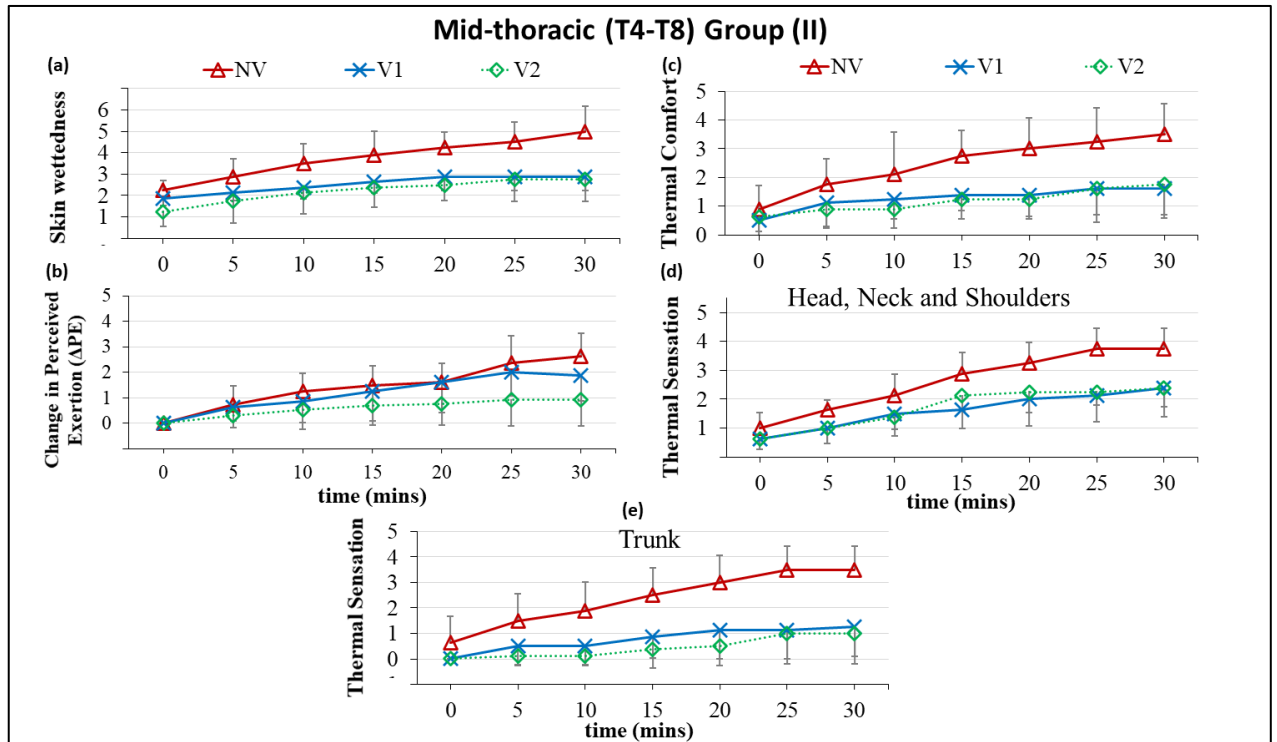
Figure 45. Plot of (a) skin wettedness (b) ΔPE (change in perceived exertion) (c) thermal comfort (d) thermal sensation at head, neck, and shoulders (e) thermal sensation at trunk for Group II

The physiological findings of **Group II** established a significant effect of the cooling vest (whether V1 or V2) on attenuating ΔT_{cr} by the end of the exercise and recovery period in hot exposure. Furthermore, using V2 provided significant effect in reducing T_{cr} values similar to that of V1 as only the sensate skin of trunk (chest and upper back) was covered. Conductive cooling at the sensate skin of trunk and active vasodilation

response at this area enhanced heat dissipation and accelerated thermal regulation in Group II (Kenny and McGinn, 2017). Furthermore, the insensate skin temperature of the trunk (pelvis and lower back) did not show preserved thermoregulation as its temperature was affected by type of vest (i.e. placement of PCM packets) rather than metabolic heat generated, then, having insignificant effect on T_{cr} values. Subjective voting of thermal comfort and sensation supported the physiological responses during exercise in heat because Group II was comfortable and slightly warm when wearing the two types of vest (V1 and V2). However, the lighter weight of V2 compared to V1 (36% less) lessened perceived exertion until the end of the exercise. Therefore, the mid-thoracic group can benefit from the lighter cooling vest that covers the sensate skin of the trunk to limit the unsafe elevation in T_{cr} values during exercise in heat.

5.2.3. Group III: Low-thoracic SCI T9-T12

At time= 0 mins, Group III showed insignificant difference in the values of HR, T_{cr} and $T_{sk,mean}$ between NV and V1 tests (85±12, 89±12 bpm; 37.16±0.3, 37.12±0.3 ℃; 31.66±1.3, 31.85±1.0 ℃). **Fig. 46(a-c)** presents values of HR, ΔT_{cr} and $\Delta T_{sk,mean}$ values during the complete one-hr. exercise. In **Fig. 46(a)**, HR values were lower in V1 compared to NV, but this difference was insignificant($p > 0.05$). **Fig. 46(b)** shows ΔT_{cr} values for **Group III** during the complete one-hr. exercise. There was no change in core temperature during preconditioning while wearing the vest ($\Delta T_{cr} \cong 0.0 \pm 0.07℃$) indicating steady neutral thermal state before exercise. This change started to increase up to $\Delta T_{cr} \cong 0.3 \pm 0.15℃$ ($p = 0.034$) followed by a significant decrease in core temperature during recovery period (time=45 mins) in V1 compared to NV. **Fig. 46(c)**

shows ΔT_{sk} values with significant reduction when using V1 compared to NV ($\Delta T_{sk} = 1.0 \pm 0.3°C, p = 1.86E - 14$).
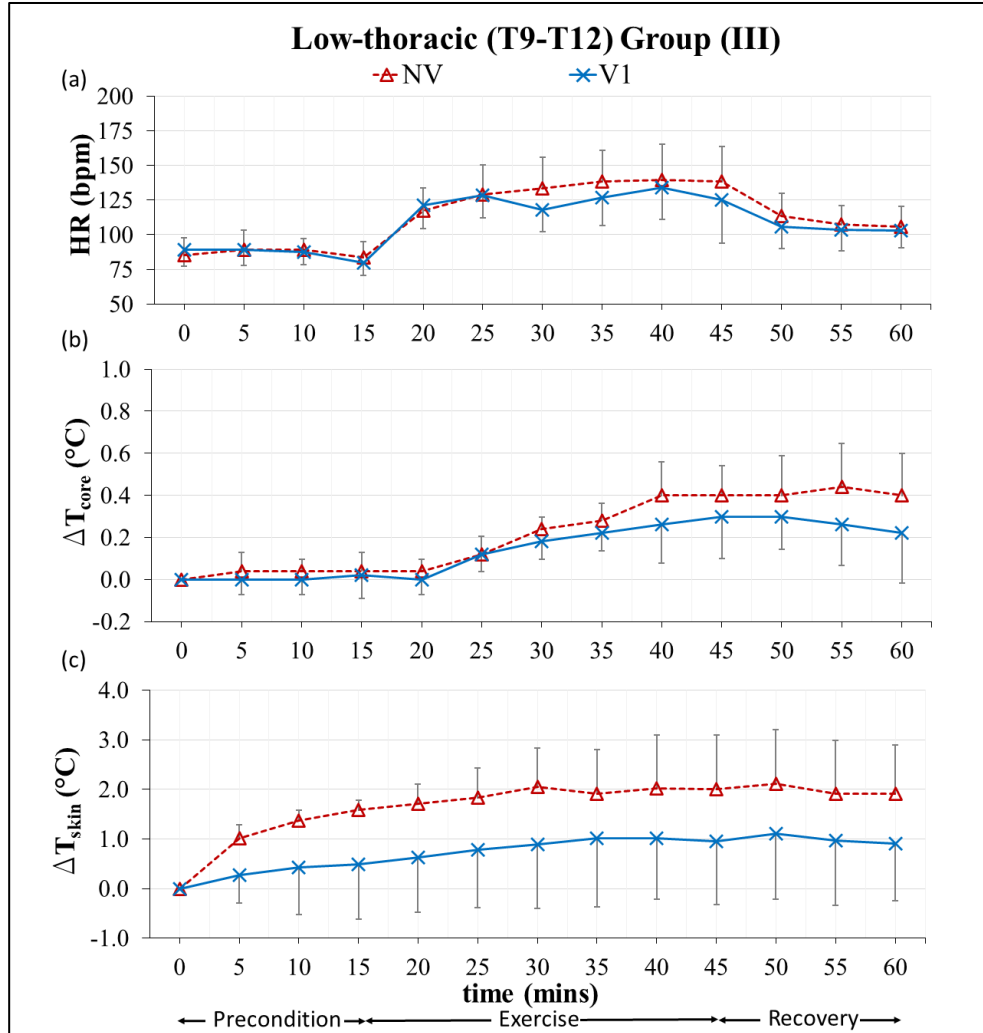
Figure 46. Plot of (a) heart rate values (b) change in core temperature (ΔT_{cr}) and (c) change in skin temperature (ΔT_{sk}) (mean ± SD) for Group (III)

No significant difference of T_{sk} values of trunk segments was found at the baseline of the experiment for NV and V1 tests (chest: 33.22±0.73, 33.24±1.29; upper back: 34.10±0.95, 34.21±2.06; pelvis: 33.62±2.21, 32.29±2.18; lower back: 34.71±1.71, 33.60±1.7; $p > 0.05$). **Fig. 47(a-d)** shows the change in segmental skin temperature (ΔT_{sk}) for the trunk segments (a) chest, (b) upper back, (c) pelvis, and (d) lower back. In

Fig. 47(a), the skin temperatures of the chest were less during preconditioning in V1 compared to NV. Yet the difference ΔT_{sk} between the two tests started to be minimal after 5 minutes of exercising. In **Fig. 47(b)**, for both tests, the upper back showed a similar trend of transient change during the one hour. Whereas in **Fig. 47(c-d)**, the lower part of trunk (lower back and pelvis) showed a decrease when using V1 during the first 5 minutes of preconditioning then remained constant throughout the hour.

Figure 47. Plot of change in skin temperature (ΔT_{sk}) (a) chest (b) upper back (c) pelvis (d) lower back for Group (III)
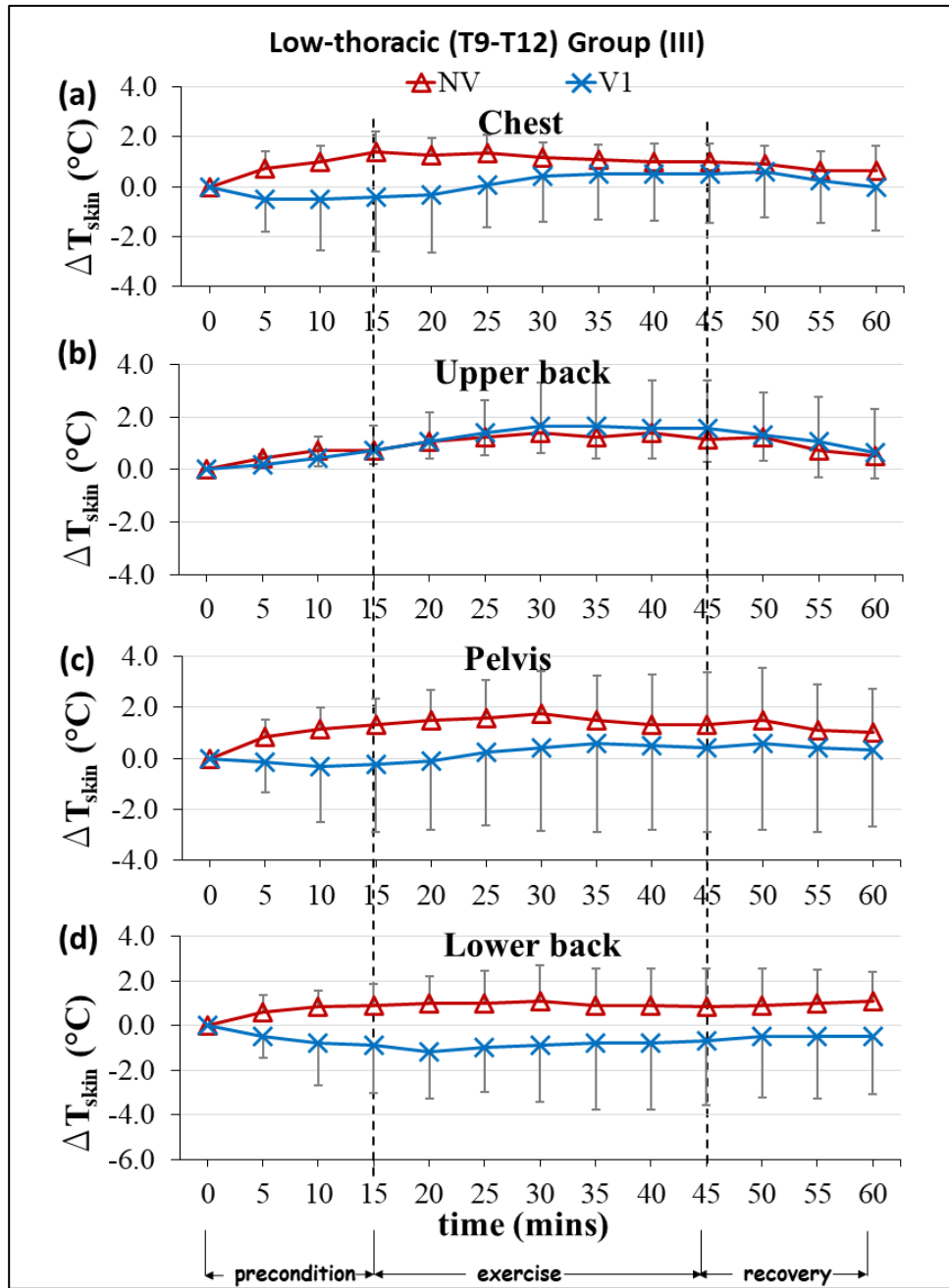
Fig. 48(a-e) demonstrates the results of subjective voting of the participants on (a) skin wettedness, (b) perceived exertion, (c) thermal comfort (d) thermal sensation at the head, shoulders and neck, and (e) thermal sensation at the trunk during exercise. Skin

wettedness was reduced when wearing the vest (see **Fig. 48a**). Change in perceived exertion improved in V1 compared to the NV test (p=0.04) (see **Fig. 48b**). Finally, thermal comfort, thermal sensation at head, neck, shoulders, as well as trunk, improved in V1 compared to the NV tests ($p<0.05$) (see **Fig. 48(c-e)**).
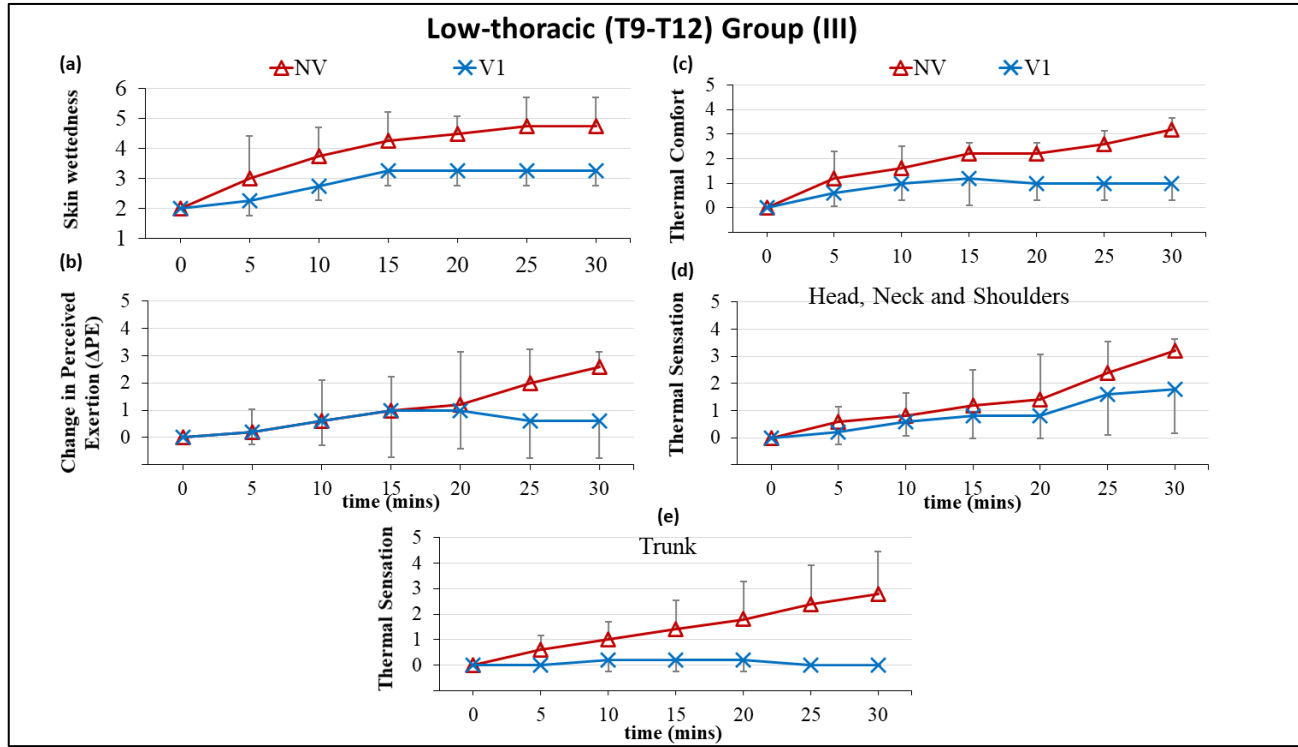
Figure 48. Plot of (a) skin wettedness (b) ΔPE (change in perceived exertion) (c) thermal comfort (d) thermal sensation at head, neck, and shoulders (e) thermal sensation at trunk, for Group (III)

The physiological findings of Group (III) showed that people with low-thoracic injury may exhibit thermal physiology similar to that of able-bodied people ($\Delta T_{cr,AB} \cong 0.42\pm0.1°C$) when performing an upper-body exercise in hot exposure (Young, 1987). Furthermore, the use of V1 had a significant cooling effect on diminishing ΔT_{cr} values during exercise and the recovery period. The large sensate skin of trunk (75% of its area)

balanced heat gain through active vasodilation at the periphery with cooler blood reaching the core. Thermal comfort and sensation were both improved while wearing V1 during exercise. Therefore, persons with low-thoracic injury can indeed benefit from a PCM cooling vest covering the sensate skin of trunk (chest, upper back, middle back, and abdomen) to reduce body thermal strain due to exercise in heat.

5.2.4. Body heat storage

The body heat storage was calculated for a complete one hour of each test using **Eq. 18(a-b)** for the three groups, presented in **Fig. 38**. For **Group I**, H_s was obtained at 37 ± 18 W for NV; 34 ± 11 W for V1. Thus, wearing the vest decreased H_s by 10% compared to NV, which confirmed the obtained results of ΔT_{cr}. For **Group II**, H_s was obtained at 60 ± 21 W for NV; 35 ± 22 W for V1; and 50 ± 21 W for V2. It was clear that the stored heat in the body was reduced by 42% with V1 of mass 3.41 kg and 16% with V2 of mass 2.17 kg, compared to NV. This difference between V1 and V2 was due to a higher $\Delta T_{sk,mean}$ value in V2. For **Group III**, H_s was obtained at 44 ± 22 W for NV and 12 ± 27 W for V1 thus covering 34% of the trunk with PCM packets reduced H_s by 73% ensuring the effectiveness of the cooling vest on reducing thermal strain in people with low-thoracic injury.
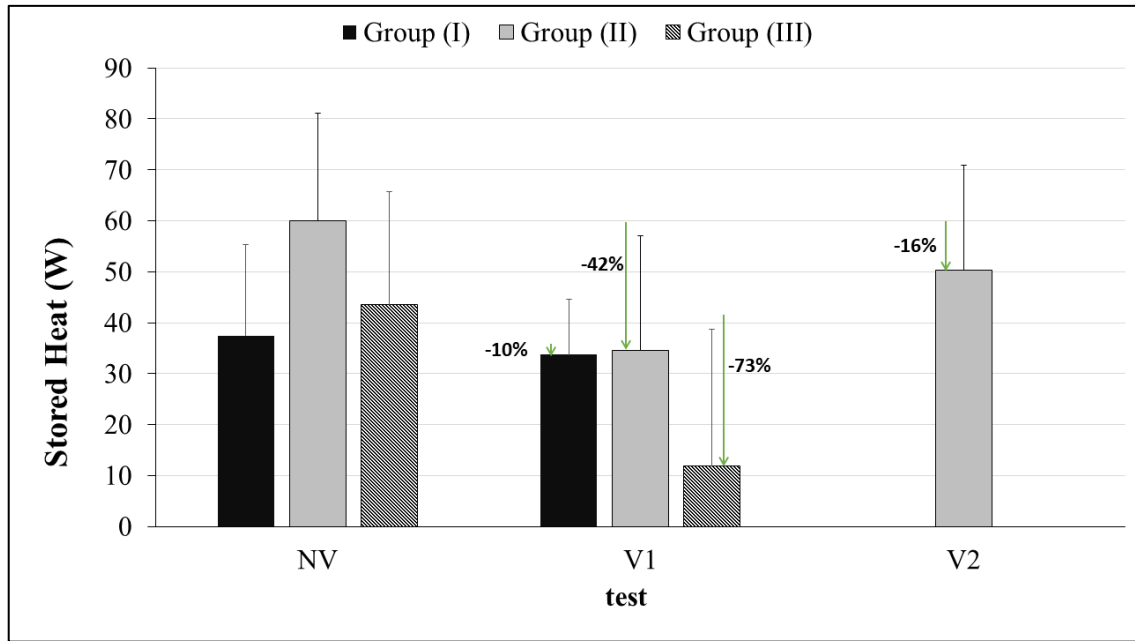
Figure 49. Plot of stored heat (mean ± SD) for the three PA groups for three tests

5.2.5. Conclusion

To sum up, the results of this experimental study indicate that the effectiveness of the PCM cooling vest is correlated to the injury level. The design of V1 showed least effectiveness in reducing core temperature for those with high-thoracic injury. The injury level limited the functional sensory portion of the trunk. Furthermore, both types of the cooling vest achieved the aim of reducing core temperature during recovery, as well as, enhancing thermal comfort in the mid-thoracic group. Furthermore, V2 can be recommended instead of V1 since it provided the same effectiveness but at a lighter weight and coverage area of trunk (36% less). For people with low-thoracic injury level, cooling the sensate skin of the trunk was effective to enhance heat dissipation (73% reduction in stored heat) during exercise and post recovery to accelerate thermal regulation and restore body neutral state. In addition, their thermal state during exercise was comparable to that of able-bodied people.

196

The drawback of not having persons with complete thoracic SCI was taken into consideration when evaluating the change in core temperature in the NV test. The findings for each group showed a gradual increase in core temperature as an indication of impaired autonomic system in persons with PA. Findings of change in T_{cr} values in NV test were similar to previous studies in literature where recruited participants with complete thoracic injury were asked to perform exercise in hot environmental temperatures (>30.0°C) (Dawson et al., 1994; Petrofsky, 1992; Price and Campbell, 2003; Trbovich et al., 2016).

5.3. Human subject experiments: Effect of melting temperature on the performance of PCM cooling vest (V20, V14 and NV tests)

To evaluate the influence of PCM temperature on the efficacy of cooling vest on the thermal response of persons with PA during exercise, a comparison of the change of core and skin temperatures ($\Delta T_{cr}, \Delta T_{sk}$), HR values, as well as reported votes for the thermal comfort, sensation, skin wettedness, and change of perceived exertion (ΔPE) was done for NV, V20, and V14 for Groups I and II. Group I was selected since the use of PCM cooling vest of melting temperature 20 °C did not show significant effect. Then, it was of great interest to check whether lowering the melting temperature of the PCM packets would improve the performance of PCM cooling vest for persons with high-thoracic SCI (T1-T3). Group II was selected to look for further enhancement in the PCM cooling vest performance for persons with mid-thoracic SCI (T4-T8).

5.3.1. Physiological responses

197

Table 29 presents the values of HR, ΔT_{cr} and $\Delta T_{sk,mean}$ during one hour of the test of the two groups. For Group I, the baseline (time=0) of HR, T_{cr} and $T_{sk,mean}$ values were insignificantly different between NV, V20 and V14 respectively (94±6, 93±6, 90±10 bpm; 37.07±0.4, 37.10±0.5, 36.90±0.2 °C; 31.3±0.2, 30.5±0.7, 31.3±1.3 °C, $p>0.05$). HR values were lower in V14 compared to V20 and NV tests, however, this difference was insignificant ($p > 0.05$). ΔT_{cr} values were reduced during exercise and recovery when using V14 compared to NV, unlike V20 that showed no difference. However, this reduction with V14 was insignificant ($p > 0.05$). $\Delta T_{sk,mean}$ was lower in V14 and V20 compared to NV at an average difference of 1.9±0.3, 0.82±0.1 °C, respectively ($p < 0.05$).

For Group II, the baseline (time=0) of HR, T_{cr} and $T_{sk,mean}$ values were insignificantly different between NV, V20 and V14 respectively (85±12, 86±10, 90±13 bpm; 37.0±0.4, 37.1±0.3, 37.1±0.3 °C; 32.2±1.1, 32.5±0.7, 32.0±1.1 °C, $p > 0.05$). HR values were insignificantly different between the three tests ($p > 0.05$). ΔT_{cr} values were reduced during exercise and recovery when using V20 and V14 compared to NV. For V20, significance was detected at time=45 mins ($p=0.024$); while for V14, it was obtained at time=35 mins ($p=0.033$) of the one hour of the experiment, compared to NV. Thus, V14 showed effectiveness at the earlier time of exercise than V20, but both were effective during recovery ($\Delta T_{cr} = 0.42 \pm 0.3$ °C for V20; 0.38 ± 0.2 °C for V14 compared to NV). $\Delta T_{sk,mean}$ was lower in V14 and V20 compared to NV at an average difference of 1.0±0.2, 0.7±0.1 °C, respectively ($p < 0.05$).

Table 29. Comparison of the mean ($\pm$ SD) of heart rate values (HR) change in core temperature (ΔT_{cr}) and change in skin temperature (ΔT_{sk}) for Group I and Group II for three tests

test		NV				V20				V14			
experimental timeline	time (mins)	group I		group II		group I		group II		group I		group II	
HR (bpm)													
baseline	0	94	±7	85	±12	94	±7	87	±10	84	±23	90	±13
end of preconditioning	15	104	±23	90	±15	100	±28	89	±12	98	±1	93	±17
mid of exercise	30	153	±30	135	±31	153	±19	141	±27	144	±18	145	±19
end of exercise	45	136	±45	153	±14	153	±18	146	±18	145	±29	145	±25
end of recovery	60	103	±24	107	±14	101	±37	106	±13	102	±29	112	±15
ΔT_{cr} (°C)													
baseline	0	0.00	±0.00	0.00	±0.00	0.00	±0.00	0.00	±0.00	0.00	±0.00	0.00	±0.00
end of preconditioning	15	0.07	±0.06	0.14	±0.20	0.07	±0.32	0.09	±0.18	0.00	±0.14	-0.01	±0.19
mid of exercise	30	0.27	±0.12	0.36	±0.18	0.30	±0.17	0.28	±0.28	0.20	±0.00	0.20	±0.14
end of exercise	45	0.47	±0.06	0.76	±0.24	0.50	±0.00	0.55*	±0.36	0.45	±0.07	0.43**	±0.26
end of recovery	60	0.47	±0.06	0.74	±0.23	0.43	±0.06	0.42*	±0.32	0.45	±0.07	0.38**	±0.33
$\Delta T_{sk,mean}$ (°C)													
baseline	0	0.00	±0.00	0.00	±0.00	0.00	±0.00	0.00	±0.00	0.00	±0.00	0.00	±0.00
end of preconditioning	15	1.38	±0.57	1.25	±0.39	0.54	±0.34	0.52	±0.25	-0.27**	±0.24	0.17*	±0.88
mid of exercise	30	1.38	±0.65	1.33	±0.64	0.39	±0.81	0.64	±0.45	-0.52**	±0.36	0.41*	±1.08
end of exercise	45	1.57	±0.60	1.65	±0.71	0.74	±0.70	0.96	±0.54	-0.51**	±0.60	0.63*	±1.10
end of recovery	60	1.74	±1.03	1.87	±0.79	0.98	±0.30	1.11	±0.53	-0.41**	±0.99	0.47*	±0.79

* $p < 0.05$, significant difference between NV and V20; ** $p < 0.05$, significant difference between NV and V14

Figure 50(a-h) demonstrates ΔT_{sk} values of sensate (chest and upper back) and insensate (pelvis and lower back) portions of the trunk for the two groups. For group (I), the baseline of skin temperatures of the chest (32.4±0.2, 32.4±1.5, 33.0±2.0), upper back (33.1±0.4, 33.4±0.5, 33.1±0.7), pelvis (33.6±1.5, 32.9±1.6, 32.8±4) and lower back (34.7±0.7, 34.9±1.4, 33.6±0.8) were significantly indifferent to NV, V20, and V14; respectively ($p>0.05$). In **Fig. 50(a)**, chest showed a lower change in V14 and V20 compared to NV during preconditioning and mid of exercise, yet this change became minimal till the end of recovery. In **Fig. 50(b)**, the upper back showed an insignificant difference between the three tests ($p>0.05$). In **Fig. 50(c-d)**, both pelvis and lower back

showed a lower change in V20 and V14 compared to NV, but more intensely in the V14 test.

For Group II, the baseline of skin temperature of the chest (33.4 ± 0.8, 33.4 ± 1.0, 33.8 ± 1.0), upper back (33.1 ± 0.8, 33.8 ± 0.1, 33.1 ± 1.7), and pelvis (32.7 ± 1.5, 32.5 ± 1.3, 32.4 ± 2.5) were significantly indifferent to NV, V20 and V14; respectively ($p>0.05$). Whereas, lower back (33.8 ± 1.6, 32.4 ± 2.1, 32.0 ± 2.4) had a significant difference at V14 test compared to NV and V20 ($p=0.008$). In **Fig. 50(e)**, the chest showed a lower change in V14 and V20 compared to NV at mean difference 1.2℃ and 0.7℃, respectively during preconditioning and mid of exercise. This change remained significant for V14 (1.0℃), while it became minimal for V20 at the end of recovery. In **Fig. 50(f)**, upper back showed lower change in V14 compared to V20 and NV tests, but it was insignificant difference between three tests ($p>0.05$). In **Fig. 50(g-h),** both pelvis and lower back showed lower change in V20 and V14 compared to NV, but more notably in V14 test in the recovery period of lower back ($p<0.05$).
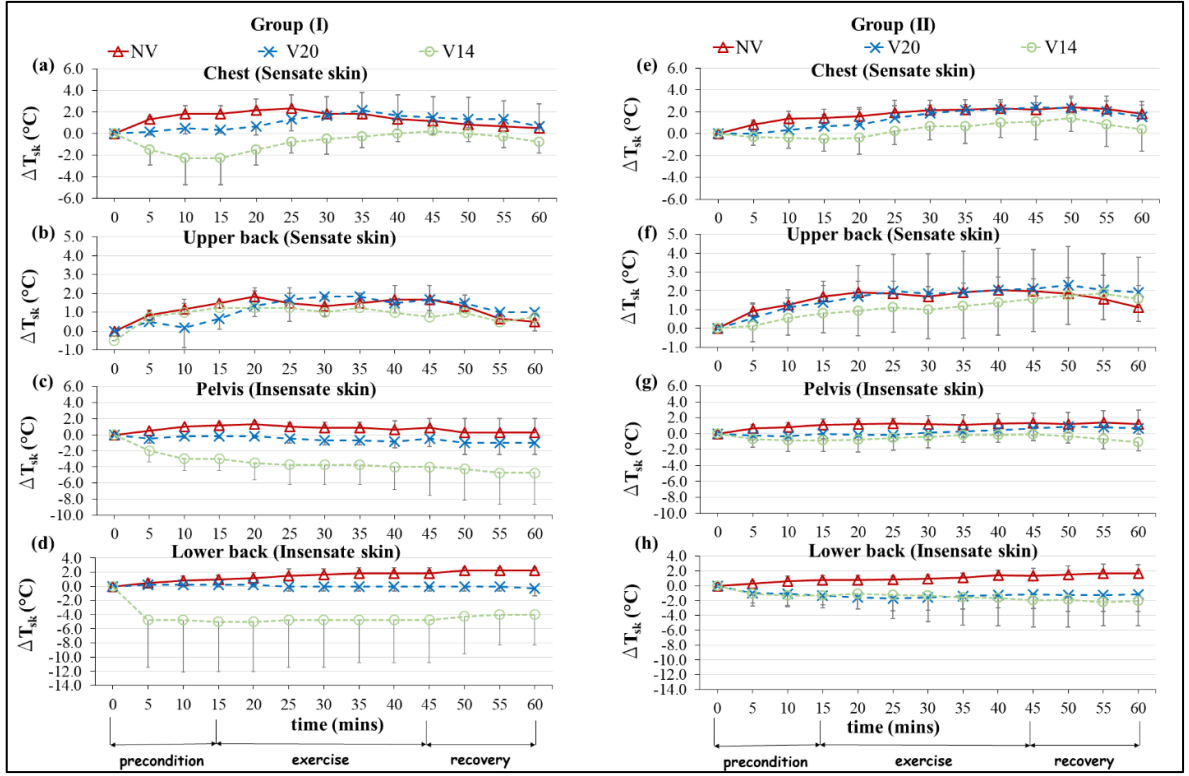
Figure 50. Comparison of change in skin temperature (ΔT_{sk}) of (a) chest (b) upper back (c) pelvis (d) lower back for Group (I) and (e) chest (f) upper back (g) pelvis (h) lower back for Group II

The heat stored in the body (H_s) at the end of each test was calculated for Groups I and II using **Eq. 18(a-b)**. In **Fig. 51**, Group I showed insignificant change in H_s when using V20, yet a strong decrease by 54% when using V14 compared to NV test. This finding in V14 test can be attributed to the significant decrease in insensate skin temperature and consequently in $T_{sk,mean}$ values while no reduction was observed in T_{cr} values at end of test for Group I. Whereas, Group II established a significant decrease in H_s at 42% and 59% while using V20 and V14 compared to NV, respectively. From this finding, it can be deduced that cooling sensate skin of trunk for Group II was greatly effective in reducing T_{cr} values and, eventually, heat gained in the body. Also, using a

201

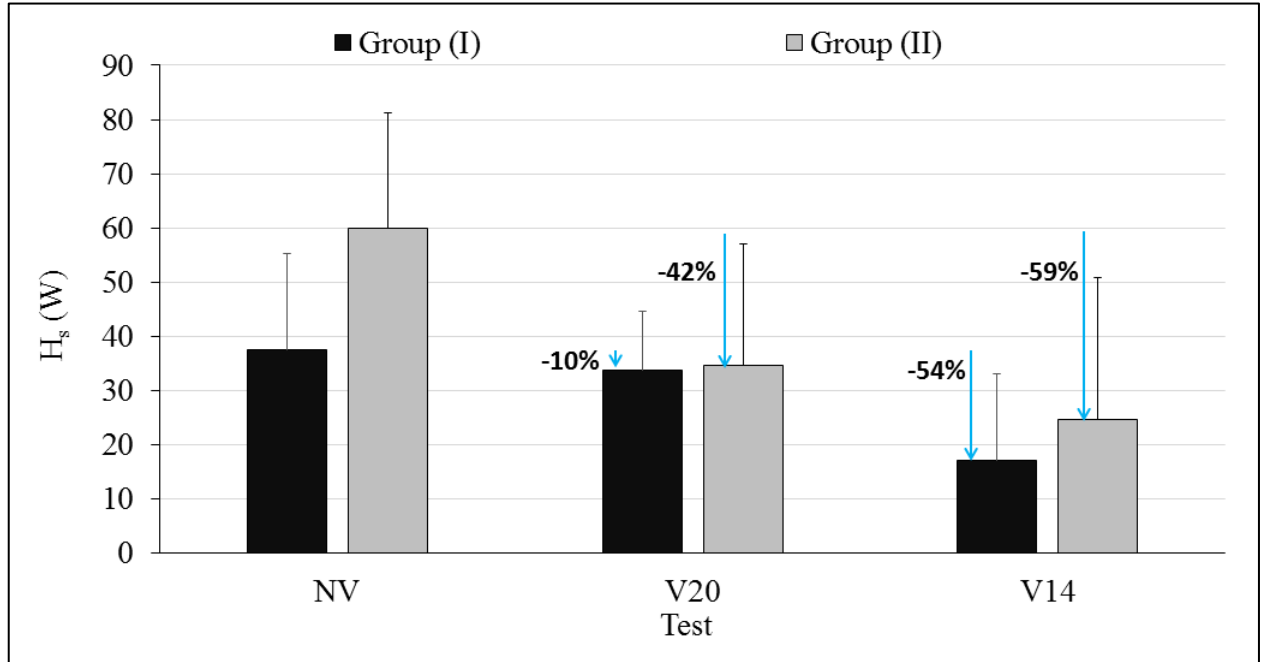lower melting temperature of PCM promoted a further reduction in H_s at the same coverage area of the trunk.

Figure 51. Comparison of stored heat (mean ± SD) for three tests for groups I and II

5.3.2. *Psychological responses*

Figure 52(a-e) presents the subjective voting of the participants during exercise on (a) thermal comfort (b) thermal sensation at head, neck, and shoulders (c) thermal sensation at trunk (d) skin wettedness (e) ΔPE (change in perceived exertion) for Group (I) during exercise. In **Fig. 52(a)**, using V20 and V14 changed the thermal comfort to "slightly uncomfortable" and "neutral" respectively, by the end of exercise compared to the NV test. In **Fig. 52(b-c)**, the thermal sensation at head, neck, shoulders (mean difference: 1±1; 2±1) and trunk (mean difference: 1.6±0.3; 2±1) was neutral while using V20 and V14 compared to NV. In **Fig. 52(d-e)**, skin wettedness, and change in perceived exertion showed an insignificant difference in three tests.
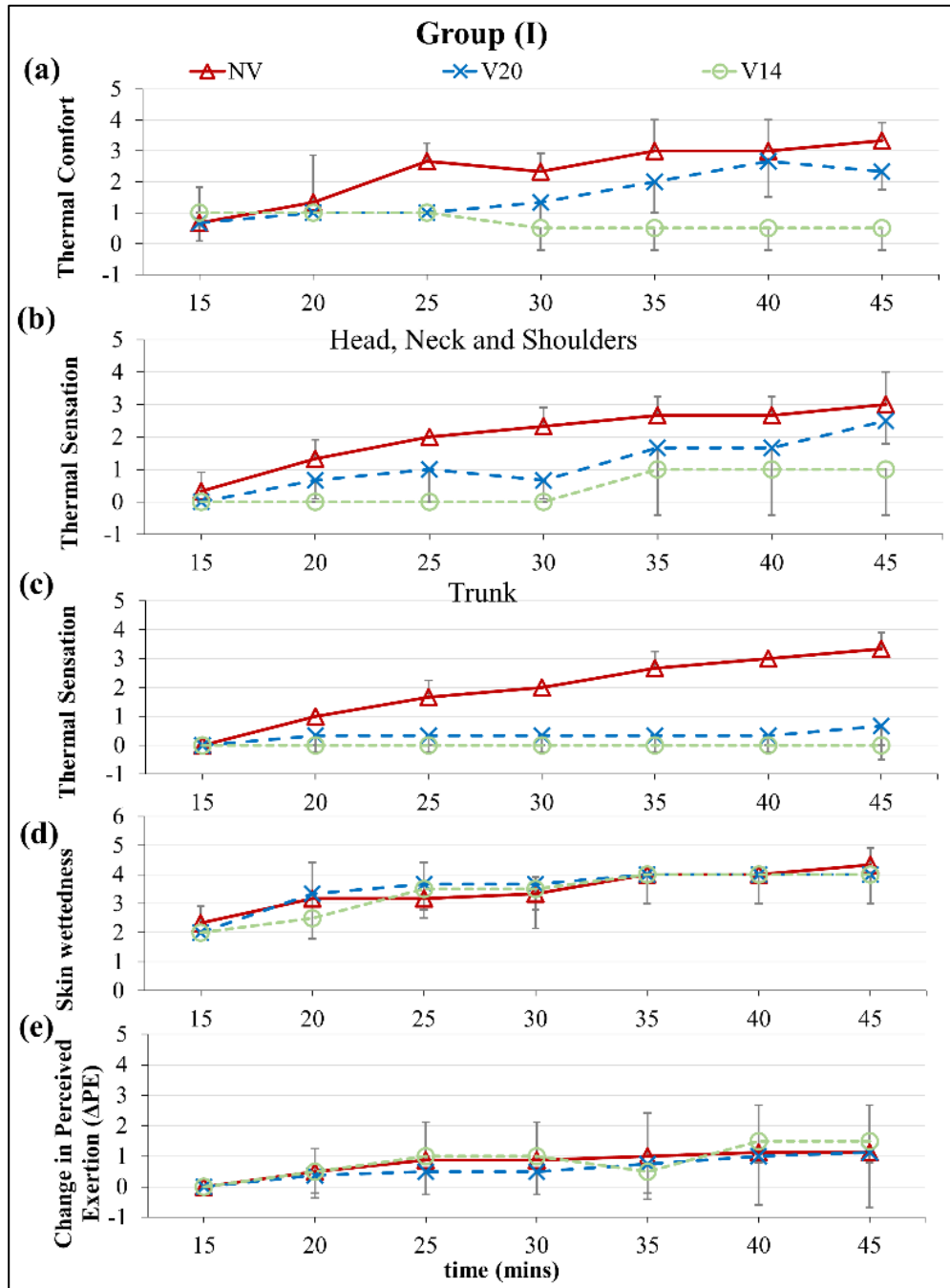
Figure 52. Comparison of (a) thermal comfort (b) thermal sensation at head, neck, and shoulders (c) thermal sensation at trunk (d) skin wettedness (e) ΔPE (change in perceived exertion) for Group (I)

Figure 53(a-e) presents the subjective voting of the participants during exercise on (a) thermal comfort (b) thermal sensation at head, neck, and shoulders (c) thermal sensation at trunk (d) skin wettedness (e) ΔPE (change in perceived exertion) for Group II during exercise. In **Fig. 53(a)**, using V20 and V14 improved thermal comfort during exercise compared to the NV test. In **Fig. 53(b-c)**, thermal sensation at head, neck, shoulders, and trunk improved while using vests compared to NV. In **Fig. 53(d)**, skin wettedness was reduced by mean difference 1.25±0.6 (*p*=0.002) when wearing the vest compared to NV. Finally, in **Fig. 53(e)**, change in perceived exertion showed a significant decrease in V14 compared to V20 and NV tests.
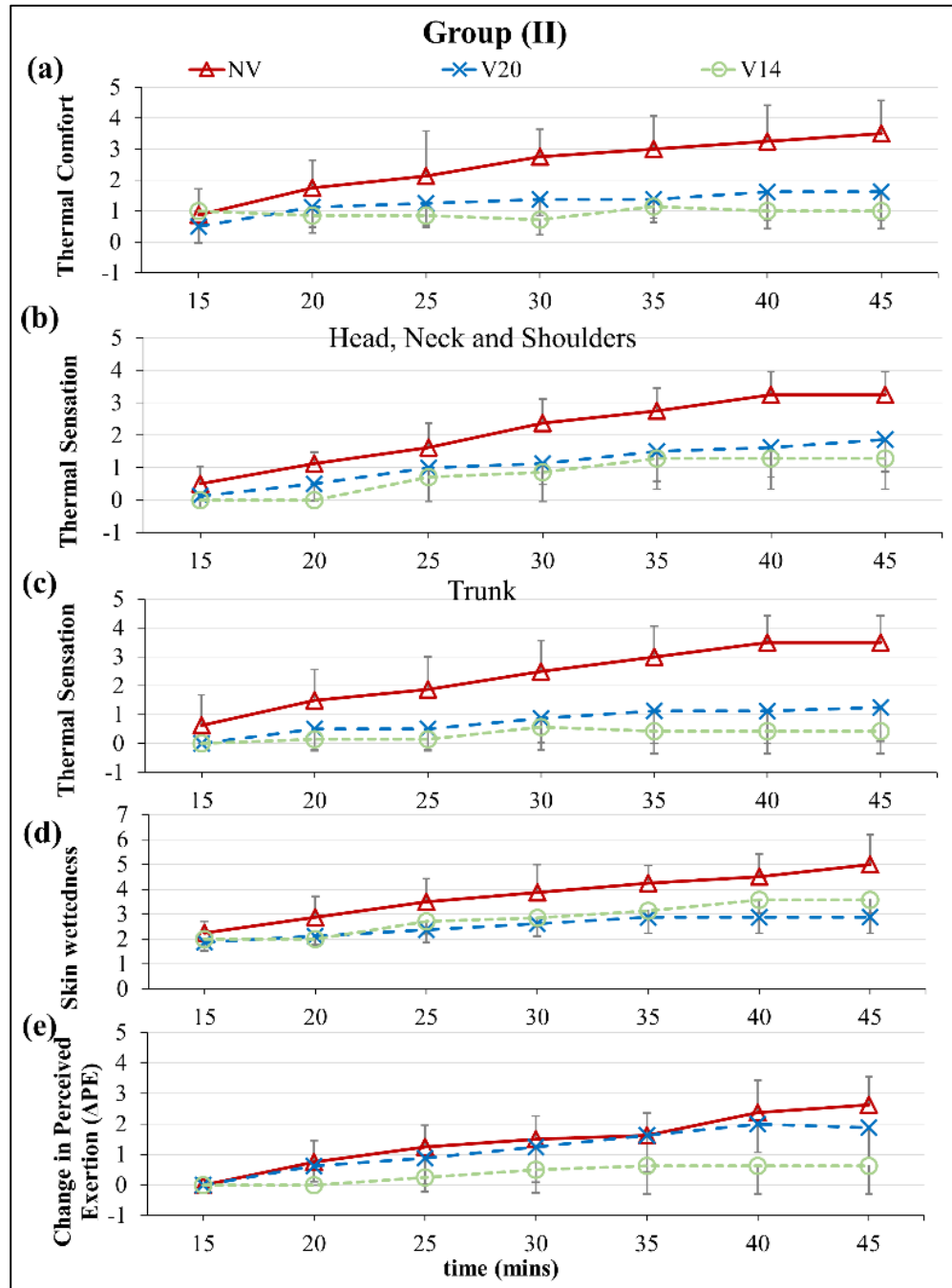
Figure 53. Comparison of (a) thermal comfort (b) thermal sensation at head, neck, and shoulders (c) thermal sensation at trunk (d) skin wettedness (e) ΔPE (change in perceived exertion) for Group II

5.3.3. Conclusion

By the findings of conveyed experiments, the physiological and psychological results revealed that the lower melting temperature of PCM enhanced the overall performance of the cooling vest in reducing thermal strain in people with high- and mid-thoracic SCI. However, the extent of this effectiveness remained dependent on the level of injury and portion of sensate skin at the trunk in persons with PA as observed in previous experiments conducted at melting temperature of 20 °C (Mneimneh et al., 2020b).

Findings of the group (I) validated that people with injury above T3 with T3 inclusive were less able to reduce the heat gained (core temperature) at high metabolic rate using a cooling vest, even at the lower melting temperature of PCM. Although V14 reduced more effectively skin temperature at the trunk, $T_{sk,mean}$ values and eventually heat stored, no reduction in core temperature occurred. This was due to i) limited portion of the sensate skin of the trunk (25%) and ii) PCM placement in the used vest, which did not target all sensate skin of the group (I). Therefore, lowering the melting temperature of PCM and locating the packets on shoulders, upper back, and upper chest would be a potential approach for effective design to be used by the high-thoracic group. The findings of subjective voting exposed that psychologically the vest did not improve thermal comfort and sensation of participants significantly during exercise, which was analogous to the insignificant change in T_{cr} values.

Findings of the group II confirmed that V14 was more effective in reducing core temperature and heat stored in the body during mid of exercise and recovery, compared to V20. Using a 14°C-PCM packets provided lower microclimate temperature near sensate skin at the chest and upper back than that of 20°C-PCM. Hence, further sensible

206

heat dissipation was promoted by a higher temperature gradient and allowed the blood to return to the core from the periphery to be cooler. Whereas, latent heat losses were minimized due to reduced sweating secretion as seen by skin wettedness subjective voting. In addition, establishing that PCM packets with lower melting temperatures have lower latent heat of fusion, the melting period duration of these packets would be shorter; therefore, a higher cooling rate occurred with V14 compared to V20 at the same duration of exercise (Gao et al., 2012; Ouahrani et al., 2017). Therefore, for people with an injury below T3, whose 50% of trunk sensate skin was preserved, lowering the melting point of PCM to 14 ℃ improved the efficacy of cooling vest by 30% in reducing stored heat compared to V20. Furthermore, subjective voting results agreed with physiological findings as perceived exertion was minimized significantly with V14 due to 20% less weight than V20.

5.4. Human subject experiments: comparison of the performance of ECV Type II and PCM cooling vest of melting temperature 20 ℃ (PCM, ECV and NV tests)

Groups **II** and **III** performed experiments using commercially available ECV Type II to be compared with the findings of NV and PCM cooling vest of melting temperature 20 ℃ which covered the chest, upper back, middle back, and abdomen tests, named in this case PCM. The comparison between two types of the vest is indicative whether ECV can provide further effectiveness for persons with PA similar to PCM cooling vest.

5.4.1. Physiological responses

Initially (time=0 min), there was insignificant difference in the values of HR, T_{cr} and T_{sk} for Group II between NV, with PCM, and with ECV tests (85±12, 86.8±10, 85±12 bpm; 36.95±0.23, 37.08±0.33, 36.96±0.39 °C; 32.2±1.05, 32.47±0.68, 31.61±0.65 °C; $p > 0.05$). **Fig. 54(a-c)** presents the transient profiles of HR, ΔT_{cr} and ΔT_{sk} for Group II during the complete one hr. of experiment. In **Fig. 54(a)**, HR values did not show significant difference between the three tests ($p > 0.05$). In **Fig. 54(b)**, ΔT_{cr} values did not indicate significant difference not until time = 45 mins by the end of exercise and during recovery period of the two tests, with PCM and with ECV, compared to NV with an average drop of $0.26 \pm 0.04°C$ ($p = 0.024$) and $0.2 \pm 0.05°C$ ($p = 0.04$); respectively, but no significant difference in values between with PCM and with ECV tests ($p > 0.05$). In **Fig. 54(c)**, by the end of exercise (time=45 mins), $\Delta T_{sk,mean}$ values were lower in the test with PCM compared to NV and with ECV test (mean difference $= 0.45 \pm 0.15°C; p = 1.03 \times 10^{-11}$); whereas, no significant drop was found between with ECV and NV tests ($p > 0.05$). The insignificant drop in case of using ECV could be justified by the fact that ECV did not cover the insensate skin of the trunk (pelvis and lower back) as much as the PCM cooling vest did. In addition, the structure of ECV is loose near the lower part of the trunk; thus, minimizing the heat transfer mechanism at this region; unlike PCM cooling vest that is tight.
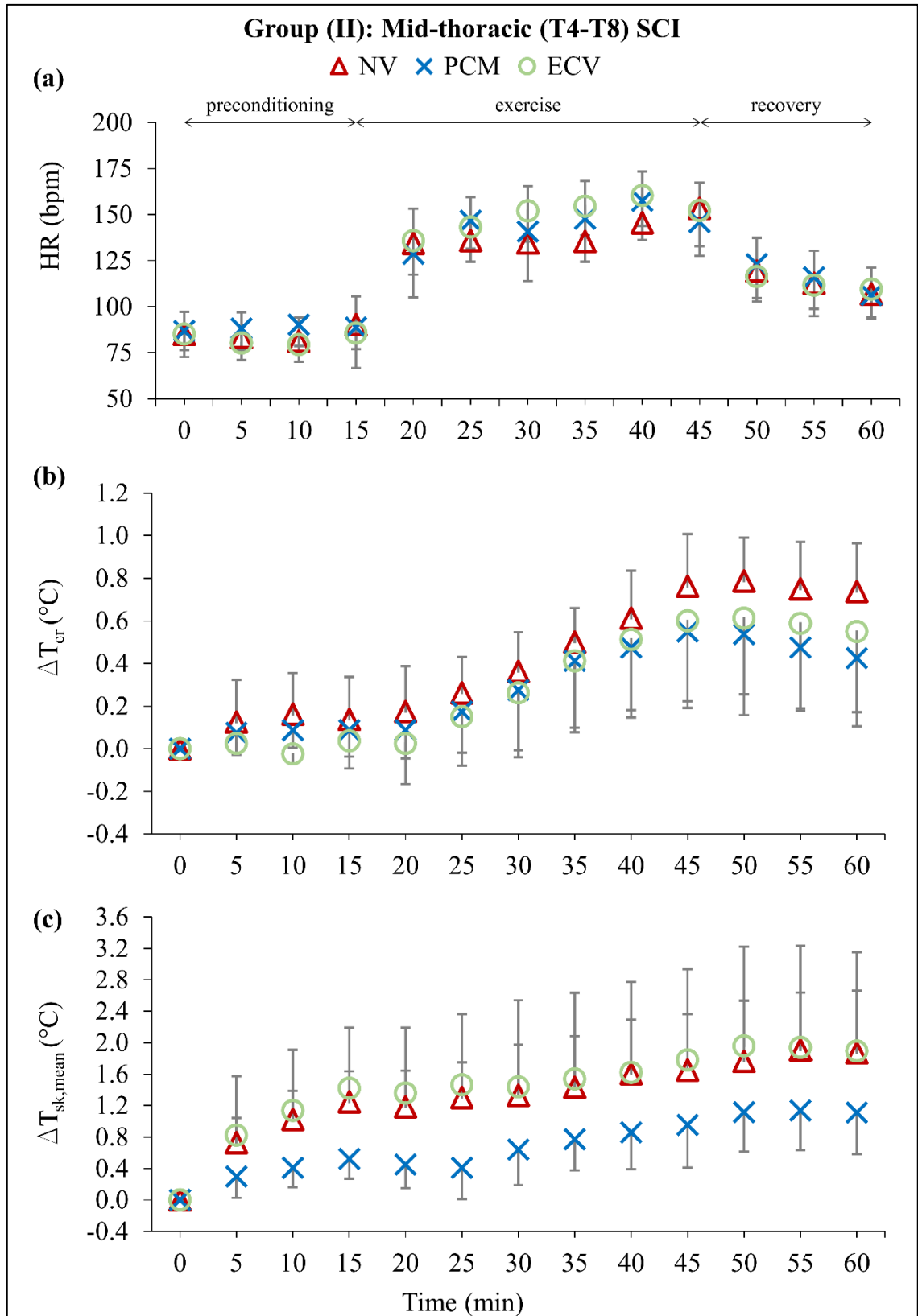
Figure 54. Plot of (a) heart rate (b) change in core temperature (ΔT_{cr}) and (c) change in skin temperature (ΔT_{sk}) (mean ± SD) for Group II

At the baseline of the experiment, T_{sk} values of trunk segments did not show significant drop for NV, with PCM, and with ECV tests (chest: 33.49±0.8, 33.43±1.0, 33.6±1.0 °C; upper back: 33.16±0.8, 33.79±1.4, 33.1±1.3 °C; pelvis: 32.72±1.5, 32.52±1.3, 32.3±2.2 °C; lower back: 33.85±1.6, 32.40±2.1, 32.9±2.2 °C; $p > 0.05$). **Fig. 55(a-d)** shows the values of ΔT_{sk} for the trunk segments (a) chest, (b) upper back, (c) pelvis, and (d) lower back. In **Fig. 55(a)**, compared to NV test, the chest segment shows drop in ΔT_{sk} values during preconditioning till mid of exercise (time=30 mins) at mean difference 0.7 °C and 1.2 °C for with PCM test and with ECV test, respectively. This difference was minimized after this period to become statistically insignificant ($p > 0.05$) during recovery. **Fig. 55(b)** shows that the upper back showed drop in ΔT_{sk} values while using ECV compared to NV test also during preconditioning and first 15-min of exercise, but this drop was diminished by the end of the experiment. Whereas, with PCM test did not show significant change ($p > 0.05$). Finally, in **Fig. 55(c-d)**, the pelvis and lower back showed significant drop with PCM test compared to NV and with ECV tests ($p = 0.001$).
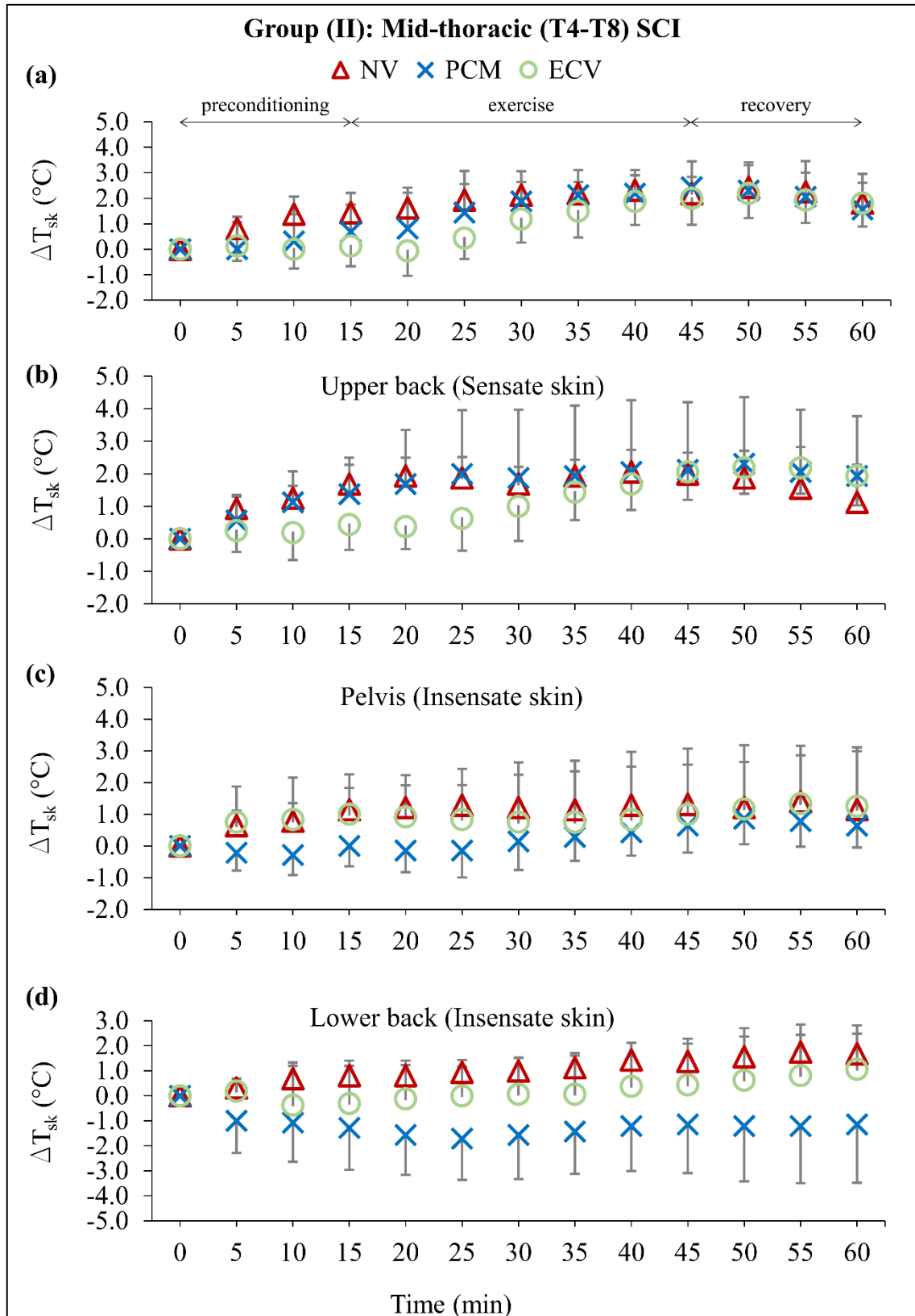
Figure 55. Plot of change in skin temperature (ΔT_{sk}) at (a) chest (b) upper back (c)

pelvis (d) lower back for Group II

Initially (time=0 min), there was insignificant difference in the values of HR, T_{cr} and T_{sk} for Group III between NV, with PCM and with ECV tests (85±12, 89±12, 84.3±5 bpm; 37.16±0.3, 37.12±0.3, 37.00±0.1 °C; 31.66±1.3, 31.85±1.0, 31.5±0.8 °C; $p >$ 0.05). **Fig. 56(a-c)** presents the transient profiles of HR, ΔT_{cr} and ΔT_{sk} for Group III during complete one hour of experiment. In **Fig. 56(a)**, HR values did not show significant difference between the three tests ($p > 0.05$). In **Fig. 56(b)**, T_{cr} values did not vary in the preconditioning while wearing ECV or PCM cooling vest ($\Delta T_{cr} \cong 0.0 \pm$ 0.07°C) indicating steady neutral thermal state before exercise. However, during exercise, ΔT_{cr} values increased up to 0.3 ± 0.15 °C ($p = 0.034$) in both with PCM and with ECV tests followed by a drop during recovery period by 0.15 ± 0.05 °C and $0.1 \pm$ 0.05 °C for with ECV and with PCM tests compared to NV tests ($p = 0.007$). In **Fig. 56(c)**, it was clear that $\Delta T_{sk,mean}$ values were significantly lower in ECV and PCM compared to NV test, more profoundly during exercise ($p < 0.05$).
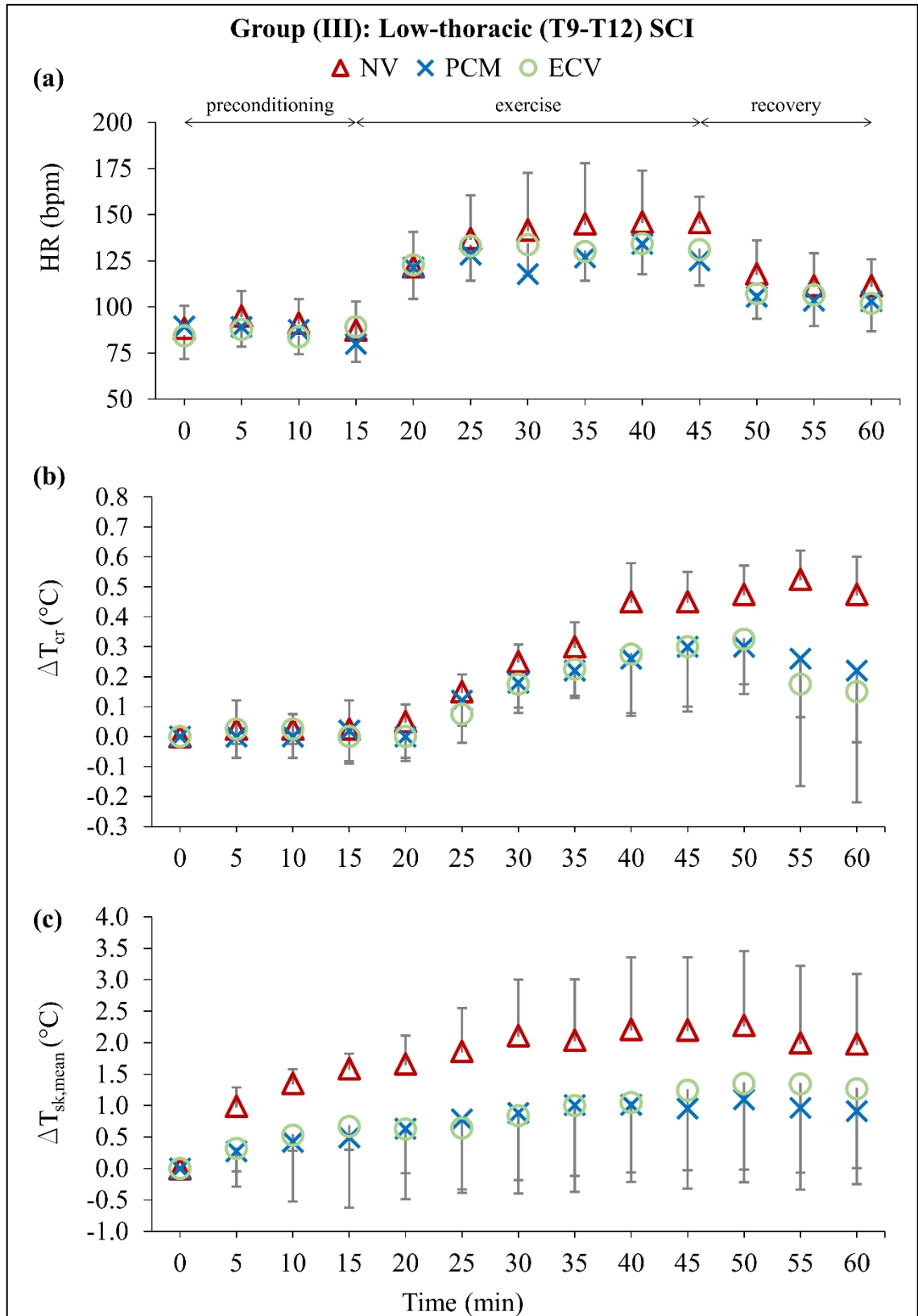
Figure 56. Plot of (a) heart rate (b) change in core temperature (ΔT_{cr}) and (c) change in skin temperature (ΔT_{sk}) (mean $\pm$ SD) for Group III

At the baseline of the experiment, T_{sk} values of trunk segments did not show significant drop for NV, with PCM, and with ECV tests (chest: 33.22±0.73, 33.24±1.29, 33.9±1.3 ℃; upper back: 34.10±0.95, 34.21±2.06, 33.1±1.8 ℃; pelvis: 33.62±2.21, 32.29±2.18, 32.0±2.8 ℃; lower back: 34.71±1.71, 33.60±1.7, 33.6±0.9 ℃; $p > 0.05$). **Fig. 57(a-d)** shows the values of ΔT_{sk} for the trunk segments (a) chest, (b) upper back, (c) pelvis, and (d) lower back. In **Fig. 57(a)**, compared to NV test, the chest segment shows drop in ΔT_{sk} values during preconditioning for with PCM test and with ECV test ($p < 0.05$). This difference was minimized after this period to become statistically insignificant ($p > 0.05$). **Fig. 57(b)** shows that the upper back showed insignificant difference in ΔT_{sk} values while using ECV or PCM compared to NV test. In **Fig. 57(c)**, the pelvis showed significant drop with PCM test and with ECV test compared to NV ($p < 0.05$). Finally, in **Fig. 57(d)**, the lower back showed significant drop with PCM test compared to with ECV and NV tests ($p < 0.05$).
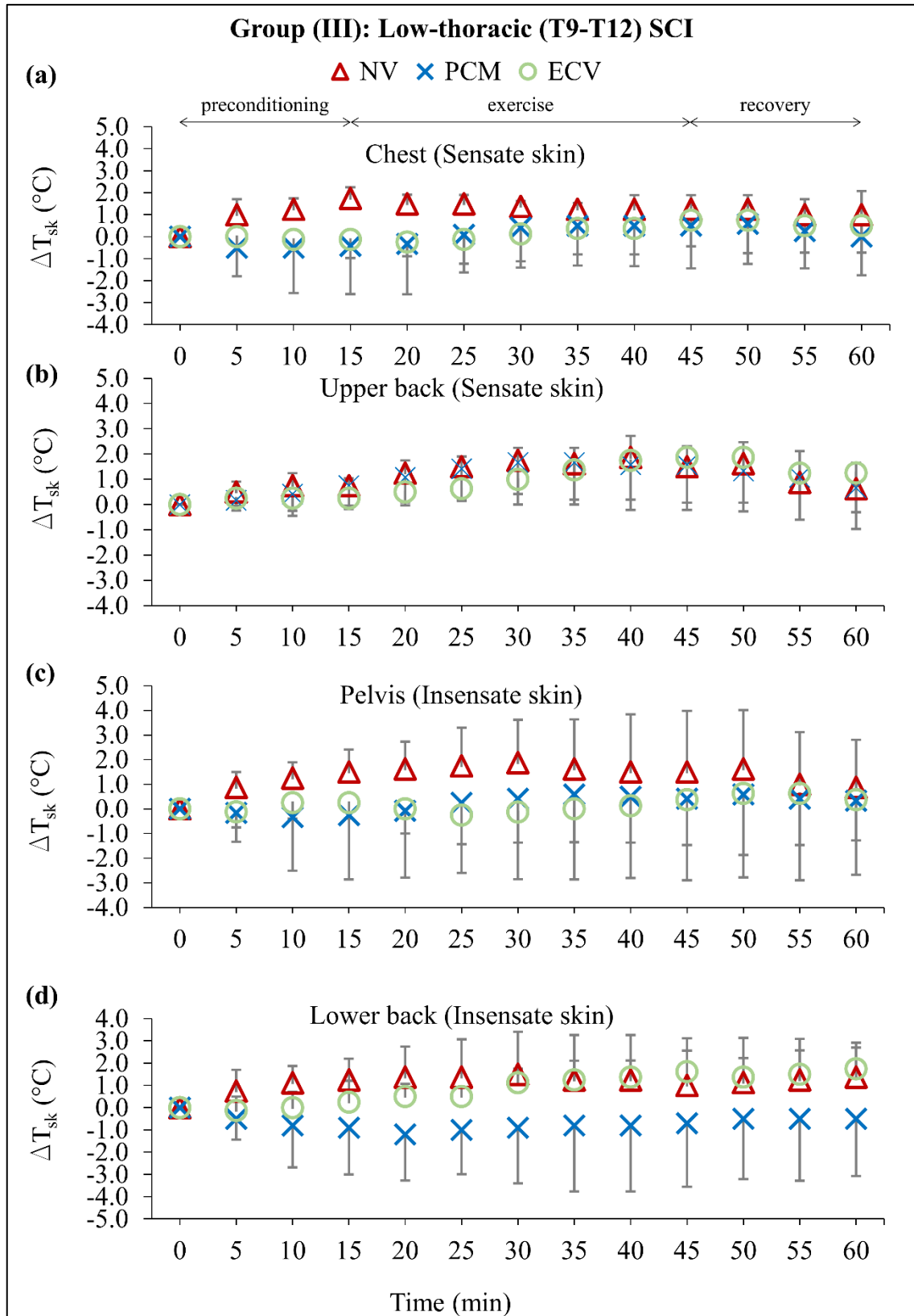
Figure 57. Plot of change in skin temperature (ΔT_{sk}) at (a) chest (b) upper back (c) pelvis (d) lower back for Group III

The heat stored in the body (H_s) at the end of each test was calculated for Groups II and III using equations 18 (a-b). Group II established a significant decrease in H_s at 42% and 16% while using PCM vest and ECV compared to NV, respectively. Group III established a significant decrease in H_s at 73% and 47% while using PCM vest and ECV compared to NV, respectively. This difference is due to the difference in $T_{sk,mean}$ values obtained from each test for the two groups. **Table 30** summarizes the values of H_s for Groups II and III by the end of each test.

Table 30. Values of H_s for Groups II and III by the end of each test

Group	NV	with PCM	with ECV
II	60 W	35 W	50 W
1II	44 W	12 W	23

5.4.2. *Psychological responses*

Figure 58(a-e) shows the results of subjective voting of the participants of Group II on (a) thermal comfort (b) thermal sensation at the head, shoulders and neck, (c) thermal sensation at trunk, (d) skin wettedness and (e) perceived exertion during exercise. In **Fig. 58(a)**, thermal comfort was improved to "comfortable" while using PCM vest (*p*=0.03) and to "slightly uncomfortable" while using ECV (*p*=0.04), compared to NV test. In **Fig. 58(b-c)**, thermal sensation at head, neck, shoulders (*p*=0.03) as well as trunk (*p*=0.001) were improved in both tests, with PCM and with ECV, compared to NV tests. In **Fig. 58(d)**, skin wettedness was reduced by mean difference 1.25 ± 0.6 ($p = 0.002$) when wearing PCM vest and by mean difference 0.4 ± 0.3 when wearing PCM vest. Finally, in **Fig. 58(e)**, change in perceived exertion (*p*=0.01) was improved while using ECV compared to with PCM and NV tests.

Figure 58. Plot of (a) thermal comfort (b) thermal sensation at head, neck, and shoulders

(c) thermal sensation at trunk (d) skin wettedness (e) change in perceived exertion

(ΔPE) for Group II

Figure 59(a-e) shows the results of subjective voting of the participants of Group III on (a) thermal comfort (b) thermal sensation at the head, shoulders and neck, (c) thermal sensation at trunk, (d) skin wettedness and (e) perceived exertion during exercise. In **Fig. 59(a)**, thermal comfort was improved to "comfortable" while using PCM vest (p=0.04) and using ECV (p=0.04), compared to NV test. In **Fig. 59(b-c)**, thermal sensation at head, neck, shoulders (p=0.03) as well as trunk (p=0.001) were improved in both tests, with PCM and with ECV, compared to NV tests. In **Fig. 59(d)**, skin wettedness was reduced by mean difference 1.7 ± 0.4 ($p = 0.002$) when wearing PCM vest and by mean difference 1.3 ± 0.4 when wearing PCM vest. Finally, in **Fig. 59(e)**, change in perceived exertion (p=0.01) was improved while using ECV analogous to the test of with PCM compared to NV test.
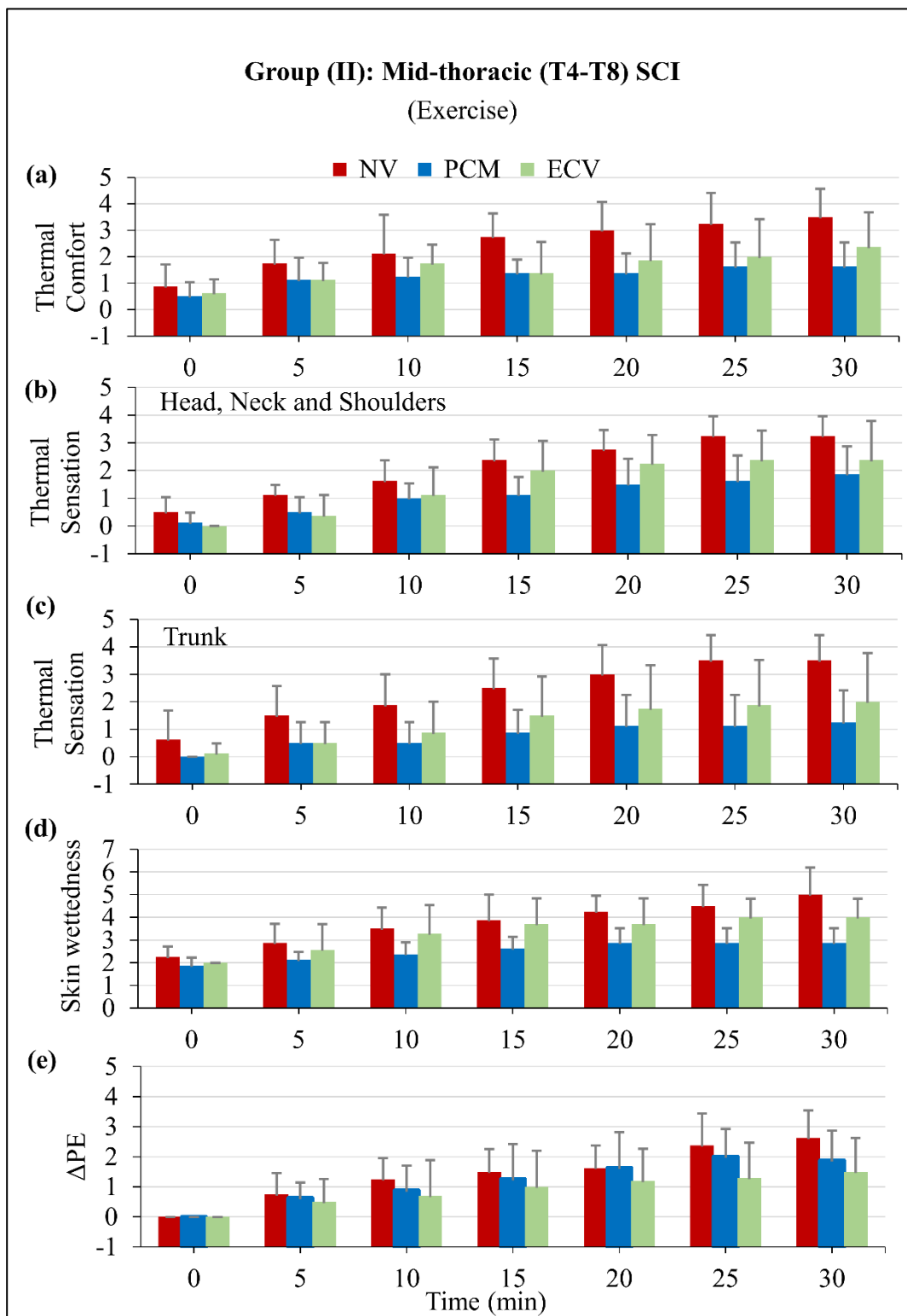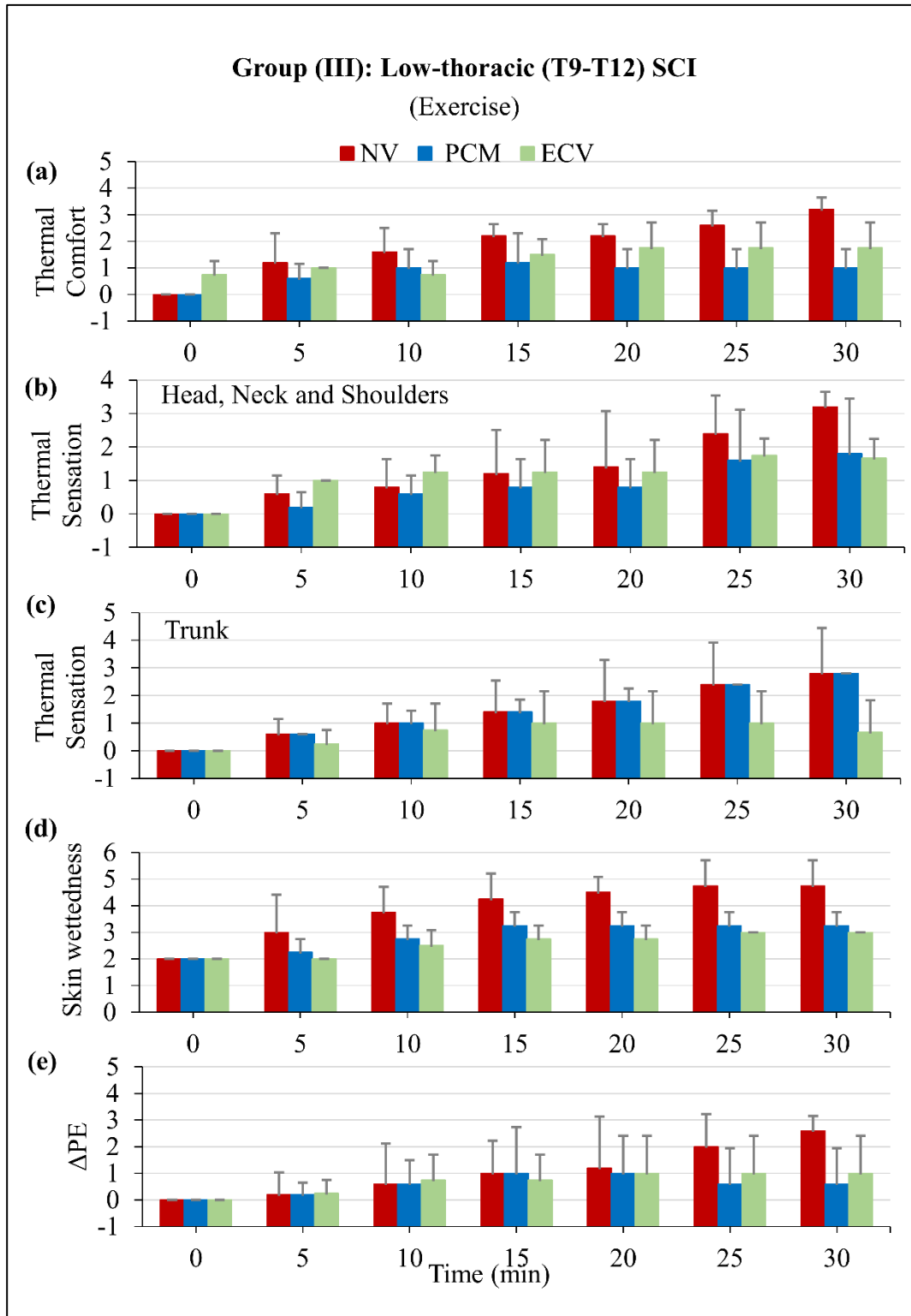
Figure 59. Plot of (a) thermal comfort (b) thermal sensation at head, neck, and shoulders

(c) thermal sensation at trunk (d) skin wettedness (e) change in perceived exertion

(ΔPE) for Group III

5.4.3. Conclusion

In this study, findings of the human subject experiments for persons with PA cleared that using ECV can be effective in reducing T_{cr} values during exercise in hot conditions with the advantage of lighter weight of the vest and less restriction of body movement compared to PCM cooling vest. However, the extent of this effectiveness varied between mid-thoracic and low-thoracic SCI groups because it was dependent on the level of injury and portion of sensate skin at the trunk in persons with PA.

Findings of the Group II confirmed that ECV can be as effective as PCM cooling vest in reducing core temperature and heat stored in the body during mid of exercise and recovery, compared to NV. Additionally, using ECV can improve perceived exertion from "somewhat hard" to "fairly light" exercising level which indicates that the exhaustion of persons with PA while engaged in high metabolic rate activity level can be reduced by wearing a light vest as ECV. Similarly, findings of Group III showed that ECV can reduce the change in T_{cr} values as that of PCM cooling vest for the same activity level and ambient conditions. Notably, because Group III possesses 75% of its trunk skin as sensate, while Group II has only 50% of its trunk skin as sensate, ECV effectiveness remains constrained by the injury level, and this was observed in the tests of PCM cooling vests for persons with PA (Mneimneh et al., 2020b).

Adding to the above, for Group II, ECV Type II resulted in a drop of ~1 °C at the trunk sensate skin compared to No-Vest case and enhanced thermal comfort and sensation levels during the exercise before sweating started. However, comfort and sensation levels deteriorated once sweat formation occurred at the sensate skin of the trunk; as an indication of restricted evaporation from the shirt when using ECV Type II. This finding

was analogous to that of previous studies that tested ECV Type II for AB to conclude that Type II had higher evaporative resistance (Ciuha et al., 2020). Therefore, it was important to investigate the performance of hybrid ECV that combined ECV Type II incorporated with ventilation fans as done in this research study.

CHAPTER 6

CONCLUSION

This study evaluated the effectiveness of PCM cooling vests and the hybrid vest in alleviating thermal strain for persons with PA at moderate/high physical activity levels performed in dry/humid and moderate/hot ambient conditions. This was achieved via the developing and validating bioheat models for persons with SCI. The PA-bioheat model was integrated with published Fabric-PCM model and newly developed hybrid ECV to be used for performing parametric study about each type of cooling vests. Furthermore, human subject experiments were conducted to test the proposed means of enhancement for PCM cooling vests and commercially available ECV Type II. The results of the parametric studies and experimental tests showed that:

Theoretical findings:

- Based on the parametric study of Fabric-PCM-PA bioheat model, the location of PCM packets should be targeting the sensate skin of the trunk.

- In addition, lowering the PCM melting temperature while covering the sensate skin of the trunk can enhance heat losses during exercise and recovery period for persons with PA.

- Based on the parametric study of hybrid ECV-PA bioheat model, enhancement in both sensible and latent heat losses for persons with PA was attained by the hybrid vest compared to No-Vest and ECV Type II, but the extent of the enhancement was dependent on the activity levels and ambient conditions.

- At moderate activity level, the hybrid vest improved heat losses at the trunk by a factor between 1.15 and 3.61, but it did not show a significant drop in local skin temperatures (< 0.6 °C) of the trunk for persons with PA compared to No-Vest.

- At high activity level, the hybrid vest improved heat losses at the trunk by a factor between 1.64 and 3.25, and its performance was effective in reducing skin temperatures at low RH for all simulated T_{amb} conditions, and at high RH but with T_{amb} lower than 32 °C, with a maximum of 0.84 °C drop in local sensate skin temperature of the trunk. This drop might be sufficient to improve the thermal comfort and sensation level for persons with PA.

- The above hybrid vest limitations imply that the use of the hybrid vest is recommended at $T_{amb} \leq 32$ °C and $RH < 60\%$ at both metabolic rates. Whereas, at $T_{amb} \geq 32$ °C and $RH \geq 60$ %, before sweat and moisture accumulation start, the use of ECV Type II is recommended over the hybrid vest.

Experimental Findings

- Based on the human subject experiments, the performance of the PCM cooling vest is dependent on the injury level of persons with PA.

- Its effectiveness in reducing body core temperature and improving thermal comfort and sensation levels is achieved when at least 50% of the trunk skin area is sensate.

- Based on the human subject experiments, ECV Type II resulted in a drop of ~1 °C at the trunk sensate skin compared to No-Vest case and enhanced thermal comfort and sensation levels during the exercise before sweating started. However, comfort and sensation levels deteriorated once sweat

formation occurred at the sensate skin of the trunk; as an indication of restricted evaporation from the shirt when using ECV Type II.

The above findings are important for improving the design of the cooling vest to be adaptive to thermal physiology of persons with PA to extend their leisure time physical activity attaining better quality of life.

6.1. Future work

Studies in literature about cooling vests for persons with SCI are still picking up, and this research provided a different perspective to evaluate the performance of cooling vests for this vulnerable population. However, there are certain limitations that need to be addressed in future work. The focus should be as follows:

- Investigate other means of cooling vests for people with high-thoracic injury (T3 and above) as they showed least beneficiary effect from using PCM cooling vest or ECV Type II. These means should overcome that limited sensate skin and limited sweating rate of the trunk for this group of injury level.

- Test the performance of the proposed hybrid vest at high activity levels that can be done through human subject experiments. This helps in assessing both the physiological and psychological responses of persons with PA, as such studies are very limited in literature.

- Because the performance of hybrid ECV depends on the sweat rate across the senate skin of the trunk of a person with PA, it is of great interest to consider the non-uniform distribution of the sweat rates at the sensate skin of the trunk (chest and upper back) for persons with PA in the integrated

hybrid ECV-PA bioheat model. This can provide improvement in evaluating the performance of cooling vests for this population while taking into consideration a better reflection of the thermal physiology of persons with PA and sweat evaporation of the trunk segments. However, this may require human subject experiments engaging people with PA for further validation of the bioheat model predictions.

- Investigate the subjective preferences of persons with PA of the PCM cooling vests and hybrid ECV via human subject experiments, taking into consideration the properties of each type of cooling vest tested (weight, practicability of activation and use, ease of body movement while using the vest…etc.).

LIST OF PUBLICATIONS

Journal Papers

- Mneimneh F, Ghaddar N, Ghali K, Itani M. The effectiveness of evaporative cooling vest with ventilation fans on the thermal state of persons with paraplegia during exercise. Building and Environment. 2021 Sep 17:108356.

- Moussalem, Charbel; Mneimneh, Farah; sarieddine, rana; Bsat, Shadi; El=Housheimy, Mohamad; Minassian, Georges; Ghaddar, Nesreen; Ghali, Kamel; Omeis, Ibrahim, 2021. Effect of phase change material cooling vests on body thermoregulation and thermal comfort of patients with paraplegia: a human subject experimental study. Global Spine Journal. Sep 27,: 21925682211049167

- Mneimneh, F., Moussalem, C., Ghaddar, N., Ghali, K. and Omeis, I., 2020. Experimental study on the effectiveness of the PCM cooling vest in persons with paraplegia of varying levels. Journal of Thermal Biology, p.102634.

- Mneimneh, F., Moussalem, C., Ghaddar, N., Aboughali, K. and Omeis, I., 2019. Influence of cervical spinal cord injury on thermoregulatory and cardiovascular responses in the human body: Literature review. Journal of Clinical Neuroscience, 69, pp.7-14.

- Mneimneh, F., Ghaddar, N., Ghali, K., Moussalem, C. and Omeis, I., 2019. Would personal cooling vest be effective for use during exercise by people with thoracic spinal cord injury?. Journal of thermal biology, 82, pp.123-141.

- Mneimneh, F., Ghaddar, N., Ghali, K., Omeis, I. and Moussalem, C., 2018. An altered Bioheat model for persons with cervical spinal cord injury. Journal of thermal biology, 77, pp.96-110.

Conference   Papers

- Mneimneh, F., Ghaddar, N., Ghali, K., Moussalem, C. and Omeis, I., 2021, June. A comparative study on the effectiveness of evaporative and phase change material cooling vests for people with paraplegia. In Heat Transfer Summer Conference. American Society of Mechanical Engineers.

- Mneimneh F, Ghaddar N, Ghali K, Moussalem C, Omeis I. Experiment Study for Evaluation of Phase Change Material Cooling Vest's Effectiveness at Two Melting Points Used by People With Paraplegia During Exercise. In ASME International Mechanical Engineering Congress and Exposition 2020 Nov 16 (Vol. 84591, p. V011T11A020). American Society of Mechanical Engineers.

- Mneimneh, F., Ghaddar, N., Ghali, K., Moussalem, C. and Omeis, I., 2019, July. Modeling the Effect of Cooling Vest on Body Thermal Response of People With Paraplegia During Exercise. In Heat Transfer Summer Conference (Vol. 59315, p. V001T13A004). American Society of Mechanical Engineers.

REFERENCES

Al-Othmani, M., Ghaddar, N., Ghali, K., 2008. A multi-segmented human bioheat model for transient and asymmetric radiative environments. International Journal of Heat and Mass Transfer 51, 5522-5533.

Altus, P., Hickman, J.W., Nord, H.J., 1985. Accidental hypothermia in a healthy quadriplegic patient. Neurology 35, 427-427.

Appolonia, M., 2002. Evaporative cooling article. Google Patents.

Armstrong, L.E., Maresh, C.M., Riebe, D., Kenefick, R.W., Castellani, J.W., Senk, J.M., Echegaray, M., Foley, M.F., 1995. Local cooling in wheelchair athletes during exercise-heat stress. Medicine and science in sports and exercise 27, 211-216.

Atasağun, H.G., Okur, A., Psikuta, A., Rossi, R.M., Annaheim, S., 2018. Determination of the effect of fabric properties on the coupled heat and moisture transport of underwear–shirt fabric combinations. Textile Research Journal 88, 1319-1331.

Attia, M., Engel, P., 1983. Thermoregulatory set point in patients with spinal cord injuries (spinal man). Spinal Cord 21, 233-248.

Avolio, A., 1980. Multi-branched model of the human arterial system. Medical and Biological Engineering and Computing 18, 709-718.

Bachnak, R., Itani, M., Ghaddar, N., Ghali, K., 2018. Performance of hybrid PCM-Fan vest with deferred fan operation in transient heat flows from active human in hot dry environment. Building and Environment 144, 334-348.

Bergman, T.L., Incropera, F.P., DeWitt, D.P., Lavine, A.S., 2011. Fundamentals of heat and mass transfer. John Wiley & Sons.

Biering-Sørensen, B., Kristensen, I.B., Kjær, M., Biering-Sørensen, F., 2009. Muscle after spinal cord injury. Muscle & Nerve 40, 499-519.

Biering-Sørensen, B., Kristensen, I.B., Kjær, M., Biering-Sørensen, F., 2009. Muscle after spinal cord injury. Muscle & Nerve: Official Journal of the American Association of Electrodiagnostic Medicine 40, 499-519.

Bongers, C.C., Eijsvogels, T.M., van Nes, I.J., Hopman, M.T., Thijssen, D.H., 2016. Effects of cooling during exercise on thermoregulatory responses of men with paraplegia. Physical therapy 96, 650-658.

Bongers, C.C.W.G., Hopman, M.T.E., Eijsvogels, T.M.H., 2017. Cooling interventions for athletes: An overview of effectiveness, physiological mechanisms, and practical considerations. Temperature 4, 60-78.

Brown, R., DiMarco, A.F., Hoit, J.D., Garshick, E., 2006. Respiratory dysfunction and management in spinal cord injury. Respiratory care 51, 853-870.

Buchholz, A.C., McGillivray, C.F., Pencharz, P.B., 2003. Differences in resting metabolic rate between paraplegic and able-bodied subjects are explained by differences in body composition. The American journal of clinical nutrition 77, 371-378.

Burton, A.C., 1935. Human calorimetry: II. The average temperature of the tissues of the body: three figures. The Journal of Nutrition 9, 261-280.

Chou, C., Tochihara, Y., Kim, T., 2008. Physiological and subjective responses to cooling devices on firefighting protective clothing. European journal of applied physiology 104, 369-374.

Chun, S., Kim, H., Shin, H.-I., 2017. Estimating the basal metabolic rate from fat free mass in individuals with motor complete spinal cord injury. Spinal cord 55, 844-847.

Ciuha, U., Valenčič, T., Mekjavic, I.B., 2020. Cooling efficiency of vests with different cooling concepts over 8-hour trials. Ergonomics, 1-15.

Ciuha, U., Valenčič, T., Mekjavic, I.B., 2021. Cooling efficiency of vests with different cooling concepts over 8-hour trials. Ergonomics 64, 625-639.

Collins, E.G., Gater, D., Kiratli, J., Butler, J., Hanson, K., Langbein, W.E., 2010. Energy cost of physical activities in persons with spinal cord injury. Med Sci Sports Exerc 42, 691-700.

Cooper, K., Ferres, H.M., Guttmann, L., 1957. Vasomotor responses in the foot to raising body temperature in the paraplegic patient. The Journal of physiology 136, 547.

Dampney, R., 1994. Functional organization of central pathways regulating the cardiovascular system. Physiological reviews 74, 323-364.

Dawson, B., Bridle, J., Lockwood, R., 1994. Thermoregulation of paraplegic and able bodied men during prolonged exercise in hot and cool climates. Spinal Cord 32, 860-870.

de Groot, P.C., Bleeker, M.W., van Kuppevelt, D.H., van der Woude, L.H., Hopman, M.T., 2006. Rapid and extensive arterial adaptations after spinal cord injury. Archives of physical medicine and rehabilitation 87, 688-696.

de Groot, P.C.E., 2005. Cardiovascular Adaptations in Spinal Cord-Injured Individuals. Timne course of arterial vascular changes. [Sl: sn].

Douzi, W., Dugué, B., Vinches, L., Al Sayed, C., Hallé, S., Bosquet, L., Dupuy, O., 2019. Cooling during exercise enhances performances, but the cooled body areas matter: A systematic review with meta-analyses. Scandinavian Journal of Medicine & Science in Sports 29, 1660-1676.

Downey, R.J., Downey, J.A., Newhouse, E., Weissman, C., 1992. Fatal hyperthermia in a quadriplegic man: possible evidence for a peripheral action of haloperidol in neuroleptic malignant syndrome. Chest 101, 1728-1730.

Dykes, R.W., Saddiki-Traki, F., Tremblay, N., Boureau, F., Morel-Fatio, X., 2002. Differences in the sensations of warmth on the anterior torso of normal and spinal-cord transected individuals. Somatosensory & motor research 19, 218-230.

Eijsvogels, T.M., Bongers, C.C., Veltmeijer, M.T., Moen, M.H., Hopman, M., 2014. Cooling during exercise in temperate conditions: impact on performance and thermoregulation. International journal of sports medicine 35, 840-846.

Fiala, D., Lomas, K.J., Stohrer, M., 2001. Computer prediction of human thermoregulatory and temperature responses to a wide range of environmental conditions. International journal of biometeorology 45, 143-159.

Finnerup, N.B., Johannesen, I., Fuglsang-Frederiksen, A., Bach, F.W., Jensen, T.S., 2003. Sensory function in spinal cord injury patients with and without central pain. Brain 126, 57-70.

Fitzgerald, P.I., Sedlock, D.A., Knowlton, R.G., 1990. Circulatory and thermal adjustments to prolonged exercise in paraplegic women. Med Sci Sports Exerc 22, 629-635.

Fontana, P., Saiani, F., Grütter, M., Croset, J.-P., Capt, A., Camenzind, M., Morrissey, M., Rossi, R.M., Annaheim, S., 2017. Exercise intensity dependent relevance of protective textile properties for human thermo-physiology. Textile Research Journal 87, 1425-1434.

Fu, G., 1995. A transient, 3-D mathematical thermal model for the clothed human. KSU, Dissertation.

Gagge, A.P., Stolwijk, J., Hardy, J., 1967. Comfort and thermal sensations and associated physiological responses at various ambient temperatures. Environmental research 1, 1-20.

Gao, C., Kuklane, K., Wang, F., Holmér, I., 2012. Personal cooling with phase change materials to improve thermal comfort from a heat wave perspective. Indoor air 22, 523-530.

Garstang, S.V., Miller-Smith, S.A., 2007. Autonomic nervous system dysfunction after spinal cord injury. Physical medicine and rehabilitation clinics of North America 18, 275-296.

Gass, E.M., Gass, G.C., Pitetti, K., 2002. Thermoregulatory responses to exercise and warm water immersion in physically trained men with tetraplegia. Spinal Cord 40, 474-480.

Gibson, P., 1996. Multiphase heat and mass transfer through hygroscopic porous media with applications to clothing materials. Army Natick Research Development and Engineering Center MA.

Ginis, K.A.M., Arbour-Nicitopoulos, K.P., Latimer, A.E., Buchholz, A.C., Bray, S.R., Craven, B.C., Hayes, K.C., Hicks, A.L., McColl, M.A., Potter, P.J., 2010. Leisure time physical activity in a population-based sample of people with spinal cord injury part II: activity types, intensities, and durations. Archives of physical medicine and rehabilitation 91, 729-733.

Golbabaei, F., Heydari, A., Moradi, G., Dehghan, H., Moradi, A., Habibi, P., 2020. The effect of cooling vests on physiological and perceptual responses: a systematic review. International Journal of Occupational Safety and Ergonomics, 1-33.

Gorgey, A., Dudley, G., 2007. Skeletal muscle atrophy and increased intramuscular fat after incomplete spinal cord injury. Spinal cord 45, 304-309.

Griggs, K.E., Havenith, G., Paulson, T.A., Price, M.J., Goosey-Tolfrey, V.L., 2017. Effects of cooling before and during simulated match play on thermoregulatory responses of athletes with tetraplegia. Journal of Science and Medicine in Sport 20, 819-824.

Griggs, K.E., Price, M.J., Goosey-Tolfrey, V.L., 2015. Cooling athletes with a spinal cord injury. Sports Medicine 45, 9-21.

Guttman, L.S.J., and Wyndham CH, 1958. Thermoregulation in spinal man. J Physiol 142, 406-419.

Guttmann, L., Silver, J., Wyndham, C.H., 1958. Thermoregulation in spinal man. The Journal of physiology 142, 406.

Hamdan, H., Ghaddar, N., Ouahrani, D., Ghali, K., Itani, M., 2016. PCM cooling vest for improving thermal comfort in hot environment. International Journal of Thermal Sciences 102, 154-167.

Havenith, G., Bröde, P., Hartog, E.d., Kuklane, K., Holmer, I., Rossi, R.M., Richards, M., Farnworth, B., Wang, X., 2013. Evaporative cooling: effective latent heat of evaporation in relation to evaporation distance from the skin. Journal of Applied Physiology 114, 778-785.

Hazra, A., Gogtay, N., 2016. Biostatistics series module 5: Determining sample size. Indian journal of dermatology 61, 496.

Hjeltnes, N., Aksnes, A.-K., Birkeland, K.I., Johansen, J., Lannem, A., Wallberg-Henriksson, H., 1997. Improved body composition after 8 wk of electrically stimulated leg cycling in tetraplegic patients. American Journal of Physiology-Regulatory, Integrative and Comparative Physiology 273, R1072-R1079.

Ho, R.M., Freed, M.M., 1991. Persistent hypertension in young spinal cord injured individuals resulting from aortic repair. Archives of physical medicine and rehabilitation 72, 743-746.

Hogancamp II, C.E., 2004. Loss of Sympathetic Control of Cardiovascular Function Following Spinal Cord Injury.

Hopman, M.T., Pistorius, M., Kamerbeek, I.C., Binkhorst, R.A., 1993. Cardiac output in paraplegic subjects at high exercise intensities. European journal of applied physiology and occupational physiology 66, 531-535.

Hostettler, S., Leuthold, L., Brechbühl, J., Illi, S.K., Spengler, C.M., 2012. Maximal cardiac output during arm exercise in the sitting position after cervical spinal cord injury. Journal of rehabilitation medicine 44, 131-136.

House, J.R., Lunt, H.C., Taylor, R., Milligan, G., Lyons, J.A., House, C.M., 2013. The impact of a phase-change cooling vest on heat strain and the effect of different cooling pack melting temperatures. European journal of applied physiology 113, 1223-1231.

Huizenga, C., Hui, Z., Arens, E., 2001. A model of human physiology and comfort for assessing complex thermal environments. Building and Environment 36, 691-699.

Ishii, K., Yamasaki, M., Muraki, S., Komura, T., Kikuchi, K., Miyagawa, T., Fujimoto, S., Maeda, K., 1995. Tympanic temperature and skin temperatures during upper limb exercise in patients with spinal cord injury. Japanese Journal of Physical Fitness and Sports Medicine 44, 447-455.

Itani, M., Bachnak, R., Ghaddar, N., Ghali, K., 2019. Evaluating performance of hybrid PCM-fan and hybrid PCM-desiccant vests in moderate and hot climates. Journal of Building Engineering 22, 383-396.

Itani, M., Ghaddar, N., Ghali, K., 2017. Innovative PCM-desiccant packet to provide dry microclimate and improve performance of cooling vest in hot environment. Energy Conversion and Management 140, 218-227.

Itani, M., Ghaddar, N., Ghali, K., Ouahrani, D., Khater, B., 2018a. Significance of PCM arrangement in cooling vest for enhancing comfort at varied working periods and climates: Modeling and experimentation. Applied Thermal Engineering 145, 772-790.

Itani, M., Ghaddar, N., Ouahrani, D., Ghali, K., Khater, B., 2018b. An optimal two-bout strategy with phase change material cooling vests to improve comfort in hot environment. Journal of Thermal Biology 72, 10-25.

Itani, M., Ouahrani, D., Ghaddar, N., Ghali, K., Chakroun, W., 2016. The effect of PCM placement on torso cooling vest for an active human in hot environment. Building and Environment 107, 29-42.

Jehl, J., Gandmontagne, M., Pastene, G., Eyssette, M., Flandrois, R., Coudert, J., 1991. Cardiac output during exercise in paraplegic subjects. European journal of applied physiology and occupational physiology 62, 256-260.

Jones, B., 1992. Transient interaction between the human and the thermal environment. ASHRAE Trans. 98, 189-195.

Karaki, W., Ghaddar, N., Ghali, K., Kuklane, K., Holmér, I., Vanggaard, L., 2013. Human thermal response with improved AVA modeling of the digits. International Journal of Thermal Sciences 67, 41-52.

Kehn, M., Kroll, T., 2009. Staying physically active after spinal cord injury: a qualitative exploration of barriers and facilitators to exercise participation. BMC Public Health 9, 168.

Kenny, G.P., McGinn, R., 2017. Restoration of thermoregulation after exercise. Journal of Applied Physiology 122, 933-944.

Kessler, K.M., Pina, I., Green, B., Burnett, B., Laighold, M., Bilsker, M., Palomo, A.R., Myerburg, R.J., 1986. Cardiovascular findings in quadriplegic and paraplegic patients and in normal subjects. The American journal of cardiology 58, 525-530.

Khan, S., Plummer, M., Martinez-Arizala, A., Banovac, K., 2007. Hypothermia in patients with chronic spinal cord injury. The Journal of Spinal Cord Medicine 30, 27-30.

Kirshblum, S.C., Burns, S.P., Biering-Sorensen, F., Donovan, W., Graves, D.E., Jha, A., Johansen, M., Jones, L., Krassioukov, A., Mulcahey, M., 2011a. International standards for neurological classification of spinal cord injury (revised 2011). The journal of spinal cord medicine 34, 535-546.

Kirshblum, S.C., Burns, S.P., Biering-Sorensen, F., Donovan, W., Graves, D.E., Jha, A., Johansen, M., Jones, L., Krassioukov, A., Mulcahey, M.J., Schmidt-Read, M., Waring, W., 2011b. International standards for neurological classification of spinal cord injury (Revised 2011). The Journal of Spinal Cord Medicine 34, 535-546.

Klinger, H., 1985. Greens' Function Formulation of the Bioheat Transfer Problem. Heat Transfer in Medicine and Biology 1, 245-260.

Klous, L., Psikuta, A., Gijsbertse, K., Mol, D., van Schaik, M., Daanen, H., Kingma, B., 2020. Two isothermal challenges yield comparable physiological and subjective responses. European Journal of Applied Physiology 120, 2761-2772.

Krause, J.S., Crewe, N.M., 1991. Chronologic age, time since injury, and time of measurement: effect on adjustment after spinal cord injury. Archives of Physical Medicine and Rehabilitation 72, 91-100.

Kume, M., Yoshida, T., Tsuneoka, H., Kimura, N., Ito, T., 2009. Relationship between body surface cooling area, cooling capacity, and thermoregulatory responses wearing water purfused suits during exercise in humans. Japanese Journal of Physical Fitness and Sports Medicine 58, 109-122.

Lehmann, K.G., Lane, J.G., Piepmeier, J.M., Batsford, W.P., 1987. Cardiovascular abnormalities accompanying acute spinal cord injury in humans: incidence, time course and severity. Journal of the American College of Cardiology 10, 46-52.

Mathias, C.J., 2004. Autonomic disturbances in spinal cord injuries, Primer on the Autonomic Nervous System. Elsevier, pp. 298-301.

Mathias, C.J., 2006. Orthostatic hypotension and paroxysmal hypertension in humans with high spinal cord injury. Progress in brain research 152, 231-243.

Maynard, F.M., Bracken, M.B., Creasey, G., Ditunno Jr, J.F., Donovan, W.H., Ducker, T.B., Garber, S.L., Marino, R.J., Stover, S.L., Tator, C.H., 1997. International standards for neurological and functional classification of spinal cord injury. Spinal cord 35, 266-274.

McKinley, W.O., Jackson, A.B., Cardenas, D.D., Michael, J., 1999. Long-term medical complications after traumatic spinal cord injury: a regional model systems analysis. Archives of physical medicine and rehabilitation 80, 1402-1410.

Melo, F.C.M., de Lima, K.K.F., Silveira, A.P.K.F., de Azevedo, K.P.M., dos Santos, I.K., de Medeiros, H.J., Leitão, J.C., Knackfuss, M.I., 2019. Physical training and upper-limb strength of people with paraplegia: a systematic review. Journal of sport rehabilitation 28, 288-293.

Miller, M.W., Ziskin, M.C., 1989. Biological consequences of hyperthermia. Ultrasound in medicine & biology 15, 707-722.

Mitchell, J.W., Myers, G.E., 1968. An analytical model of the counter-current heat exchange phenomena. Biophysical journal 8, 897-911.

Mneimneh, F., Ghaddar, N., Ghali, K., Moussalem, C., Omeis, I., 2019a. Modeling the Effect of Cooling Vest on Body Thermal Response of People With Paraplegia During Exercise, Heat Transfer Summer Conference. American Society of Mechanical Engineers, p. V001T013A004.

Mneimneh, F., Ghaddar, N., Ghali, K., Moussalem, C., Omeis, I., 2019b. Would personal cooling vest be effective for use during exercise by people with thoracic spinal cord injury? Journal of thermal biology 82, 123-141.

Mneimneh, F., Ghaddar, N., Ghali, K., Moussalem, C., Omeis, I., 2020a. Experiment Study for Evaluation of Phase Change Material Cooling Vest's Effectiveness at Two Melting Points Used by People With Paraplegia During Exercise, ASME International Mechanical Engineering Congress and Exposition. American Society of Mechanical Engineers, p. V011T011A020.

Mneimneh, F., Ghaddar, N., Ghali, K., Omeis, I., Moussalem, C., 2018. An altered Bioheat model for persons with cervical spinal cord injury. Journal of thermal biology 77, 96-110.

Mneimneh, F., Moussalem, C., Ghaddar, N., Aboughali, K., Omeis, I., 2019c. Influence of cervical spinal cord injury on thermoregulatory and cardiovascular responses in the human body: Literature review. Journal of Clinical Neuroscience 69, 7-14.

Mneimneh, F., Moussalem, C., Ghaddar, N., Ghali, K., Omeis, I., 2020b. Experimental study on the effectiveness of the PCM cooling vest in persons with paraplegia of varying levels. Journal of Thermal Biology 91, 102634.

Mortan, W., Hearle, L., 1975. Physical properties of textile fibers. Heinemann, London.

Muraki, S., Yamasaki, M., Ishii, K., Kikuchi, K., Seki, K., 1996. Relationship between core temperature and skin blood flux in lower limbs during prolonged arm exercise in persons with spinal cord injury. European journal of applied physiology and occupational physiology 72, 330-334.

Nightingale, T.E., Gorgey, A.S., 2018. Predicting Basal Metabolic Rate in Men with Motor Complete Spinal Cord Injury. Med Sci Sports Exerc 50, 1305-1312.

Ouahrani, D., Itani, M., Ghaddar, N., Ghali, K., Khater, B., 2017. Experimental study on using PCMs of different melting temperatures in one cooling vest to reduce its weight and improve comfort. Energy and Buildings 155, 533-545.

Pennes, H.H., 1948. Analysis of tissue and arterial blood temperatures in the resting human forearm. Journal of applied physiology 1, 93-122.

Petrofsky, J.S., 1992. Thermoregulatory stress during rest and exercise in heat in patients with a spinal cord injury. European journal of applied physiology and occupational physiology 64, 503-507.

Pledger, H., 1962. Disorders of temperature regulation in acute traumatic tetraplegia. The Journal of bone and joint surgery. British volume 44, 110-113.

Popa, C., Popa, F., Grigorean, V.T., Onose, G., Sandu, A.M., Popescu, M., Burnei, G., Strambu, V., Sinescu, C., 2010. Vascular dysfunctions following spinal cord injury. Journal of medicine and life 3, 275.

Price, M., Campbell, I., 1997a. Thermoregulatory responses of 1 paraplegic and able-bodied athletes at rest and during prolonged upper body 2 exercise and passive recovery. Eur J Appl Physiol Occup Physiol 76, 552-560.

Price, M.J., Campbell, I.G., 1997b. Thermoregulatory responses of paraplegic and able-bodied athletes at rest and during prolonged upper body exercise and passive recovery. European journal of applied physiology and occupational physiology 76, 552-560.

Price, M.J., Campbell, I.G., 2003. Effects of spinal cord lesion level upon thermoregulation during exercise in the heat. Medicine & Science in Sports & Exercise 35, 1100-1107.

Procter, J., The Effect of an Evaporative Cooling Vest During 40km Time Trial Performance in the Heat.

Procter, J., 2017. The Effect of an Evaporative Cooling Vest During 40km Time Trial Performance in the Heat.

Salloum, M., Ghaddar, N., Ghali, K., 2007. A new transient bioheat model of the human body and its integration to clothing models. International journal of thermal sciences 46, 371-384.

Schmidt-Trucksäss, A., Schmid, A., Brunner, C., Scherer, N., Zach, G., Keul, J., Huonker, M., 2000. Arterial properties of the carotid and femoral artery in endurance-trained and paraplegic subjects. Journal of applied physiology 89, 1956-1963.

Sekhon, L.H., Fehlings, M.G., 2001. Epidemiology, demographics, and pathophysiology of acute spinal cord injury. Spine 26, S2-S12.

Singh, R., Rohilla, R.K., Saini, G., Kaur, K., 2014. Longitudinal study of body composition in spinal cord injury patients. Indian journal of orthopaedics 48, 168-177.

Song, Y.-G., Won, Y.H., Park, S.-H., Ko, M.-H., Seo, J.-H., 2015. Changes in body temperature in incomplete spinal cord injury by digital infrared thermographic imaging. Annals of rehabilitation medicine 39, 696.

Spungen, A.M., Adkins, R.H., Stewart, C.A., Wang, J., Pierson Jr, R.N., Waters, R.L., Bauman, W.A., 2003a. Factors influencing body composition in persons with spinal cord injury: a cross-sectional study. Journal of applied physiology 95, 2398-2407.

Spungen, A.M., Adkins, R.H., Stewart, C.A., Wang, J., Pierson, R.N., Waters, R.L., Bauman, W.A., 2003b. Factors influencing body composition in persons with spinal cord injury: a cross-sectional study. Journal of Applied Physiology 95, 2398-2407.

Stephan, K., Laesecke, A., 1985. The thermal conductivity of fluid air. Journal of physical and chemical reference data 14, 227-234.

Stolwijk, J., Hardy, J., 1966. Temperature regulation in man—a theoretical study. Pflüger's Archiv für die gesamte Physiologie des Menschen und der Tiere 291, 129-162.

Takahashi, M., Sakaguchi, A., Matsukawa, K., Komine, H., Kawaguchi, K., Onari, K., 2004. Cardiovascular control during voluntary static exercise in humans with tetraplegia. Journal of Applied Physiology 97, 2077-2082.

Tanabe, S.-i., Kobayashi, K., Nakano, J., Ozeki, Y., Konishi, M., 2002. Evaluation of thermal comfort using combined multi-node thermoregulation (65MN) and radiation models and computational fluid dynamics (CFD). Energy and Buildings 34, 637-646.

Teasell, R.W., Arnold, J.M.O., Krassioukov, A., Delaney, G.A., 2000. Cardiovascular consequences of loss of supraspinal control of the sympathetic nervous system after spinal cord injury. Archives of physical medicine and rehabilitation 81, 506-516.

Theisen, D., Vanlandewijck, Y., 2002. Cardiovascular responses and thermoregulation in individuals with spinal cord injury. European bulletin of adapted physical activity 1.

Thijssen, D.H., De Groot, P.C., van den Bogerd, A., Veltmeijer, M., Cable, N.T., Green, D.J., Hopman, M.T., 2012. Time course of arterial remodelling in diameter and wall thickness above and below the lesion after a spinal cord injury. European journal of applied physiology 112, 4103-4109.

Toner, M.M., Drolet, L.L., Pandolf, K.B., 1986. Perceptual and physiological responses during exercise in cool and cold water. Perceptual and motor skills 62, 211-220.

Trbovich, M., 2019. Efficacy of various cooling techniques during exercise in persons with spinal cord injury: a pilot crossover intervention study. Topics in spinal cord injury rehabilitation 25, 74-82.

Trbovich, M., Ortega, C., Schroeder, J., Fredrickson, M., 2014. Effect of a cooling vest on core temperature in athletes with and without spinal cord injury. Topics in spinal cord injury rehabilitation 20, 70-80.

Trbovich, M.B., Kiratli, J.B., Price, M.J., 2016. The effects of a heat acclimation protocol in persons with spinal cord injury. Journal of Thermal Biology 62, 56-62.

Umeno, T., Hokoi, S., Takada, S., 2001. Prediction of skin and clothing temperatures under thermal transient considering moisture accumulation in clothing/Discussion. ASHRAE Transactions 107, 71.

Urbański, P.K., Conners, R.T., Tasiemski, T., 2021. Leisure time physical activity in persons with spinal cord injury across the seasons. Neurological Research 43, 22-28.

van Marken Lichtenbelt, W.D., Daanen, H.A., Wouters, L., Fronczek, R., Raymann, R.J., Severens, N.M., Van Someren, E.J., 2006. Evaluation of wireless determination of skin temperature using iButtons. Physiology & behavior 88, 489-497.

Veeger, H., YAHMED, M., Van der Woude, L., Charpentier, P., 1991. Peak oxygen uptake and maximal power output of Olympic wheelchair-dependent athletes. Medicine & Science in Sports & Exercise 23, 1201-1209.

Wan, X., Fan, J., 2008. A transient thermal model of the human body–clothing–environment system. Journal of Thermal Biology 33, 87-97.

Wang, F., Song, W., 2017. An investigation of thermophysiological responses of human while using four personal cooling strategies during heatwaves. Journal of thermal biology 70, 37-44.

West, C., Mills, P., Krassioukov, A., 2012. Influence of the neurological level of spinal cord injury on cardiovascular outcomes in humans: a meta-analysis. Spinal cord 50, 484-492.

WICKS, J., OLDRIDGE, N., CAMERON, B., JONES, N., 1983. Arm cranking and wheelchair ergometry in elite spinal cord-injured athletes. Medicine & Science in Sports & Exercise 15, 224-231.

Wijnen, J., Kuipers, H., Kool, M., Hoeks, A., Van Baak, M., HA, S.B., Verstappen, F., Van Bortel, L., 1991. Vessel wall properties of large arteries in trained and sedentary subjects. Basic research in cardiology 86, 25-29.

Wilsmore, B.R., 2007. Thermoregulation in people with spinal cord injury.

Wulff, W., 1974. The energy conservation equation for living tissue. IEEE transactions on biomedical engineering, 494-495.

Xu, X., Gonzalez, J., 2011. Determination of the cooling capacity for body ventilation system. European journal of applied physiology 111, 3155-3160.

Yamasaki, M., Kim, K.T., Choi, S.W., Muraki, S., Shiokawa, M., Kurokawa, T., 2001. Characteristics of body heat balance of paraplegics during exercise in a hot environment. Journal of physiological anthropology and applied human science 20, 227-232.

Yi, W., Zhao, Y., Chan, A.P., 2017. Evaluation of the ventilation unit for personal cooling system (PCS). International Journal of Industrial Ergonomics 58, 62-68.

Yilmaz, B., Yasar, E., Goktepe, A.S., Onder, M.E., Alaca, R., Yazicioglu, K., Mohur, H., 2007. The relationship between basal metabolic rate and femur bone mineral density in men with traumatic spinal cord injury. Archives of physical medicine and rehabilitation 88, 758-761.

Young, A., 1987. Sawka MN, Epstein Y, Decristofano B, and Pandolf KB. Cooling different body surfaces during upper and lower body exercise. J Appl Physiol 63, 1218-1223.

Zhao, M., Gao, C., Wang, F., Kuklane, K., Holmér, I., Li, J., 2013. A study on local cooling of garments with ventilation fans and openings placed at different torso sites. International Journal of Industrial Ergonomics 43, 232-237.